MIXOTROPHY IN PROTISTS: FROM MODEL SYSTEMS TO MATHEMATICAL MODELS,
2nd Edition

EDITED BY: Matthew D. Johnson and Holly V. Moeller
PUBLISHED IN: Frontiers in Marine Science

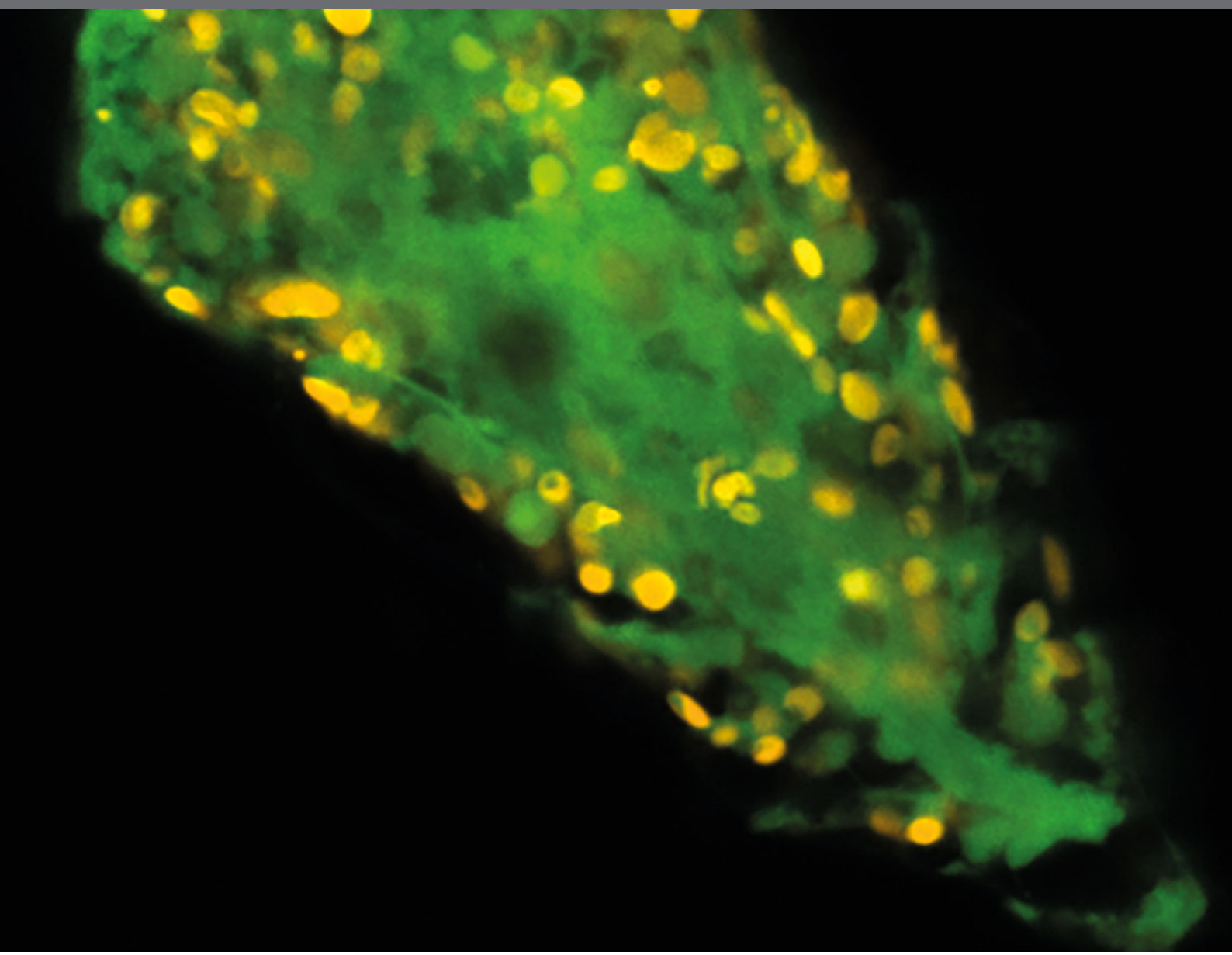

frontiers Research Topics

ISSN 1664-8714
ISBN 978-2-88963-148-3
DOI 10.3389/978-2-88963-148-3

About Frontiers

Frontiers is more than just an open-access publisher of scholarly articles: it is a pioneering approach to the world of academia, radically improving the way scholarly research is managed. The grand vision of Frontiers is a world where all people have an equal opportunity to seek, share and generate knowledge. Frontiers provides immediate and permanent online open access to all its publications, but this alone is not enough to realize our grand goals.

Frontiers Journal Series

The Frontiers Journal Series is a multi-tier and interdisciplinary set of open-access, online journals, promising a paradigm shift from the current review, selection and dissemination processes in academic publishing. All Frontiers journals are driven by researchers for researchers; therefore, they constitute a service to the scholarly community. At the same time, the Frontiers Journal Series operates on a revolutionary invention, the tiered publishing system, initially addressing specific communities of scholars, and gradually climbing up to broader public understanding, thus serving the interests of the lay society, too.

Dedication to Quality

Each Frontiers article is a landmark of the highest quality, thanks to genuinely collaborative interactions between authors and review editors, who include some of the world's best academicians. Research must be certified by peers before entering a stream of knowledge that may eventually reach the public - and shape society; therefore, Frontiers only applies the most rigorous and unbiased reviews.
Frontiers revolutionizes research publishing by freely delivering the most outstanding research, evaluated with no bias from both the academic and social point of view. By applying the most advanced information technologies, Frontiers is catapulting scholarly publishing into a new generation.

What are Frontiers Research Topics?

Frontiers Research Topics are very popular trademarks of the Frontiers Journals Series: they are collections of at least ten articles, all centered on a particular subject. With their unique mix of varied contributions from Original Research to Review Articles, Frontiers Research Topics unify the most influential researchers, the latest key findings and historical advances in a hot research area! Find out more on how to host your own Frontiers Research Topic or contribute to one as an author by contacting the Frontiers Editorial Office: researchtopics@frontiersin.org

MIXOTROPHY IN PROTISTS: FROM MODEL SYSTEMS TO MATHEMATICAL MODELS,
2nd Edition

Topic Editors:
Matthew D. Johnson, Woods Hole Oceanographic Institution, United States
Holly V. Moeller, University of California, Santa Barbara, United States

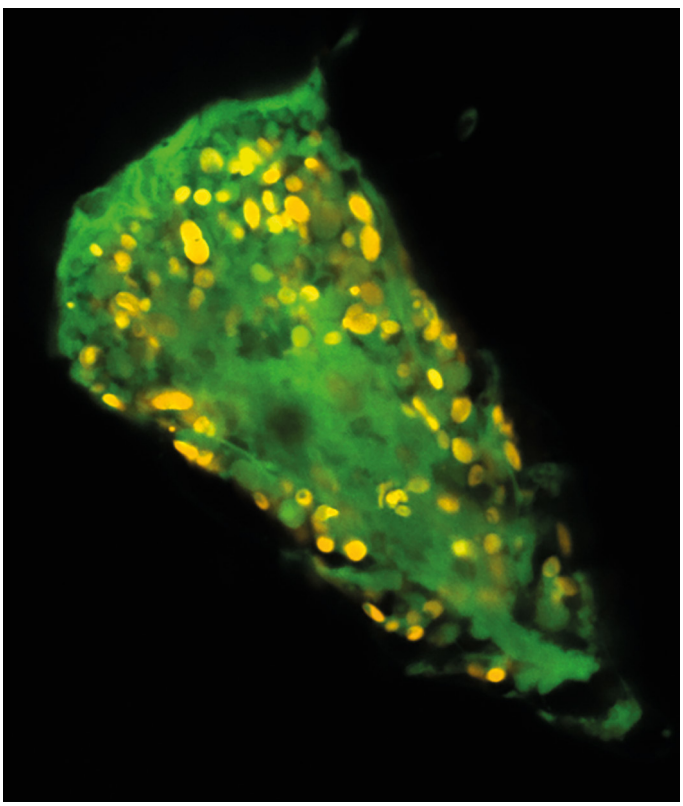

A fluorescence confocal micrograph of the mixotrophic ciliate *Laboea strobila*
Image: Matthew Johnson

Publisher's note: In this 2nd edition, the following article has been updated: Gomes HdR, McKee K, Mile A, Thandapu S, Al-Hashmi K, Jiang X and Goes JI (2018) Influence of Light Availability and Prey Type on the Growth and Photo-Physiological Rates of the Mixotroph *Noctiluca scintillans*. *Front. Mar. Sci*. 5:374. doi: 10.3389/fmars.2018.00374

Citation: Johnson, M. D., Moeller, H. V., eds. (2019). Mixotrophy in Protists: From Model Systems to Mathematical Models, 2nd Edition. Frontiers Media SA. doi: 10.3389/978-2-88963-148-3

Table of Contents

frontiers in Marine Science

EDITORIAL
published: 18 December 2018
doi: 10.3389/fmars.2018.00490

Editorial: Mixotrophy in Protists: From Model Systems to Mathematical Models

Matthew D. Johnson[1]* *and Holly V. Moeller*[2]

[1] Biology Department, Woods Hole Oceanographic Institution, Woods Hole, MA, United States, [2] Ecology, Evolution & Marine Biology, University of California, Santa Barbara, Santa Barbara, CA, United States

Keywords: mixotrophy, protists, marine microbial ecology, plankton ecology and pelagic food webs, Ocean biochemistry

Editorial on the Research Topic

Mixotrophy in Protists: From Model Systems to Mathematical Models

Mixotrophy in marine protists is now recognized as a fundamentally important mechanism for acquiring energy or limiting nutrients. This move to center stage follows decades of research establishing that mixotrophy occurs broadly across the eukaryotic tree of life (Selosse et al., 2016) and is more commonplace in aquatic ecosystems than previously thought (Worden et al., 2015). Its ubiquity among microbial eukaryotes in sunlit oligotrophic oceans, and its important roles in coastal temperate and polar ecosystems, has propelled a reevaluation of microbial food web trophic dynamics. Changes in how the broader oceanographic community perceives the role of mixotrophy is evident in the growing interest by theoretical and mathematical ecologists in modeling these phenomena.

The prevalence of mixotrophs among most protist lineages is not surprising, considering that phagotrophy is an ancestral trait in eukaryotes and that most major lineages have members that have acquired stable plastids (Raven, 1997). This metabolic duality can be seen in the ebb and flow of photosynthetic and phagotrophic traits within lineages, and is most vividly reflected within the dinoflagellates (Saldarriaga et al., 2001). Rarely are heterotrophy and phototrophy balanced even within a species, but rather seem to function in a tug of war for cellular resources (Skovgaard, 1996; Adolf et al., 2006; Flynn and Mitra, 2009). Mixotrophs can be broadly categorized as being constitutive (CM), and possessing a stable plastid, or non-constitutive (NCM) and lacking a plastid (Mitra et al., 2016). The NCM are also referred to as acquired phototrophs, since they host endosymbiotic algae or steal their plastids. Both CMs and NCMs practice photosynthesis and phagotrophy simultaneously to fulfill the energetic and nutritional requirements.

While cellular and ecosystem drivers and the physiological role of mixotrophy are well understood for some protists, major gaps remain in our understanding of the broader biogeochemical and trophic implications of mixotrophy. The growing emphasis of mixotrophy in community and ecosystem ecology is helping to bridge this divide and to better focus research efforts. In this Research Topic, Lin et al. use a dynamic mathematical model to illustrate the effects of temperature and nutrients on autotrophic and mixotrophic growth in the harmful alga *Karlodinium veneficum*. This research suggests that in a warming climate, both the occurrence of mixotrophy and the availability of suitable prey will likely increase for this harmful algal bloom species.

OPEN ACCESS

Edited and reviewed by:
Angel Borja,
Centro Tecnológico Experto en Innovación Marina y Alimentaria (AZTI), Spain

***Correspondence:**
Matthew D. Johnson
mattjohnson@whoi.edu

Specialty section:
This article was submitted to Marine Ecosystem Ecology, a section of the journal Frontiers in Marine Science

Received: *19 November 2018*
Accepted: *04 December 2018*
Published: *18 December 2018*

Citation:
Johnson MD and Moeller HV (2018) Editorial: Mixotrophy in Protists: From Model Systems to Mathematical Models. Front. Mar. Sci. 5:490. doi: 10.3389/fmars.2018.00490

These findings support the conclusions of Wilken et al. (2013), who found that a warming climate would select for more mixotrophic organisms due to their nutritional flexibility in conditions that will likely result in greater respiration rates and lower nutrient availability.

In a review of mixotrophy in polar seas, Stoecker and Lavrentyev provide a strong case for mixotrophic protists dominating an alternative food web during much of the year that includes mixotrophic flagellates and oligotrich ciliates. Mixotrophic oligotrichs, feeding on mixotrophic flagellates, represent the majority of community chlorophyll within the mixed layer during summer in the Arctic, and provide an important link to mesozooplankton. Stoecker and Lavrentyev highlight the pivotal role of mixotrophs in Arctic food webs, and outline future directions to investigate mixotrophic contributions to community and ecosystem dynamics through empirical research and modeling.

Despite a rich history of research on the physiological ecology of mixotrophs, we still lack fundamental trait based knowledge for many protist groups. This is particularly true of most of Radiolaria and Foraminifera taxa, which are generally not possible to culture and can be difficult to work with due to their delicate structures. Villar et al. reveal that under thermal stress, dinoflagellate symbionts of *Collozoum pelagicum* (Retaria) undergo a bleaching-like response that may involve activation of a lysogenic virus. While numerous studies have documented the role of thermal stress in cnidarians, this is the first such study for radiolarians. In another study of a NCM, Gomes et al. show that feeding by the dinoflagellate *Noctiluca scintillans* does not enhance photophysiology of their symbionts when nutrients are not limiting, and that the dinoflagellate is able to fine-tune intracellular nutrient levels when feeding. Finally, McManus et al. found that while the NCM ciliate *Strombidium rassoulzadegani* displays some flexibility in the types of phytoplankton from which it could steal plastids, it was unable to do so with 6 of the algal prey species investigated, suggesting some degree of variability in prey compatibility and/or selectivity by the ciliate.

Two studies employed state-of-the-art approaches to gain insights into cellular processes in mixotrophs. McKie-Krisberg et al. used transcriptomics to identify genes involved in phagotrophy within *Micromonas polaris* and *Pyramimonas tychotreta*, but found little difference in expression levels of these genes under conditions that selected for predominantly phototrophic or phagotrophic metabolism. Carpenter et al. used nanometer-scale secondary ion mass spectrometry (NanoSIMS) to quantify the role of phagotrophy among *P. parvum* cells in acquiring C and N. They discovered that *P. parvum* was feeding mainly to acquire N, but that a large degree of variation occurs between individual cells in their assimilation of N. These studies provided novel insights into genomic and metabolic processes within mixotrophs, and illustrate the need for basic research to understand how mixotrophs function.

Finally, several studies in this Research Topic focus on identifying and quantifying *in situ* interactions between mixotrophs and their prey using a variety of approaches. *In situ* dynamics of prey selection by mixotrophs remains largely unstudied. Johnson et al. focused on the trophic role of cryptophyte algae in Chesapeake Bay, finding high grazing rates and selective grazing by certain protist predators among cryptophyte species. They demonstrated that *in situ* grazing helps to shape community cryptophyte diversity by using a combination of molecular approaches and traditional dilution experiments. Lee and Park used single cell approaches to sequence ingested prey of the harmful benthic dinoflagellate *Ostreopsis* in coastal Korean waters, revealing that it ingests gametes of Rhodophyte macroalgae. Gast et al. studied the contribution of CMs to bacterivory in the Ross Sea during spring and summer, finding that mixotrophs were less abundant than heterotrophic flagellates, but had higher per capita ingestion rates of bacterial prey and were most important during spring. Using bromodeoxyuridine-labeled bacteria as food and immunoprecipitation of labeled DNA, they were also able to identify potential mixotrophs in these samples.

The papers in this Research Topic provide a small sampling of current mixotrophy research and a window into the complex and fascinating interactions within marine microbial food webs. With the growing interest in mixotrophy research and an emphasis on contextualizing this research within theoretical and ecological frameworks, we are entering a period of quickening discoveries and progress in understanding the role of mixotrophy in marine ecosystems.

AUTHOR CONTRIBUTIONS

All authors listed have made a substantial, direct and intellectual contribution to the work, and approved it for publication.

ACKNOWLEDGMENTS

MJ thanks the National Science Foundation (OCE 1436169) for providing support for this research.

REFERENCES

Adolf, J. E., Stoecker, D. K., and Harding, L. W. (2006). The balance of autotrophy and heterotrophy during mixotrophic growth of Karlodinium micrum (Dinophyceae). *J. Plankton Res.* 28, 737–751. doi: 10.1093/plankt/fbl007

Flynn, K. J., and Mitra, A. (2009). Building the "perfect beast": modelling mixotrophic plankton. *J. Plankton Res.* 31, 965–992. doi: 10.1093/plankt/fbp044

Mitra, A., Flynn, K. J., Tillmann, U., Raven, J. A., Caron, D., Stoecker, D. K., et al. (2016). Defining planktonic protist functional groups on mechanisms for energy and nutrient acquisition: incorporation of diverse mixotrophic strategies. *Protist* 167, 106–120. doi: 10.1016/j.protis.2016.01.003

Raven, J. A. (1997). Phagotrophy in phototrophs. *Limnol. Oceanogr.* 42, 198–205. doi: 10.4319/lo.1997.42.1.0198

Saldarriaga, J. F., Taylor, F. J., Keeling, P. J., and Cavalier-Smith, T. (2001). Dinoflagellate nuclear SSU rRNA phylogeny suggests multiple plastid

losses and replacements. *J. Mol. Evol.* 53, 204–213. doi: 10.1007/s002390010210

Selosse, M. A., Charpin, M., and Not, F. (2016). Mixotrophy everywhere on land and in water: the grand écart hypothesis. *Ecol. Lett.* 20, 246–263. doi: 10.1111/ele.12714

Skovgaard, A. (1996). Mixotrophy in Fragilidium subglobosum (Dinophyceae): growth and grazing responses as functions of light intensity. *Mar. Ecol. Prog. Ser.* 143, 247–253. doi: 10.3354/meps143247

Wilken, S., Huisman, J., Naus-Wiezer, S., and Donk, E. (2013). Mixotrophic organisms become more heterotrophic with rising temperature. *Ecol. Lett.* 16, 225–233. doi: 10.1111/ele.12033

Worden, A. Z., Follows, M. J., Giovannoni, S. J., Wilken, S., Zimmerman, A. E., and Keeling, P. J. (2015). Rethinking the marine carbon cycle: factoring in the multifarious lifestyles of microbes. *Science* 347:1257594. doi: 10.1126/science.1257594

Conflict of Interest Statement: The authors declare that the research was conducted in the absence of any commercial or financial relationships that could be construed as a potential conflict of interest.

frontiers in Marine Science

ORIGINAL RESEARCH
published: 10 September 2018
doi: 10.3389/fmars.2018.00320

Simulating Effects of Variable Stoichiometry and Temperature on Mixotrophy in the Harmful Dinoflagellate *Karlodinium veneficum*

Chih-Hsien Lin[1], Kevin J. Flynn[2], Aditee Mitra[2] and Patricia M. Glibert[1]*

[1] Horn Point Laboratory, University of Maryland Center for Environmental Science, Cambridge, MD, United States,
[2] Department of Biosciences, Wallace Building, Swansea University, Swansea, United Kingdom

OPEN ACCESS

Edited by:
Matthew D. Johnson,
Woods Hole Oceanographic Institution, United States

Reviewed by:
Lasse Tor Nielsen,
Technical University of Denmark, Denmark
Shovonlal Roy,
University of Reading, United Kingdom

***Correspondence:**
Kevin J. Flynn
k.j.flynn@swansea.ac.uk

Specialty section:
This article was submitted to Marine Ecosystem Ecology, a section of the journal Frontiers in Marine Science

Received: 28 March 2018
Accepted: 22 August 2018
Published: 10 September 2018

Citation:
Lin C-H, Flynn KJ, Mitra A and Glibert PM (2018) Simulating Effects of Variable Stoichiometry and Temperature on Mixotrophy in the Harmful Dinoflagellate Karlodinium veneficum. Front. Mar. Sci. 5:320. doi: 10.3389/fmars.2018.00320

Results from a dynamic mathematical model are presented simulating the growth of the harmful algal bloom (HAB) mixotrophic dinoflagellate *Karlodinium veneficum* and its algal prey, *Rhodomonas salina*. The model describes carbon-nitrogen-phosphorus-based interactions within the mixotroph, interlinking autotrophic and phagotrophic nutrition. The model was tuned to experimental data from these species grown under autotrophic conditions and in mixed batch cultures in which nitrogen:phosphorus stoichiometry (input molar N:P of 4, 16, and 32) of both predator and prey varied. A good fit was attained to all experimentally derived carbon biomass data. The potential effects of temperature and nutrient changes on promoting growth of prey and thus *K. veneficum* bloom formation were explored using this simulation platform. The simulated biomass of *K. veneficum* was highest when they were functioning as mixotrophs and when they consumed prey under elevated N:P conditions. The scenarios under low N:P responded differently, with simulations showing larger deviation between mixotrophic and autotrophic growth, depending on temperature. When inorganic nutrients were in balanced proportions, lower biomass of the mixotroph was attained at all temperatures in the simulations, suggesting that natural systems might be more resilient against *Karlodinium* HAB development in warming conditions if nutrients were available in balanced proportions. These simulations underscore the need for models of HAB dynamics to include consideration of prey; modeling HAB as autotrophs is insufficient. The simulations also imply that warmer, wetter springs that may bring more N with lower N:P, such as predicted under climate change scenarios for Chesapeake Bay, may be more conducive to development of these HABs. Prey availability may also increase with temperature due to differential growth temperature responses of *K. veneficum* and its prey.

Keywords: mixotrophy, *Karlodinium veneficum*, *Rhodomonas salina*, harmful algal blooms, mathematical model, stoichiometry, temperature responses

INTRODUCTION

In conjunction with the growing recognition that harmful algal blooms (HABs) are promoted by increasing nutrient loads to marine and freshwaters (e.g., Anderson et al., 2002; Glibert et al., 2005; Heisler et al., 2008; Glibert and Burford, 2017), there is also an enhanced appreciation for the importance of mixotrophy in the nutrition of many HAB taxa (Jeong et al., 2005a,b; Burkholder et al., 2008; Flynn et al., 2013; Stoecker et al., 2017). The complexities of understanding the dynamics of HABs dominated by mixotrophs compound the already difficult study of system regulation by simple autotrophic physiology (Flynn, 2009; Mitra and Flynn, 2010; Ghyoot et al., 2017; Flynn and McGillicuddy, 2018; Glibert et al., 2018). For instance, some mixotroph species are primarily autotrophic but ingest prey under light limitation or conditions of nutrient limitation or imbalance, while some others appear to be primarily heterotrophic but photosynthesize under certain conditions by retaining chloroplasts from their prey (Stoecker, 1998). The challenge in understanding HAB dynamics where mixotrophy is an important nutritional mode is thus further complicated by the need to not only understand the ecophysiology of the HAB species, but also that of its prey species. Additionally, mixotrophy may also be related to toxin production in some HABs (e.g., Blossom et al., 2012).

Mixotrophy in protists is not a simple additive process of autotrophy plus phagotrophy, but rather a complex integration of physiological interactions (Flynn and Mitra, 2009; Mitra and Flynn, 2010). Only a few physiological experiments (Lundgren et al., 2016; Lin et al., 2017)–and even fewer model constructs–consider the feedback function of rates of change during mixotrophic feeding, the nutritional status of both predator and prey, and linkages to nutrient physiological interactions (Mitra and Flynn, 2006; Flynn, 2010). At present, predictive capabilities that include the role of mixotrophy in bloom formation are just beginning to be developed (Flynn, 2005, 2010; Glibert et al., 2010; Mitra et al., 2014, 2016; Flynn and McGillicuddy, 2018; Flynn et al., 2018).

There is also a growing appreciation that changes in climate may expand the potential niches for some harmful or toxic algal blooms (Hallegraeff, 2010; Fu et al., 2012; Wells et al., 2015; Glibert and Burkholder, 2018). The most direct effects of climate change are those associated with rising temperatures. The frequency and severity of blooms may be exacerbated due to temperature-driven competitive advantages for HAB species over non-HAB species (Hallegraeff, 2010) and other HAB-favorable conditions may expand, such as increased stratification or altered precipitation patterns that affect the timing of freshwater and associated nutrient delivery (e.g., Heisler et al., 2008; Moore et al., 2015; Glibert and Burkholder, 2018). The mixotrophic chrysophyte *Ochromonas* sp., for example, has been found to become more heterotrophic with increased temperature (Wilken et al., 2013). However, other climate changes events such as ocean acidification with (de)eutrophication may also affect the consortium of organisms that co-occur with the HAB species, and which can be food sources for these mixotrophs (e.g., Fu et al., 2012; Flynn et al., 2015; Wells et al., 2015; Glibert et al., 2018). There is evidence that ingestion, growth rates and cell volume of the heterotrophic dinoflagellate *Oxyrrhis marina* respond differently to temperature-prey interactions, indicating complex and non-linear predator-prey dynamics with increasing temperatures (Montagnes et al., 2003; Kimmance et al., 2006). Many important questions related to the interactive effects of temperature changes and mixotrophy on HAB dynamics clearly remain.

The mixotrophic dinoflagellate *Karlodinium veneficum* (formerly *Gymnodinium galatheanum* and *K. micrum*) is a common toxigenic species that can produce a suite of unique polyketide compounds, karlotoxins (Van Dolah, 2000; Kempton et al., 2002). This species is a constitutive mixotroph (Mitra et al., 2016), possessing the ability to make its own chloroplasts, and is capable of forming blooms of up to 10^7–10^8 cells L^{-1} (e.g., Adolf et al., 2008) that have been associated with fish and shellfish mortality, both in natural waters and aquaculture farms worldwide (Braarud, 1957; Nielsen, 1993; Glibert and Terlizzi, 1999; Deeds et al., 2002; Stoecker et al., 2008; Zhou et al., 2011). Blooms of *K. veneficum* appear to be increasing in size and frequency of occurrence in estuaries such as Chesapeake Bay, MD, United States (Li et al., 2015) and elsewhere worldwide (Place et al., 2012 and references therein; Dai et al., 2013; Adolf et al., 2015). This mixotroph is also a species for which there are considerable physiological data related to mixotrophy (e.g., Li et al., 1999, 2000; Place et al., 2012; Lin et al., 2017). Given its prevalence and potential threats to natural resources around the world, improved forecasting and predictive ability of this HAB taxon would be an aid to managers.

Here, applying both previously published and newly acquired experimental data, a model was developed to improve our understanding of the interactions of the growth of this mixotroph and its common prey, *Rhodomonas salina*, under varying nutrient and temperature conditions. The resultant simulations were used to address the hypothesis that growth of this mixotroph may increase due to the combination of increased nutrient concentrations, altered nutrient ratios, and raised temperature, combinations of conditions that may be expected under future climate conditions in eutrophic estuaries. While such responses may seem intuitive, the extent to which changes in nutrient (in form and proportion) together with temperature alter growth of the mixotroph and its prey are not well resolved and therefore simulations enable such interactions to be explored for multiple temperature and nutrient conditions. Results from using such models may help inform nutrient management plans under future climate conditions.

MATERIALS AND METHODS

Overall Approach

A mechanistic model was developed based on the framework of an existing variable stoichiometric, photo-acclimative mixotrophy model, namely the "perfect beast" construct of Flynn and Mitra (2009). This describes carbon-nitrogen-phosphorus (C-N-P)-based interactions within a mixotroph cell, and builds upon the variable stoichiometric zooplankton model of Mitra (2006) and the phytoplankton model of Flynn (2001). To

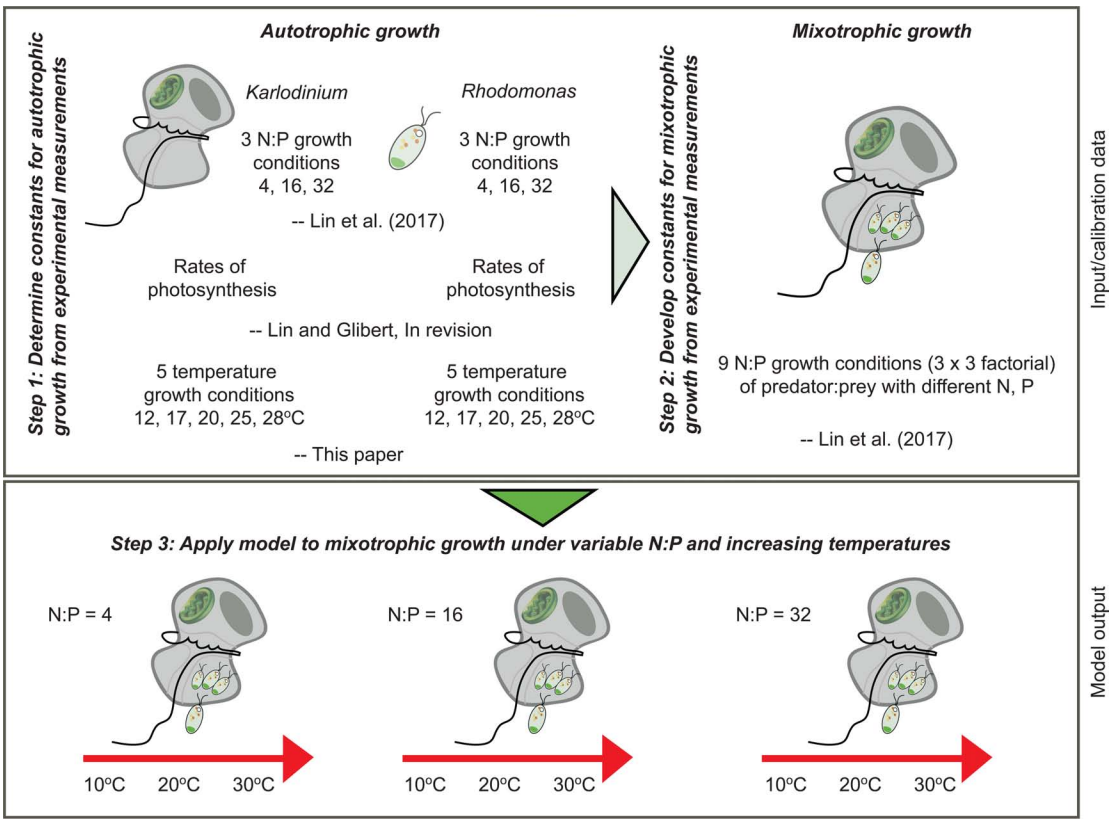

FIGURE 1 | Schematic diagram to illustrate the steps taken to determine the constants required for development of the "perfect beast" model (Flynn and Mitra, 2009) of mixotrophy of *Karlodinium veneficum* and its application under varying nutrient conditions and increasing temperature.

parameterize the model, previously published data as well as new data on temperature responses of both the mixotroph and prey were applied (**Figure 1**).

In brief, the "perfect beast" model has eight state variables (**Figure 2**) describing C, N, and P and chlorophyll (Chl) associated with the core mixotroph (m) biomass (mC, NC, PC, and ChlC) and also the same constituents associated with the contents of the food (F) vacuole (namely, FC, FNC, FPC, and FChlC) after the m have fed on algal prey. The amount of material associated with the F vacuole is relative to the core mC biomass. Thus, the total C associated with the m is mC·(1+FC) with the unit of gC L^{-1}. Here the m model was configured to be consistent with the status of *K. veneficum* as a constitutive m, with its own photoacclimative description of Chl:C. Prey were described using the variable stoichiometric photoacclimative phytoplankton model of Flynn (2001), as deployed in Flynn and Mitra (2009). The full model accounts for predator stoichiometry, prey stoichiometry (i.e., F quality) and their feedback interactions (**Figure 2**). The model operates using ordinary differential equations (ODEs) using an Euler integration routine with a timestep of 0.0039 d (5.625 min). Equations are provided in the associated **Supplementary Table S1**; these are given in a linear form to aid reconstruction in the modeling platform of choice.

The model was built, and simulations run, using the Powersim Constructor platform, with tuning (calibration) to experimental data performed using the evolutionary algorithm supported by Powersim Solver v2 (Isdalstø, Norway). This algorithm maximizes the likelihood of resolving a global, rather than a local, minimum, and produces the fit closest to the presented data (Haefner, 2005; Flynn, 2018). Most of the constants within the model are not tuned (**Tables 1**, **2**); they are used to modulate physiological feedback processes and the model is not sensitive to their precise value (see source papers for further details).

To configure the full model describing both the mixotroph and its prey, the constants that constrain the autotrophic physiology of predator and prey were first determined from experimental data (**Figure 1**). Once rates of photosynthesis and inorganic nutrient uptake for these species were calculated for varying nutrients and temperatures, the parameters that control mixotrophic performance of the predator were then ascertained (again through reference to experimental data), for conditions in which predator and prey were both grown under varying nutrient stoichiometry. Finally, the tuned model was run to simulate (predict) growth of *K. veneficum* and its prey under variable N:P and temperature conditions.

Data Sources, Experimental Conditions and Model Parameters

Previously available experimental data were first exploited. These included rates of autotrophic growth of both *K. veneficum* and

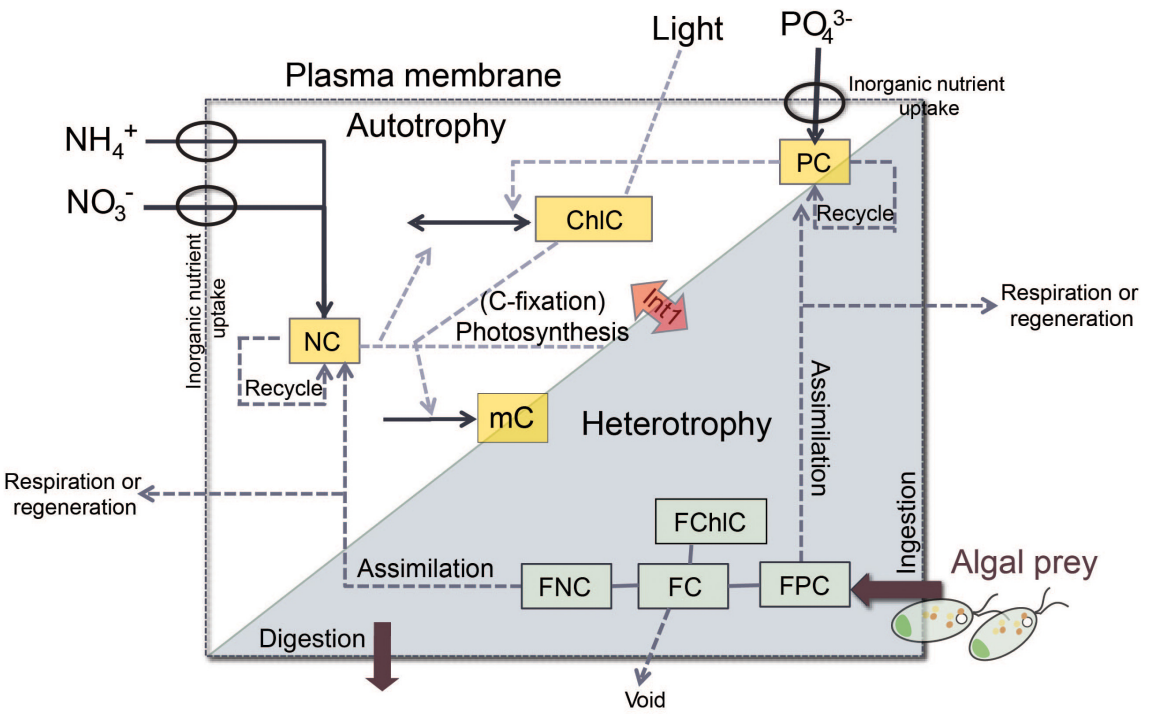

FIGURE 2 | Schematic of the structure of the "perfect beast" model, showing major flows in and out of state variables (solid arrows and boxes) from the external parameters (NO_3^-, PO_4^{3-}, and Light), and the major feedback processes (dashed arrows). Autotrophic growth uses inorganic nutrients and light via the photosystems of the mixotroph (phototrophy; white part). A proportion of activity leading to growth is required to support synthesis of those photosystems. Predation brings algal prey into the food vacuole within the confines of the mixotroph cell (heterotrophy; gray part). Interactions between phototrophic and heterotrophic nutrition (Int1) influence the growth of the mixotrophy (Flynn and Mitra, 2009). The state variables (yellow boxes) that describe carbon (C), nitrogen (N), phosphorus (P), and chlorophyll (Chl) associated with core mixotroph biomass are mC (C-biomass of the mixotroph), ChlC (chlorophyll C quota), NC (cellular NC quota), and PC (cellular PC quota), while the same constituents (green boxes) associated with the content of food vacuole are FC (food vacuole C content relative to mC), FChlC (food vacuole Chl content relative to mC), FNC (food vacuole N content relative to mC), and FPC (food vacuole P content relative to mC).

R. salina under varied N:P stoichiometry (molar N:P of 4, 16, and 32) in exponential growth phase (Lin et al., 2017; **Figure 1**); these experimental data are provided in the **Supplementary Table S2**). In order to establish the variable N:P conditions in those experiments, NO_3^- concentrations were held constant at ~1232 μg N L^{-1}, while initial PO_4^{3-} concentrations were varied. The constants that describe the autotrophic physiology of prey (e.g., half saturation constants for N and P uptake, aK_{Ni}, aK_P, and of growth, $a\mu max^{phot}$) and m (e.g., mK_{Ni}, and mK_P) were obtained from model tuning based on the change in residual NO_3^- and PO_4^{3-} concentrations (nutrient kinetics), and Chl and C biomass (see below) during culture growth (**Table 1**). From a second set of experiments, based on monocultures of *K. veneficum* and *R. salina,* growing autotrophically, initial

TABLE 1 | Autotrophic state constants that were calculated and gained from tuning against changes in experimental monoculture cultures of *Rhodomonas salina* and *Karlodinium veneficum*.

		Rhodomonas salina		*Karlodinium veneficum*		
Parameters	**Units**	**Abbr.**	**Values**	**Abbr.**	**Values**	**Sources**
Half saturation for NO_3^- transport	μg N L^{-1}	aK_{Ni}	57.437	mK_{Ni}	14.628	Tuned herein
Half saturation for PO_4^{3-} transport	μg P L^{-1}	aK_P	1.550	mK_P	118.490	Tuned herein
Chl-specific initial slope to PI curve (α)	($m^2 g^{-1}$ Chl *a*) (mgC micromol photon^{-1})	$a\alpha^{Chl}$	0.192	$m\alpha^{Chl}$	0.011	Lin and Glibert, unpublished
Maximum N:C	gN gC^{-1}	*aNCmax*	0.200	*mNCmax*	0.200	Calculated herein
Minimum N:C	gN gC^{-1}	*aNCmin*	0.050	*mNCmin*	0.050	Calculated herein
Maximum P:C	gP gC^{-1}	*aPCmax*	0.020	*mPCmax*	0.020	Calculated herein
Minimum P:C	gP gC^{-1}	*aPCmin*	0.005	*mPCmin*	0.001	Calculated herein
Maximum rate of phototrophic growth	d^{-1}	$a\mu max^{phot}$	1.280	$m\mu max^{phot}$	ND	Tuned herein

*Autotrophic growth rate of K. veneficum was not tuned here (ND; not determined, but see **Table 2**).*

TABLE 2 | Constants obtained from tuning the "perfect beast" model of Flynn and Mitra (2009) against experimentally derived changes in carbon biomass in mixed cultures of *Karlodinium veneficum* (mixotroph) with *Rhodomonas salina* (prey) when each was grown separately in different N:P condition (low NP = 4, Redfield = 16, and high N:P = 32 on a molar basis) and also combined in a total of 9 combinations.

	Scenario		
Parameters	**Low-N:P prey**	**Redfield-N:P prey**	**High-N:P prey**
Low-N:P *K. veneficum*			
mAEmin	0.658	0.840	0.814
mcap_a	0.050	0.050	0.050
mKas	0.999	0.835	0.647
mKIng	0.490	0.295	0.204
$m\mu max^{phot}$	0.200	0.400	0.400
$m\mu max^{het}$	0.450	0.477	0.504
Redfield-N:P *K. veneficum*			
mAEmin	0.743	0.370	0.736
mcap_a	0.050	0.050	0.050
mKas	0.010	0.840	0.997
mKIng	0.086	0.551	0.464
$m\mu max^{phot}$	0.200	0.400	0.400
$m\mu max^{het}$	0.451	0.887	0.842
High-N:P *K. veneficum*			
mAEmin	0.537	0.821	0.832
mcap_a	0.163	0.050	0.050
mKas	0.363	0.450	0.720
mKIng	0.010	0.296	0.309
$m\mu max^{phot}$	0.200	0.400	0.400
$m\mu max^{het}$	0.545	0.501	0.759

mAEmin, minimum assimilation efficiency; mcap_a, the likelihood of ingestion following encounter; mKas, mixotroph half saturation for digestion rate; mKIng, mixotroph half saturation for ingestion; $m\mu max^{phot}$*:mixotroph maximum rate of phototrophic growth;* $m\mu max^{het}$*, mixotroph maximum rate of heterotrophic growth.*

slopes of photosynthesis-irradiance (PI) curves were calculated (Lin and Glibert, unpublished). Additional physiological data (**Supplementary Table S1**) for parameterizing the autotrophic component of the model were obtained from Flynn and Mitra (2009). The C biomass of *K. veneficum* was estimated based on a cellular C-volume relationship for dinoflagellates (Menden-Deuer and Lessard, 2000) and a conversion factor of 0.2 pg C μm^{-3} from volume to C for *R. salina* was applied (Jakobsen and Hansen, 1997). Cell size of predator and prey were recorded in parallel with the cell densities in the study of Lin et al. (2017); cellular volume (CV) was estimated from these data using the following equation:

$$CV = 0.1875WL^2$$

where W and L are the width and length of cells.

To parameterize temperature responses, new experimental data were also obtained on rates of autotrophic growth of *K. veneficum* and *R. salina* across a temperature gradient (**Figure 1**). The same strains of *K. veneficum* and *R. salina* used in Lin et al. (2017) were inoculated separately into *f*/2 media (Guillard, 1975) and maintained at 12, 17, 20, 25, 28°C under irradiance of 430 micromol photons m^{-2} s^{-1} in a 12 h light:12 h dark cycle in batch cultures. The strains were acclimated for 2 weeks to the experimental conditions, after which growth was monitored over 96 h. Aliquots (2 mL) were collected for cell enumeration at 0, 24, 48, 72, and 96 h from each flask and were preserved in paraformaldehyde (final concentrations of 1% v/v) at 4°C for later cell enumeration. The cells were identified and gated based on size, shapes, and auto-fluorescence using a BD Accurri C6 flow cytometry. Then, cell-specific growth rates of predator and prey were determined separately based on the rates of changes in the slopes of the regression of natural log-transformed cell-densities change over 96 h.

After the mixotroph model was calibrated, and after autotrophic temperature responses of predator and prey were experimentally determined (and assumed to remain the same under mixotrophic conditions), the model was used to simulate 10-day growth responses of the mixotroph and its prey under 3 nutrient conditions (N:P = 4, N:P = 16, and N:P = 32 for both predator and prey) under varying temperatures (**Figure 1**). Rates of maximum growth of *K. veneficum* are reported in autotrophic and in mixotrophic nutritional modes.

Statistical Analyses

All statistical analyses were performed with *R.* The Shapiro–Wilk test was used to verify normality of the experimental data while the Levenes' test was used to assess the homogeneity of variance. Cell-specific growth rates of *K. veneficum* and *R. salina* were compared for statistical differences in slopes of regression of natural log-transformed data under each temperature conditions (ANCOVA test). Two-way analysis of variance was applied to test for the interactive effects between temperature and species. Regressions were considered significant at $p < 0.05$ with the adjusted r^2 value.

RESULTS

Temperature Effects on Growth

The responses to temperature of the mixotroph and its prey differed. Autotrophic growth rates of *K. veneficum* ranged between 0.06 and 0.29 d^{-1} and increased with increasing temperature up to 20°C above which growth rates fell sharply (**Figure 3**). The growth rates of *R. salina* had a similar range as those in the predator, from 0.06 to 0.26 d^{-1}, but the prey grew significantly faster than its predator at temperatures > 20°C (ANCOVA, $p < 0.001$; **Figure 3**). Variations between temperature responses of the maximal growth rates of *K. veneficum* and *R. salina* were statistically significant (two-way ANOVA: *F*-value = 2.88, $p = 0.011$; **Figure 3**).

Model Tuning to Experimental Data Sets

Model tuning was undertaken in 2 steps. Half saturation values (i.e., mK_{Ni}, mK_P, aK_{Ni}, and aK_P) were calculated based on nutrient depletion to determine transport of nutrients in relation to the cell quotas, and photosynthetic rates were used to determine cell C when cells were in autotrophic growth.

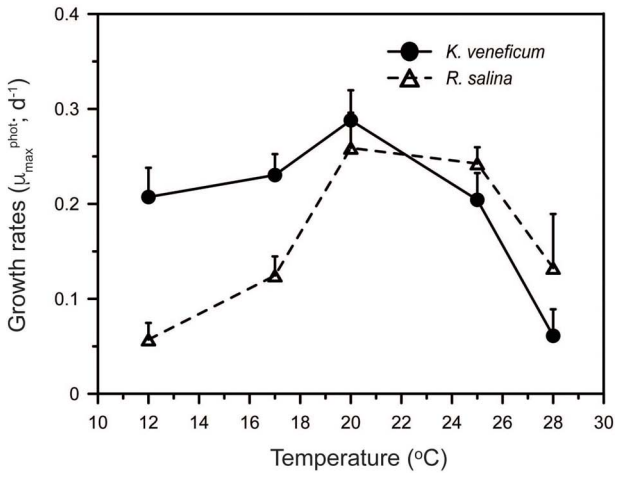

FIGURE 3 | Effect of temperature on cell-specific, autotrophic growth rates (μ_{max}^{phot}) of *Karlodinium veneficum* and *Rhodomonas salina*.

Maximum and minimum ratios of N:C and P:C define the nutrient status of the cells (**Table 1**). These parameters were then applied to mixotrophic growth.

The mixotroph model was successfully calibrated against previously available data on the growth of the mixotroph and its prey as a function of variable nutrient stoichiometry (**Figure 4**). Between 67 and 97% of the variations in the nine experimental data sets could be explained by the simulations for biomass of the mixotroph, with no significant difference between the observed and predicted data ($p < 0.05$).

The parameters that control mixotrophic growth showed variability with the nutritional status (C:N:P) of *K. veneficum* and its prey (**Table 2**). The most sensitive parameters were assimilation efficiency (*mAEmin*) and half saturation constant for ingestion (*mKIng*) and maximum growth rate of heterotrophic growth ($m\mu max^{het}$; **Table 2**). For example, the minimum assimilation efficiency (*mAEmin*) of C in the mixotroph from the ingested prey ranged from 0.370 under conditions in which both the mixotroph and prey were grown with nutrients supplied in Redfield conditions (N:P = 16), to 0.840 when the prey was under Redfield growth conditions but *K. veneficum* was grown under low N:P conditions. Thus, there was significantly higher *mAEmin* when the mixotroph was initially under low N:P conditions than when it was under Redfield N:P conditions and given the same quality prey. In addition, the half saturation for ingestion (*mKIng*) for *K. veneficum* grown under low N:P conditions was significantly lower when they were mixed with the high N:P prey than when *K. veneficum* in the same nutrient state was given prey grown under Redfield N:P and low N:P conditions (0.204 vs. 0.295 and 0.490, respectively). For those *K. veneficum* grown under high N:P conditions, their *mKIng* ranged from 0.010 to 0.309 with the lowest value corresponding to prey grown under low N:P. Maximum growth rate of *K. veneficum* as a photo-heterotroph ($m\mu max^{het}$) was consistently higher than maximum growth rate of *K. veneficum* as an autotroph ($m\mu max^{phot}$) by factors of 1.19 (low N:P *K. veneficum* with Redfield N:P prey) to 2.72 (high N:P *K. veneficum* with low N:P prey; **Table 2**).

Simulating Growth Under Variable Stoichiometry and Temperature

Using the tuned mixotroph-prey models, and having established individual temperature responses of *K. veneficum* and *R. salina*, scenarios were developed to estimate growth of both species under variable stoichiometry and temperature conditions (**Figure 1**). For *K. veneficum*, growth as an autotroph and as a mixotroph were compared, and for *R. salina*, growth with and without the predator were estimated. Three stoichiometric conditions were simulated, holding both species in the same N:P condition for each scenario (N:P = 4, 16, 32).

In the low N:P scenario, a significantly higher C biomass of *K. veneficum* in mixotrophic growth was attained in simulations with increased temperature (≥25°C) compared with that under comparable autotrophic conditions (ANCOVA, $p < 0.001$; **Figures 5A,D**). The highest mixotrophic growth rate, 0.30 d^{-1}, was attained at 25°C, which was 1.5-fold higher than the simulation without prey at this temperature. In the Redfield N:P scenarios, there were no significant differences between autotrophic and mixotrophic growth rates of *K. veneficum* (ANCOVA, $p = 0.161$) and relatively low overall C biomass of the mixotroph was attained in the 10-day simulation (**Figures 5B,E**). Differences between mixotrophic and autotrophic growth of *K. veneficum* under high N:P conditions considered a distinct trend toward statistical significance (ANCOVA, $p = 0.072$). The growth patterns of *K. veneficum* in the two nutritional modes were very similar, showing increases in biomass reaching the maximum value of ∼2200 μgC L^{-1} at 20°C under mixotrophic conditions, but a lower growth rate and corresponding lower C biomass accumulation at the highest temperature (**Figures 5C,F**).

The accumulation of C biomass and growth rates of *R. salina* in the presence and absence of the mixotroph were also estimated under variable nutrient and temperature conditions (**Figure 6**). In the presence of the mixotroph, prey biomass in all N:P conditions declined, but the patterns of decline varied depending on the nutrient conditions (**Figures 6A–C**). Under low N:P conditions, prey biomass gradually declined to zero within the 10-day simulation. Under Redfield conditions, prey remained detectable, but low, throughout this period. In the highest N:P simulation, prey biomass declined most quickly, to a near-zero biomass within 4 days. The patterns of the changes in prey biomass without predator were comparable among the three nutrient conditions, but higher biomass values were usually attained in the N-rich conditions at the near-highest temperatures (**Figure 6F**).

Changes in cellular N:P of *K. veneficum* with time was also explored in the model output in autotrophic and mixotrophic growth to determine the extent to which the mixotroph was using inorganic nutrients under the different stoichiometric and temperature conditions. The cellular elemental ratios of *K. veneficum* under low N:P and Redfield N:P growth conditions varied considerably in the first 2 days of simulated growth, then converged at a value of ∼7, but those of *K. veneficum* grown

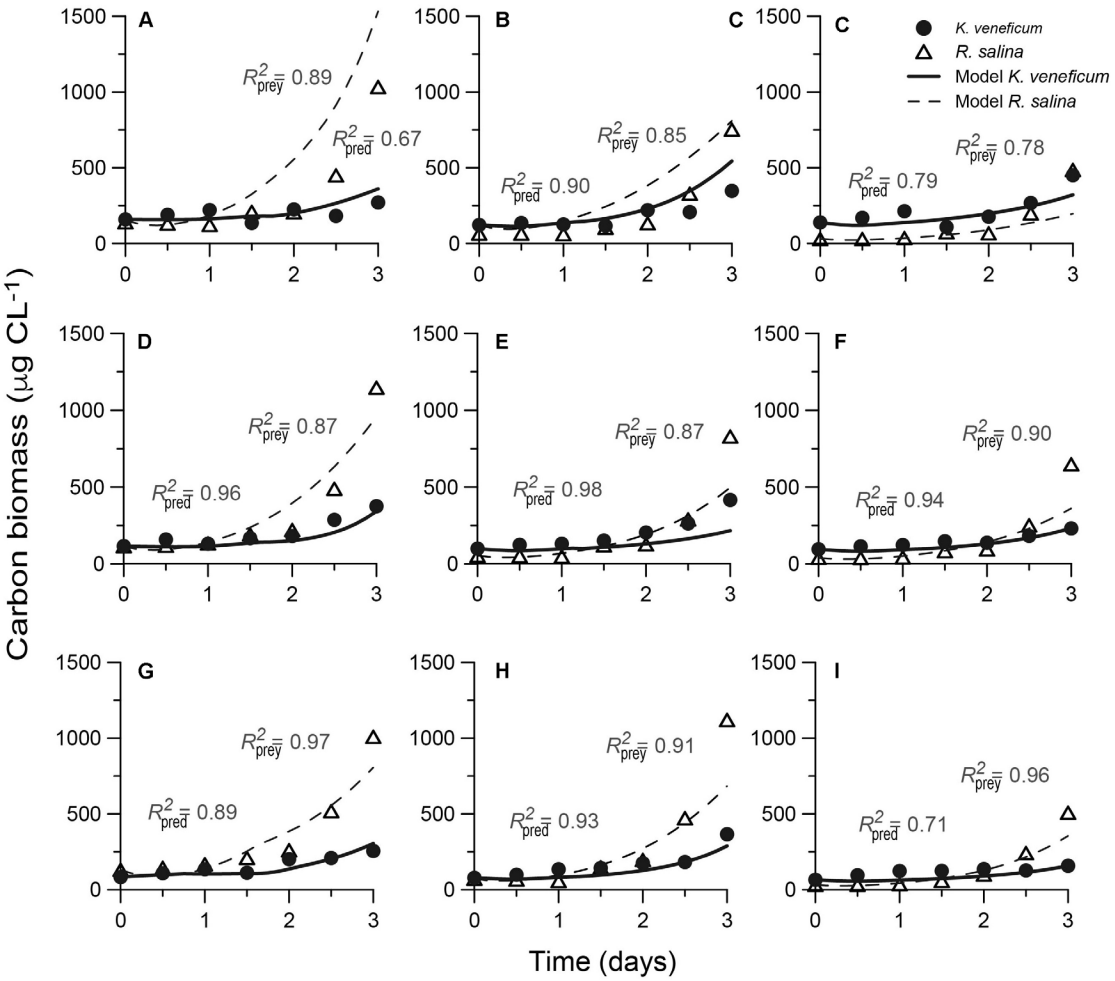

FIGURE 4 | Fits of the "perfect beast" model (lines) to experimental data (symbols) for carbon biomass from nine mixed-culture systems. The low-NP *Karlodinium veneficum* **(A–C)** Redfield-NP *K. veneficum* **(D–F)** and high-NP *K. veneficum* **(G–I)** provided with low-NP, Redfield-NP and high-NP prey *Rhodomonas salina* during mixed-culture experiments, respectively. N, nitrogen; P, phosphorus. R^2 coefficients are determined for the predator and prey under varying nutrient conditions.

in high N:P conditions converged on a value of ∼5 within 2 days under all temperatures conditions (**Figure 7**). Thus, in the simulations, under the condition of excess N (high N:P), *K. veneficum* appeared to become increasingly enriched with internal P through mixotrophy.

DISCUSSION

Despite the increasing recognition of the importance of mixotrophy in planktonic communities, especially HABs (Jeong et al., 2005a,b; Burkholder et al., 2008; Flynn et al., 2013; Stoecker et al., 2017), modeling of plankton dynamics that incorporates mixotrophy is in its infancy (but see Thingstad et al., 1996; Stickney et al., 2000; Ward et al., 2011; Våge et al., 2013; Mitra et al., 2014; Berge et al., 2017; Ghyoot et al., 2017). For simplicity, most model approaches have assumed independence between phototrophic and phagotrophic regulations (e.g., Thingstad et al., 1996; Baretta-Bekker et al., 1998; Jost et al., 2004; Våge et al., 2013; Ward and Follows, 2016). The "perfect beast' model (Flynn and Mitra, 2009) integrates phototrophy vs. phagotrophy with feedback functions to better represent a nearly true of mixotrophic behaviors, especially for predicting rates of ingestion (Mitra and Flynn, 2010). The "perfect beast" is a construct that can be configured to represent different types of constitutive and non-constitutive mixotrophs, and is consistent with our understanding of the different physiologies associated withthese different types of mixotrophs (Mitra et al., 2016). Although the model has been previously configured to represent different generic mixotroph types, and used to explore the implications of different types of mixotrophy in oligotrophic through to eutrophic conditions (Flynn and Mitra, 2009; Mitra and Flynn, 2010; Flynn and Hansen, 2013; Mitra et al., 2014), this is the first time that this, or indeed any, multi-stoichiometric model of protist mixotrophy has been specifically tuned to simulate experimental data of the complexity explored here. In large measure, this reflects the paucity of such data not only for mixotroph activity but also for the prey. Indeed, very

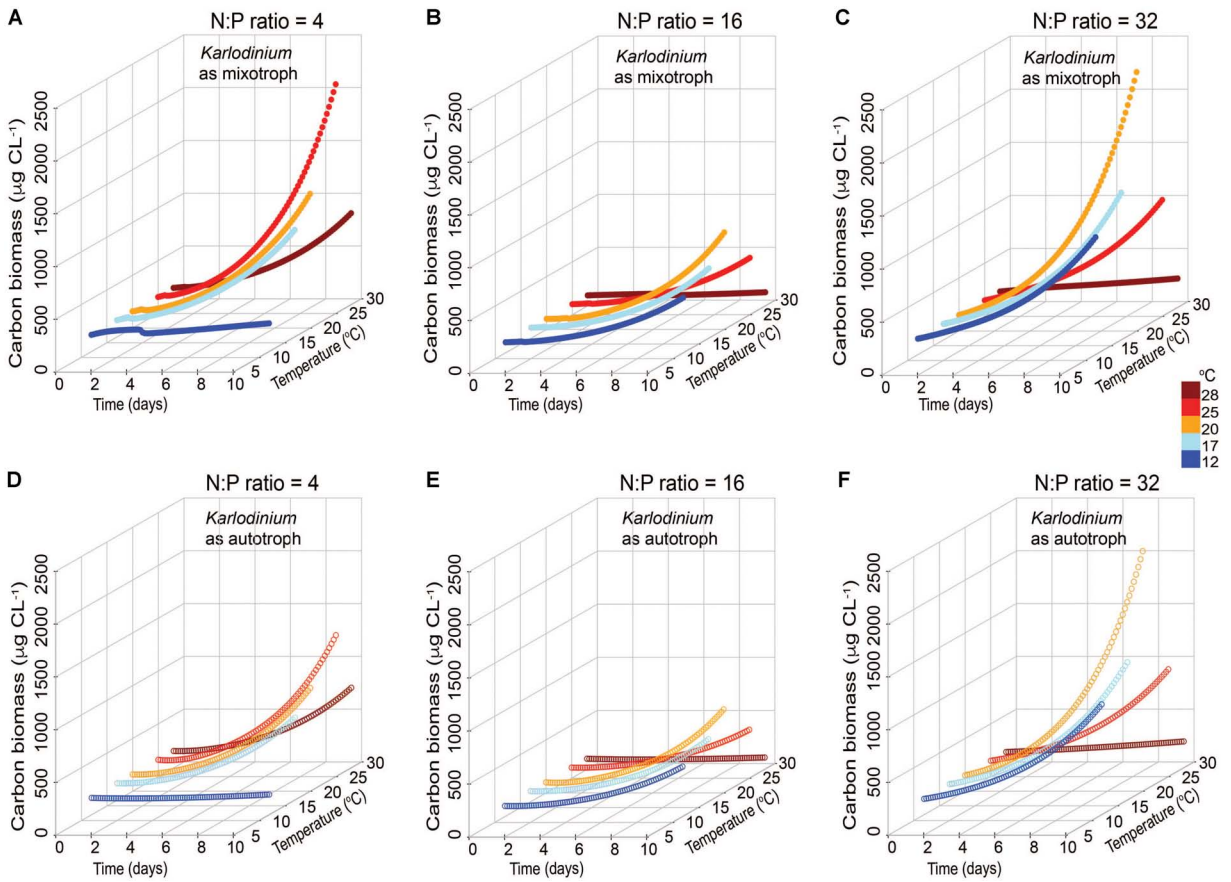

FIGURE 5 | Simulated changes in carbon biomass of *Karlodinium veneficum* in mixotrophic **(A–C)** and autotrophic **(D–F)** growth under low N:P (=4), Redfield N:P (=16) and high N:P (=32) conditions, and variable temperature conditions over 10-day simulations.

few empirical or modeling studies of phytoplankton describe multiple stoichiometries (i.e., C:N:P), despite increasing evidence that in nature such multiple nutrient states are important features structuring ecology and that nutrient stoichiometry is changing in many systems with anthropogenic nutrient loads (e.g., Peñuelas et al., 2012; Sutton et al., 2013; Glibert, 2017).

This study has successfully tuned the "perfect beast" to experimental data sets of the harmful dinoflagellate, *K. veneficum* and its prey, *Rhodomonas* sp., under varying nutrient conditions. Temperature growth responses were added to the original 'perfect beast' construct, thus allowing scenarios of mixotrophic growth under both varying nutrient and temperature conditions to be explored. The modeled scenarios highlighted several distinct differences in responses of *K. veneficum* as an autotroph and as a mixotroph in different nutrient and temperature conditions. Both autotrophic and mixotrophic *K. veneficum* attained much higher biomass in non-Redfieldian nutrient conditions compared to balanced nutrient growth. The modeled results in autotrophic *K. veneficum* biomass were quite consistent with the experimental data from Lin et al. (2017). Thus, simple stoichiometric relationships for predicting HAB developments need careful reconsideration, particularly in eutrophic systems where the corresponding changes in nutrient ratios and forms as well as prey stoichiometry may ultimately affect cellular functions (such as C:N:P ratio) within the harmful algal mixotrophs (Mitra and Flynn, 2005, 2010). Indeed, it has been increasingly recognized that the benefits of mixotrophy to cells are synergistic, not additive (e.g., Mitra and Flynn, 2010).

In both low N:P and high N:P simulations, *K. veneficum* appeared to be more mixotrophic and attained higher biomass with increasing temperature compared with growth under Redfield conditions or growth as an autotroph (**Figure 5**). Under low N:P condition, temperature effects on mixotrophic growth rates of *K. veneficum* were also significant, with mixotrophic growth rates increasing faster than autotrophic growth rates at the highest temperature (i.e., 25°C; **Figure 5A**). This growth stimulation may imply a higher demand for C from prey. These growth patterns support the notion that mixotrophy is likely to be greater under nutrient imbalanced conditions, that is, that mixotrophy is not just a mechanism to acquire C, but also a mechanism by which nutrients are acquired (e.g., Glibert and Burkholder, 2011). For example, the assimilation efficiency (*mAEmin*) in the mixotrophs was the highest for those *K. veneficum* grown under low N:P conditions and mixed with prey in Redfield N:P conditions, indicating nutrient sources from

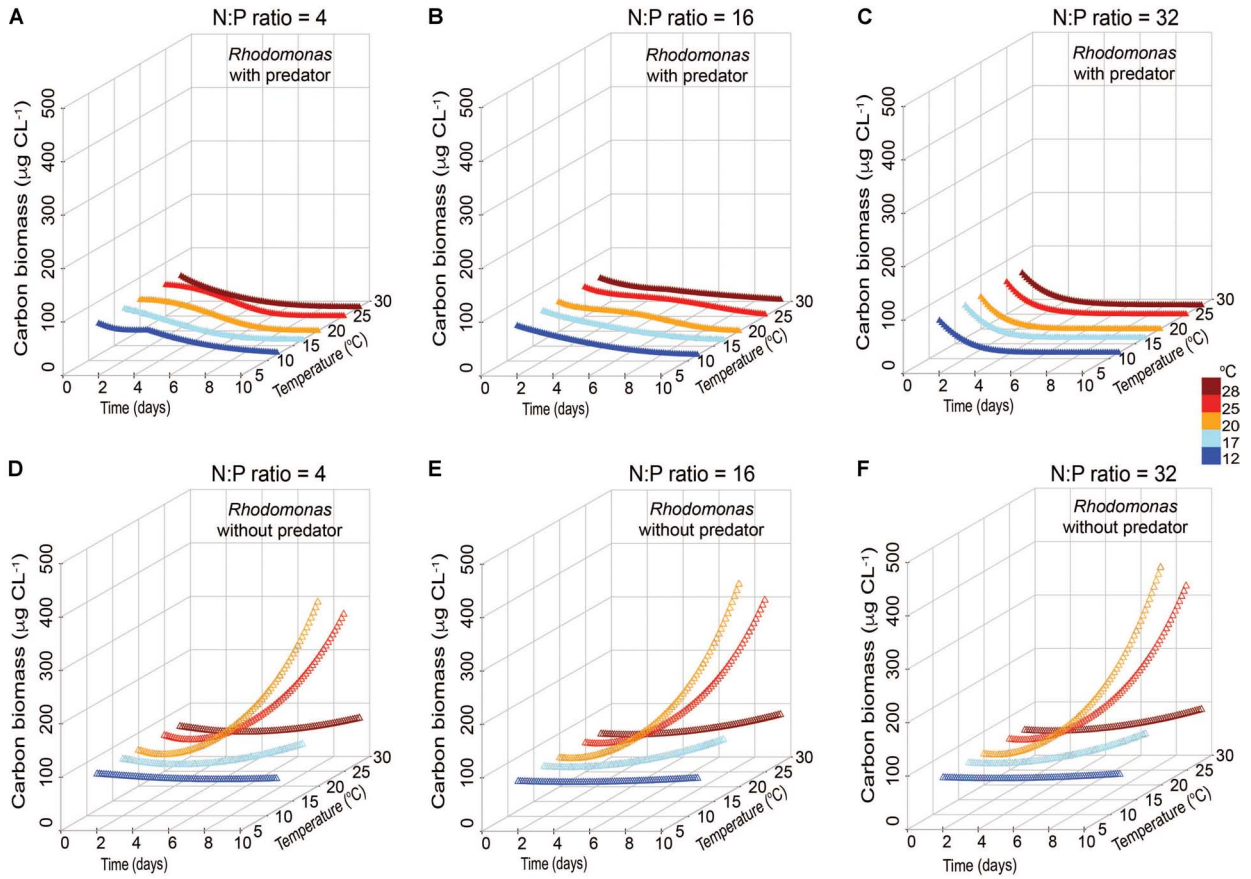

FIGURE 6 | Simulated changes in carbon biomass of prey *Rhodomonas salina* with *Karlodinium veneficum* as predator **(A–C)** and without predator **(D–F)** under low N:P (=4), Redfield N:P (=16) and high N:P (=32) conditions, and variable temperature conditions over 10-day simulations.

ingested prey were required (**Table 2**). On the other hand, the cellular N:P of *K. veneficum* in simulations under high N:P was low compared to the other nutrient conditions for this mixotroph (**Figure 7C**). The present simulations agreed with laboratory data: the incidence of *K. veneficum* feeding are enhanced when ambient nutrient ratios deviated from Redfield ratio with either N and/or P deficiency depending on the cellular status of the mixotrophic dinoflagellate (Lin et al., 2017). These results also suggest that under the warmest temperatures simulated, increased growth rates of prey could contribute to an increased growth of the mixotroph (**Figure 6**). The growth rates of *R. salina* were higher than those of *K. veneficum* > 20°C, and thus prey availability increases faster at these temperatures. This situation may be enhanced in the environments that deviate from balanced nutrient proportions.

Outputs from these simulated scenarios have implications for growth of this HAB in eutrophic conditions in warming environments. In eutrophic estuaries such as Chesapeake Bay, there are large seasonal variations in nutrient loads and in their stoichiometry (e.g., Kemp et al., 2005; Li et al., 2015). A conceptual model was previously developed of summer blooms of *K. veneficum* in Chesapeake Bay that incorporates the role of prey with a high N:P ratio originating from river inputs and a source inocula of *K. veneficum* from southern Bay waters with a lower N:P content (Lin et al., 2018). Nutrient inputs through tributaries are greatest during the high-flow period, typically starting through March to May. During this period, prey can accumulate in the tributaries and are typically characterized by high N:P ratios due to disproportionate high N loading (Fisher et al., 1992; Kemp et al., 2005). The peak in summer *K. veneficum* blooms generally occurs 1–3 months later relative to these inputs, in June through September (Li et al., 2015). In this regard, according to previous laboratory experiments, growth performance of low NP-*K. veneficum* had a two-fold increase when fed upon prey with N-rich conditions compared to same nutrient conditions of prey (Lin et al., 2017). Thus, the enhanced growth of *K. veneficum* derived from the oceanic end member of the Bay may be enhanced if they encountered prey originating from the tributaries with different patterns of nutrient loading.

With accelerating climate change, mean temperatures may rise by 2–6°C by the end of the century in all seasons for Chesapeake Bay (Muhling et al., 2018). This may expand the window for *K. veneficum* growth in several ways. Prey availability may increase due to growth stimulation at higher temperatures. Also, recent Mid-Atlantic climate projections show that warming will likely increase current interannual variability, and that

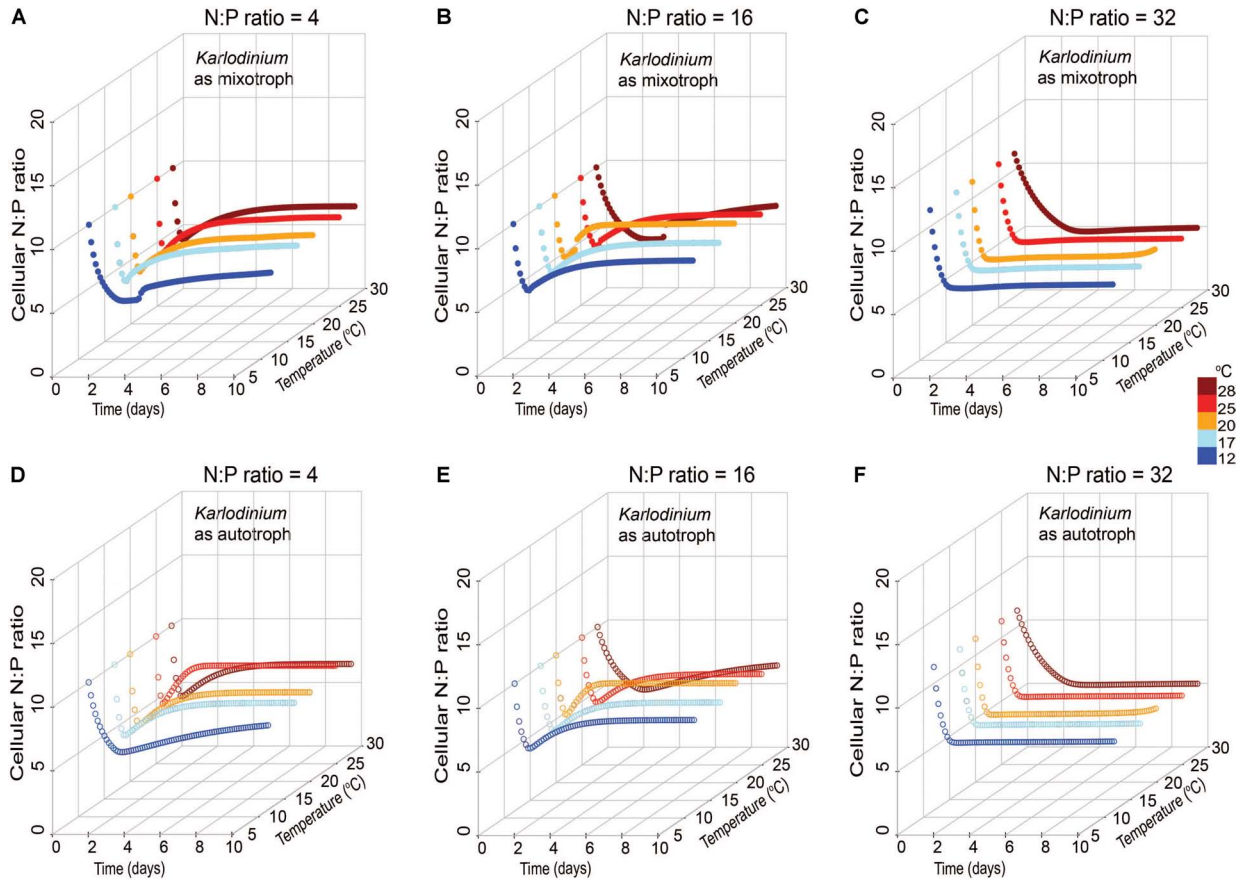

FIGURE 7 | Simulated changes in cellular N:P ratio of *Karlodinium veneficum* in mixotrophic **(A–C)** and autotrophic **(D–F)** growth under low N:P (=4), Redfield N:P (=16) and high N:P (=32) conditions, and variable temperature conditions over 10-day simulations.

winter/spring increases in precipitation are likely (e.g., Najjar et al., 2010), bringing increased N and high N:P conditions with these flows. These wetter spring conditions, with more nutrients may lead to more N-rich and/or P-deplete prey that may further support the development of these HABs. As mixotrophs may be more temperature sensitive than their autotrophic prey, the increased temperatures could enhance their ingestion capabilities and effectively control the growth of autotrophic prey (e.g., Yang et al., 2016). The modeled biomass of *K. veneficum* as a mixotroph was found to achieve the highest biomass when they consumed prey under high N:P conditions (**Figure 5**). Interestingly, the model suggests that while the highest biomass for *K. veneficum* is attained at 20°C under high N:P, and falls off rapidly above 20°C, under low N:P conditions, highest biomass is attained at 25°C. These differing temperature responses raise important questions that warrant further exploration experimentally.

Using models of mixotrophy, based on food uptake and photosynthesis measurements of *K. veneficum* and its congener, *K. armiger*, and assuming constant Redfield ratios, Berge et al. (2017) predicted succession of these species and their relative investments in autotrophy and phagotrophy. Their model suggested that nutrient uptake and high investments in photosynthesis would yield high autotrophic growth rates in spring, but increased phagotrophy in summer. In another recent model, Ghyoot et al. (2017) developed a flexible model in which a distinction was made between constitutive mixotrophs, those that synthesize and maintain their chloroplasts, and non-constitutive mixtrophs, those that acquire chloroplasts. The next important step in mixotroph modeling will be to incorporate variable nutrient stoichiometry in a model of seasonal succession of both constitutive and non-constitutive mixotrophs.

CONCLUSION

In conclusion, the current study expanded modeling of mixotrophic growth to conditions of variable stoichiometry and temperature. These simulations have highlighted the consideration of particulate prey in modeling HAB dynamics under future warming; it is insufficient to only consider dissolved nutrients. The complexities shown here in consideration of differential impacts of temperature upon the growth of mixotroph predator and prey, parallel those expected under (de)eutrophication scenarios with ocean acidification (Flynn et al., 2015). Such changes in species competitive advantage under multi-stressor environments (light, temperature, pH, nutrients)

will require a concerted effort in physiology-modeling research to conceptualize adequately to aid ecosystem management. Even though the current models are based only on bottom-up, nutrient conditions, and are focused on only one typical prey species without modeling the role of the toxic contents of *K. veneficum* in predation purpose (Sheng et al., 2010), they have provided some insight into the potential trend in HABs under future eutrophication and warming conditions.

AUTHOR CONTRIBUTIONS

C-HL and PG conceived and designed the experiments and analyzed the simulation model outputs. KF and AM developed the model structures. C-HL and KF performed the model tuning. PG contributed the experimental materials, reagents, and tools. CL wrote the paper with editorial contributions from all authors.

FUNDING

C-HL was supported by funding from the Taiwanese Government, the Bay and Rivers Fellowship from the Horn Point Laboratory, and travel support from the Ryan Saba Memorial Fellowship. Additional support for this work was provided by the National Oceanic and Atmospheric Administration National Centers for Coastal Ocean Science Competitive Research program under award no. NA17NOS4780180. This is contribution number 5519 from the University of Maryland Center for Environmental Science.

ACKNOWLEDGMENTS

This work honors the memory of a friend of C-HL, Ryan Saba.

SUPPLEMENTARY MATERIAL

The Supplementary Material for this article can be found online at: https://www.frontiersin.org/articles/10.3389/fmars.2018.00320/full#supplementary-material

REFERENCES

Adolf, J. E., Bachvaroff, T., and Place, A. R. (2008). Can cryptophyte abundance trigger toxic *Karlodinium veneficum* blooms in eutrophic estuaries? *Harmful Algae* 8, 119–128. doi: 10.1016/j.hal.2008.08.003

Adolf, J. E., Bachvaroff, T. R., Deeds, J. R., and Place, A. R. (2015). Ichthyotoxic *Karlodinium veneficum* (Ballantine) J Larsen in the upper Swan river estuary (Western Australia): ecological conditions leading to a fish kill. *Harmful Algae* 48, 83–93. doi: 10.1016/j.hal.2015.07.006

Anderson, D. M., Glibert, P. M., and Burkholder, J. M. (2002). Harmful algal blooms and eutrophication: nutrient sources, composition, and consequences. *Estuaries* 25, 704–726. doi: 10.1007/BF02804901

Baretta-Bekker, J. G., Baretta, J. W., Hansen, A. S., and Riemann, B. (1998). An improved model of carbon and nutrient dynamics in the microbial food web in marine enclosures. *Aquat. Microb. Ecol.* 14, 91–108. doi: 10.3354/ame014091

Berge, T., Chakraborty, S., Hansen, P. J., and Andersen, K. H. (2017). Modeling succession of key resource-harvesting traits of mixotrophic plankton. *ISME J.* 11, 212–223. doi: 10.1038/ismej.2016.92

Blossom, H. E., Daugbjerg, N., and Hansen, P. J. (2012). Toxic mucus traps: a novel mechanism that mediates prey uptake in the mixotrophic dinoflagellate *Alexandrium pseudogonyaulax*. *Harmful Algae* 17, 40–53. doi: 10.1016/j.hal.2012.02.010

Braarud, T. (1957). A red water organism from Walvis Bay (*Gymnodinium galatheanum* n. sp.). *Galathea Deep Sea Exped.* 1, 137–138.

Burkholder, J. M., Glibert, P. M., and Skelton, H. M. (2008). Mixotrophy, a major mode of nutrition for harmful algal species in eutrophic waters. *Harmful Algae* 8, 77–93. doi: 10.1016/j.hal.2008.08.010

Dai, X., Lu, D., Guan, W., Wang, H., He, P., Xia, P., et al. (2013). Newly recorded *Karlodinium veneficum* dinoflagellate blooms in stratified water of the East China Sea. *Deep Sea Res. II* 101, 237–243. doi: 10.1016/j.dsr2.2013.01.015

Deeds, J. R., Terlizzi, D. E., Adolf, J. E., Stoecker, D. K., and Place, A. R. (2002). Toxic activity from cultures of *Karlodinium micrum* (= *Gyrodinium galatheanum*)(Dinophyceae)—a dinoflagellate associated with fish mortalities in an estuarine aquaculture facility. *Harmful Algae* 1, 169–189. doi: 10.1016/S1568-9883(02)00027-6

Fisher, T. R., Peele, E. R., Ammerman, J. W., and Harding Jr, L. W. (1992). Nutrient limitation of phytoplankton in Chesapeake Bay. *Mar. Ecol. Prog. Ser.* 82, 51–63. doi: 10.3354/meps082051

Flynn, K. J., Mitra, A., Glibert, P. M., and Burkholder, J. M. (2018). "Mixotrophy in HABs: by whom, on whom, when, why and what next," in *Global Ecology and Oceanography of Harmful Algal Blooms*, eds P. M. Glibert, E. Berdalet, M. A. Burford, G. C. Pitcher, and M. Zhou (Cham: Springer Press), 113–132.

Flynn, K. J. (2001). A mechanistic model for describing dynamic multi-nutrient, light, temperature interactions in phytoplankton. *J. Plankt. Res.* 23, 977–997. doi: 10.1093/plankt/23.9.977

Flynn, K. J. (2005). Castles built on sand: dysfunctionality in plankton models and the inadequacy of dialogue between biologists and modellers. *J. Plankt. Res.* 27, 1205–1210. doi: 10.1093/plankt/fbi099

Flynn, K. J. (2009). Going for the slow burn: why should possession of a low maximum growth rate be advantageous for microalgae? *Plant Ecol. Divers.* 2, 179–189. doi: 10.1080/17550870903207268

Flynn, K. J. (2010). Do external resource ratios matter?: implications for modelling eutrophication events and controlling harmful algal blooms. *J. Mar. Syst.* 83, 170–180. doi: 10.1016/j.jmarsys.2010.04.007

Flynn, K. J. (2018). *Dynamic Ecology - An Introduction to the Art of Simulating Trophic Dynamics*. Swansea: Swansea University.

Flynn, K. J., Clark, D. R., Mitra, A., Fabian, H., Hansen, P. J., Glibert, P. M., et al. (2015). Ocean acidification with (de)eutrophication will alter future phytoplankton growth and succession. *Proc. R. Soc. Lond. B Biol. Sci.* 282:20142604. doi: 10.1098/rspb.2014.2604

Flynn, K. J., and Hansen, P. J. (2013). Cutting the canopy to defeat the "selfish gene"; conflicting selection pressures for the integration of phototrophy in mixotrophic protists. *Protist* 164, 811–823. doi: 10.1016/j.protis.2013.09.002

Flynn, K. J. and McGillicuddy, D. J. Jr. (2018). "Modeling marine harmful algal blooms; current status and future prospects," in *Harmful Algal Blooms: A Compendium Desk Reference*, eds. S. E. Shumway, J.-A.M. Burkholder, and S. Morton (New York, NY: Wiley Science Publishers).

Flynn, K. J., and Mitra, A. (2009). Building the "perfect beast": modelling mixotrophic plankton. *J. Plankt. Res.* 31, 965–992. doi: 10.1093/plankt/fbp044

Flynn, K. J., Stoecker, D. K., Mitra, A., Raven, J. A., Glibert, P. M., Hansen, P. J., et al. (2013). Misuse of the phytoplankton–zooplankton dichotomy: the need to assign organisms as mixotrophs within plankton functional types. *J. Plankt. Res.* 35, 3–11. doi: 10.1093/plankt/fbs062

Fu, F. X., Tatters, A. O., and Hutchins, D. A. (2012). Global change and the future of harmful algal blooms in the ocean. *Mar. Ecol. Prog. Ser.* 470, 207–233. doi: 10.3354/meps10047

Ghyoot, C., Flynn, K. J., Mitra, A., Lancelot, C., and Gypens, N. (2017). Modeling plankton mixotrophy: a mechanistic model consistent with the Shuter-type biochemical approach. *Front. Ecol. Evol.* 5:78. doi: 10.3389/fevo.2017.00078

Glibert, P. M. (2017). Eutrophication, harmful algae and biodiversity—challenging paradigms in a world of complex nutrient changes. *Marine Poll. Bull.* 124, 591–606. doi: 10.1016/j.marpolbul.2017.04.027

Glibert, P. M., Allen, J. I., Bouwman, A. F., Brown, C. W., Flynn, K. J., Lewitus, A. J., et al. (2010). Modeling of HABs and eutrophication: status, advances, challenges. *J. Mar. Syst.* 83, 262–275. doi: 10.1016/j.jmarsys.2010.05.004

Glibert, P. M., and Burford, M. A. (2017). Globally changing nutrient loads and harmful algal blooms: recent advances, new paradigms, and continuing challenges. *Oceanography* 30, 58–69. doi: 10.5670/oceanog.2017.110

Glibert, P. M., and Burkholder, J. M. (2011). Harmful algal blooms and eutrophication: "strategies" for nutrient uptake and growth outside the Redfield comfort zone. *Chin. J. Oceanogr. Limnol.* 29, 724–738.doi: 10.1007/s00343-011-0502-z

Glibert, P. M., and Burkholder, J. M. (2018). "Causes of harmful algal blooms," in *Harmful Algal Blooms: A Compendium Desk Reference*, eds S. Shumway, J. M. Burkholder, and S. L. Morton (West Sussex: Wiley Press), 1–21.

Glibert, P. M., Heil, C. A., Wilkerson, F. P., and Dugdale, R. C. (2018). "Nutrients and harmful algal blooms: dynamic kinetics and flexible nutrition," in *Global Ecology and Oceanography of Harmful Algal Blooms*, eds P. M. Glibert, E. Berdalet, M. A. Burford, G. C. Pitcher, and M. Zhou (Cham: Springer Press), 93–112.

Glibert, P. M., Seitzinger, S., Heil, C. A., Burkholder, J. M., Parrow, M. W., Codispoti, L. A., et al. (2005). The role of eutrophication in the global proliferation of harmful algal blooms. *Oceanography* 18, 198–209. doi: 10.5670/oceanog.2005.54

Glibert, P. M., and Terlizzi, D. E. (1999). Cooccurrence of elevated urea levels and dinoflagellate blooms in temperate estuarine aquaculture ponds. *Appl. Environ. Microbiol.* 65, 5594–5596.

Guillard, R. R. (1975). "Culture of phytoplankton for feeding marine invertebrates," in *Culture of Marine Invertebrate Animals*, eds W. L. Smith and M. H. Chanley (New York, NY: Plenum Press), 29–60.

Haefner, J. W. (2005). *Modeling Biological Systems: Principles and Applications*. Berlin: Springer Science & Business Media.

Hallegraeff, G. M. (2010). Ocean climate change, phytoplankton community responses, and harmful algal blooms: a formidable predictive challenge1. *J. Phycol.* 46, 220–235. doi: 10.1111/j.1529-8817.2010.00815.x

Heisler, J., Glibert, P. M., Burkholder, J. M., Anderson, D. M., Cochlan, W., Dennison, W. C., et al. (2008). Eutrophication and harmful algal blooms: a scientific consensus. *Harmful Algae* 8, 3–13. doi: 10.1016/j.hal.2008.08.006

Jakobsen, H. H., and Hansen, P. J. (1997). Prey size selection, grazing and growth response of the small heterotrophic dinoflagellate *Gymnodinium* sp. and the ciliate *Balanion comatum*—a comparative study. *Mar. Ecol. Prog. Ser.* 158, 75–86. doi: 10.3354/meps158075

Jeong, H. J., Park, J. Y., Nho, J. H., Park, M. O., Ha, J. H., Seong, K. A., et al. (2005a). Feeding by red-tide dinoflagellates on the cyanobacterium *Synechococcus*. *Aquat. Microb. Ecol.* 41, 131–143. doi: 10.3354/ame041131

Jeong, H. J., Yoo, Y. D., Park, J. Y., Song, J. Y., Kim, S. T., Lee, S. H., et al. (2005b). Feeding by phototrophic red-tide dinoflagellates: five species newly revealed and six species previously known to be mixotrophic. *Aquat. Microb. Ecol.* 40, 133–150. doi: 10.3354/ame040133

Jost, C., Lawrence, C. A., Campolongo, F., Van de Bund, W., Hill, S., and DeAngelis, D. L. (2004). The effects of mixotrophy on the stability and dynamics of a simple planktonic food web model. *Theor. Popul. Biol.* 66, 37–51. doi: 10.1016/j.tpb.2004.02.001

Kemp, W., Boynton, W., Adolf, J., Boesch, D., Boicourt, W., Brush, G., et al. (2005). Eutrophication of Chesapeake Bay: historical trends and ecological interactions. *Mar. Ecol. Prog. Ser.* 303, 1–29. doi: 10.3354/meps303001

Kempton, J. W., Lewitus, A. J., Deeds, J. R., Law, J. M., and Place, A. R. (2002). Toxicity of *Karlodinium micrum* (Dinophyceae) associated with a fish kill in a South Carolina brackish retention pond. *Harmful Algae* 1, 233–241. doi: 10.1016/S1568-9883(02)00015-X

Kimmance, S. A., Atkinson, D., and Montagnes, D. J. S. (2006). Do temperature–food interactions matter? Responses of production and its components in the model heterotrophic flagellate *Oxyrrhis marina*. *Aquat. Microb. Ecol.* 42, 63–73. doi: 10.3354/ame042063

Li, A., Stoecker, D. K., and Adolf, J. E. (1999). Feeding, pigmentation, photosynthesis and growth of the mixotrophic dinoflagellate *Gyrodinium galatheanum*. *Aquat. Microb. Ecol.* 19, 163–176. doi: 10.3354/ame019163

Li, A., Stoecker, D. K., and Coats, D. W. (2000). Mixotrophy in *Gyrodinium galatheanum* (Dinophyceae): grazing responses to light intensity and inorganic nutrients. *J. Phycol.* 36, 33–45. doi: 10.1046/j.1529-8817.2000.98076.x

Li, J., Glibert, P. M., and Gao, Y. (2015). Temporal and spatial changes in Chesapeake Bay water quality and relationships to *Prorocentrum* minimum, *Karlodinium veneficum*, and CyanoHAB events, 1991–2008. *Harmful Algae* 42, 1–14. doi: 10.1016/j.hal.2014.11.003

Lin, C.-H., Accoroni, S., and Glibert, P. M. (2017). *Karlodinium veneficum* feeding responses and effects on larvae of the eastern oyster *Crassostrea virginica* under variable nitrogen: phosphorus stoichiometry. *Aquat. Microb. Ecol.* 79, 101–114. doi: 10.3354/ame01823

Lin, C.-H., Lyubchich, V., and Glibert, P. M. (2018). Time series models of decadal trends in the harmful algal species *Karlodinium veneficum* in Chesapeake Bay. *Harmful Algae* 73, 110–118. doi: 10.1016/j.hal.2018.02.002

Lundgren, V. M., Glibert, P. M., Granéli, E., Vidyarathna, N. K., Fiori, E., Ou, L., et al. (2016). Metabolic and physiological changes in *Prymnesium parvum* when grown under, and grazing on prey of, variable nitrogen: phosphorus stoichiometry. *Harmful Algae* 55, 1–12. doi: 10.1016/j.hal.2016.01.002

Menden-Deuer, S., and Lessard, E. J. (2000). Carbon to volume relationships for dinoflagellates, diatoms, and other protist plankton. *Limnol. Oceanogr.* 45, 569–579. doi: 10.4319/lo.2000.45.3.0569

Mitra, A. (2006). A multi-nutrient model for the description of stoichiometric modulation of predation in micro-and mesozooplankton. *J. Plankt. Res.* 28, 597–611. doi: 10.1093/plankt/fbi144

Mitra, A., and Flynn, K. J. (2005). Predator–prey interactions: is 'ecological stoichiometry'sufficient when good food goes bad? *J. Plankt. Res.* 27, 393–399. doi: 10.1093/plankt/fbi022

Mitra, A., and Flynn, K. J. (2006). Accounting for variation in prey selectivity by zooplankton. *Ecol. Model.* 199, 82–92. doi: 10.1016/j.ecolmodel.2006.06.013

Mitra, A., and Flynn, K. J. (2010). Modelling mixotrophy in harmful algal blooms: more or less the sum of the parts? *J. Mar. Syst.* 83, 158–169. doi: 10.1016/j.jmarsys.2010.04.006

Mitra, A., Flynn, K. J., Burkholder, J., Berge, T., Calbet, A., Raven, J. A., et al. (2014). The role of mixotrophic protists in the biological carbon pump. *Biogeosciences* 10, 13535–13562. doi: 10.5194/bg-11-995-2014

Mitra, A., Flynn, K. J., Tillmann, U., Raven, J. A., Caron, D., Stoecker, D. K., et al. (2016). Defining planktonic protist functional groups on mechanisms for energy and nutrient acquisition: incorporation of diverse mixotrophic strategies. *Protist* 167, 106–120. doi: 10.1016/j.protis.2016.01.003

Montagnes, D. J. S., Kimmance, S. A., and Atkinson, D. (2003). Using Q10: can growth rates increase linearly with temperature? *Aquat. Microb. Ecol.* 32, 307–313. doi: 10.3354/ame032307

Moore, S. K., Johnstone, J. A., Banas, N. S., and Salathe, E. P. Jr. (2015). Present-day and future climate pathways affecting *Alexandrium* blooms in Puget Sound, WA, USA. *Harmful Algae* 48, 1–11. doi: 10.1016/j.hal.2015.06.008

Muhling, B. A., Gaitán, C. F., Stock, C. A., Saba, V. S., Tommasi, D., and Dixon, K. W. (2018). Potential salinity and temperature futures for the Chesapeake Bay using a statistical downscaling spatial disaggregation framework. *Estuar. Coast.* 41, 349–372. doi: 10.1007/s12237-017-0280-8

Najjar, R. G., Pyke, C. R., Adams, M. B., Breitburg, D., Hershner, C., Kemp, M., et al. (2010). Potential climate-change impacts on the Chesapeake Bay. *Estuar. Coast. Shelf. Sci.* 86, 1–20. doi: 10.1016/j.ecss.2009.09.026

Nielsen, M. V. (1993). Toxic effect of the marine dinoflagellate *Gymnodinium galatheanum* on juvenile cod *Gadus morhua*. *Mar. Ecol. Prog. Ser.* 93, 273–277. doi: 10.3354/meps095273

Peñuelas, J., Sardans, J., Rivas-ubach, A., and Janssens, I. A. (2012). The human-induced imbalance between C, N and P in Earth's life system. *Glob. Change Biol.* 18, 3–6. doi: 10.1111/j.1365-2486.2011.02568.x

Place, A. R., Bowers, H. A., Bachvaroff, T. R., Adolf, J. E., Deeds, J. R., and Sheng, J. (2012). *Karlodinium veneficum* —the little dinoflagellate with a big bite. *Harmful Algae* 14, 179–195. doi: 10.1016/j.hal.2011.10.021

Sheng, J., Malkiel, E., Katz, J., Adolf, J. E., and Place, A. R. (2010). A dinoflagellate exploits toxins to immobilize prey prior to ingestion. *Proc. Natl. Acad. Sci. U.S.A.* 107, 2082–2087. doi: 10.1073/pnas.0912254107

Stickney, H. L., Hood, R. R., and Stoecker, D. K. (2000). The impact of mixotrophy on planktonic marine ecosystems. *Ecol. Model.* 125, 203–230. doi: 10.1146/annurev-marine-010816-060617

Stoecker, D. K. (1998). Conceptual models of mixotrophy in planktonic protists and some ecological and evolutionary implications. *Eur. J. Protistol.* 34, 281–290. doi: 10.1016/S0932-4739(98)80055-2

Stoecker, D. K., Adolf, J. E., Place, A. R., Glibert, P. M., and Meritt, D. W. (2008). Effects of the dinoflagellates *Karlodinium veneficum* and *Prorocentrum* minimum on early life history stages of the eastern oyster (*Crassostrea virginica*). *Mar. Biol.* 154, 81–90. doi: 10.1007/s00227-007-0901-z

Stoecker, D. K., Hansen, P. J., Caron, D. A., and Mitra, A. (2017). Mixotrophy in the marine plankton. *Annu. Rev. Mar. Sci.* 9, 311–335. doi: 10.1146/annurev-marine-010816-060617

Sutton, M. A., Bleeker, A., Howard, C. M., Erisman, J. W., Abrol, Y. P., Bekunda, M., et al. (2013). *Our Nutrient World. The Challenge to Produce More Food and Energy with Less Pollution*. Edinburgh: Centre for Ecology & Hydrology.

Thingstad, T. F., Havskum, H., Garde, K., and Riemann, B. (1996). On the strategy of "eating your competitor": a mathematical analysis of algal mixotrophy. *Ecology* 77, 2108–2118. doi: 10.2307/2265705

Våge, S., Castellani, M., Giske, J., and Thingstad, T. F. (2013). Successful strategies in size structured mixotrophic food webs. *Aquat. Ecol.* 47, 329–347. doi: 10.1007/s10452-013-9447-y

Van Dolah, F. M. (2000). Marine algal toxins: origins, health effects, and their increased occurrence. *Environ. Health Perspect.* 108, 133–141.

Ward, B. A., Dutkiewicz, S., Barton, A. D., and Follows, M. J. (2011). Biophysical aspects of resource acquisition and competition in algal mixotrophs. *Am. Nat.* 178, 98–112. doi: 10.1086/660284

Ward, B. A., and Follows, M. J. (2016). Marine mixotrophy increases trophic transfer efficiency, mean organism size, and vertical carbon flux. *Proc. Natl. Acad. Sci. U.S.A.* 113, 2958–2963. doi: 10.1073/pnas.1517118113

Wells, M. L., Trainer, V. L., Smayda, T. J., Karlson, B. S. O., Trick, C. G., Kudela, R. M., et al. (2015). Harmful algal blooms and climate change: learning from the past and present to forecast the future. *Harmful Algae* 49, 68–93. doi: 10.1016/j.hal.2015.07.009

Wilken, S., Huisman, J., Naus-Wiezer, S., and Donk, E. (2013). Mixotrophic organisms become more heterotrophic with rising temperature. *Ecol. Lett.* 16, 225–233. doi: 10.1111/ele.12033

Yang, Z., Zhang, L., Zhu, X., Wang, J., and Montagnes, D. J. S. (2016). An evidence-based framework for predicting the impact of differing autotroph-heterotroph thermal sensitivities on consumer–prey dynamics. *ISME J.* 10, 1767–1778. doi: 10.1038/ismej.2015.225

Zhou, C., Fernández, N., Chen, H., You, Y., and Yan, X. (2011). Toxicological studies of *Karlodinium micrum* (Dinophyceae) isolated from East China Sea. *Toxicon* 57, 9–18. doi: 10.1016/j.toxicon.2010.08.014

Conflict of Interest Statement: The authors declare that the research was conducted in the absence of any commercial or financial relationships that could be construed as a potential conflict of interest.

The handling Editor declared a past co-authorship with the authors KF and PG.

frontiers in Marine Science

REVIEW
published: 22 August 2018
doi: 10.3389/fmars.2018.00292

Mixotrophic Plankton in the Polar Seas: A Pan-Arctic Review

Diane K. Stoecker[1]* *and Peter J. Lavrentyev*[2]

[1] Horn Point Laboratory, University of Maryland Center for Environmental Science, Cambridge, MD, United States,
[2] Department of Biology, University of Akron, Akron, OH, United States

Polar marine ecosystems are characterized by low water temperatures, sea ice cover, and extreme annual variation in solar irradiance and primary productivity. A review of the available information from the Arctic suggests that mixotrophy (i.e., the combination of photosynthetic and phagotrophic modes of nutrition in one cell) is wide spread among plankton. In the central Arctic Ocean (AO) in summer, mixotrophic flagellates such as *Micromonas* and *Dinobryon* can account for much of bacterivory. Planktonic ciliates with acquired phototrophy form the bulk of microzooplankton biomass in both the ultra-oligotrophic deep basins of AO and its productive shelf seas. With the exception of the diatom bloom in the marginal ice zone, mixotrophic ciliates often dominate total chlorophyll in the mixed layer in summer taking advantage of the 24-h insolation. Their relatively high growth rates at low temperatures indicate that they are an important component of primary and secondary production. The key Arctic copepod species preferentially feed on chloroplast-bearing ciliates, which form an important link in the planktonic food web. The limited available year round data indicate that mixotrophic plankton persist in the water column during the long polar winter when irradiance is low or absent and ice cover further reduces light penetration. These observations suggest that at high latitudes an alternative food web based on mixotrophy may dominate the pelagic lower food web during much of the year.

Keywords: mixotrophy, Arctic plankton, mixotrophic flagellates, mixotrophic ciliates, Arctic Ocean

OPEN ACCESS

Edited by:
Holly V. Moeller,
University of California, Santa Barbara, United States

Reviewed by:
Rebecca Gast,
Woods Hole Oceanographic Institution, United States
Suzanne Strom,
Western Washington University, United States

***Correspondence:**
Diane K. Stoecker
stoecker@umces.edu

Specialty section:
This article was submitted to Marine Ecosystem Ecology, a section of the journal Frontiers in Marine Science

Received: *02 April 2018*
Accepted: *30 July 2018*
Published: *22 August 2018*

Citation:
Stoecker DK and Lavrentyev PJ (2018) Mixotrophic Plankton in the Polar Seas: A Pan-Arctic Review. Front. Mar. Sci. 5:292. doi: 10.3389/fmars.2018.00292

INTRODUCTION

Mixotrophy, defined as the combination of phagotrophy and photosynthesis in an individual cell, is increasingly recognized as an important trophic mode among planktonic protists, both "phytoplankton" and "microzooplankton," in the global ocean (reviewed in Caron, 2017; Leles et al., 2017; Selosse et al., 2017; Stoecker et al., 2017) but in polar waters mixotrophy has not received much attention. In fact, this mixed mode of nutrition is so wide-spread that the above dichotomy may be no longer suitable for an accurate description of the role of unicellular eukaryotes in the ocean (Flynn et al., 2013). Ecosystem models that include mixotrophy indicate that this trophic mode has profound effects on biogeochemical cycling, including increasing carbon fixation, decreasing loss of dissolved organic carbon and increasing vertical carbon flux (Mitra et al., 2014; Ward and Follows, 2016). Mixotrophy also influences the structure and function of food webs. Modeling indicates that mixotrophy can increase mean organism size and trophic transfer, potentially resulting in increased production at upper levels in the food web (Mitra et al., 2014; Ward and Follows, 2016).

It is particularly important to understand the effects of mixotrophy in the Arctic because its marine environment is changing rapidly. The Arctic Ocean may have lost over 50% of its sea ice volume (Kwok and Rothrock, 2009), with the largest decreases in the Barents, Kara, and Siberian sectors, particularly over the continental shelf (Pabi et al., 2008). In just 12 years, the open-water growing season has increased by 45 days, promoting a pan-Arctic 20% increase in net primary production (Brown and Arrigo, 2012). Climate change is causing a patchwork of altered environmental conditions in the Arctic. Decreases in sea ice thickness, extensions in the length of the ice free season, increased water temperatures, and freshening have led to increased stratification in some seas, whereas increased mixing due to storms have been observed in other areas (Metfies et al., 2016; Blais et al., 2017; Oziel et al., 2017). Although the rising trend in primary production (Slagstad et al., 2011) may be hindered by stronger stratification and nutrient limitation in offshore areas (Ardyna et al., 2011, 2017; Brown and Arrigo, 2012), these changes are expected to bolster the pelagic system at the expense of the benthic components, with profound impacts on trophic structure and carbon fluxes (Wassmann and Reigstad, 2011). Recent studies in the Arctic indicate that a major portion of pelagic primary production is channeled to the higher trophic levels through unicellular grazers such as ciliates and dinoflagellates (Olson and Strom, 2002; Verity et al., 2002; Calbet et al., 2011b; Sherr et al., 2013; Stoecker et al., 2014; Franzè and Lavrentyev, 2017). This warrants investigation of the effects of climate change on microbial plankton as even minor effects at the base of food webs could be amplified through trophic chains (Sarmento et al., 2010). Given the rapid changes in Arctic ecosystems, it is increasingly important to determine the trophic modes of plankton in Arctic seas and predict how trophic modes may change with the environment and how this may affect ecosystem processes.

The Objectives and Material

Few attempts have been made to directly examine the physiological rates of mixotrophic plankton in the Arctic due to logistical and methodological constraints (Putt, 1990; Sanders and Gast, 2012; Franzè and Lavrentyev, 2014). Nevertheless, there is evidence in the literature that mixotrophic plankton play an important role(s) in the Arctic marine ecosystems. Our objectives are to review existing data, identify data gaps, and present hypotheses about the roles of mixotrophy in Arctic Seas and how these may be altered due to changes in the physical environment.

In this review we primarily focus on the following contrasting regions of the Arctic: the deep oligotrophic Canada Basin of the Arctic Ocean, the relatively shallow and productive Barents and Kara shelf seas, and the main entrance for the Atlantic water into the Arctic Ocean, the Fram Strait (**Figure 1**). In addition we consider data from the productive shelf of the sub-Arctic Bering Sea, which has been subjected to similar climatic changes as the Arctic shelf seas (Hunt and Megrey, 2005). Each of the above polar regions is unique in terms of bathymetry, circulation, sea-ice cover, and food webs (Carmack and Wassmann, 2006). Thus, they are ideally suited for a pan-Arctic comparison.

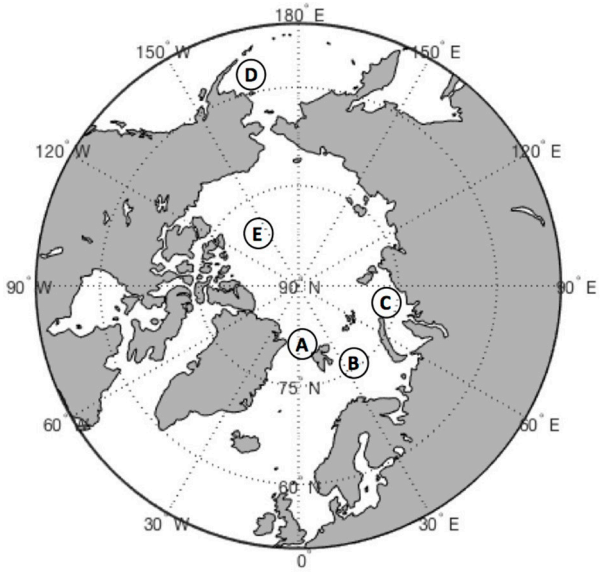

FIGURE 1 | Map of the Arctic Ocean showing the main study locations: A, Fram Strait; B, Barents Sea; C, Kara Sea; D, Bering Sea; E, Canada Basin.

REVIEW

Evidence for Mixotrophy Among Arctic Plankton

Although mixotrophy among planktonic protists is well documented in temperate and tropical waters, less is known about mixotrophy in Arctic seas. Phagotrophy by phytoflagellates is usually underestimated, particularly in remote locations such as the Arctic, where field experiments are logistically difficult or which are difficult to sample in all seasons. Ingestion of prey by small, pigmented cells is difficult to detect and is often underestimated, even in experimental studies designed to measure it (Anderson et al., 2017). Ciliates with plastids are more readily distinguished from heterotrophs than phagotrophic phytoflagellates from strict autotrophs. Measurements of feeding and photosynthesis in both mixotrophic flagellates and ciliates are rare. However, there are ample reasons to hypothesize that mixotrophy is common among Arctic plankton. Below we list mixotrophic flagellate and ciliate taxa reported from Arctic Seas and provide evidence that the taxa are mixotrophic. The evidence for mixotrophy ranges from observation of food vacuoles or plastids in preserved specimens to field or laboratory measurements of feeding and photosynthesis. For some species the evidence is very limited, whereas other species have been studied intensively. For well-studied species, we have included only a few key references.

Chrysophyta

Arctic plankton assemblages include nanoplanktonic chrysophytes such as *Ochromonas* spp. that are often bacterivorous as well as photosynthetic (Estep et al., 1986; Andersson et al., 1989; Keller et al., 1994). The colonial

chrysophyte, *Dinobryon balticum*, is a common component of the microplankton in Arctic and sub-Arctic seas (**Table 1**) and is often associated with low irradiance and the deep chlorophyll maximum (DCM) layer (McKenzie et al., 1995). The colonies are a significant contributor to particle flux during summer in the Barents Sea (Olli et al., 2002) and probably other coastal Arctic seas. Although *D. balticum* has plastids and requires light, this species supplements it nutrition with bacterivory (McKenzie et al., 1995).

Cryptophyta

Cryptophytes are another algal group often associated with low light conditions and that are known to contribute to bacterivory (**Table 1**). In phytoplankton investigations and *in situ* studies of phagotrophy by algae, cryptophytes have rarely been identified to species. *Teleaulax amphioxeia*, a widespread species found in temperate and Arctic waters (**Table 1**) has been shown to be mixotrophic (Yoo et al., 2017).

Haptophyta (Prymnesiophyta)

Although many haptophytes are mixotrophic and often dominate the mixotrophic phytoplankton assemblage in temperate waters (Unrein et al., 2014), the dominant haptophyte in Arctic waters, *Phaeocystis pouchetii*, is yet to be shown to be phagotrophic. Another photosynthetic prymnesiophyte genus found in Arctic water is *Chrysochromulina* (**Table 1**). At low irradiances, feeding can enhance growth in some *Chrysochromulina* species (Hansen and Hjorth, 2002).

Chlorophyta

A well-documented case of mixotrophy among Arctic chlorophyte flagellates is bacterivory by *Micromonas* sp. This picoplankton-sized member of the Prasinophyceae is widely distributed and abundant in the Arctic (Not et al., 2005). During autumn, when the Beaufort Sea and Canada Basin were highly oligotrophic, photosynthetic picoflagellates numerically dominated the phytoplankton and accounted for as much or sometimes more bacterivory than heterotrophic flagellates (Sanders and Gast, 2012). Genetic analysis indicated that *Micromona*s was a common and probably abundant component of the picoflagellate assemblage (Sanders and Gast, 2012). In laboratory experiments with a culture of Arctic *Micromonas*, McKie-Krisberg and Sanders (2014) observed the greatest bacterivory under conditions of high light and inorganic nutrient limitation, conditions similar to the oligotrophic polar seas in summer.

Dinophyta

Dinoflagellates possess feeding structures that allow them to consume prey of equal to or greater than their own cell size. Most plastidic dinoflagellates are probably mixotrophic (reviewed in Jeong et al., 2010; Hansen, 2011). Mixotrophic as well as heterotrophic dinoflagellates are common in the Arctic (**Table 1**). Nanoplanktonic dinoflagellates have often been overlooked, but they appear to be important components of the polar plankton. For example, plastidic nano-sized gymnodiniids formed 55–85% of total dinoflagellate abundance in the Barents Sea (Franzè and Lavrentyev, 2017). Among the small size mixotrophic dinoflagellates are *Karlodinium* and small *Gymnodinium*-like spp. Some taxa, like *Karlodinium*, can ingest prey most of the time although inorganic nutrient limitation often stimulates feeding (Li et al., 1999, 2000; Calbet et al., 2011a). A small photosynthetic dinoflagellate that occurs in the Arctic as well as in temperate low salinity waters is *Heterocapsa rotundata* (**Table 1**). In temperate waters it blooms in winter and is stimulated to feed by light limitation (Millette et al., 2017). *H. rotundata* may be an important mixotrophic alga in low salinity, turbid waters, such as the coastal Beaufort Sea and Kara Sea. Among the larger thecate photosynthetic dinoflagellates, many species have been observed to capture and digest prey about their own size or larger, including diatoms, other flagellates, and ciliates (reviewed in Hansen, 2011). This group includes *Alexandrium* and *Tripos (formerly Ceratium)* spp. that have been observed in the Arctic (**Table 1**). Mixotrophic *Dinophysis* spp. prey on ciliates and obtain their plastids from ingestion of photosynthetic *Mesodinium* spp. (Park et al., 2006; Hansen, 2011) and are reported in Arctic Seas (**Table 1**).

Ciliophora

Phagotrophic protists that feed on phytoplankton can also be mixotrophic due to acquired phototrophy; among marine ciliates this usually involves sequestration of plastids and sometimes other organelles from their algal prey (reviewed in Stoecker et al., 2009). In field studies, presence of plastids in ciliates is easier to recognize than phagotrophy in phytoplankton. Epifluorescence microscopy is used to detect the chlorophyll (plastids) in fresh or aldehyde fixed samples that have been stored under conditions (refrigeration and darkness) that minimize chlorophyll degradation. However, many field studies of microzooplankton rely solely on acid Lugol's fixed samples. Thus, mixotrophy among the ciliates often is overlooked.

Among the oligotrich ciliates, plastid-retention is a species-specific attribute. In investigations that lack data from epifluorescence microscopy, the presence of certain species is a good indicator of mixotrophy among the oligotrichs. *Laboea strobila*, a very distinctive plastid-retaining species, several plastidic *Strombidium* spp. and *Tontonia* spp. which always seem to be plastidic, are reported from many Arctic Seas (**Table 2**). In addition, several plastidic prostomatid and haptorid ciliates such as *Askenasia*, *Cyclotrichium*, *Didinium*, *Prorodon,* and *Urotricha* occur in ice-covered waters and open waters of the Barents Sea and Kara Sea (Lavrentyev, 2012; Franzè and Lavrentyev, 2014, 2017). In field studies in which epifluorescence microscopy is utilized, plastid-retaining oligotrichs usually comprise 30–40% of the oligotrich assemblage in the euphotic zone (Stoecker et al., 2017), but in the Arctic they often dominate the ciliate assemblage (**Table 3**).

Contributions of mixotrophic ciliates to chlorophyll are highly variable even in ecosystems in which they are abundant (**Table 3**), partially because of the large variations in total chlorophyll *a*. Putt (1990) estimated that mixotrophic ciliates contributed ∼15% of the total chlorophyll *a* at 2 m in the Barents Sea. In the deep chlorophyll maximum (DCM) of the Barents Sea, Franzè and Lavrentyev (2017) estimated that mixotrophic ciliates (predominantly plastidic oligotrichs) contributed between 0.5 and 46% of the chlorophyll *a*. The contribution of mixotrophs to ciliate abundance and

TABLE 1 | Common mixotrophic flagellates in the Arctic.

Taxa	Arctic regions	Evidence for mixotrophy
CHRYSOPHYTA		
Ochromonas crenata, Ochromonas marina, Ochromonas sp.	Barents Sea (Olli et al., 2002; Franzè and Lavrentyev, 2017); Kongsfjorden, Svalbard (Iversen and Seuthe, 2011)	Ingestion of prey (Estep et al., 1986; Andersson et al., 1989); Ingestion of fluorescently labeled bacteria (Keller et al., 1994)
Dinobryon balticum	Barents Sea (Olli et al., 2002; Rat'kova and Wassmann, 2002); Kongsfjorden, Svalvard (Keck et al., 1999; Iversen and Seuthe, 2011); Beaufort Sea (Ardyna et al., 2017); Arctic Ocean NW of Svalbard (Johnsen et al., 2018)	Ingestion of beads (McKenzie et al., 1995)
CRYPTOPHYTA		
	Kongsfjorden, Svalvard (Iversen and Seuthe, 2011); SE Bering Sea (Olson and Strom, 2002); Beaufort Sea (Ardyna et al., 2017); Barents Sea (Rat'kova and Wassmann, 2002; Franzè and Lavrentyev, 2017); Arctic Ocean NW of Svalbard (Johnsen et al., 2018)	Ingestion of beads by *Geminigera cryophilia* (McKie-Krisberg et al., 2015); Ingestion of prey by *Teleaulax amphioxeia* (Yoo et al., 2017); Ingestion of bacteria (Unrein et al., 2007, 2014)
HAPTOPHYTA		
Chrysochromulina spp.	Beaufort Sea (Ardyna et al., 2017)	Ingestion of prey (Jones et al., 1993)
CHLOROPHYTA		
Pyramimonas spp.	Beaufort Sea (Estrada et al., 2009; Ardyna et al., 2017); Arctic Ocean NW of Svalbard (Johnsen et al., 2018)	Ingestion of beads by *P. tychotreta* (McKie-Krisberg et al., 2015)
Micromonas spp.	Barents Sea (Not et al., 2005; Franzè and Lavrentyev, 2017); Beaufort Sea (Estrada et al., 2009); Beaufort Sea & Canada Basin (Sanders and Gast, 2012); Central Arctic Ocean, Fram Strait (Metfies et al., 2016)	Ingestion of fluorescently labeled bacteria and beads (Sanders and Gast, 2012); Ingestion of beads (McKie-Krisberg and Sanders, 2014)
DINOPHYTA		
Alexandrium tamarense	Chukchi Sea (Yokoi et al., 2016)	Ingestion of small phytoplankton (Jeong et al., 2005); Ingestion of *Skeletonema costatum* (Yoo et al., 2009)
Dinophysis acuminata, D. norvegica	Kongsfjorden, Svalbard (Seuthe et al., 2011a); Barents Sea (Franzè and Lavrentyev, 2014, 2017)	Photosynthetic *Dinophysis* spp. obtain plastids and other organelles from ciliate prey (reviewed in Hansen, 2011; Stoecker et al., 2017)
Heterocapsa triquetra, H. rotundata	Beaufort Sea (Ardyna et al., 2017)	*H. triquetra*, ingestion of bacteria (Legrand et al., 1998); *H. triquetra* & *H. rotundata* ingestion of prey (Jeong et al., 2005); *H. rotundata* ingestion of beads & bacteria (Millette et al., 2017)
Karlodinium veneficum (syn. Karlodinium micrum, Gyrodinium galatheanum)	Kongfjorden, Svalbard (Seuthe et al., 2011a)	Ingestion of cryptophytes (Li et al., 1999, 2000; Calbet et al., 2011a)
Prorocentrum minimum	Chukchi Sea (Yokoi et al., 2016)	Ingestion of cryptophytes (Johnson, 2015)
Tripos arcticus (syn. *Ceratium arcticum, C. longipes*), *Tripos fusus* (syn. *C. fusus*), *Tripos macroceros* (syn. *C. macroceros*)	Kongsfjorden, svalbard (Seuthe et al., 2011a); Barents Sea (Franzè and Lavrentyev, 2014, 2017); Kara Sea (Lavrentyev, 2012)	*T. arcticus,* observation of food vacuoles with ingested prey (Jacobson and Anderson, 1996)

total chlorophyll *a* peaked at the Polar Front primarily due to populations of the large mixotrophic oligotrichs *L. strobila, Strombidium conicum*, and *S. wulffi* (**Figure 2**). In the productive eastern Bering Sea during summer, mixotrophic ciliates abundance (also predominantly plastid oligotrichs) and their estimated contribution to total chlorophyll *a* was also very variable. The contribution of mixotrophs to ciliate abundance was relatively low at stations near the shelf edge and in upwelling around the Pribilof Islands. However, mixotrophic ciliate abundance was greatest and estimated contribution of ciliates to total chlorophyll was often 50% or more in highly stratified waters in the middle of the northern shelf (Stoecker et al., 2014). Similarly, in the shallow waters of the Kara Sea, mixotrophic ciliates were responsible for up to 46% of total chlorophyll *a* (Lavrentyev, 2012). In the western Fram Strait, mixotrophic oligotrichs formed a spring bloom in the mixed layer within the Atlantic Drift ($>200\ \mu g\ C\ L^{-1}$, Lavrentyev and Franzè, 2017); this is the highest ciliate biomass recorded so far in the Arctic.

The above estimates of mixotrophic contributions are conservative. Mixotrophic chlorophyll *a* content was calculated based on ciliate volume (Montagnes et al., 1994), assuming that the volume to chlorophyll *a* relationship is similar to that in autotrophic plankton (Dolan and Perez, 2000). The chlorophyll *a* cellular quota calculated based on these assumptions for *S. conicum* (30,000 μm^3, 55 pg chlorophyll $cell^{-1}$) was similar to that measured directly in the Barents Sea (48 pg chlorophyll *a* $cell^{-1}$, Putt, 1990). However, oligotrich chlorophyll *a* content can be much higher (Stoecker et al., 1988; McManus et al., 2012). Laboratory and field studies have demonstrated that plastidic ciliates graze on pico- and nano-phytoplankton, can have about the same biovolume specific chlorophyll *a* content

TABLE 2 | Common mixotrophic ciliates in the Arctic.

Ciliophora	Arctic regions	Evidence for mixotrophy
Laboea strobila	Iceland/Greenland Seas & N. Svalbard/Barents Sea (Putt, 1990); Greenland Sea (Möller et al., 2006); W. Arctic Ocean (Lovejoy et al., 2002, 2007; Sherr et al., 2009); East Siberian Sea & Chukchi Sea (Jiang et al., 2015); Disko Bay, Greenland (Levinsen et al., 2000a); Eastern Bering Sea (Olson and Strom, 2002; Strom and Fredrickson, 2008; Stoecker et al., 2014); Barents Sea (Rat'kova and Wassmann, 2002; Franzè and Lavrentyev, 2014, 2017); Kara Sea (Lavrentyev, 2012)	Detection of plastids with epifluorescence microscopy, measurement of chlorophyll *a* /ciliate (Putt, 1990); Measurement of chlorophyll *a*/ciliate and photosynthesis in cultures (Stoecker et al., 1988); Detection of plastids with epifluorescence microscopy (Franzè and Lavrentyev, 2014)
Mesodinium rubrum/M. major (syn. *Myrionecta rubra*)	Iceland/Greenland Seas & N Svalbard/Barents Sea (Putt, 1990); Barents Sea (Hansen et al., 1996; Rat'kova and Wassmann, 2002; Franzè and Lavrentyev, 2014, 2017); East Siberian Sea & Chukchi Sea (Jiang et al., 2015); Disko Bay, Greenland (Levinsen et al., 2000a); NW Fram Strait (Seuthe et al., 2011b); Barents Sea & Bering Sea (Johnson et al., 2016), Kongfjorden, Svalbard (Seuthe et al., 2011a), Kara Sea (Lavrentyev, 2012)	Growth, photosynthesis and feeding experiments with cultures (Gustafson et al., 2000; Park et al., 2007; Smith and Hansen, 2007).
Strombidium acutum	East Siberian Sea & Chukchi Sea (Jiang et al., 2015)	Measurement of chlorophyll *a*/ciliate and photosynthesis in cultures (Stoecker et al., 1988/1989)
Strombidium capitatum	East Siberian Sea & Chukchi Sea (Jiang et al., 2015)	Measurement of chlorophyll *a*/ciliate and photosynthesis in cultures (Stoecker et al., 1988/1989)
Strombidium conicum	NW Fram Strait (Seuthe et al., 2011b); Barents Sea (Franzè and Lavrentyev, 2014, 2017); Kongsfjorden, Svalbard (Seuthe et al., 2011a); Kara Sea (Lavrentyev, 2012)	Measurement of chlorophyll *a*/ciliate and photosynthesis in cultures (Stoecker et al., 1988/1989); Detection of plastids with epifluorescence microscopy (Franzè and Lavrentyev, 2017)
Strombidium wulffi	Kongsfjorden, Svalbard (Seuthe et al., 2011a); Barents Sea (Franzè and Lavrentyev, 2017)	Detection of plastids with epifluorescence microscopy (Franzè and Lavrentyev, 2017)
Strombidium spp. *A and B*	Iceland/Greenland Seas & N Svalbard/Barents Sea (Putt, 1990)	Detection of plastids with epifluorescence microscopy, measurement of chlorophyll *a*/ciliate and photosynthesis (Putt, 1990)
Tontonia spp.	East Siberian Sea & Chukchi Sea (Jiang et al., 2015); Iceland/Greenland Seas & N Svalbard/Barents Sea (Putt, 1990); Chukchi Sea (Yokoi et al., 2016); Kongsfjorden, Svalbard (Seuthe et al., 2011a); Barents Sea (Franzè and Lavrentyev, 2014)	Detection of plastids with epifluorescence microscopy, measurement of chlorophyll *a* /ciliate (Putt, 1990). Many (all?) *Tontonia* spp. have plastids (reviewed in Stoecker et al., 2009).

as their phytoplankton prey and are photosynthetic (reviewed in Stoecker et al., 2009, 2017). One of the few field studies in which chlorophyll *a* content and photosynthesis were measured in oligotrichs from natural assemblages was conducted by Putt (1990) in Arctic seas. In *Strombidium* sp. "A," carbon: chlorophyll ratios varied from 87 to 103 and in *L. strobila* from 200 to 232. In *Strombidium* sp. "A," light saturated photosynthetic rates (P_{max}) averaged 2.1 pg C (pg chlorophyll *a*)$^{-1}$h^{-1}, which was equivalent ∼2.8% of body carbon h^{-1} (Putt, 1990; **Table 3**).

The "red" ciliates *Mesodinium rubrum* and *M. major* are important mixotrophic ciliates in coastal and upwelling waters globally (Johnson et al., 2016). In Arctic waters they are a common component of the microplankton (**Table 2**). *M. major* was described as a separate species from *M. rubrum* relatively recently (Garcia-Cuetos et al., 2012) so in **Table 2** we refer to them together. In some cases, red *Mesodinium* are responsible for dense blooms in the Arctic (Johnson et al., 2016). In contrast with the plastid retaining oligotrichs, that can retain plastids from several algal taxa (reviewed in Stoecker et al., 2009; McManus et al., 2012), the red *Mesodinium* spp. are specialized and primarily retain plastids, nuclei and other cell components from phycoerythrin-containing cryptophytes in the *Teleaulax* and *Plagioselmis* species complex (Johnson et al., 2016). The metabolism of *M. rubrum/M. major* is primarily photosynthetic, although polar strains are capable of survival in the dark for long periods (Johnson and Stoecker, 2005). *M. rubrum* is often considered to be more a component of the phytoplankton than the microzooplantkon because of their high chlorophyll content, high rates of photosynthesis and ability to form blooms (reviewed in Crawford, 1989). In the Arctic, as elsewhere, red *Mesodinium* spp. are routinely a significant component of the protist plankton in meso- and eutrophic waters, particularly under low light conditions which also favor their cryptophyte prey. Blooms are usually associated with fronts or upwelling events and can be "hotspots" of primary and secondary production which influence biogeochemical cycling (Herfort et al., 2012).

Factors Influencing Mixotrophy in the Arctic

Although there have been fewer studies of mixotrophy in the Arctic than in temperate seas, the environmental conditions in the Arctic should often favor mixotrophs over strict heterotrophs or autotrophs. Mixotrophy is advantageous in environments in which resource availability is highly variable and/or does

TABLE 3 | Relative contributions of mixotrophic ciliates to ciliate abundance, biomass, and total chlorophyll *a* (chl *a*) in the Arctic during summer.

Location	% Ciliate Abundance	% Ciliate Biomass	% Total chlorophyll *a*	References
Iceland/Greenland Seas	Meso-Avg. 6% PO-Avg. 52%	Avg. 63% of aloricate ciliates	Estimated 4%	Putt, 1990
Barents Sea/N. Svarbard	Meso-Avg. 25% PO-Avg. 40%	Avg. 59% of aloricate ciliates	Estimated 15%	Putt, 1990
Disko Bay, Greenland	Range 45–85% of oligotrich ciliates	ND	ND	Levinsen et al., 2000a
Barents Sea	Range 22–73% of total ciliates	Avg. 54% (Range 12–93%) of total ciliates	Estimated range, DCM (0.5–46%)	Franzè and Lavrentyev, 2017
Pechora (SE Barents) & Kara Seas	Avg. 48% (Range 30–60%) of total ciliates	Avg. 69% (Range 47–91%) of total ciliates	Estimated 22% (Range 7–46%) mixed layer	Lavrentyev, 2012
Eastern Fram Strait and AO Eurasian Basin slope north of Svalbard	Avg. 25% (Range 12–49%) of total ciliates	Avg. 71% (Range 40–99%) of total ciliates	ND	Lavrentyev and Franzè, 2017
Eastern Bering Sea	Range 68–75% on shelf	~65%	Variable; Estimated >50% at some stations on middle shelf	Stoecker et al., 2014

Meso, Mesodinium rubrum/major; PO, plastidic oligotrich ciliates; ND, no data; AO, the Arctic Ocean; DCM, deep chlorophyll maximum; MIZ, marginal ice zone; Avg., Average.

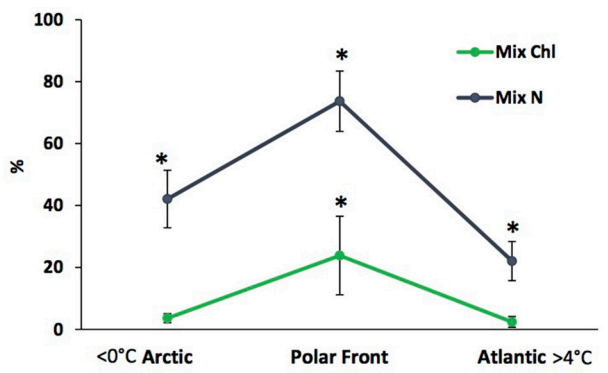

FIGURE 2 | Relative abundance and contribution to total chlorophyll a of mixotrophic ciliates in the deep chlorophyll layer along the latitudinal gradient in the Barents Sea (modified from Franzè and Lavrentyev, 2017). Vertical bars,standard deviation; asterisks denote significant difference ($p < 0.05$) based on ANOVA and Fisher LSD test. Mix N, relative abundance of mixotrophic ciliates; Mix Chl, estimated contribution of mixotrophic ciliates to total chlorophyll a.

not support balanced growth (reviewed in Mitra et al., 2016; Stoecker et al., 2017). Mixotrophic strategies vary among planktonic protists (Mitra et al., 2016). For example, many small phytoflagellates and photosynthetic dinoflagellates can grow as strict autotrophs, using light and dissolved inorganic nutrients for growth, but nitrogen (N), phosphorus (P), and iron limitation or skewed N:P ratios induce or increase phagotrophy (Maranger et al., 1998; Li et al., 2000; Smalley et al., 2003). Less well-known are marine phytoflagellates and photosynthetic dinoflagellates that are stimulated to feed by light or carbon limitation. A freshwater mixotrophic *Ochromonas* sp. (chrysophyte) primarily obtains carbon and nitrogen from ingestion of bacteria and only assimilates inorganic nutrients to appreciable degree when bacterial abundances are very low (Terrado et al., 2017). The same strategy may occur in some marine *Ochromonas* spp. However, at least one marine *Ochromonas* sp. is primarily photosynthetic and is stimulated to feed by low light and low nutrients (Keller et al., 1994). In the marine dinoflagellate *H. rotundata*, light limitation stimulates ingestion of bacteria (Millette et al., 2017) but it is unclear how common this response is in photosynthetic dinoflagellates. Interaction of light and inorganic nutrient availability is important in regulating the relative contributions of phototrophy and phagotrophy to survival and growth in most mixotrophic flagellates. For example, species-specific responses of both photosynthesis and feeding to light and nutrients were observed in cultured Antarctic mixotrophic flagellates (McKie-Krisberg et al., 2015).

Among the microzooplankton with acquired phototrophy (which in the Arctic plankton, is primarily mixotrophic ciliates), most use photosynthesis as a carbon and energy supplement (reviewed in Stoecker et al., 2009). Except in the case of *M. rubrum*, which has nitrate reductase, most plastidic ciliates obtain most of their nitrogen from food. In the plastidic oligotrichs, photosynthate is used primarily to cover respiratory demands for carbon and thus can increase survival times during starvation and, particularly when prey are limiting, increase gross growth efficiency and growth rate (McManus et al., 2012; reviewed in Stoecker et al., 2017).

Environmental parameters, including temperature, inorganic nutrient availability, and light availability are all expected to influence mixotrophy among both "phytoplankton" and "microzooplankton" mixotrophs in Arctic Seas.

Temperature

Sub-zero sea temperatures typical for the Arctic Ocean may be conducive to mixotrophy, particularly among microzooplankton such as ciliates, because photosynthetic plankton are thought to be less constrained by low temperatures than their heterotrophic consumers (Rose and Caron, 2007). The latitudinal trends in

mixotrophic ciliate growth rates in the Barents Sea seem to support this idea (Franzè and Lavrentyev, 2014). However, mixotrophic ciliates also peaked at relatively warm summer temperatures in the Kara (Lavrentyev, 2012) and Bering Seas (Stoecker et al., 2014). In the Fram Strait the highest concentration of ciliates in the Arctic was found in the Atlantic drift warm core (Lavrentyev and Franzè, 2017).

Little information is available on latitudinal or temperature gradients in mixotrophy among phytoflagellates. Laboratory experiments with a freshwater mixotrophic flagellate suggest that some mixotrophs become more heterotrophic with increases in temperature (Wilken et al., 2013). However, it is not clear that this is a general response among mixotrophic flagellates.

Oligotrophy

Oligotrophic conditions favor bacterivorous pico- and nanoplankton in tropical and temperate seas (Zubkov and Tarran, 2008; Hartmann et al., 2012; Mitra et al., 2016). In temperate seas, mixotrophic flagellates are often most abundant during summer stratification which can result in inorganic nutrient limitation of phytoplankton growth in the surface mixed layer (Mitra et al., 2014). Oligotrophic conditions are common during the ice-free season in some parts of the Arctic including the central Arctic Ocean, Beaufort Sea and parts of the Amundsen Sea.

Seasonally low phytoplankton biomass and small phytoplankton cell size can, in turn, select for mixotrophic oligotrich ciliates over strictly heterotrophic microzooplankton (Mitra et al., 2016). In large ciliates, photosynthetic carbon could cover a significant fraction of their metabolism (reviewed in Stoecker et al., 2009, 2017) due to relatively low volume-specific respiration rates (Dolan and Perez, 2000). The Barents Sea Polar Front, where the relative abundance of mixotrophic ciliates peaked, has relatively low phytoplankton biomass in summer compared to receding ice edges and does not stimulate phytoplankton productivity in summer (Reigstad et al., 2011; Erga et al., 2014). However, large mixotrophic oligotrichs are not restricted to oligotrophic conditions in the Arctic. *Laboea strobila* was abundant under phytoplankton bloom conditions in the Bering Sea (Olson and Strom, 2002), Kara Sea (Lavrentyev, 2012), and the Fram Straight (Lavrentyev and Franzè, 2017). In the Gulf of Ob, *M. rubrum* reached its maximum of 75 μg C L^{-1} at total chlorophyll *a* >17 μg L during a cyanobacterial bloom (Lavrentyev, 2012). Mixotrophs contributed up to 46% of total chlorophyll *a* in the deep chlorophyll maximum (DCM) at the pycnocline in the Barents Sea, where phytoplankton accumulate in summer (Franzè and Lavrentyev, 2017).

Light

In contrast to temperate and especially low latitudes, the Arctic is characterized by extremes in solar irradiance. During the polar day, 24-h insolation may favor mixotrophic metabolism over strictly heterotrophic metabolism in planktonic protists. For example, given the same prey concentration, a mixotrophic oligotrich grew faster under luxury light (McManus et al., 2012). The combination of high irradiance and low inorganic nutrients stimulates phagotrophy in many mixotrophic flagellates and dinoflagellates (reviewed in Stoecker et al., 2017). The proportion of phagotrophic and autotrophic-derived carbon in a mixotrophic dinoflagellate diet changed dynamically in response to light conditions and food availability (Riisgaard and Hansen, 2009). Mixotrophic ciliate abundance often peaks in the upper part of the mixed layer (Putt, 1990; Rat'kova and Wassmann, 2002; Lavrentyev, 2012; Franzè and Lavrentyev, 2014; Jiang et al., 2015). Some mixotrophic ciliates and dinoflagellates can migrate between prey or nutrient rich deep chlorophyll maximum layers and well-lit surface waters (Crawford and Lindholm, 1997; Ji and Franks, 2007).

During winter and in/under sea-ice, prolonged dark or low irradiance may also favor mixotrophic phytoplankton over strict autotrophs. Many mixotrophic phytoflagellates and some dinoflagellates use phagotrophy to supplement carbon budgets when light limited (Czypionka et al., 2011; McKie-Krisberg et al., 2015; Millette et al., 2017). Phagotrophy has been hypothesized to be an important mechanism supporting survival and limited growth of phytoflagellates during the polar winter (Zhang et al., 2003).

Although mixotrophy would not appear to be an advantage in ciliates during the dark polar winter, the plastidic ciliates *L. strobila* and *M. rubrum* persist under the ice in West Greenland (Levinsen et al., 2000a). The advantages of mixotrophy during the summer may outweigh the disadvantages of obtaining and maintaining chloroplasts during the winter. Levinsen et al. (2000a) suggested that mixotrophic ciliates survive long periods of darkness due to reduced metabolic demands at low winter temperatures. During the polar winter, photo-degradation is non-existent or minimal, which may contribute to long survival times of plastids in the ciliates. Although mixotrophic oligotrichs have been thought to require both algal prey and light (reviewed in Stoecker et al., 2017), under winter conditions some species may be able to survive and grow as heterotrophs. McManus et al. (2012) observed that a temperate mixotrophic ciliate could grow for several weeks in the dark when supplied with a small dinoflagellate as food, although the dinoflagellate did not support good growth of the ciliate in the light.

Role of Mixotrophy in the Pelagic Food Webs

Mixotrophy has important consequences for primary and secondary production and transfer of carbon to upper levels in Arctic planktonic food webs. Major differences between an Arctic food web with mixotrophy and the microbial loop sensu Azam et al. (1983) are conceptualized in **Figure 3**. In the traditional microbial loop, bacteria are consumed by heterotrophic nanoflagllates, which are then consumed by larger grazers such as ciliates. Most carbon collected by bacteria is respired in the subsequent trophic steps. In the mixotrophic microbial loop bacteria are consumed by both photosynthetic (exemplified by mixotrophic *Micromonas*) and heterotrophic nanoflagellates. The flagellates then become food for ciliates, which in addition to phagotrophy also use functional chloroplasts acquired from their photosynthetic prey. Thus, at each trophic step, energy dissipated through respiration is partially or

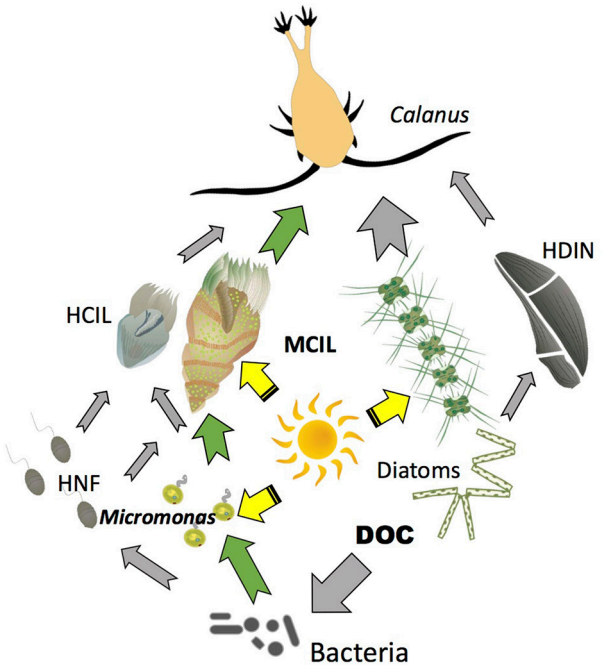

FIGURE 3 | Conceptual model of Arctic food web with mixotrophy. Yellow arrows indicate flow of energy from the sun to photosynthetic organisms (autotrophs and mixotrophs); Gray arrows indicate flow of carbon to heterotrophs; Green arrows indicate major pathways of carbon flow to or from mixotrophs. HCIL, Strictly heterotrophic ciliates; MCIL, Mixotrophic ciliates; HNF, Heterotrophic nanoflagellates; DOC, Dissolved organic carbon; HDIN, Heterotrophic dinoflagellates.

completely replaced by solar energy. This is particularly important under oligotrophic conditions, when inorganic nutrient supply limits primary production. With mixotrophy among the photosynthetic plankton, primary production at the base of the food web can be enhanced (Zubkov and Tarran, 2008; Mitra et al., 2014). Studies in freshwater ecosystems indicate that mixotrophy can stabilize the stoichiometry (C:N:P) of the primary producers, which may in turn stabilize the efficiency of trophic transfer to secondary producers under varying nutrient regimes (Moorthi et al., 2017). Another benefit may be enhanced survival of plastidic ciliates and flagellates in a physiologically active state during the polar winter (Levinsen et al., 2000a; Zhang et al., 2003). When light becomes available, mixotrophic plankton can rapidly respond with high growth rates despite low sea temperatures (Franzè and Lavrentyev, 2014).

Laboratory studies indicate that plastidic oligotrichs ingest and digest phytoplankton and, at least in temperate waters under moderate light intensities, derive much of their carbon, and probably almost all of their nitrogen and phosphorus from phagotrophy (Stoecker et al., 1988; McManus et al., 2012; Schoener and McManus, 2012). Particularly under prey limitation, photosynthesis can increase their gross growth efficiency (McManus et al., 2012) probably because photosynthesis can cover all or part of their respiratory demand for carbon in the light (Stoecker and Michaels, 1991). In the food web with mixotrophy, the sun's energy is directly transferred to relatively large size microzooplankton (the mixotrophic ciliates) as well as to traditional phytoplankton (such as diatoms and phytoflagellates). This augments microzooplankton production, which is important because microzooplankton are a large component of the diet of large size Arctic copepods, such as *Calanus* spp. (Campbell et al., 2009; Saiz et al., 2013). Mixotrophic ciliates in particular are a preferred prey of copepods (Levinsen et al., 2000b; Dutz and Peters, 2008). Such mixotrophic interactions have the potential to temporarily sustain mesozooplankton under low phytoplankton biomass conditions such as occur pre- and post-bloom in many polar seas. Modeling indicates that mixotrophy has the potential to increase food web transfer efficiencies, help retain inorganic nutrients (nitrogen and phosphorous) in the upper water column, and enhance transfer of carbon to larger size organisms (Mitra et al., 2014; Ward and Follows, 2016).

Potential Significance of Mixotrophy in the Changing Arctic

Below we outline three specific examples in which mixotrophs may be affected by changing climate and or how this could affect Arctic ecosystems now and in the future:

1. McMinn and Martin (2013) have suggested that phytoplankton will need to survive the same period of seasonal darkness, but at higher temperatures in the future, thus exhausting stored metabolic resources more quickly. In dark survival, phagotrophic phytoflagellates can have an advantage over diatoms (Zhang et al., 2003; Millette et al., 2017). This could result in changes in the composition of spring blooms, with an increase in phytoflagellates over diatoms.
2. Some areas of the Arctic are becoming more oligotrophic due to increased stratification. For example, offshore areas in the Western Arctic Ocean are becoming more oligotrophic. These changes have already resulted in the phytoplankton composition shift toward small sized-taxa in the Canada Basin (Li et al., 2009). Under such conditions, the presence of mixotrophy among photosynthetic flagellates and ciliates may moderate the negative climate change impacts on energy transfer to higher trophic levels and on particle flux out of surface waters (**Figure 3**).
3. Mixotrophy can facilitate blooms of unpalatable or harmful algae (Burkholder et al., 2008). Incursions of warmer waters, containing potentially bloom-forming, harmful species, already occur in the Arctic. Toxic *Alexandrium, Dinophysis, Karlodinium,* and *Chrysochromulina* spp. are all mixotrophic taxa that often proliferate in highly stratified or freshened waters and have been reported from the Arctic (**Table 1**).

To understand plankton dynamics in a changing Arctic environment, we obviously need information on the magnitude and spatial distribution of the physical and chemical changes. To understand and predict how these changes will alter the structure and function of Arctic planktonic food webs, we need information about alterations near the base of

the food web, among the microbial plankton (bacteria and protists) because these changes will affect higher trophic levels through prey availability, palatability and size and alterations to biogeochemical cycles. In the Arctic, as elsewhere in aquatic food webs, many planktonic protists are not strict autotrophs or heterotrophs and this can have profound effects primary production and secondary production. We need to incorporate mixotrophy into our thinking, into our work on cruises and laboratory studies of Arctic "phytoplankton" and "microzooplankton," and into models of Arctic marine ecosystems.

CONCLUSIONS AND QUESTIONS FOR FUTURE RESEARCH

In summary, many mixotrophic flagellates are found in Arctic waters, but there is only one reported field investigation (Sanders and Gast, 2012) of mixotrophy from Arctic Seas. Most of the data on Arctic phytoplankton relate to bloom-forming diatom species and *Phaeocystis pouchetti* but little data exist on the distribution and abundance of potentially mixotrophic phytoflagellate taxa. Mixotrophy by taxa that are traditionally categorized as "phytoplankton" has been overlooked in most Arctic seas where it may be particularly important in oligotrophic waters during summer and in light limiting conditions for phytoplankton growth year round. Under-ice phytoplankton blooms appear to be increasing in the Arctic (Arrigo et al., 2014); mixotrophs as well as diatoms may be a component of some of these blooms. Field investigations in the Antarctic have shown that mixotrophic flagellates are an important component of sea-ice algal assemblages (Moorthi et al., 2009) but the role of mixotrophs in this habitat in the Arctic appears to be unexplored.

An important task for future research is to determine if mixotrophy among flagellates is widespread in the Arctic and its role in planktonic food webs. For example, in the study by Sanders and Gast (2012), *Micromonas* and other mixotrophic flagellates preferred inert beads over the commonly used fluorescently labeled bacteria. In real life, they may consume a variety of prokaryotic and eukaryotic microorganisms. Genomic techniques for identification and quantification of populations will need to be combined with innovative measurements of both feeding and photosynthesis to accomplish this task (Anderson et al., 2017; Terrado et al., 2017). The degree of mixotrophy in protists (i.e., phagotrophy vs. photosynthesis) can be difficult to establish and its investigation requires novel approaches, involving both field and laboratory experiments. One important question is the effect of warming water temperatures and stratification on the balance between heterotrophy and autotrophy both within species and within assemblages of phytoplankton. Will mixotrophic flagellates increase in dominance because they can survive winter darkness better than strictly autotrophic phytoplankton at higher temperatures? Will stronger stratification and oligotrophy in summer in some regions increasingly favor mixotrophs over strictly autotrophic phytoplankton? How will this influence zooplankton populations and higher trophic levels?

Mixotrophic ciliates are undoubtedly a major component of pelagic food webs across the Arctic and surprisingly, also a major component of photosynthetic biomass. The routine methods of chlorophyll *a* collection need to be revised in the light of recent data showing the importance of green ciliates in total photosynthetic biomass. Specifically, vacuum filtration through membrane filters may result in significant losses of mixotrophic chlorophyll as fragile plankton cells are destroyed and release their cellular content to the filtrate. We still know little about the physiological ecology of mixotrophs in polar waters and a number of important questions remain to be answered. Is high mixotrophic ciliate biomass linked to blooms of particular types of phytoplankton as a source of nutrients and plastids? Are *Micromonas* sp. and other mixotrophic flagellates such as cryptophytes the primary prey and source of plastids for ciliates? This appears to be true for *Mesodinium* spp. which consume certain cryptophytes (Johnson et al., 2016), but is it true for plastid-retaining oligotrichs as well? *Micromonas* is a good source of plastids for at least some species of plastid-retaining oligotichs (Stoecker et al., 1988/1989). How does seasonal 24-h light or darkness influence their survival and growth? What effects do mixotrophs have on primary and secondary production in the Arctic? How does mixotrophy among protistan prey influence trophic transfer efficiencies to macrozooplankton and fish? Does a mixotrophic microbial food web, starting with small mixotrophic flagellates that are in turn consumed large mixotrophic ciliates, support zooplankton production during most of the year? To answer these questions will take a variety of approaches: field sampling to quantify populations of mixotrophic and non-mixotrophic planktonic protists, laboratory and field experiments to determine the contributions of phagotrophy and photosynthesis to the metabolism and growth of Arctic mixotrophs, experimental manipulations to determine the effects of temperature, irradiance, and inorganic nutrient concentrations and ratios on the balance of heterotrophy and autotrophy within mixotrophs as well as the contribution of strict heterotrophs, strict autotrophs and mixotrophs to plankton assemblages. Modeling will be necessary to understand the effects of mixotrophy on food webs and biogeochemical cycling in Arctic planktonic ecosystems and to predict what effects climate change might have on mixotrophs and their roles in Arctic Seas.

AUTHOR CONTRIBUTIONS

DS and PL co-wrote the manuscript. DS had primary responsibility for constructing the tables, PL for drafting the figures.

ACKNOWLEDGMENTS

DS thanks UMCES, Horn Point Laboratory for providing the resources needed to prepare this contribution and MD Johnson for suggesting we review mixotrophy in polar ecosystems.

REFERENCES

Anderson, R., Jurgens, K., and Hansen, P. J. (2017). Mixotrophic phytoflagellate bacterivory field measurements strongly biased by standard approaches: a case study. *Front. Microbiol.* 8:1398. doi: 10.3389/fmicb.2017.01398

Andersson, A., Falk, S., Samuelsson, G., and Hagström, A. (1989). Nutritional characteristics of a mixotrophic nanoflagellate, *Ochromonas* sp. *Microb. Ecol.* 17, 251–262. doi: 10.1007/BF02012838

Ardyna, M., Babin, M., Devred, E., Forest, A., Grosselin, M., Raimbault, P., et al. (2017). Shelf-basin gradients shape ecological phytoplankton niches and community composition in the coastal Arctic Ocean (Beaufort Sea). *Limnol. Oceanogr.* 62, 2113–2132. doi: 10.1002/lno.10554

Ardyna, M., Gosselin, M., Michel, C., Poulin, M., and Tremblay, J. E. (2011). Environmental forcing of phytoplankton community structure and function in the Canadian High Arctic: contrasting oligotrophic and eutrophic regions. *Mar. Ecol. Prog. Ser.* 442, 37–57. doi: 10.3354/meps09378

Arrigo, K. R., Perovich, D. K., Pickart, R. S., Brown, Z. W., van Dijken, G. L., Lowry, K. E., et al. (2014). Phytoplankton blooms beneath the sea ice in the Chukchi sea. *Deep Sea Res. II* 105, 1–16. doi: 10.1016/j.dsr2.2014.03.018

Azam, F., Fenchel, T., Field, J. G.,Gray, J. S., Meyer Reil, L. A., and Thingstad, F. (1983). The ecological role of water-column microbes in the sea. *Mar. Ecol. Prog. Ser.* 10, 257–263. doi: 10.3354/meps010257

Blais, M., Ardyna, M., Gosselin, M., Dumont, D., Belanger, S., and Tremblay, J. E. (2017). Contrasting interannual changes in phytoplankton productivity and community structure in the coastal Canadian Arctic Ocean. *Limnol. Oceanogr.* 62, 2480–2497. doi: 10.1002/lno.10581

Brown, Z. W., and Arrigo, K. R. (2012). Contrasting trends in sea ice and primary production in the Bering Sea and Arctic Ocean. *ICES J. Mar. Sci.* 69, 1180–1193 doi: 10.1093/icesjms/fss113

Burkholder, J. M., Glibert, P. M., and Skelton, H. M. (2008). Mixotrophy, a major mode of nutrition for harmful algal species in eutrophic waters. *Harm. Algae* 8, 77–93. doi: 10.1016/j.hal.2008.08.010

Calbet, A., Bertos, M., Fuentes-Grunewald, C., Alacid, E., Figueroa, R., Renom, B., et al. (2011a). Intraspecific variability in *Karlodinium veneficum*: growth rates, mixotrophy, and lipid composition. *Harm. Algae* 10, 654–667. doi: 10.1016/j.hal.2011.05.001

Calbet, A., Riisgaard, K., Saiz, E., Zamora, S., Stedmon, C., and Nielsen, T. G. (2011b). Phytoplankton growth and microzooplankton grazing along a sub-Arctic fjord (Godthåbsfjord, west Greenland). *Mar. Ecol. Prog. Ser.* 442, 11–22. doi: 10.3354/meps09343

Campbell, R. G., Sherr, E. B., Ashjian, C. J., Plourde, S., Sherr, B. F., Hill, V., et al. (2009). Mesozooplankton prey preference and grazing impact in the western Arctic Ocean. *Deep Sea Res. II* 56, 1274–1289. doi: 10.1016/j.dsr2.2008.10.027

Carmack, E., and Wassmann, P. (2006). Food webs and physical-biological coupling on pan-Arctic shelves: unifying concepts and comprehensive perspectives. *Prog. Oceanogr.* 71, 446–477. doi: 10.1016/j.pocean.2006.10.004

Caron, D. A. (2017). Acknowledging and incorporating mixed nutrition into aquatic protistan ecology, finally. *Environ. Microbiol. Rep.* 9, 41–43. doi: 10.1111/1758-2229.12514

Crawford, D. W. (1989). *Mesodinium rubrum*: the phytoplankter that wasn't. *Mar. Ecol. Prog. Ser.* 58, 161–174.

Crawford, D. W., and Lindholm, T. (1997). Some observations on vertical distribution and migration of the phototrophic ciliate *Mesodinium rubrum* (=*Myrionecta rubra*) in a stratified brackish inlet. *Aquat. Microb. Ecol.* 13, 267–274. doi: 10.3354/ame013267

Czypionka, T., Vargas, C. A., Silva, N., Daneti, G., Gonzalez, H. E., and Iriate, J. L. (2011). Importance of mixotrophic nanoplankton in Aysen Fjord (Southern Chile) during austral winter. *Cont. Shelf Res.* 31, 216–224. doi: 10.1016/j.csr.2010.06.014

Dolan, J. R., and Perez, M. T. (2000). Costs, benefits and characteristics of mixotrophy in marine oligotrichs. *Freshw. Biol.* 45, 227–238. doi: 10.1046/j.1365-2427.2000.00659.x

Dutz, J., and Peters, J. (2008). Importance and nutritional value of large ciliates for the reproduction of *Acartia clausi* during the post spring-bloom period in the North Sea. *Aquat. Microb. Ecol.* 50, 261–277. doi: 10.3354/ame01168

Erga, S. R., Ssebiyonga, N., Hamre, B., Frette, O., Rey, F., and Drinkwater, K. (2014). Nutrients and phytoplankton biomass distribution and activity at the Barents Sea Polar Front during summer near Hopen and Storbanken. *J. Mar. Syst.* 130, 181–192. doi: 10.1016/j.jmarsys.2012.12.008

Estep, K. W., Davis, P. G., Keller, M. D., Sieburth, J., and Mc, N. (1986). How important are oceanic algal nanoflagellates in bacterivory? *Limnol. Oceanogr.* 31, 646–650.

Estrada, M., Bayer-Giraldi, M., Felipe, J., Marrase, C., Sala, M. M., and Vidal, M. (2009). Light and nutrient effects on microbial communities collected during spring and summer in the Beaufort Sea. *Aquat. Microb. Ecol.* 54, 217–231. doi: 10.3354/ame01268

Flynn, K. J., Stoecker, D. K., Mitra, A., Raven, J. A., Glibert, P. M., Hansen, P. J., et al. (2013). Misuse of the phytoplankton zooplankton dichotomy: the need to assign organisms as mixotrophs within plankton functional types. *J. Plankton Res.* 35, 3–11. doi: 10.1093/plankt/fbs062

Franzè, G., and Lavrentyev, P. J. (2014). Microzooplankton growth rates examined across a temperature gradient in the Barents Sea. *PLoS ONE* 9:e86429. doi: 10.1371/journal.pone.0086429

Franzè, G., and Lavrentyev, P. J. (2017). Microbial food web structure and dynamics across a natural temperature gradient in a productive polar shelf system. *Mar. Ecol. Prog. Ser.* 569, 89–102. doi: 10.3354/meps12072

Garcia-Cuetos, L., Moestrup, O., and Hansen, P. J. (2012). Studies on the genus *Mesodinium*, II. Ultrastructural and molecular investigations of five marine species help clarifying the taxonomy. *J. Eukaryt. Microbiol.* 59, 374–400. doi: 10.1111/j.1550-7408.2012.00630.x

Gustafson, D. E., Stoecker, D. K., Johnson, M. D., Van Heukelem, W. F., and Sneider, K. (2000). Cryptophyte algae are robbed of their organelles by the marine ciliate *Mesodinium rubrum*. *Nature* 405, 1049–1052. doi: 10.1038/35016570

Hansen, B., Christiansen, S., and Pedersen, G. (1996). Plankton dynamics in the marginal ice zone of the central Barents Sea during spring: carbon flow and structure of the grazer food chain. *Polar Biol.* 16, 115–128. doi: 10.1007/BF02390432

Hansen, P. J. (2011). The role of photosynthesis and food uptake for the growth of marine mixotrophic dinoflagellates. *J. Eukaryot. Microbiol.* 58, 203–214. doi: 10.1111/j.1550-7408.2011.00537.x

Hansen, P. J., and Hjorth, M. (2002). Growth and grazing responses of *Chrysochromulina ericina* (Prymnesiophyceae): the role of irradiance, prey concentration and pH. *Mar. Biol.* 141, 975–983. doi: 10.1007/s00227-002-0879-5

Hartmann, M., Grub, C., Tarran, G. A., Martin, A. P., Burkill, P. H., Scanlan, D. J., et al. (2012). Mixotrophic basis of Atlantic oligotrophic ecosystem. *Proc. Natl. Acad. Sci. U.S.A.* 109, 5756–5760. doi: 10.1073/pnas.1118179109

Herfort, L., Peterson, T. D., Prahl, F. G., McCue, L. A., Needoba, J. A., Crump, B. C., et al. (2012). Red waters of *Myrionecta rubra* are biogeochemical hotspots for the Columbia River estuary with impacts on primary/secondary productions and nutrient cycles. *Estuar. Coasts* 35, 878–891. doi: 10.1007/s12237-012-9485-z

Hunt, G. L., and Megrey, B. (2005). Comparison of the biophysical and trophic characteristics of the Bering and Barents Seas. *ICES J. Mar. Sci.*62, 1245–1255. doi: 10.1016/j.icesjms.2005.04.008

Iversen, K. R., and Seuthe, L. (2011). Seasonal microbial processes in a high-latitude fjord (Kongsfjorden, Svalbard): I. Heterotrophic bacteria, picoplankton and nanoflagellates. *Polar Biol.* 34, 731–749. doi: 10.1007/s00300-010-0929-2

Jacobson, D. M., and Anderson, D. M. (1996). Widespread phagocytosis of ciliates and other Protists by marine mixotrophic and heterotrophic thecate dinoflagellates. *J. Phycol.* 32, 279–285. doi: 10.1111/j.0022-3646.1996.00279.x

Jeong, H. J., Doo, D., Park, J. Y., Song, J. Y., Kim, S. T., Lee, S. H., et al. (2005). Feeding by phototrophic red-tide dinoflagellates: five species newly revealed and six species previously known to be mixotophic. *Aquat. Microb. Ecol.* 40, 133–150. doi: 10.3354/ame040133

Jeong, H. J., Yoo, Y. D., Kim, J. S., Seong, K. A., Kang, N. S., and Kim, T. H. (2010). Growth, feeding and ecological roles of the mixotrophic and heterotrophic dinoflagellates in marine planktonic food webs. *Ocean Sci. J.* 45, 65–91. doi: 10.1007/s12601-010-0007-2

Ji, R. B., and Franks, P. J. S. (2007). Vertical migration of dinoflagellates: model analysis of strategies, growth, and vertical distribution patterns. *Mar. Ecol. Prog. Ser.* 344, 49–61. doi: 10.3354/meps06952

Jiang, Y., Yang, E. J., Min, J. O., Kim, T. W., and Kang, S. H. (2015). Vertical variation of pelagic ciliate communities in the western Arctic Ocean. *Deep Sea Res. II* 120, 103–113. doi: 10.1016/j.dsr2.2014.09.005

Johnsen, G., Norli, M., Moline, M., Robbins, I., von Quillfeldt, C., Sørensen, K., et al. (2018). The advective origin of an under-ice spring bloom in the Arctic Ocean using multiple observational platforms. *Polar Biol.* 41, 1197–1216. doi: 10.1007/s00300-018-2278-5

Johnson, M. D. (2015). Inducible mixotrophy in the dinoflagellate *Prorocentrum minimum*. *J Eukaryt. Microbiol.* 62, 431–443. doi: 10.1111/jeu.12198

Johnson, M. D., Beaudoin, D. J., Laza-Martinez, A., Dyhrman, S. T., and Fensin, E., Lin, S. et al. (2016). The genetic diversity of *Mesodinium* and associated cryptophytes. *Front. Microbiol.* 7:2017. doi: 10.3389/fmicb.2016.02017

Johnson, M. D., and Stoecker, D. K. (2005). Role of feeding in growth and photophysiology of *Myrionecta rubra*. *Aquat. Microb. Ecol.* 39, 303–312. doi: 10.3354/ame039303

Jones, H. L. J., Leadbeater, B. S. C., and Green, J. C. (1993). Mixotrophy in marine species of *Chrysochromulina* (Prymnesiophyceae): ingestion and digestion of a small green flagellate. *J. Mar. Biol. Assoc. U.K.* 73, 283–296. doi: 10.1017/S0025315400032859

Keck, A., Wiktor, J., Hapter, R., and Nilsen, R. (1999). Phytoplankton assemblages related to physical gradients in an arctic, glacier-fed fjord in summer. *ICES J. Mar. Sci.* 56, 203–214. doi: 10.1006/jmsc.1999.0631

Keller, M. D., Shapiro, L. P., Haugen, E. M., Cucci, T. L., Sherr, E. B., and Sherr, B. F. (1994). Phagotrophy of fluorescently labeled bacteria by an oceanic phytoplankter. *Microb. Ecol.* 28, 39–52. doi: 10.1007/BF00170246

Kwok, R., and Rothrock, D. A. (2009). Decline in Arctic sea ice thickness from submarine and ICES records: 1958–2008. *Geophys. Res. Lett.* 36:L15501. doi: 10.1029/2009GL039035

Lavrentyev, P. J. (2012). Microzooplankton studies in the Kara Sea during the Yamal-Arctic 2012 expedition. *Russ. Polar Res.* 10, 24–26.

Lavrentyev, P. J., and Franzè, G. (2017). *CarbonBridge May 2014: Microzooplankton Biomass Distribution in the Waters Northwest of Spitsbergen*. University of Akron, PANGAEA. doi: pangaea.de/10.1594/PANGAEA.881808

Legrand, C., Granéli, E., and Carlsson, P. (1998). Induced phagotrophy in the photosynthetic dinoflagellate *Heterocapsa triqueta*. *Aquat. Microb. Ecol.* 15, 65–75. doi: 10.3354/ame015065

Leles, S. G., Mitra, A., Flynn, K. J., Stoecker, D. K., Hansen, P. J., Calbet, A., et al. (2017). Oceanic protists with different forms of acquired phototrophy display contrasting biogeographies and abundance. *Proc. R. Soc. B.* 284:20170664. doi: 10.1098/rspb.2017.0664

Levinsen, H., Nielsen, T. G., and Hansen, B. W. (2000a). Annual succession of marine pelagic protozoans in Disko Bay, West Greenland, with emphasis on winter dynamics. *Mar. Ecol. Prog. Ser.* 206, 119–134. doi: 10.3354/meps206119

Levinsen, H., Turner, J. T., Nielsen, T. G., and Hansen, B. W. (2000b). On trophic coupling between protists and copepods in arctic marine ecosystems. *Mar. Ecol. Prog. Ser.* 204, 65–77. doi: 10.3354/meps204065

Li, A., Stoecker, D. K., and Adolf, J. E. (1999). Feeding, pigmentation, photosynthesis and growth of the mixotrophic dinoflagellate *Gyrodinium galatheanum*. *Aquat. Microb. Ecol.* 19, 163–176.

Li, A., Stoecker, D. K., and Coats, D. W. (2000). Mixotrophy in *Gyrodinium galatheanum* (Dinophyceae): grazing responses to light intensity and inorganic nutrients. *J. Phycol.* 36, 33–45. doi: 10.1046/j.1529-8817.2000.98076.x

Li, W. K., McLaughlin, F. A., Lovejoy, C., and Carmack, E. C. (2009). Smallest algae thrive as the Arctic Ocean freshens. *Science* 326, 539–539. doi: 10.1126/science.1179798

Lovejoy, C., Legendre, L., Martineau, M. J., Bacle, J., and von Quillfeldt, C. H. (2002). Distribution of phytoplankton and other protists in the North Water. *Deep Sea Res. II* 49, 5027–5047. doi: 10.1016/S0967-0645(02)00176-5

Lovejoy, C., Vincent, W. F., Bonilla, S., Roy, S., Martineau, M. J., Terrado, R., et al. (2007). Distribution, phylogeny, and growth of cold-adapted picoprasinophytes in Arctic Seas. *J. Phycol.* 43, 78–89. doi: 10.1111/j.1529-8817.2006.00310.x

Maranger, R., Bird, D. F., and Price, N. M. (1998). Iron acquisition by photosynthetic marine phytoplankton from ingested bacteria. *Nature* 396, 248–251 doi: 10.1038/24352

McKenzie, C. H., Deibel, D., Paranjape, M. A., and Thompson, R. J. (1995). The marine mixotroph *Dinobryon balticum* (Chrysophyceae) – phagotrophy and survival in a cold ocean. *J. Phycol.* 31, 19–24. doi: 10.1111/j.0022-3646.1995.00019.x

McKie-Krisberg, Z. M., Gast, R. J., and Sanders, R. W. (2015). Physiological responses of three species of Antarctic mixotrophic phytoflagellates to changes in light and dissolved nutrients. *Microb. Ecol.* 70. 21–29. doi: 10.1007/s00248-014-0543-x

McKie-Krisberg, Z. M., and Sanders, R. W. (2014). Phagotrophy by the picoeukaryotic green alga *Micromonas*: implications for Arctic Oceans. *ISME J.* 8, 1953–1961. doi: 10.1038/ismej.2014.16

McManus, G. B., Schoener, D. M., and Haberlandt, K. (2012). Chloroplast symbiosis in a marine ciliate: ecophysiology and the risks and rewards of hosting foreign organelles. *Front. Microbiol.* 3:321. doi: 10.3389/fmicb.2012.00321

McMinn, A., and Martin, A. (2013). Dark survival in a warming world. *Proc. R. Soc. B* 280:20122909. doi: 10.1098/rspb.2012.2909

Metfies, K., von Appen, W. J., Kilias, E., Nicolaus, A., and Nothig, E. M. (2016). Biogeography and photosynthetic biomass of Arctic marine pico-eukaryotes during summer of the record sea ice minimum 2012. *PLoS ONE* 11:e0148512. doi: 10.1371/journal.pone.0148512

Millette, N. C., Pierson, J. J., Aceves, A., and Stoecker, D. K. (2017). Mixotrophy in *Heterocapsa rotundata*: a mechanism for dominating the winter phytoplankton. *Limnol. Oceangr.* 62, 836–845. doi: 10.1002/lno.10470

Mitra, A., Flynn, K. A., Tillmann, U., Raven, J. A., Caron, D., Stoecker, D. K., et al. (2016).Defining planktonic functional groups on mechanisms for energy and nutrient acquisition: incorporation of diverse mixotrophic strategies. *Protist* 167, 106–120. doi: 10.1016/j.protis.2016.01.003

Mitra, A., Flynn, K. J., Burkholder, J. M., Berge, T., Calbet, A., Raven, J. A., et al. (2014). The role of mixotrophic protists in the biological carbon pump. *Biogeosciences* 11, 995–1005. doi: 10.5194/bg-11-995-2014

Möller, E. F., Nielsen, T. G., and Richardson, K. (2006). The zooplankton community in the Greenland Sea: composition and role in carbon turnover. *Deep Sea Res. I.* 53, 76–93. doi: 10.1016/j.dsr.2005.09.007

Montagnes, D. J. S., Berges, J. A., Harrison, P. J., and Taylor, F. J. R. (1994). Estimating carbon, nitrogen, protein, and chlorophyll-*a* from volume in marine-phytoplankton. *Limnol. Oceangr.* 39, 1044–1060.

Moorthi, S., Caron, D. A., Gast, R. J., and Sanders, R. W. (2009). Mixotrophy: a widespread and important ecological strategy for planktonic and sea-ice nanoflagellates in the Ross Sea, Antarctica. *Aquat. Microb. Ecol.* 54, 269–277. doi: 10.3354/ame01276

Moorthi, S. D., Ptacnik, R., Sanders, R. W., Fischer, R., Busch, M., and Hillebrand, H. (2017). The functional role of planktonic mixotrophs in altering seston stoichiometry. *Aquat. Microb. Ecol.* 79, 235–245. doi: 10.3354/ame01832

Not, F., Massana, R., Latasa, M., Marie, D., Colson, C., Eikrem, W., et al. (2005). Late summer community composition and abundance of photosynthetic picoeukaryotes in Norwegian and Barents Seas. *Limnol. Oceanogr.* 50, 1677–1686. doi: 10.4319/lo.2005.50.5.1677

Olli, K., Riser, C. W., Wassmann, P., Rat'kova, T., Arashkevich, E., and Pasternak, A. (2002). Seasonal variation in vertical flux of biogenic matter in the marginal ice zone and the central Barents Sea. *J. Mar. Syst.* 38, 189–204. doi: 10.1016/S0924-7963(02)00177-X

Olson, M. B., and Strom, S. L. (2002). Phytoplankton growth, microzooplankton herbivory and community structure in the southeast Bering Sea: insight into the formation and temporal persistence of an *Emiliania huxleyi* bloom. *Deep Sea Res. II* 49, 5969–5990. doi: 10.1016/S0967-0645(02)00329-6

Oziel, L., Neukermans, G., Ardyna, M., Lancelot, C., Tison, J. L., Wassmann, P., et al. (2017). Role for Atlantic inflows and sea ice loss on shifting phytoplankton blooms in the Barents Sea. *J. Geophys. Res. Oceans* 122, 5121–5139. doi: 10.1002/2016JC012582

Pabi, S., van Dijken, G. L., and Arrigo, K. R. (2008). Primary production in the Arctic Ocean, 1998-2006. *J. Geophys. Res. Oceans* 113:C08005. doi: 10.1029/2007JC004578

Park, J. S., Myung, G., Kim, H. S., Cho, B. C., and Yih, W. (2007). Growth responses of the marine photosynthetic ciliate *Myrionectra rubra* to different cryptomonad strains. *Aquat. Microb. Ecol.* 48, 83–90. doi: 10.3354/ame048083

Park, M. G., Kim, S., Kim, H. S., Myung, G., Kang, Y. G., and Yih, W. H. (2006). First successful culture of the marine dinoflagellate *Dinophysis acuminata*. *Aquat. Microb. Ecol.* 45, 101–106. doi: 10.3354/ame045101

Putt, M. (1990). Abundance, chlorophyll content and photosynthesis rates of ciliates in the Nordic Seas during summer. *Deep Sea Res.* 37, 1713–1731. doi: 10.1016/0198-0149(90)90073-5

Rat'kova, T. N., and Wassmann, P. (2002). Seasonal variation and spatial distribution of phyto- and protozooplankton in the central Barents Sea. *J. Mar. Syst.* 38, 47–75. doi: 10.1016/S0924-7963(02)00169-0

Reigstad, M., Carroll, J., Slagstad, D., Ellingsen, I. H., and Wassmann, P. (2011). Intra-regional comparison of productivity, carbon flux and ecosystem composition within the northern Barents Sea. *Prog. Oceanogr.* 90, 33–46. doi: 10.1016/j.pocean.2011.02.005

Riisgaard, K., and Hansen, P. J. (2009). Role of food uptake for photosynthesis, growth and survival of the mixotrophic dinoflagellate *Dinophysis acuminata*. *Mar. Ecol. Prog. Ser.* 381, 51–62. doi: 10.3354/meps07953

Rose, J. M., and Caron, D. A. (2007). Does low temperature constrain the growth rates of heterotrophic protists? Evidence and implications for algal blooms in cold waters. *Limnol. Oceanogr.* 52, 886–895. doi: 10.4319/lo.2007.52.2.0886

Saiz, E., Calbet, A., Isari, S., Antó, M., and others (2013). Zooplankton distribution and feeding in the Arctic Ocean during a *Phaeocystis pouchetii* bloom. *Deep Sea Res. I* 72, 17–33. doi: 10.1016/j.dsr.2012.10.003

Sanders, R. W., and Gast, R. J. (2012). Bacterivory by phototrophic picoplankton and nanoplankton in Arctic waters. *FEMS Microbiol. Ecol.* 82, 42–253. doi: 10.1111/j.1574-6941.2011.01253.x

Sarmento, H., Montoya, J. M., Vázquez-Domínguez, E., Vaqué, D., and Gasol, J. M. (2010). Warming effects on marine microbial food web processes: how far can we go when it comes to predictions? *Philos. Trans. R. Soc. Lond. Ser. B. Biol. Sci.* 365, 2137–2149. doi: 10.1098/rstb.2010.0045

Schoener, D. M., and McManus, G. B. (2012). Plastid retention, use, and replacement in a kleptoplastidic ciliate. *Aquat. Microb. Ecol.* 67, 177–187. doi: 10.3354/ame01601

Selosse, M. A., Charpin, M., and Not, F. (2017). Mixotrophy everywhere on land and in water: the *grand ecart* hypothesis. *Ecol. Lett.* 20, 246–263. doi: 10.1111/ele.12714

Seuthe, L., Iversen, K. R., and Narcy, F. (2011a). Microbial processes in a high–latitude fjord (Kongsfjorden, Svalbard): ciliates and dinoflagellates. *Polar Biol.* 34, 751–766. doi: 10.1007/s00300-010-0930-9

Seuthe, L., Topper, B., Reigstad, M., Thyrhaug, R., and Vaquer-Sunyer, R. (2011b). Microbial communities and processes in ice covered Arctic waters of the northwestern Fram Strait (75 to 80° N) during the vernal pre-bloom phase. *Aquat. Microb. Ecol.* 64, 253–266. doi: 10.3354/ame01525

Sherr, E. B., Sherr, B. F., and Hartz, A. J. (2009). Microzooplankton grazing impact in the Western Arctic Ocean. *Deep Sea Res. II* 56, 1264–1273. doi: 10.1016/j.dsr2.2008.10.036

Sherr, E. B., Sherr, B. F., and Ross, C. (2013). Microzooplankton grazing impact in the Bering Sea during spring sea ice conditions. *Deep Sea Res II* 94, 57–67. doi: 10.1016/j.dsr2.2013.03.019

Slagstad, D., Ellingsen, I. H., and Wassmann, P. (2011). Evaluating primary and secondary production in an Arctic Ocean void of summer sea ice: an experimental simulation approach. *Prog. Oceanogr.* 90, 117–131. doi: 10.1016/j.pocean.2011.02.009

Smalley, G. W., Coats, D. W., and Stoecker, D. K. (2003). Feeding in the mixotrophic dinoflagellate *Ceratium furca* is influenced by intracellular nutrient concentrations. *Mar. Ecol. Prog. Ser.* 262, 137–151. doi: 10.3354/meps262137

Smith, M., and Hansen, P. J. (2007). Interaction between *Mesodinium rubrum* and its prey: importance of prey concentration, irradiance and pH. *Mar. Ecol. Prog. Ser.* 338, 61–70. doi: 10.3354/meps338061

Stoecker, D. K., Hansen, P. J., Caron, D. A., and Mitra, A. (2017). Mixotrophy in the marine plankton. *Annu. Rev. Mar. Sci.* 9, 311–335. doi: 10.1146/annurev-marine-010816-060617

Stoecker, D. K., Johnson, M. D., de Vargas, C., and Not, F. (2009).Acquired phototrophy in aquatic protists. *Aquat. Microb. Ecol.* 57, 279–310. doi: 10.3354/ame01340

Stoecker, D. K., and Michaels, A. E. (1991). Respiration, photosynthesis and carbon metabolism in planktonic ciliates. *Mar. Biol.* 108, 441–447. doi: 10.1007/BF01313654

Stoecker, D. K., Silver, M. W., Michaels, A. E., and Davis, L. H. (1988). Obligate mixotrophy in *Laboea strobila*, a ciliate which retains chloroplasts. *Mar. Biol.* 99, 415–423.

Stoecker, D. K., Silver, M. W., Michaels, A. E., and Davis, L. H. (1988/1989). Enslavement of algal chloroplasts by four *Strombidium* spp. (Ciliophora, Oligotrichida). *Mar. Microb. Fd. Webs* 3, 79–100.

Stoecker, D. K., Weigel, A. C., Stockwell, D. A., and Lomas, M. W. (2014). Microzooplankton: abundance, biomass and contribution to chlorophyll in the Eastern Bering Sea in summer. *Deep Sea Res. II.* 109, 134–144. doi: 10.1016/j.dsr2.2013.09.007

Strom, S. L., and Fredrickson, K. A. (2008). Intense stratification leads to phytoplankton nutrient limitation and reduced microzooplankton grazing in the Southeastern Bering Sea. *Deep Sea Res. II* 55, 1761–1774. doi: 10.1016/j.dsr2.2008.04.008

Terrado, R., Pasulka, A. L., Lie, A. A., Orphan, V. J., Heidelberg, K. B., and Caron, D. A. (2017). Autotrophic and heterotrophic acquisition of carbon and nitrogen by a mixotrophic chrysophyte established through stable isotope analysis. *ISME J.* 11, 2022–2034. doi: 10.1038/ismej.2017.68

Unrein, F., Gasol, J. M., Not, F., Forn, I., and Massana, R. (2014). Mixotrophic haptophytes are key bacterial grazers in oligotrophic coastal waters. *ISME J.* 8, 164–176. doi: 10.1038/ismej.2013.132

Unrein, F., Massana, R., Alonso-Saez, L., and Gasol, J. M. (2007). Significant year-round effect of small mixotrophic flagellates on bacterioplankton in an oligotrophic coastal system. *Limnol. Oceanogr.* 52, 456–469. doi: 10.4319/lo.2007.52.1.0456

Verity, P. G., Wassmann, P., Frischer, M. E., Howard-Jones, M. H., and Allen, A. E. (2002). Grazing of phytoplankton by microzooplankton in the Barents Sea during early summer. *J. Mar. Syst.* 38, 109–123. doi: 10.1016/S0924-7963(02)00172-0

Ward, B. A., and Follows, M. J. (2016). Marine mixotrophy increases trophic transfer efficiency, mean organism size and vertical carbon flux. *Proc. Nat. Acad. Sci. U.S.A.* 113, 2958–2963. doi: 10.1073/pnas.1517118113

Wassmann, P., and Reigstad, M. (2011). Future Arctic Ocean seasonal ice zones and implications for pelagic-benthic coupling. *Oceanography* 24, 220–231. doi: 10.5670/oceanog.2011.74

Wilken, S., Huisman, J., Naus-Weier, S., and Van Donk, E. (2013). Mixotrophic organisms become more heterotrophic with rising temperature. *Ecol. Lett.* 16, 225–233. doi: 10.1111/ele.12033

Yokoi, N., Matsuno, K., Ichinomiya, M., Yamaguchi, A., Nishino, S., Onodera, J., et al. (2016). Short-term changes in a microplankton community in the Chukchi Sea during autumn: consequences of a strong wind event. *Biogeosciences* 13, 913–923. doi: 10.5194/bg-13-913-2016

Yoo, Y. D., Jeong, H. J., Kim, M. S., Kang, N. S., Song, J. Y., Shin, W., et al. (2009). Feeding by phototrophic red-tide dinoflagellates on the ubiquitous marine diatom *Skeletonema costatum*. *J. Eukaryt. Microbiol.* 56, 413–420. doi: 10.1111/j.1550-7408.2009.00421.x

Yoo, Y. D., Seong, K. A., Jeong, H. J., Yih, W., Rho, J. R., Nam, S. W., et al. (2017). Mixotrophy in the marine red-tide cryptophyte *Teleaulax amphioxeia* and ingestion and grazing impact of cryptophytes on natural populations of bacteria in Korean coastal waters. *Harm. Algae* 68, 105–117. doi: 10.1016/j.hal.2017.07.012

Zhang, Q., Gradinger, R., and Zhou, Q. S. (2003). Competition within the marine microalgae over the polar dark period in the Greenland Sea of high Arctic. *Acta Oceanol. Sin.* 22, 233–242.

Zubkov, M. V., and Tarran, G. A. (2008). High bacterivory by the smallest phytoplankton in the North Atlantic Ocean. *Nature* 455, 224–226. doi: 10.1038/nature07236

Conflict of Interest Statement: The authors declare that the research was conducted in the absence of any commercial or financial relationships that could be construed as a potential conflict of interest.

frontiers in Marine Science

ORIGINAL RESEARCH
published: 29 October 2018
doi: 10.3389/fmars.2018.00387

Symbiont Chloroplasts Remain Active During Bleaching-Like Response Induced by Thermal Stress in *Collozoum pelagicum* (Collodaria, Retaria)

Emilie Villar[1], Vincent Dani[2], Estelle Bigeard[1], Tatiana Linhart[1], Miguel Mendez-Sandin[1], Charles Bachy[1], Christophe Six[1], Fabien Lombard[3], Cécile Sabourault[2] and Fabrice Not[1]**

[1] Sorbonne Université, CNRS – UMR7144 – Ecology of Marine Plankton Group – Station Biologique de Roscoff, Roscoff, France, [2] Université Côte d'Azur, Institut de Biologie Valrose UMR7277, Nice, France, [3] Sorbonne Université, CNRS – UMR 7093, Laboratoire d'Océanographie de Villefranche (LOV), Observatoire Océanologique, Villefranche-sur-Mer, France

OPEN ACCESS

Edited by:
Matthew D. Johnson, Woods Hole Oceanographic Institution, United States

Reviewed by:
Anthony William Larkum, University of Technology Sydney, Australia
Manuel F. G. Weinkauf, Université de Genève, Switzerland

***Correspondence:**
Emilie Villar
emilie.villar1@gmail.com
Fabrice Not
not@sb-roscoff.fr

Specialty section:
This article was submitted to Marine Ecosystem Ecology, a section of the journal Frontiers in Marine Science

Received: *08 June 2018*
Accepted: *03 October 2018*
Published: *29 October 2018*

Citation:
Villar E, Dani V, Bigeard E, Linhart T, Mendez-Sandin M, Bachy C, Six C, Lombard F, Sabourault C and Not F (2018) Symbiont Chloroplasts Remain Active During Bleaching-Like Response Induced by Thermal Stress in Collozoum pelagicum (Collodaria, Retaria). Front. Mar. Sci. 5:387. doi: 10.3389/fmars.2018.00387

Collodaria (Retaria) are important contributors to planktonic communities and biogeochemical processes (e.g., the biologic pump) in oligotrophic oceans. Similarly to corals, Collodaria live in symbiosis with dinoflagellate algae, a relationship that is thought to explain partly their ecological success. In the context of global change, the robustness of the symbiotic interaction, and potential subsequent bleaching events are of primary interest for oceanic ecosystems functioning. In the present study, we compared the ultrastructure, morphology, symbiont density, photosynthetic capacities and respiration rates of colonial Collodaria exposed to a range of temperatures corresponding to natural conditions (21°C), moderate (25°C), and high (28°C) thermal stress. We showed that symbiont density immediately decreased when temperature rose to 25°C, while the overall Collodaria holobiont metabolic activity increased. When temperature reached 28°C, the holobiont respiration nearly stopped and the host morphological structure was largely damaged, as if the host tolerance threshold has been crossed. Over the course of the experiment, the photosynthetic capacities of remaining algal symbionts were stable, chloroplasts being the last degraded organelles in the microalgae. These results contribute to a better characterization and understanding of temperature-induced bleaching processes in planktonic photosymbioses.

Keywords: heat stress, photosymbiosis, bleaching, dinoflagellate, Collodaria, Radiolaria, Retaria, plankton

INTRODUCTION

Retaria encompass Foraminifera and Radiolaria *sensu stricto* or Radiozoa. Within Radiozoa, Collodaria have been recently unraveled as key players in oceanic ecosystems (Biard et al., 2016; Guidi et al., 2016). Previously overlooked because of their fragility, the use of non-destructive, *in situ*, imaging tools showed that Collodaria represents nearly 30% of zooplankton biomass at subsurface in oligotrophic oceans (Biard et al., 2016). Collodaria were also reported as central actors in plankton community networks related to carbon export to the deep ocean via both primary

production and vertical flux (Guidi et al., 2016). Initially described by E. Haeckel toward the end of the 19th century (Haeckel, 1887), Collodaria have been little studied so far, with only a few landmark studies conducted on radiolarian morphology and physiology (Anderson, 1983).

Collodaria are unicellular organisms that live either solitary (cell size ∼1 mm) or form colonies up to a few centimeters long. Each colony is composed of hundreds to thousands of cells agglomerated in a gelatinous matrix. All cells, individually represented by a spherical structure called the central capsule, are connected together through cytoplasmic extensions and some particular species can bear a siliceous skeleton (Anderson, 1976a,b). Collodaria feed on prey from the surrounding environment but can be considered as mixotrophic organisms, since they also rely on symbiotic interactions with photosynthetic dinoflagellates. Swanberg (1983) suggested that photosymbiosis provides Retaria with the minimum energy to subsist, while their energy and nutrients for growth would come from their heterotrophic regime. Collodaria can consume 4% of their symbionts everyday (Anderson, 1983) and a part of the photosynthates are transferred to the host, mostly as lipid storage pool (Anderson et al., 1983). Microalgae symbionts isolated from the collodarian species *Collozoum* spp. have been recently identified as *Brandtodinium nutricula*, a dinoflagellate species belonging to the Peridiniales order (Probert et al., 2014). As *B. nutricula* can be cultivated in host-free media and has been found in association with different radiolarian hosts and even with the jellyfish *Velella velella*, this microalga is thought to be a generalistic symbiont having free-living stages (Decelle et al., 2015).

The breakdown of the symbiotic associations in corals, so-called coral bleaching, has been originally described by Glynn (1984), who depicted coral bleaching as a reaction to environmental constraints, due to the massive loss of symbiotic algae, or alternatively as a decline of their photosynthetic pigment content. Recent projections suggest that more than half of the coral reefs worldwide will experience several bleaching events by the year 2100, as a consequence of ocean temperature rise of 1–1.8°C (Logan et al., 2014). Coral bleaching has significant deleterious consequences on coral reef ecosystem functioning and as a result, on several countries economy and food supply (Hoegh-Guldberg et al., 2007). Numerous studies have tried to decipher the relationships between corals -or other cnidarians such as sea anemones- and their symbionts upon environmental perturbations. Although bleaching events involve the whole holobiont and all possible interactions between its biotic components (Baird et al., 2009), in cnidarians most studies considered bleaching as being induced by the microalgal partner release (reviewed in Lesser, 2011). One of the proposed mechanisms suggests the production of reactive oxygen species (ROS) when symbiont photosynthesis is impaired by heat stress (Lesser, 2006). These ROS lead to the death of the host cells by triggering apoptosis, notably through the induction of protease enzymes (Cikala et al., 1999). During the stress and death of the host cells, microalgal symbiotic cells can be either healthy (Baghdasarian and Muscatine, 2000) or damaged (Fujise et al., 2014). In the later case, it is unclear whether the symbiont damages are due to the host cell apoptosis or to other symbiont related processes, such as programmed cell death (PCD) or host autophagic digestion (Dunn et al., 2007; Paxton et al., 2013).

Considering the potential impact of bleaching in Collodaria on the marine ecosystem functioning and the lack of recent studies on their biology, this study aims at a better characterization of their functional behavior. We performed a controlled thermal stress experiment on Collodaria to investigate potential plankton bleaching and the photosymbiosis response to elevated temperatures using both morphological and physiological analyses.

MATERIALS AND METHODS

Experimental Design

Collodarian colonies were collected in the bay of Villefranche-sur-Mer (France, 43°41′10″ N, 7°18′50″ E) using a Regent plankton net (680 μm mesh size) handheld from a boat, immediately handpicked and transferred into clean beakers filled with seawater filtered over 0.2 μm filters. Colonies were incubated at ambient seawater temperature (21°C) for 3–4 h to allow self-cleaning of particles embedded in their gelatinous matrix. A total of 300 colonies with similar morphotypes were transferred individually into two 17L-Kreisel tank aquaria (JHT-17G, Exotic Aquaculture, Hong-Kong) filled with 0.2 μm filtered seawater and placed in two distinct thermostatic incubators set at 21°C (TC135S, Lovibond Water testing, United Kingdom). As treatments were performed in single experimental units (called pseudoreplication by Hurlbert, 1984), colonies were randomly placed in the two aquaria. Two liters of 0.2 μm filtered seawater from the Kreisel tanks were changed on a daily basis. Electroluminescent diode ramps (Easyled 6800 K°, Aquatlantis, Portugal) provided constant white light at 100 μmol photon m^{-2} s^{-1}. Colonies were further exposed to two thermal treatments during 3 days (T0, T1, and T2). In one aquarium, the control treatment (CT) remained at 21°C over the course of the experiment. In the other aquarium, the temperature of the stressed treatment (ST) was raised from 21°C (T0), to 25°C (T1) on the first day and then from 25°C to 28°C (T2) on the second day. The water temperature increased by 1°C per hour sufficiently in advance to enable a 12 h-acclimation before sampling. In the following text, a "condition" refers to the unique combination of a treatment and a sampling time point (e.g., CT-T0).

Phylogenetic Analysis

18S ribosomal DNA gene sequences from the Collodarian host and the dinoflagellate symbionts of 30 holobiont specimens collected during the experiment were retrieved from the transcriptome data (see details in **Supplementary Text 1**). Briefly, for each sample, host and symbiont sequences were aligned separately with reference sequences using MAFFT (Katoh et al., 2002). Phylogenetic trees were obtained using maximum likelihood reconstruction method in RAxML (Stamatakis, 2014), allowing the genetic identification of the host and the symbiont species.

Transmission Electron Microscopy (TEM)

For each condition, Collodarian specimens were collected in triplicates and independently fixed for 2 h at room temperature with 2.5% glutaraldehyde in a mix of cacodylate buffer (0.1 M, pH 7.4)/artificial seawater, then washed with 0.1 M cacodylate buffer (pH 7.4) and postfixed with 1% osmium tetroxide in cacodylate buffer containing 1% potassium ferrocyanide. Each samples were embedded in Epon resin after 10 min dehydration in 90% acetone and 2 baths of 10 min in acetone 100%. Ultrathin sections (70–80 nm) of colony parts were obtained using a diamond knife mounted on an ultramicrotome (Ultracut S, Leica) and placed on copper TEM grids coated with formvar film. To increase the contrast, the grids were treated with conventional uranyl acetate stain followed by lead citrate. Samples were observed under a JEOL JEM 1400 transmission electron microscope equipped with a CCD camera (Morada, Olympus SIS).

Oxygen Measurements

Oxygen consumption was measured using oxygen optodes, as described in Lilley et al. (2014). Each sample was made of two colonies incubated together in 5 mL tubes filled with filtered seawater and equipped with light-sensitive oxygen spots (PreSens Precision Sensing GmbH, Germany). For each condition, 6 measurements were made: 5 replicates and an additional control tube filled with 0.2 μm filtered seawater only that was used for blank corrections. This control tube therefore records the background respiration of the few organisms still present since neither 0.2 μm filtered seawater nor containers were sterile. After 30 min of dark-acclimation, oxygen was measured using a Fibox 3 optical oxygen meter (PreSens) every 20 min during 2 h. Light (100 μmol photon m^{-2} s^{-1}) was then switched on for 2 h and oxygen was measured again every 20 min for 2 h under light exposure.

After calibration, the phase delay measured by the sensor was converted into O_2 concentration (in μmol L^{-1}). Linear regressions between oxygen concentration against time were fitted through all data points for each replicate and for dark and light measurements separately. Values showing standardized residues <-1.5 and >1.5 were considered as outliers and removed from the dataset to ensure linearity (54 out of 384 measures). Slopes of the fitted regression gave individual consumption rates (μmol O_2 $L^{-1}h^{-1}$) and blank slopes were removed from experimental slopes to remove the water background respiration associated with the use of non–sterile water/containers [see Lilley et al. (2014)]. In all cases, this background O_2 change was negligible (average slope: 0.08) compared to the respiration/photosynthesis signal recorded (average slope: 0.21). Respiration rates were estimated as the slope during the dark experiment and gross photosynthesis rates were computed as differences of slopes between light (net photosynthesis) and dark. The respiration/photosynthesis signal recorded corresponds then to the net respiration and photosynthesis of the holobiont (including host, symbionts, and the associated microbiota). For normalization, rates were divided by the colony biomass estimated from binocular inspection (see the following morphological measurement methods). The Q_{10} temperature coefficient is the factor by which the reaction rate increases when the temperature is raised by ten degrees. It has been calculated using the following equation: $Q_{10} = \left(\frac{R_2}{R_1}\right)^{\left(\frac{10}{T_2-T_1}\right)}$ where R_1 and R_2 are the reaction rates at the corresponding temperatures T_1 and T_2.

Chlorophyll Fluorescence Measurements Coupled With Microscopy

For each condition, 5 collodarian colonies were transferred to cavity slides and maintained with a coverslip to prevent them from moving. For every 5 replicated colonies, photosynthetic parameters of individual symbiotic microalgae were measured on three different fields of observation using a Pulse Amplitude Modulated fluorometer coupled to a microscope (MICROSCOPY-PAM; Walz, Effeltrich, Germany), equipped with a 10 × objective lens. After the colonies were incubated in the dark for at least 5 min, the basal level of fluorescence (F_0) was measured under modulated light (9 μmol photons m^{-2} s^{-1}, frequency: 8 Hz at 625 nm), and a saturating light pulse (1707 μmol photons m^{-2} s^{-1}, during 8 × 60 ms at 625 nm) allowed determining the maximum fluorescence level (F_M). The Dark-adapted maximal quantum Yield (F_V/F_M) of photosystem II (PSII) was computed as follows:

$$F_V/F_M = (F_M - F_0)/F_M$$

The colonies were then exposed to actinic light (463 μmol photons m^{-2} s^{-1} at 625 nm) during 2 min followed by another saturating light pulse to measure the light-adapted PSII fluorescence yield (F_V'/F_M'; Genty et al., 1989). Pilot experiments and light curves were previously performed to determine the optimal duration of the dark incubation and actinic light intensity. The saturating pulse settings were adjusted according to preliminary experiments performed on cultures of *B. nutricula* (**Supplementary Text 2**).

For every colony, a number of 6 to 15 areas of interest, corresponding to single symbiotic cells, were selected on each picture (see **Supplementary Figure S1**). Outliers were removed when measured values were inconsistent (e.g., $F_V/F_M = 0$ or 1), being mostly due to field depth impairments. Overall, we obtained between 13 and 45 measurements for each of the 5 replicate colonies per experimental condition. To avoid bias due to these sampling size differences between conditions to compare, the F_V/F_M medians were computed for each microscopic field (3 microscopic fields per colony; 5 replicated colonies per condition).

Morphological Measurements

Images of all colonies used for oxygen and PAM fluorescence analyses were acquired under a binocular microscope (Zeiss Stemi SV11 mounted with an Olympus DP21 camera system) and analyzed using the ImageJ software (Rasband, 1997)[1]. Stressed colonies at sampling time 2 (ST-T2) were too degraded to be manipulated and observed under binocular microscope. For this

[1]https://imagej.nih.gov/ij/

specific condition, morphological measurements were performed for one colony and data are provided as indicative trends, while 13 to 17 replicates were accounted for other conditions. Correction factors were applied to normalize measurements in function of the different magnifications used to take each picture. On large field of view, we used image thresholding of ImageJ to measure full colonies area, width and we derived biovolume estimates from the prolate ellipsoid equation described in Biard et al. (2016). We also enumerated the total number of central capsules present on the observable part of the colonies using the automated cell count functionality of ImageJ. On zoomed in fields of view, we measured each central capsule area along with central capsule area covered by microalgal symbionts. As previously, we counted the total number of central capsules on the observable part of the colonies. We also enumerated the symbionts observed between central capsules (i.e., in the matrix) and measured their areas. At this magnification the symbiont cell area was homogeneous, we derived the number of symbionts per central capsule by dividing their total area by the average area of a symbiont ($3x10^{-4}mm^2$). Symbiont density was thus expressed as the number of symbionts per area. Carbon content was derived from the central capsule counts using a conversion factor of 131 ng C per capsule (Michaels et al., 1995).

Statistical Analysis

All the statistical analysis and associated figures were performed using R version 3.5.1 (R Core Team, 2013). For fluorescence and oxygen analyses, pairwise permutation tests from the rcompanion library have been used to test for significance of the interaction treatment-sampling time effect.

For symbiont density analysis, a *t*-test was applied to compare the regression slopes at each sampling time between the two treatments.

RESULTS

Colonies were identified as *Collozoum pelagicum* by phylogenetic analysis of the 18S rDNA gene sequences (NCBI accession MG907123, **Supplementary Figure S2**) onto a reference tree published in Biard et al. (2015). We were also able to retrieve 18S rDNA sequences of a dinoflagellate identified as *B. nutricula* by phylogenetic placement (NCBI accession MG905637, **Supplementary Figure S3**), confirming that *C. pelagicum* hosts *B. nutricula* as symbiotic algae.

C. pelagicum Morphological Changes Upon Heat Stress

Depending on colony size, an average of 800 (*SD* = 300) *C. pelagicum* cells were agglomerated in the gelatinous matrix, corresponding to an average density of 10 cells per mm^2 of colony surface. (**Table 1** and **Supplementary Table S1**). Cells were distributed in the matrix forming defined compartments (**Figure 1a**). Central capsules, appearing bright under the microscope (**Figure 1a**), exhibited a size ranging from 100 to 150 μm. Each central capsule contained a large electron dense droplet, an endoplasm and an ectoplasm (**Figure 1b**). Sudan Black staining suggested that this droplet, surrounded by a vacuolar membrane was constituted of fibrous elements and lipids. The endoplasm contained multiple nuclei displaying fibrillar nucleoplasm chord-like structures of chromatin attached to the inner surface of the nuclear membrane (**Figures 1c,d**). The endoplasm was delimited from the ectoplasm by a multiple layer membrane (**Figure 1e**).

Brandtodinium nutricula cells were always within cytoplasmic structures, either spread in the gelatinous matrix or closely associated to the central capsules (**Figures 1a,b**) and exhibited a thick cell wall and no flagella. *B. nutricula* were enclosed in a vacuole and separated from the *C. pelagicum* ectoplasm by a vacuolar membrane (**Figure 1f**). *B. nutricula* cells contained pyrenoid-bearing lobed chloroplasts, located essentially at the cell periphery, and associated with starch granules. Comparisons of phenotypes from control colonies (CT at 21°C) to heat stressed colonies (ST) at 3 sampling times (T0:21°C, T1:25°C, and T2:28°C) demonstrated that the general morphology of control colonies was preserved during the entire experiment. The polysaccharide matrix surrounded the evenly distributed central capsules and the compartments forming the colony remained visible (**Figures 2a,b**). In heat-stressed conditions, the central capsules from the colonies were still observable but irregularly distributed (**Figures 2c,d**). The gelatinous matrix was altered at 25°C and completely disorganized at 28°C, while colony compartments disappeared, being replaced by large bubbles inside the colonies (**Figure 2d**). With respect to ultrastructural features, ectoplasms were degraded, revealing large spaces around vacuoles, at T2 for CT colonies (**Figures 2e,f**) and earlier (from T1) in ST colonies (**Figure 2g**). Ectoplasm of ST-T2 colonies completely shrunk (**Figure 2h**). Compared to freshly collected specimens, both control and thermal stress experiments showed highly condensed chromatin in their nuclei, with an increase in electron-dense filaments (**Figures 1c,d**, **2i–l**).

Physiological Impact of Heat Stress on *C. pelagicum*

At seawater temperature, the respiration rate was of 3.94 (*SD* = 0.99) $\mu LO_2\ mgC^{-1}\ h^{-1}$ (**Table 1**, **Figure 3**, and **Supplementary Tables S1, S2**). The incubation conditions did not affect significantly the respiration rates in control colonies, with values of 4.58 (*SD* = 0.83) $\mu LO_2\ mgC^{-1}\ h^{-1}$ at T1 and 4.84 (*SD* = 1.25) $\mu LO_2\ ind^{-1}\ h^{-1}$ at T2. For heat-stressed colonies, the respiration rates slightly increased at 25°C, reaching 5.82 (*SD* = 1.62) $\mu LO_2\ mgC^{-1}\ h^{-1}$, and decreased markedly to 2.94 (*SD* = 1.56) $\mu LO_2\ mgC^{-1}\ h^{-1}$ at 28°C.

The experimental conditions induced a decrease of the average *B. nutricula* cell density, from nearly 80 symbionts mm^{-2} at T0 and T1, down to 59 symbionts mm^{-2} at T2, for control colonies (**Table 1** and **Figure 4**). The symbiont density decrease occurred significantly faster in heat-stress conditions with as few as 60 symbionts mm^{-2} at T1 (25°C) already. The regression line slopes between T0 and T1 were significantly different with a stronger drop in symbiont densities in stressed colonies compared to controls (*p*-value = 0.05). At T2 (28°C), symbiont density kept decreasing down to 50 symbionts mm^{-2}, but the reaction norm

TABLE 1 | Summary of the statistics of the morphological and physiological measurements in control (CT) and heat-stressed (ST) colonies of *Collozoum pelagicum* at 3 sampling times (T0, T1, and T2).

Sampling time	Treatment	Central capsule density (nb/mm_2)	Central capsule average size (mm_2)	Holobiont biovolume (mm^3)	Symbiont density (nb/mm_2)	Respiration rate (µl O2.mgC-1.h-1)	Photosynthesis rate (µl O2.mgC-1.h-1)	Fv/Fm
T0	CT	9 ± 2 (*n* = 16)	0.017 ± 0.004 (*n* = 16)	135 ± 49 (*n* = 16)	74 ± 17 (*n* = 16)	3,9 ± 1 (*n* = 4)	4,4 ± 2 (*n* = 4)	0.569 ± 0.021 (*n* = 6)
T1	CT	10 ± 1 (*n* = 13)	0.018 ± 0.004 (*n* = 13)	164 ± 38 (*n* = 13)	81 ± 20 (*n* = 13)	4,6 ± 0,8 (*n* = 5)	4,2 ± 0,7 (*n* = 5)	0.578 ± 0.017 (*n* = 5)
T1	ST	10 ± 1 (*n* = 14)	0.016 ± 0.004 (*n* = 14)	120 ± 57 (*n* = 15)	60 ± 9 (*n* = 14)	4,8 ± 1,3 (*n* = 4)	3,3 ± 1,3 (*n* = 4)	0.603 ± 0.04 (*n* = 5)
T2	CT	12 ± 3 (*n* = 15)	0.015 ± 0.003 (*n* = 15)	159 ± 31 (*n* = 14)	59 ± 17 (*n* = 15)	5,8 ± 1,6 (*n* = 5)	3,5 ± 1,8 (*n* = 5)	0.591 ± 0.035 (*n* = 5)
T2	ST	6 (*n* = 1)	0.022 (*n* = 1)	114 (*n* = 1)	50 (*n* = 1)	2,9 ± 1,6 (*n* = 5)	4,1 ± 0,8 (*n* = 5)	0.584 ± 0.052 (*n* = 5)

Average, standard deviation and sample size (n) were obtained from the full dataset presented in ***Supplementary Tables S1–S3****.*

slopes were not significantly different from the control conditions between T1 and T2 (**Table 1** and **Figure 4**). The *B. nutricula* cells were mainly located in the vicinity of the central capsules, with nearly 8% of the symbionts found in the cytoplasmic extension throughout the gelatinous matrix. During our experiment, the symbiont density varied nearby the central capsule but remained stable for those in the matrix (**Figure 4**).

With respect to photosynthetic parameters, we first measured the oxygen production of entire colonies to globally estimate their overall photosynthesis, then we carried out fluorometric measurements coupled to microscopy to evaluate the photosynthetic efficiency of photosystem II for individual symbiotic cells. Both methods demonstrated that the photosynthetic apparatus was not impacted by neither the stalling nor the thermal stress conditions. Photosynthetic rates remained stable at about 4 $\mu LO_2\ mgC^{-1}\ h^{-1}$ with no significant changes across all conditions (**Table 1**, **Figure 5a**, and **Supplementary Tables S1, S2**) and the maximal photosystem II quantum yield (F_V/F_M) average was 0.58 (*SD* = 0.04), a nearly optimal value for phytoplanktonic cells (**Table 1**, **Figure 5b**, and **Supplementary Tables S1, S3**). No photoprotective processes of energy dissipation were observed (**Supplementary Tables S1, S3**). Coupling fluorometry analysis to microscopy enabled to measure individual cells photosynthetic capacities. The PAM microscopy analysis thus revealed that at CT-T2 and during the entire heat-stress experiment, the number of observed *B. nutricula* cells per microscopic field decreased, as also suggested by the symbiont density counts. During the experiment, we also observed that the variability of the F_V/F_M increased both within colonies and between colonies, particularly in the stressed treatment where the coefficient of variation significantly increased from T0 to T1 and T2 (**Figure 5b**, **Supplementary Figure S4**, and **Supplementary Tables S1, S4**).

Symbionts Morphological Changes

TEM micrographs were used to monitor ultrastructural changes of the symbiotic *B. nutricula* cells. In control colonies, vacuolar structures containing filamentous particles were observed in cells at T1 (**Figure 6a** and **Supplementary Figure S5**). At T2, these filamentous particles were still present and electron-dense bodies containing membrane-packaged cellular debris appeared within the symbiotic cells (**Figure 6b**) but nuclei as well as chloroplast ultrastructure remained preserved (**Supplementary Figure S6**).

In thermally stressed colonies, filamentous particles were also observed but to a lesser extent. Instead, an important vacuolization around the *B. nutricula* cells, thylakoid disorganization, nucleus dissolution and destabilized organelles structures were observed at 25°C (**Figure 6c**), suggesting autophagic processes. At 28°C, the *B. nutricula* cells from heat-stressed colonies showed marked necrosis patterns with numerous apoptotic bodies and their cellular content appeared completely shrunk, with abundant electron-dense bodies (**Figure 6d**). Inside decaying symbiotic cells, chloroplasts were the only healthy looking organelles, consistent with the maintenance of the photosynthetic capacities observed in the physiological study (**Figure 6** and **Supplementary Figure S6**).

DISCUSSION

Bleaching is commonly described in the phylum Cnidaria as a loss of color originating in the exclusion of the symbiotic dinoflagellates (i.e., genus *Symbiodinium*) from the animal, and/or the degradation of photosynthetic pigments in the chloroplasts of the symbionts (Douglas, 2003). Bleaching has also been shown to occur in the benthic protists Foraminifera (Rhizaria) hosting symbiotic diatoms (Schmidt et al., 2011; Edgar et al., 2013). Here, as symbionts were lightly arranged around the central capsule, the color loss was not detectable to the naked eye, but we observed a decrease of the dinoflagellate symbiont (*B. nutricula*) density in the planktonic species *C. pelagicum* (Collodaria, Retaria) during a heat stress experiment. This study shows that bleaching processes, as initially defined by Kleppel et al. (1989), are not restricted to benthic fauna, but likely constitute a broader stress response in marine organisms harboring photosymbionts. *C. pelagicum* belongs to the most diverse and abundant collodarian clade C7 from the Sphaerozoidae family, which is particularly dominant in coastal

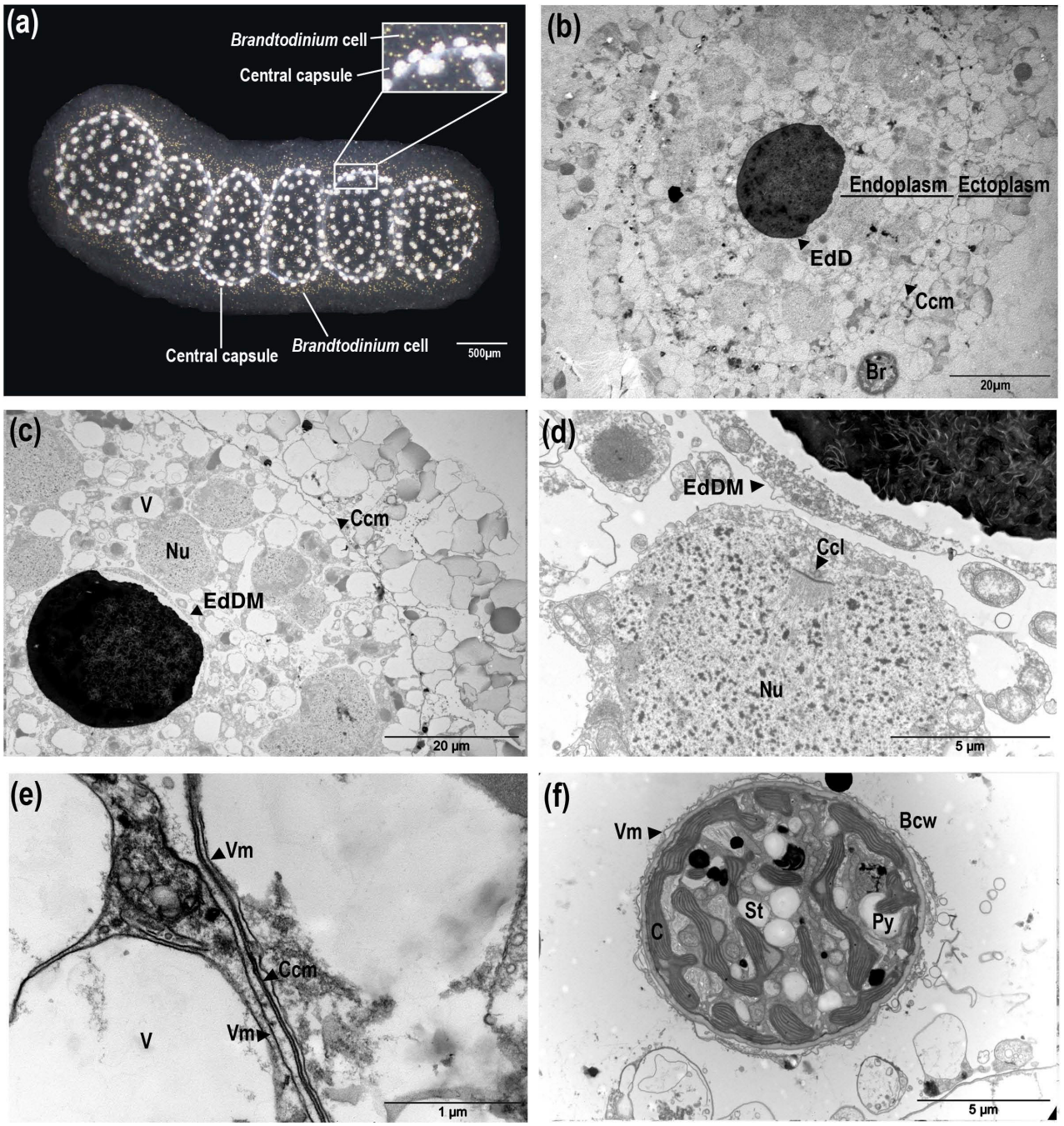

FIGURE 1 | Description of *Collozoum pelagicum* morphology and ultrastructure. *Collozoum pelagicum* colony morphological aspect by binocular observation **(a)**. Observation of the general organization of a central capsule observed by Transmission Electron Microscopy **(b,c)**. Focus on nuclei in the endoplasm of the central capsule **(d)**, membranes at the periphery of the central capsule **(e)** and *in hospite Brandtodinium nutricula* cells **(f)**, observed by electron microscopy. Bcw, *B. nutricula* cell wall; C, Chloroplast; Ccl, cord-like Chromatin; Ccm, Central capsule membrane; EdD, Electron-dense Droplet; EdDM, Electron-dense Droplet Membrane; Nu, Nuclei; Py, Pyrenoid; St, Starch granule; V, Vacuole; Vm, Vacuolar membrane.

biomes and in the western part of the Mediterranean Sea (Biard et al., 2017), stressing out the potential ecological impact of such symbiont loss events in the environment.

Although we cannot exclude that cellular processes involved in the symbiont loss can be radically distinct among different taxa, one might consider that, as described for cnidarians (Weis, 2008), the decrease of symbiont density in *C. pelagicum* could originate in the digestion and/or expulsion of *B. nutricula* cells. Indeed, it has been shown that, under standard conditions, cnidarians continuously expel degraded forms of *Symbiodinium*

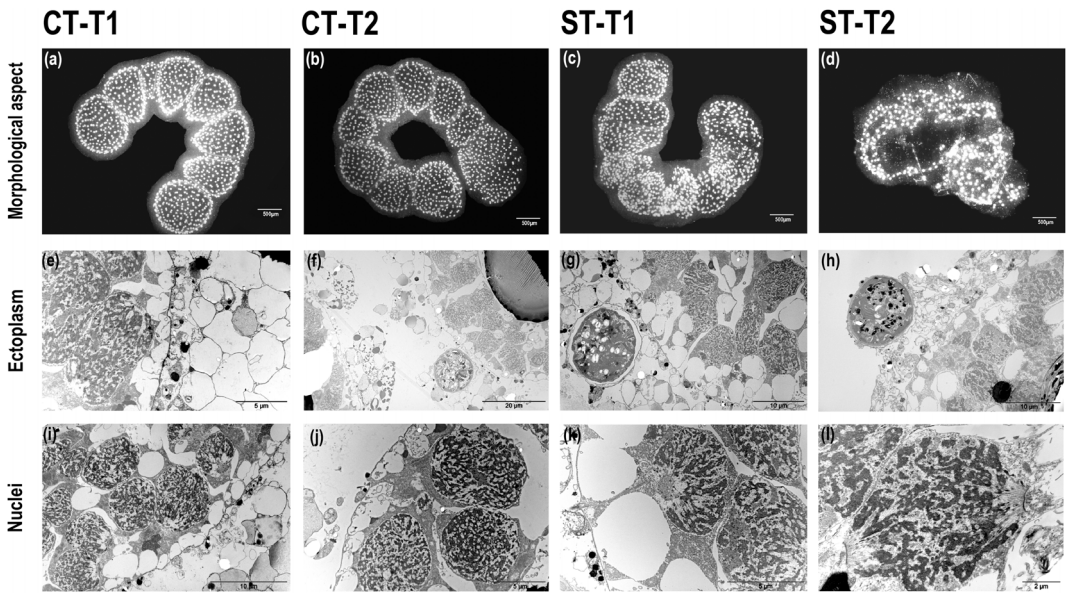

FIGURE 2 | Morphological and ultrastructural changes in control and heat-stressed *Collozoum pelagicum*. Observation of colonies overall morphological aspect at control T1 **(a)** and control T2 **(b)** at 21°C, thermal stress T1 at 25°C **(c)** and thermal stress T2 at 28°C **(d)**. Focus on the ultrastructure of ectoplasm at control T1 **(e)**, control T2 **(f)**, thermal stress T1 **(g),** and thermal stress T2 **(h)**. Focus on the nuclei ultrastructure at control T1 **(i)** and control T2 **(j)**, thermal stress T1 **(k)**, and thermal stress T2 **(l)** arrows.

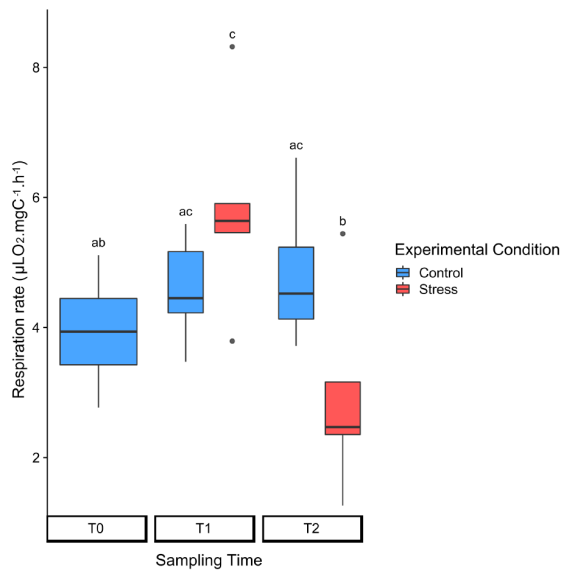

FIGURE 3 | Normalized respiration rates in control (blue) and heat-stressed (red) colonies of *Collozoum pelagicum*. The rates are normalized to the surface area of the colony. Control colonies were maintained at 21°C, while stressed colonies were sampled at 25°C (T1) and 28°C (T2). Pairwise comparison from permutation test between each condition was represented by letters. Statistical supports are described in **Supplementary Tables 1, 4A**.

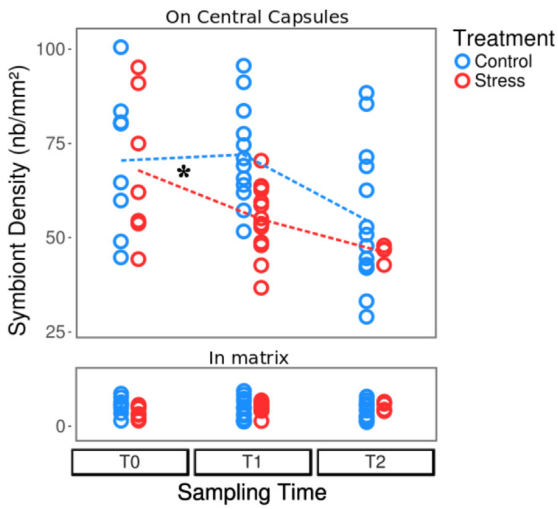

FIGURE 4 | Variations of the symbiont density in control (blue) and heat-stressed colonies (red) of *Collozoum pelagicum*. Control colonies were maintained at 21°C, while stressed colonies were sampled at 21°C (T0), 25°C (T1) and 28°C (T2). The upper and bottom parts represent the density of symbionts attached to central capsules and in the gelatinous matrix, respectively. As indicated by a star, slopes of reaction norms for symbionts from central capsule (represented as dotted lines) were significantly different between T0 and T1 (p-value < 0.025), but not between T1 and T2. Statistical supports are described in **Supplementary Tables 1, 4B,C**.

cells to maintain a healthy population in symbiosis, whereas in stress conditions healthy algal cells are also released in the environment (Ralph et al., 2001; Fujise et al., 2014). In our study, the number of *B. nutricula* cells located at the vicinity of the central capsules decreased, but symbiont density in the gelatinous matrix remained constant. Assuming that expulsion of

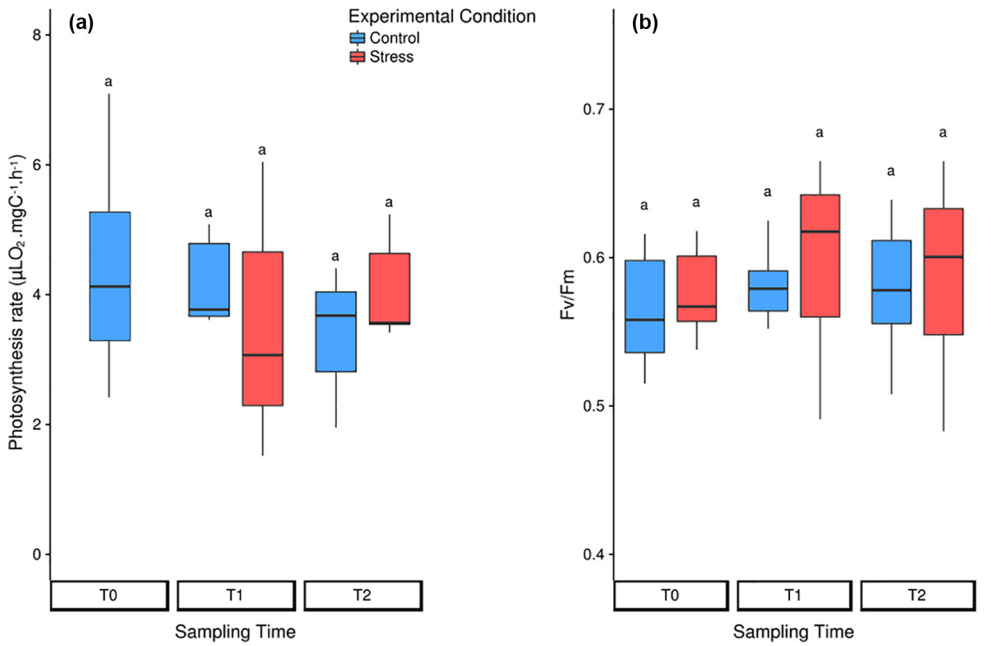

FIGURE 5 | Photosynthetic rates of the symbionts in control (blue) and heat-stressed (red) colonies of *Collozoum pelagicum*. **(a)** Box-plots of photosynthesis rates measured by oxygen production, when normalized by the symbiont surface of the colony. **(b)** Box-plots of PAM-microscopy measurements. Pairwise comparison from permutation test between each condition was represented by letters. Statistical supports are described in **Supplementary Tables 1, 4D,E**.

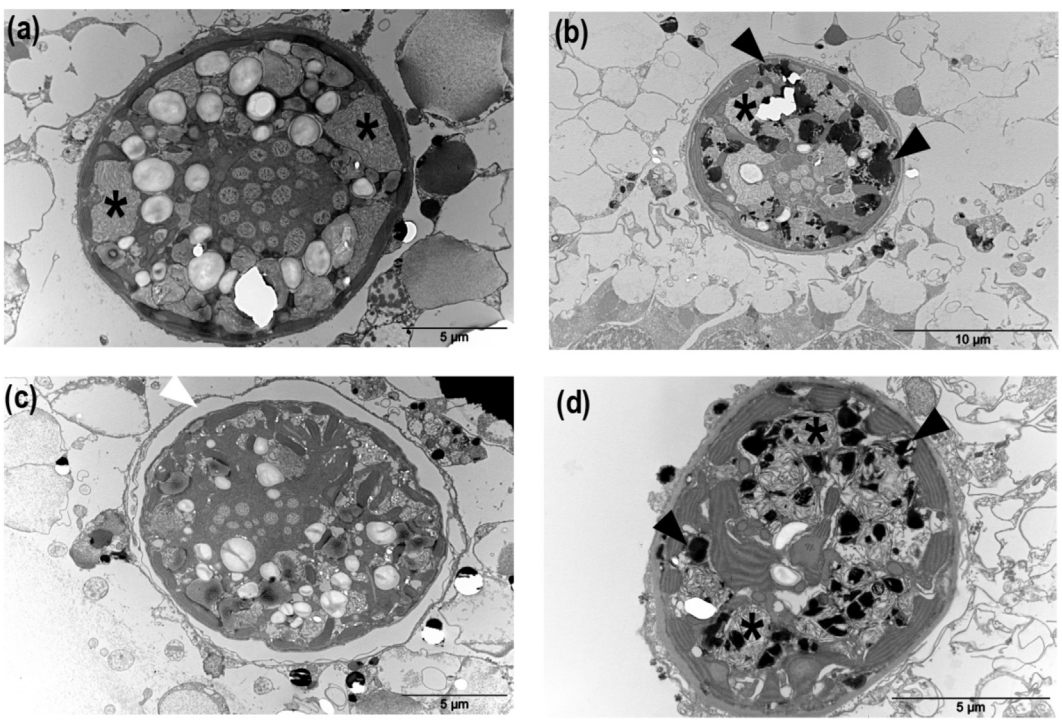

FIGURE 6 | Morphological structures corresponding to the main cellular responses induced in *in hospite B. nutricula* cells in control and heat-stressed colonies of *Collozoum pelagicum*. Transmission electron microscopy of *C. pelagicum* cross section in control T1 **(a)**, control T2 **(b)** at 21°C, and thermal stress T1 at 25°C **(c)** and thermal stress T2 at 28°C **(d)**. Asterisks: filamentous particles, black triangles: apoptotic bodies, white triangles: vacuolar matrix.

B. nutricula cells requires to go through the gelatinous matrix, an increased density would have been expected.

In our study, the respiration rate increase between 21 and 25°C could be related to symbiont digestion. The estimated temperature coefficient Q_{10} for *C. pelagicum* reached the value of 2.66, falling into the Q_{10} range of 2 to 3 estimated for zooplankton (Hernández-León and Ikeda, 2005; Ikeda, 2014). Respiration rate increase as a function of temperature has already been reported in a large panel of zooplankton groups such as Rhizaria, Copepods, Tintinnids (Vidal, 1980; Verity, 1985; Lombard et al., 2005) and could be due to several processes. The global rates of chemical reactions generally increase with temperature (Arrhenius, 1889) and, until enzymatic structure is altered, most biological enzymatic processes require oxygen, so that oxygen demand usually increases with temperature. Also, higher temperatures likely enhance the growth of prokaryotes associated to the host and in turn could contribute to a not negligible part of the holobiont respiration (del Giorgio et al., 1997). Finally, it has also been shown that digestion increases the respiration rate of organisms (Conover, 1978).

Looking at the ultrastructure to characterize the observed bleaching process, all *B. nutricula* cells inside the hosts showed signs of programmed cell death (PCD) mechanisms, such as autophagy (vacuolization) or apoptosis (cell shrinkage, chromatin condensation), suggesting overall cell decay. Apoptosis is triggered by a series of controlled cellular processes involving caspases, which cleave key proteins, cytoskeletal elements and cell adhesion molecules (Dunn et al., 2007). In the autophagic pathway, the target is enveloped in a membrane structure before lysosomal fusion, which initiates digestion by hydrolytic enzymes (Cuervo, 2004). Both apoptosis and autophagy have been observed during cnidarian bleaching and can occur simultaneously (Dunn et al., 2007) or alternatively in response to hyperthermal stress (Richier et al., 2006; Dani et al., 2016). In addition, another process related to symbiotic dinoflagellate autophagy has been reported in cnidarians and is referred to as "symbiophagy," which results in the digestion of the resident dinoflagellates (Downs et al., 2009). TEM observations in *C. pelagicum* suggested that a similar diversity of PCD-like mechanisms would be involved in planktonic symbiosis breakdown. Originally reported in metazoans, PCD-like mechanisms have also been described in phytoplankton in the case of nutrient stress and could occur during viral infections (see review by Bidle, 2015).

Our observations also evidenced the presence of filamentous structures, probably virus-like particles (VLPs), potentially involved in the collapsing of *B. nutricula* cells, whose features appeared similar to the single stranded RNA viruses previously described in *Symbiodinium* cells (Weynberg et al., 2017; Buerger and van Oppen, 2018). These authors indeed proposed that the cnidarian endosymbiont *Symbiodinium* harbors a lysogenic virus within its genome that would induce a lytic infection cycle under stressed conditions. Such lysis of symbiotic dinoflagellates by viruses supports the microbial bleaching hypothesis, which suggests that bleaching could be initiated by the microbial community shift induced by heat-stress (Correa et al., 2016; Thurber et al., 2017). Levin et al. (2017) also described that only thermosensitive *Symbiodinium* showed a marked transcriptional response to viral infection when heat stressed. To our knowledge, only one study has described large icosahedral virus-like particles associated with vacuolar structures in phaeodarians, a taxonomic group close to radiolarians, within the Rhizaria lineage (Gowing, 1993). This study suggests that VLPs could have been acquired by the host through feeding on sinking particles, while in our case, it seems that the viral attack was restricted to the *B. nutricula* cells.

Viral infections in marine algae have been shown to promote ROS activity, triggering subsequent caspase activity and further PCD processes in host cells (Bidle and Vardi, 2011; Bidle, 2015). Nevertheless, as ROS could also be generated by the over-reduction of photosystem I reaction centers (Roberty et al., 2015) during the thermal stress, it was not possible to attribute the cause of the observed PCD directly to the abiotic stress or as a consequence of the pathogen pressure. Weynberg et al. (2017) observed that if nuclear structures were rapidly degraded by virus infection, other organelles like chloroplasts and mitochondria remained almost intact until infectious particles filled the entire cell structure. This is consistent with our observation showing that chloroplasts remained morphologically intact and active, even though other *B. nutricula* organelles were severely damaged. Both oxygen production and fluorometry measurements demonstrated that photosynthesis rates were not altered by heat stress as *B. nutricula* photosynthetic efficiencies remained globally stable. The increased variability of individual photosynthetic efficiencies during heat-stress treatments suggests that healthy *B. nutricula* could compensate for damaged symbionts so as to buffer the holobiont photosynthetic activity.

Based on our observations (e.g., respiration virtually stopped, morphological structure altered), a temperature of 28°C (i.e., T2) likely exceeded the *C. pelagicum* colonies tolerance threshold. The pronounced thermal stress we applied in our experiment aimed at observing and characterizing a marked response of the symbiotic system, likely preventing the potentially existing acclimation period required for the host plastic response. The free-living stage of the microalgal symbionts *B. nutricula* tolerates temperatures up to 29°C when grown in batch culture, displaying relatively high growth rates and photosynthetic efficiency (**Supplementary Figure S7**). *Symbiodinium* physiology was also more affected by heat stress when in symbiosis with corals than when maintained free-living in culture (Buxton et al., 2009). Photosymbiosis induces critical symbiont morphological and physiological changes (i.e., loss of motility) likely leading to a greater sensitivity when host protection is altered and prevent buffering external stressors.

In this study, we show that *C. pelagicum* can exhibit heat-induced bleaching. We unveiled several features of the processes, such as host cells degradation, partial digestion and potential viral infection of the *B. nutricula* cells, while the chloroplast was clearly the last structure to remain active. These results raise questions regarding the underlying cellular processes involved in symbiont loss in *C. pelagicum* and preservation mechanisms of chloroplast activity during *B. nutricula* cell collapsing. Further analysis using complementary approaches like transcriptomics or metabolomics would certainly be helpful to decipher more

precisely the *C. pelagicum* holobiont response to elevated temperatures.

AUTHOR CONTRIBUTIONS

EV, MM-S, CB, EB, TL, and FN performed the experiments. EV performed the PAM fluorometry measurements, image analyses, the statistical treatments and wrote the manuscript. VD contributed to the TEM analyses and manuscript writing. MM-S performed the oxygen measurements. CB performed the sequence analyses. CB, FL, CSi, CSa, and FN commented and contributed to the final version of the manuscript. FN planned and designed the research.

FUNDING

This work benefited from the support of the projects IMPEKAB ANR-15-CE02-0011 and inSIDE ANR-12-JSV7-0009-01 of the French National Research Agency (ANR). This research was supported by the research infrastructure EMBRC-Fr (www.embrc-france.fr). CB received funding from the European Union's Horizon 2020 research and innovation program under the Marie Skłodowska-Curie grant agreement no. 706430 (DYNAMO).

ACKNOWLEDGMENTS

The authors greatly acknowledge the Centre Commun de Microscopie Appliquée (Université Côte d'Azur), especially Sophie Pagnotta who performed the TEM image acquisitions. The authors acknowledge the members of Villefranche-sur-mer oceanological observatory for their help during the experimental work, especially Simon Ramondenc, Guillaume de Liege, David Luquet, Sophie Marro, and Régis Lasbleiz. The manuscript was deposited before peer-review on the pre-print server biorXiv (Villar et al., 2018).

SUPPLEMENTARY MATERIAL

The Supplementary Material for this article can be found online at: https://www.frontiersin.org/articles/10.3389/fmars.2018.00387/full#supplementary-material

REFERENCES

Anderson, O. R. (1976a). Fine structure of a collodarian radiolarian (*Sphaerozoum punctatum* Müller 1858) and cytoplasmic changes during reproduction. *Mar. Micropaleontol.* 1, 287–297. doi: 10.1016/0377-8398(76)90012-8

Anderson, O. R. (1976b). Ultrastructure of a colonial radiolarian *Collozoum inerme* and a cytochemical determination of the role of its zooxanthellae. *Tissue Cell* 8, 195–208. doi: 10.1016/0040-8166(76)90046-X

Anderson, O. R. (1983). *Radiolaria*. New York, NY: Springer New York, doi: 10.1007/978-1-4612-5536-9

Anderson, O. R., Swanberg, N. R., and Bennett, P. (1983). Assimilation of symbiont-derived photosynthates in some solitary and colonial radiolaria. *Mar. Biol.* 77, 265–269. doi: 10.1007/BF00395815

Arrhenius, S. (1889). Über die Reaktionsgeschwindigkeit bei der Inversion von Rohrzucker durch Säuren. *Z. Phys. Chem.* 4, 226–248. doi: 10.1515/zpch-1889-0116

Baghdasarian, G., and Muscatine, L. (2000). Preferential expulsion of dividing algal cells as a mechanism for regulating algal-cnidarian symbiosis. *Biol. Bull.* 199, 278–286. doi: 10.2307/1543184

Baird, A. H., Bhagooli, R., Ralph, P. J., and Takahashi, S. (2009). Coral bleaching: the role of the host. *Trends Ecol. Evol.* 24, 16–20. doi: 10.1016/j.tree.2008.09.005

Biard, T., Bigeard, E., Audic, S., Poulain, J., Gutierrez-Rodriguez, A., Pesant, S., et al. (2017). Biogeography and diversity of Collodaria (Radiolaria) in the global ocean. *ISME J.* 11, 1331–1344. doi: 10.1038/ismej.2017.12

Biard, T., Pillet, L., Decelle, J., Poirier, C., Suzuki, N., and Not, F. (2015). Towards an integrative morpho-molecular classification of the Collodaria (Polycystinea, Radiolaria). *Protist* 166, 374–388. doi: 10.1016/j.protis.2015.05.002

Biard, T., Stemmann, L., Picheral, M., Mayot, N., Vandromme, P., Hauss, H., et al. (2016). In situ imaging reveals the biomass of giant protists in the global ocean. *Nature* 532, 504–507. doi: 10.1038/nature17652

Bidle, K. D. (2015). The molecular ecophysiology of programmed cell death in marine phytoplankton. *Annu. Rev. Mar. Sci.* 7, 341–375. doi: 10.1146/annurev-marine-010213-135014

Bidle, K. D., and Vardi, A. (2011). A chemical arms race at sea mediates algal host–virus interactions. *Curr. Opin. Microbiol.* 14, 449–457. doi: 10.1016/j.mib.2011.07.013

Buerger, P., and van Oppen, M. J. H. (2018). Viruses in corals: hidden drivers of coral bleaching and disease? *Microbiol. Aust.* 2:4. doi: 10.1071/MA18004

Buxton, L., Badger, M., and Ralph, P. (2009). Effects of moderate heat stress and dissolved inorganic carbon concentration on photosynthesis and respiration of *Symbiodinium* Sp. (dinophyceae) in culture and in symbiosis. *J. Phycol.* 45, 357–365. doi: 10.1111/j.1529-8817.2009.00659.x

Cikala, M., Wilm, B., Hobmayer, E., Böttger, A., and David, C. N. (1999). Identification of caspases and apoptosis in the simple metazoan Hydra. *Curr. Biol.* 9, 959–962. doi: 10.1016/S0960-9822(99)80423-0

Conover, R. (1978). "Transformation of organic matter," in *Marine Ecology, Dynamics*, Vol. 4, ed. O. Kinne (New York, NY: Wiley), 221–499.

Correa, A. M. S., Ainsworth, T. D., Rosales, S. M., Thurber, A. R., Butler, C. R., and Vega Thurber, R. L. (2016). Viral outbreak in corals associated with an in situ bleaching event: atypical herpes-like viruses and a new Megavirus infecting *Symbiodinium*. *Front. Microbiol.* 7:127. doi: 10.3389/fmicb.2016.00127

Cuervo, A. M. (2004). Autophagy: many paths to the same end. *Mol. Cell. Biochem.* 263, 55–72. doi: 10.1023/B:MCBI.0000041848.57020.57

Dani, V., Priouzeau, F., Pagnotta, S., Carette, D., Laugier, J.-P., and Sabourault, C. (2016). Thermal and menthol stress induce different cellular events during sea anemone bleaching. *Symbiosis* 69, 175–192. doi: 10.1007/s13199-016-0406-y

Decelle, J., Colin, S., and Foster, R. A. (2015). "Photosymbiosis in marine planktonic protists," in *Marine Protists*, eds S. Ohtsuka, T. Suzaki, T. Horiguchi, N. Suzuki, and F. Not (Tokyo: Springer), 465–500. doi: 10.1007/978-4-431-55130-0_19

del Giorgio, P. A., Cole, J. J., and Cimbleris, A. (1997). Respiration rates in bacteria exceed phytoplankton production in unproductive aquatic systems. *Nature* 385, 148–151. doi: 10.1038/385148a0

Douglas, A. E. (2003). Coral bleaching—how and why? *Mar. Pollut. Bull.* 46, 385–392. doi: 10.1016/S0025-326X(03)00037-7

Downs, C. A., Kramarsky-Winter, E., Martinez, J., Kushmaro, A., Woodley, C. M., Loya, Y., et al. (2009). Symbiophagy as a cellular mechanism for coral bleaching. *Autophagy* 5, 211–216. doi: 10.4161/auto.5.2.7405

Dunn, S. R., Schnitzler, C. E., and Weis, V. M. (2007). Apoptosis and autophagy as mechanisms of dinoflagellate symbiont release during cnidarian bleaching: every which way you lose. *Proc. R. Soc. B Biol. Sci.* 274, 3079–3085. doi: 10.1098/rspb.2007.0711

Edgar, K. M., Bohaty, S., Gibbs, S., Sexton, P., Norris, R., and Wilson, P. (2013). Symbiont 'bleaching'in planktic foraminifera during the Middle Eocene Climatic Optimum. *Geology* 41, 15–18. doi: 10.1130/G33388.1

Fujise, L., Yamashita, H., Suzuki, G., Sasaki, K., Liao, L. M., and Koike, K. (2014). Moderate thermal stress causes active and immediate expulsion of

photosynthetically damaged zooxanthellae (*Symbiodinium*) from corals. *PLoS One* 9:e114321. doi: 10.1371/journal.pone.0114321

Genty, B., Briantais, J.-M., and Baker, N. R. (1989). The relationship between the quantum yield of photosynthetic electron transport and quenching of chlorophyll fluorescence. *Biochim. Biophys. Acta* 990, 87–92. doi: 10.1016/S0304-4165(89)80016-9

Glynn, P. W. (1984). Widespread coral mortality and the 1982–83 el Niño warming event. *Environ. Conserv.* 11, 133–146. doi: 10.1017/S0376892900013825

Gowing, M. M. (1993). Large virus-like particles from vacuoles of phaeodarian radiolarians and from other marine samples. *Mar. Ecol. Prog. Ser.* 101, 33–43. doi: 10.3354/meps101033

Guidi, L., Chaffron, S., Bittner, L., Eveillard, D., Larhlimi, A., Roux, S., et al. (2016). Plankton networks driving carbon export in the oligotrophic ocean. *Nature* 532, 465–470. doi: 10.1038/nature16942

Haeckel, E. (1887). "Report on Radiolaria collected by HMS Challenger during the years 1873-1876. Volume XVIII (Part 1) p. xcix-c," in *The Voyage of HMS Challenger*, eds C. W. Thompson and J. Murray (London: Her Majesty's Stationary Office).

Hernández-León, S., and Ikeda, T. (2005). *Zooplankton Respiration. Respiration in Aquatic Systems*. New York, NY: Oxford University Press, 57–82.

Hoegh-Guldberg, O., Mumby, P. J., Hooten, A. J., Steneck, R. S., Greenfield, P., Gomez, E., et al. (2007). Coral reefs under rapid climate change and ocean acidification. *Science* 318, 1737–1742. doi: 10.1126/science.1152509

Hurlbert, S. H. (1984). Pseudoreplication and the design of ecological field experiments. *Ecol. Monogr.* 54, 187–211. doi: 10.2307/1942661

Ikeda, T. (2014). Respiration and ammonia excretion by marine metazooplankton taxa: synthesis toward a global-bathymetric model. *Mar. Biol.* 161, 2753–2766. doi: 10.1007/s00227-014-2540-5

Katoh, K., Misawa, K., Kuma, K., and Miyata, T. (2002). MAFFT: a novel method for rapid multiple sequence alignment based on fast Fourier transform. *Nucleic Acids Res.* 30, 3059–3066. doi: 10.1093/nar/gkf436

Kleppel, G., Dodge, R. E., and Reese, C. (1989). Changes in pigmentation associated with the bleaching of stony corals. *Limnol. Oceanogr.* 34, 1331–1335. doi: 10.4319/lo.1989.34.7.1331

Lesser, M. P. (2006). Oxidative stress in marine environments: biochemistry and physiological ecology. *Annu. Rev. Physiol.* 68, 253–278. doi: 10.1146/annurev.physiol.68.040104.110001

Lesser, M. P. (2011). "Coral Bleaching: Causes and Mechanisms," in *Coral Reefs: An Ecosystem in Transition*, eds Z. Dubinsky and N. Stambler (Dordrecht: Springer), 405–419. doi: 10.1007/978-94-007-0114-4_23

Levin, R. A., Voolstra, C. R., Weynberg, K. D., and van Oppen, M. J. H. (2017). Evidence for a role of viruses in the thermal sensitivity of coral photosymbionts. *ISME J.* 11, 808–812. doi: 10.1038/ismej.2016.154

Lilley, M. K. S., Thibault-Botha, D., and Lombard, F. (2014). Respiration demands increase significantly with both temperature and mass in the invasive ctenophore *Mnemiopsis leidyi*. *J. Plankton Res.* 36, 831–837. doi: 10.1093/plankt/fbu008

Logan, C. A., Dunne, J. P., Eakin, C. M., and Donner, S. D. (2014). Incorporating adaptive responses into future projections of coral bleaching. *Glob. Chang. Biol.* 20, 125–139. doi: 10.1111/gcb.12390

Lombard, F., Sciandra, A., and Gorsky, G. (2005). Influence of body mass, food concentration, temperature and filtering activity on the oxygen uptake of the appendicularian *Oikopleura dioica*. *Mar. Ecol. Prog. Ser.* 301, 149–158. doi: 10.3354/meps301149

Michaels, A. F., Caron, D. A., Swanberg, N. R., Howse, F. A., and Michaels, C. M. (1995). Planktonic sarcodines (Acantharia, Radiolaria, Foraminifera) in surface waters near Bermuda: abundance, biomass and vertical flux. *J. Plankton Res.* 17, 131–163. doi: 10.1093/plankt/17.1.131

Paxton, C. W., Davy, S. K., and Weis, V. M. (2013). Stress and death of cnidarian host cells play a role in cnidarian bleaching. *J. Exp. Biol.* 216, 2813–2820. doi: 10.1242/jeb.087858

Probert, I., Siano, R., Poirier, C., Decelle, J., Biard, T., Tuji, A., et al. (2014). *Brandtodinium* gen. nov. and B. nutricula comb. Nov. (Dinophyceae), a dinoflagellate commonly found in symbiosis with polycystine radiolarians. *J. Phycol.* 50, 388–399. doi: 10.1111/jpy.12174

R Core Team (2013). *R: A Language and Environment for Statistical Computing*. Vienna: R Foundation for Statistical Computing.

Ralph, P. J., Gademann, R., and Larkum, A. W. (2001). Zooxanthellae expelled from bleached corals at 33°C are photosynthetically competent. *Mar. Ecol. Prog. Ser.* 220, 163–168. doi: 10.3354/meps220163

Rasband, W. (1997). *ImageJ*. Bethesda, MD: US National Institutes of Health.

Richier, S., Sabourault, C., Courtiade, J., Zucchini, N., Allemand, D., and Furla, P. (2006). Oxidative stress and apoptotic events during thermal stress in the symbiotic sea anemone, *Anemonia viridis*. *FEBS J.* 273, 4186–4198. doi: 10.1111/j.1742-4658.2006.05414.x

Roberty, S., Fransolet, D., Cardol, P., Plumier, J.-C., and Franck, F. (2015). Imbalance between oxygen photoreduction and antioxidant capacities in Symbiodinium cells exposed to combined heat and high light stress. *Coral Reefs* 34, 1063–1073. doi: 10.1007/s00338-015-1328-5

Schmidt, C., Heinz, P., Kucera, M., and Uthicke, S. (2011). Temperature-induced stress leads to bleaching in larger benthic foraminifera hosting endosymbiotic diatoms. *Limnol. Oceanogr.* 56, 1587–1602. doi: 10.4319/lo.2011.56.5.1587

Stamatakis, A. (2014). RAxML version 8: a tool for phylogenetic analysis and post-analysis of large phylogenies. *Bioinformatics* 30, 1312–1313. doi: 10.1093/bioinformatics/btu033

Swanberg, N. R. (1983). The trophic role of colonial Radiolaria in oligotrophic oceanic environments1,2. *Limnol. Oceanogr.* 28, 655–666. doi: 10.4319/lo.1983.28.4.0655

Thurber, R. V., Payet, J. P., Thurber, A. R., and Correa, A. M. S. (2017). Virus–host interactions and their roles in coral reef health and disease. *Nat. Rev. Microbiol.* 15, 205–216. doi: 10.1038/nrmicro.2016.176

Verity, P. G. (1985). Grazing, respiration, excretion, and growth rates of tintinnids. *Limnol. Oceanogr.* 30, 1268–1282. doi: 10.4319/lo.1985.30.6.1268

Vidal, J. (1980). Physioecology of zooplankton. IV. Effects of phytoplankton concentration, temperature, and body size on the net production efficiency of *Calanus pacificus*. *Mar. Biol.* 56, 203–211. doi: 10.1007/BF00645344

Villar, E., Dani, V., Bigeard, E., Linhart, T., Mendez-Sandin, M., Bachy, C., et al. (2018). Chloroplasts of symbiotic microalgae remain active during bleaching induced by thermal stress in Collodaria (Radiolaria). *bioRxiv* [Preprint]. doi: 10.1101/263053

Weis, V. M. (2008). Cellular mechanisms of Cnidarian bleaching: stress causes the collapse of symbiosis. *J. Exp. Biol.* 211, 3059–3066. doi: 10.1242/jeb.009597

Weynberg, K. D., Neave, M., Clode, P. L., Voolstra, C. R., Brownlee, C., Laffy, P., et al. (2017). Prevalent and persistent viral infection in cultures of the coral algal endosymbiont Symbiodinium. *Coral Reefs* 36, 773–784. doi: 10.1007/s00338-017-1568-7

Conflict of Interest Statement: The authors declare that the research was conducted in the absence of any commercial or financial relationships that could be construed as a potential conflict of interest.

frontiers in Marine Science

ORIGINAL RESEARCH
published: 23 October 2018
doi: 10.3389/fmars.2018.00374

Influence of Light Availability and Prey Type on the Growth and Photo-Physiological Rates of the Mixotroph *Noctiluca scintillans*

Helga do Rosario Gomes[1], Kali McKee[1], Anxhela Mile[2], Sharanya Thandapu[3], Khalid Al-Hashmi[4], Xiaojian Jiang[1,5] and Joaquim I. Goes[1]*

[1] *Lamont-Doherty Earth Observatory at Columbia, Palisades, NY, United States,* [2] *Elisabeth Haub School of Law at Pace University, White Plains, NY, United States,* [3] *Washington University in St. Louis, St. Louis, MO, United States,* [4] *Department of Marine Science and Fisheries Sultanate of Oman, Sultan Qaboos University, Muscat, Oman,* [5] *School of Life Sciences, Huaiyin Normal University, Huai'an, China*

OPEN ACCESS

Edited by:
Matthew D. Johnson, Woods Hole Oceanographic Institution, United States

Reviewed by:
Jelena Godrijan, Bigelow Laboratory for Ocean Sciences, United States
Kemal Can Bizsel, Dokuz Eylül University, Turkey

***Correspondence:**
Helga do Rosario Gomes
helga@ldeo.columbia.edu

Specialty section:
This article was submitted to Marine Ecosystem Ecology, a section of the journal Frontiers in Marine Science

Received: *28 June 2018*
Accepted: *26 September 2018*
Published: *23 October 2018*

Citation:
Gomes HdR, McKee K, Mile A, Thandapu S, Al-Hashmi K, Jiang X and Goes JI (2018) Influence of Light Availability and Prey Type on the Growth and Photo-Physiological Rates of the Mixotroph Noctiluca scintillans. Front. Mar. Sci. 5:374. doi: 10.3389/fmars.2018.00374

A strain of the mixotrophic green *Noctiluca scintillans* (*Noctiluca*) isolated from the Arabian Sea afforded us an opportunity to investigate the photosynthetic and feeding characteristics of this organism which has recently replaced the once diatom dominated food chain of winter blooms in the Arabian Sea. Here we present the first in a series of experiments undertaken to study the interactive effects of irradiance and grazing response of this mixotroph to four phytoplankton species provided as food. *Noctiluca* showed a distinct preference for the dinoflagellate *Peridinium foliaceum* and the pennate diatom *Phaeodactylum tricornutum*, but not for the chlorophyte *Pyramimonas* sp., nor the chain forming diatom *Thalassiosira weissflogii.* However, irrespective of the food provided, adequate light was required for *Noctiluca* to grow as evidenced by its maximum growth rates of 0.3 day^{-1} when fed the preferred dinoflagellate *Peridinium* and exposed to optimal irradiance of 250 $\mu E\ m^{-2}\ s^{-1}$ vs. growth rates of 0.13 day^{-1} with the same food but at a low irradiance of 10 $\mu E\ m^{-2}\ s^{-1}$. Measurements of *Noctiluca*'s electron transport rates (ETR) per PSII Reaction Center as a function of irradiance also indicated severe light limitation of photosynthesis at 10 $\mu E\ m^{-2}\ s^{-1}$. The active fluorescence derived ETR vs. Irradiance curves also revealed an interesting finding in that there was no significant difference in photosynthetic parameters such as the maximum photosynthetic capacity (ETR_{max}) nor α, the rate of increase of photosynthesis with light between fed and unfed cells under optimal light conditions. These results suggest that feeding does not enhance the photosynthetic activity of the endosymbionts when nutrients are not limiting as was the case in these experiments. Measurements of *Noctiluca*'s intracellular ammonium concentrations under optimal light conditions, the first for this strain, show significant accumulation of NH_4^+ (0.003–0.012 $\mu M\ NH_4^+\ cell^{-1}$) after 14 days for fed and unfed *Noctiluca* which was undetectable 4 days later. A similar 14-day increase but of significantly higher

concentrations (0.005–0.08 μM NH_4^+ $cell^{-1}$) was obtained under low light conditions. For *P. tricornutum* and *T. weissflogii* fed cultures under light limitation, NH_4^+ continued to increase past the 14-day period suggesting a strong and efficient mechanism for regulation of intracellular nutrients by *Noctiluca*.

Keywords: mixotroph, blooms, Arabian Sea, feeding, green *Noctiluca scintillans*, photosynthesis

INTRODUCTION

Several informative reviews (Stoecker et al., 2009, 2017; Caron, 2016; Mitra et al., 2016; Leles et al., 2017) now urge researchers to recognize that autotrophy (obtaining energy for growth from light) and heterotrophy (utilizing preformed organic matter produced by autotrophs to meet their energy and carbon needs) may often not be mutually exclusive behaviors and many plankton do in fact exhibit some combination of these nutritional modes, an ability generally referred to as mixotrophy (Caron, 2017). Mixotrophy is not confined to just a few unique taxonomic groups but, rather is ubiquitous and occurs amongst different species and in diverse habitats from marine coastal to open ocean systems as well as in freshwater systems (Mitra et al., 2014).

Recognizing that the majority of protists are mixotrophs and engaged in varying proportions of phototrophy and phagotrophy, Mitra et al. (2016) and Stoecker et al. (2017) grouped them into one of three general behavioral categories. Firstly, phagotrophic phytoflagellates that possess chloroplasts but also engulf and digest small prey by phagocytosis, secondly, kleptoplastidic protists, heterotrophic species that feed on algae, partially digest them, but retain their chloroplasts in a functional state (Caron, 2017). The third and perhaps least studied of categories are protists or zooplankton with algal endosymbionts of only one species or very closely related algal species (Stoecker et al., 2017). The best example of such mixotrophy is the dinoflagellate *Noctiluca scintillans* (herein referred to as *Noctiluca* as there is only one species in the genus *Noctiluca*) which harbors thousands of free-swimming endosymbiotic green algae. In contrast, to the exclusively heterotrophic red *Noctiluca* which is globally ubiquitous, green *Noctiluca*, is much more restricted and limited mainly to tropical southeast Asian waters and parts of the Arabian Sea, Gulf of Oman, and the Red Sea (Harrison et al., 2011). Localized blooms of this green endosymbiont carrying *Noctiluca* have been recurring in Southeast Asian waters such as in the Manila Bay, the upper Gulf of Thailand, and Jakarta Bay (Furuya et al., 2006a,b), in the coastal waters of Vietnam and Cambodia (Harrison et al., 2011) and further west in the Sea of Oman (also known as the Gulf of Oman) (Al-Azri et al., 2012; Al-Hashmi et al., 2015). In the early 2000s, using microscopy in conjunction with ocean color imagery we reported (Gomes et al., 2008, 2009) for the first time, large scale and recurrent blooms of the green *Noctiluca* in the northern Arabian Sea. The *Noctiluca* of the Arabian Sea is large (diameter of ∼600–1000 μm), bulbous and harbors thousands of endosymbionts, which swim freely within its large central vacuole (**Figure 1**). On the basis of molecular analysis and the priority rule of nomenclature, the ecological characteristics of the endosymbionts within *Noctiluca* have been reclassified as *Protoeuglena noctilucae* (Wang et al., 2016) instead of *Pedinomonas noctilucae*, the earlier species name given in Sweeney (1976).

Thick surface blooms of *Noctiluca* are now becoming more pervasive and widespread throughout the northern and central AS, causing a radical shift in the usually diatom dominant winter monsoonal blooms, one of the two high productivity periods in the otherwise oligotrophic Arabian Sea (Gomes et al., 2008; Goes et al., 2018). In Gomes et al. (2014) we showed that a combination of its ability to feed on extraneous phytoplankton prey and the recent spread of hypoxia in the Arabian Sea were favoring the growth of *Noctiluca* over that of diatoms.

Specifically, we observed that *Noctiluca* have higher rates of carbon fixation in hypoxic waters as compared to diatoms (Gomes et al., 2014). O_2 deficiency (<4 μM) and a permanent oxygen minimum zone (OMZ) at mid-depths (>120 m) is a unique feature of the northeastern Arabian Sea, a consequence of high surface productivity of the semi-annual phytoplankton blooms (Goes et al., 2005), sub-thermocline source waters that have naturally low dissolved O_2 content flowing from the Southern Ocean and poor ventilation of subsurface waters in the landlocked north (Morrison et al., 1999). Comparison of O_2 saturation data from our recent studies with historic data (Gomes et al., 2014) showed that the Arabian Sea's euphotic zone was indeed experiencing an influx of hypoxic waters from an expanding OMZ. A recent study by Lachkar et al. (2017) confirmed the findings of Gomes et al. (2014). This phenomenon is not confined only to the Arabian Sea but is being experienced in many regions of the world (Breitburg et al., 2018) because of human activities that have increased global temperatures and nutrients discharged to coastal waters. Coupled with this unique functional and adaptive response of *Noctiluca* and its endosymbiont to hypoxia, is its voracious predation of diatoms and other phytoplankton that form the winter blooms of the Arabian Sea fueled by new nitrogen inputs from convective mixing (Banse and McClain, 1986).

Noctiluca's requirement for inorganic nutrients for photosynthesis by its endosymbionts, and its ability to graze on other phytoplankton suggests that it competes for resources (nutrients and prey) with both its prey and predators but little is known about how it regulates its photosynthetic and heterotrophic processes. The few studies, reviewed in Harrison et al. (2011) suggest that although *Noctiluca* can grow photo-autotrophically for several generations, phagotrophy promotes faster growth and is a requirement for bloom formation (Sriwoon et al., 2008). Feeding experiments conducted during a bloom in the Arabian Sea to elucidate the

FIGURE 1 | A single cell of *Noctiluca scintillans* with free-swimming endosymbionts *Protoeuglena noctilucae* using its tentacle to capture algal cells for feeding. Image was produced with a epifluorescence microscope (OMAX 40X–2500X) with a 40× objective.

interplay between dependence of *Noctiluca* on its autotrophic endosymbionts and its facultative phagotrophy (Gomes et al., 2014) showed that growth rates of *Noctiluca* were much lower in the dark even with addition of food as compared to rates for cells grown in the light indicating the importance of autotrophic endosymbionts for growth. Even more interesting was the fact that growth rates in samples where light and nutrients were provided were comparable to those where light and food (but not nutrients) were provided. Growth rates did not increase when nutrients were added to flasks containing food and exposed to light, suggesting that when food is available, *Noctiluca* is capable of meeting a large fraction of its metabolic requirements via phagotrophy. What was lacking in this study was knowledge of whether *Noctiluca* had food preferences although the general consensus based on experimental evidence with red *Noctiluca* is that it is not particularly selective (Elbrachter and Qi, 1998; Zhang et al., 2016).

On account of the paucity of information on this unique and novel organism, little is known on the regulation and interplay between photosynthetic and heterotrophic processes, key information required to understand its recent proliferation in tropical waters (Furuya et al., 2006a,b; Harrison et al., 2011; Al-Azri et al., 2012; Al-Hashmi et al., 2015). An isolate from the Arabian Sea afforded us with an opportunity to conduct controlled, laboratory experiments. This culture is more akin to that of Furuya et al. (2006b) and Saito et al. (2006) from the Manila Bay because it grows in a 12 h light-dark cycle, without food for more than a year and even without the addition of fresh media. It differs from the one described by Sweeney (1971) and Hansen et al. (2004) which could survive and divide in the light with or without addition of food for only about a month.

In this series of experiments described in detail below, we fed the laboratory grown strain of *Noctiluca* with four phytoplankton species *viz*. Two diatoms, *Phaeodactylum tricornutum* and *Thalassiosira weissflogii*, a dinoflagellate *Peridinium foliaceum* and a green alga *Pyramimonas* sp. In addition to counting *Noctiluca* cells to ascertain growth with the different foods provided, we also assessed the photosynthetic efficiency of the green endosymbionts using photosynthesis-irradiance responses (Platt and Jassby, 1976).

Additionally, we conducted preliminary measurements on the NH_4^+ content of *Noctiluca* cells. This aspect of *Noctiluca* has rarely been addressed although it is known that the heterotrophic red variety of *Noctiluca* accumulates large quantities of NH_4^+ (Okaichi and Nishio, 1976) which makes it buoyant (Furuya et al., 2006a). This is also the case with *Noctiluca* blooms in the Arabian Sea which form green carpets over large expanses of the sea even though this exposes them to inhibitory light levels (Goes and Gomes, 2016).

MATERIALS AND METHODS

Prey and Predator Cultures

Noctiluca cells isolated from the open waters of the Arabian Sea are maintained in f/20 medium without silicate (f/20 – Si) in polycarbonate bottles at 26°C and exposed to a light intensity of approximately 200 µE m^{-2} s^{-1} and a photoperiod of 11.5 h light: 12.5 h dark. This culture is maintained without extraneous food.

The four prey cultures used in the feeding experiments were isolated from warm tropical waters and include a pennate diatom (*P. tricornutum*; CCMP632, cell dimensions of 18–26 µm), a centric diatom (*T. weissflogii*; CCMP1336, cell dimensions of 12–22 µm), and one chlorophyte (*Pyramimonas* c.f. sp.; CCMP1239, cell dimensions of 5–10 µm) all obtained from the NCMA, Bigelow Laboratory for Ocean Sciences, ME, United States). A fourth, the dinoflagellate *P. foliaceum* (cell dimensions of 5–10 µm) was obtained from Dr. E. J. Buskey, University of Texas, TX, United States. *P. tricornutum* and *T. weissflogii* are grown in f/2 medium; while *Pyramimonas* and *P. foliaceum* are grown in f/2 – Si. All prey cultures are maintained at 26°C with a light intensity of approximately 200 µE m^{-2} s^{-1} and a photoperiod of 11 h Light: 13 h Dark. Growth media for the prey cultures was prepared in 0.22 µm membrane filtered seawater (FSW) according to protocols provided by NCMA. Growth and grazing experiments were started once all cultures had reached exponential phase.

Experimental Setup

All polycarbonate bottles in which the experiments were conducted were acid-washed and soaked overnight with 5% technical grade HCl, rinsed with Milli-Q distilled water, and autoclaved prior to use. A schematic of the experimental setup is shown in **Supplementary Figure S1**.

Twenty cleaned 250 mL polycarbonate bottles were filled with 200 mL of sterile f/20 – Si medium and 50 *Noctiluca* cells

were added to each of them. Cells were picked individually using plastic transfer pipettes, and washed in sterile FSW before being introduced into the bottles. Ten of these bottles containing *Noctiluca* were placed in light replete (HL, 250 $\mu E\ m^{-2}\ s^{-1}$) conditions and 10 in light limited (LL, 10 $\mu E\ m^{-2}\ s^{-1}$) conditions in an incubator at 26°C. LL conditions were simulated by covering the cool white light fluorescent tubes of the lower tiers of the incubator with neutral density filters. Aliquots of each of the four prey suspensions were added to eight bottles reserved for the HL treatment so that each prey treatment had two duplicate bottles. The volume of prey approximated 1–2 $\mu g\ L^{-1}$ Chlorophyll *a* (Chl *a*, a proxy for biomass) per bottle (volume of culture was 3.29 mL for *Pyramimonas* sp. and <1 mL for the other three prey cultures). No food was added to the remaining two *Noctiluca* bottles which served as controls. The setup for the 10 LL bottles was identical to the one described for the 10 HL bottles. Four additional bottles with only prey cultures were placed in the HL section of the incubator. Based on preliminary work, *Noctiluca* was allowed to adapt to the four prey cultures for 7 days. All bottles were maintained at 26°C with a photoperiod of 11.5 h light: 12.5 h dark for 27 days on three dimensional gyratory rockers to gently agitate the cells and encourage natural interaction between predator and prey.

Details of the sampling protocols and of all measurements conducted are presented below.

Sampling and Measurements

Measurements were made to assess the growth and feeding rates of *Noctiluca* and the photo-physiology of the cells as follows:

Chl *a*

Chl *a*, was measured fluorometrically (Holm-Hansen and Riemann, 1978) using a Turner® Designs Trilogy Laboratory Fluorometer to determine the initial biomass of the four stock prey cultures prior to being fed to *Noctiluca*. Chl *a* was extracted in acetone in cells filtered through 0.7 μm Whatman® GF/F glass filters. The same procedure was employed to measure Chl *a* during the course of the experiment.

Cell Counts

Cell counts of prey prior to being fed and during the course of the experiment were undertaken using FlowCAM®, an imaging particle analyzer that combines imaging and laser light to detect particles and capture their images which are then identified from pre-built libraries (Poulton, 2016). Prey counts were made by drawing 4.9 mL of culture in duplicate from each of the bottles, which was preserved with 0.1 mL neutral Lugol's iodine solution. Care was taken to draw this sub-sample from the bottom, and if any *Noctiluca* cells were observed in the transfer pipette the process was repeated until we are assured that the sub-sample had no *Noctiluca* cells.

To obtain *Noctiluca* counts, 5 ml of media from each bottle was drawn into a sterile plastic transfer pipette and the number of individual cells in the pipette was counted before the volume was returned to the bottle. This process was repeated five times to ascertain accuracy. *Noctiluca*'s large size allowed us to count cells using this non-invasive method.

Photophysiology Using Fluorescence Inductance and Relaxation (FIRe)

A suite of photosynthetic and physiological characteristics of *Noctiluca*'s endosymbionts was assessed using the Fluorescence Inductance and relaxation technique in a mini-FIRe benchtop instrument (Gorbunov and Falkowski, 2004; Park et al., 2013).

Variable Fluorescence, a unique property of the photosynthetic machinery (Gorbunov and Falkowski, 2004) is related to the efficiency of photosynthetic processes and provides us with estimates of the physiological status of photosynthetic organisms (Kolber et al., 1998). Variable Fluorescence (F_V) is calculated using initial (F_0) and maximum (F_M) fluorescence after illumination with a high-energy flash ($F_V = F_M - F_0$). Quantum efficiency of the photochemistry in Photosystem II (PSII), a relative measure of the electron transport efficiency is the ratio of the Variable Florescence Fv and the maximum Fluorescence Fm, i.e., F_V/F_M. High F_V/F_M is associated with a functioning PSII and, therefore, is a proximal measurement of cellular integrity and metabolic capability while fluctuations may indicate "stressful growth" such as nutrient starvation or excessive light (Suggett et al., 2009). Variable Fluorescence can then be used to calculate parameters that characterize photosynthetic light-harvesting processes, the photochemistry in PSII, and the photosynthetic electron transport down to carbon fixation. In addition to the quantum efficiency of PSII (F_V/F_M) our FIRe system also provides the cross section of PSII (σPSII), which is a measure of the size of the light-harvesting antenna system associated with PSII (Bibby et al., 2008).

Using these parameters we can then calculate the photosynthetic ETR per PSII Reaction Center (RC) as described in Park et al. (2013) which is related to the rate of primary production or carbon fixation (Gorbunov and Falkowski, 2004). Using FIRe, ETR measurements were performed over a range of light levels using an Actinic Light Source to obtain ETR rates as a function of irradiance. These ETR-Irradiance curves (ETR-E) are similar to the Photosynthesis-Irradiance curves (P-E) (Platt and Sathyendranath, 1988) that have been used widely to measure primary productivity at basin or global scales (Platt et al., 1980; Bouman et al., 2005) and serve to understand the acclimation state of the phytoplankton and as indicators of the influences of environmental factors such as light and nutrients on primary production (Falkowski et al., 1981; Henley, 1993). These ETR-E curves like the Photosynthesis-Irradiance curves provide parameters such as maximum ETR (ETRmax), α, the initial light-limited slope and saturation irradiance E_k (Platt et al., 1980; Park et al., 2013; Houliez et al., 2017). Depending on the presence or absence of photoinhibition two different models of (Platt et al., 1980) were fitted to the ETR data. All curve fitting was done using MATLAB 2016b routines.

In order to conduct the above measurements, 10 *Noctiluca* cells from each bottle were carefully picked with transfer pipettes,

cleaned in sterile FSW to prevent the carryover of prey and suspended into glass tubes containing sterile FSW. The glass cuvette was inserted into the compartment and the actinic light source (ALS) was placed on top of the holder. The length of the multi-turnover flash (MTF) was set to 100 ms, the number of pulses in the relaxation sequence (MTRP) was set to 40, while the maximum PAR for the ALS was set to 1200 μmole/m^2/s. The number of PAR steps was set to 10, and the time delay in which the ALS was on prior to data acquisition was set to 5 s. To acquire the parameters described above the data was further processed with a program supplied with the instrument.

Known aliquots of f/20 – Si medium were added to the sample bottles to account for any loss in volume occurring after sampling. After the FIRe measurements, the same samples containing the 10 *Noctiluca* cells were used to measure Chl *a* of the endosymbionts using the fluorometric method described above. FIRe measurements were also conducted with prey samples without *Noctiluca* to estimate the photophysiological status of the prey. We could not conduct weekly FIRe or Chl *a* estimates of the prey in the bottles because we have observed in our routine maintenance of *Noctiluca* that it ejects out its endosymbionts. So we instead relied on FlowCAM® derived cell counts of prey samples which were more accurate.

Intracellular Ammonium Concentrations

NH_4^+ accumulation in *Noctiluca* cells was measured at the start of the experiment, and after 14 and 18 days. This was done by placing five washed and cleaned cells into 15 mL plastic centrifuge tubes containing 10 mL Milli-Q distilled water. The process was repeated with five more cells to obtain replicates. Samples were collected in duplicate, vortexed, and frozen at −80°C prior to analysis. Ammonium was measured colorimetrically with the Turner Designs Trilogy laboratory fluorometer according to Holmes et al. (1999).

Growth Rate Calculations

Growth Rates (μ) of *Noctiluca*, measured as the change in cell number over time, were computed using the formula:

$$\mu = [ln(Nt_1/Nt_0)]t^{-1} \quad (1)$$

where Nt_0 = concentration of cells at time 0 (cells ml^{-1}), Nt_1 = concentration of cells at time 1 (cells ml^{-1}), and t = duration of each experiment (d).

Statistics

All statistical tests used to test the significance of differences in growth of *Noctiluca* as well as differences in photosynthetic

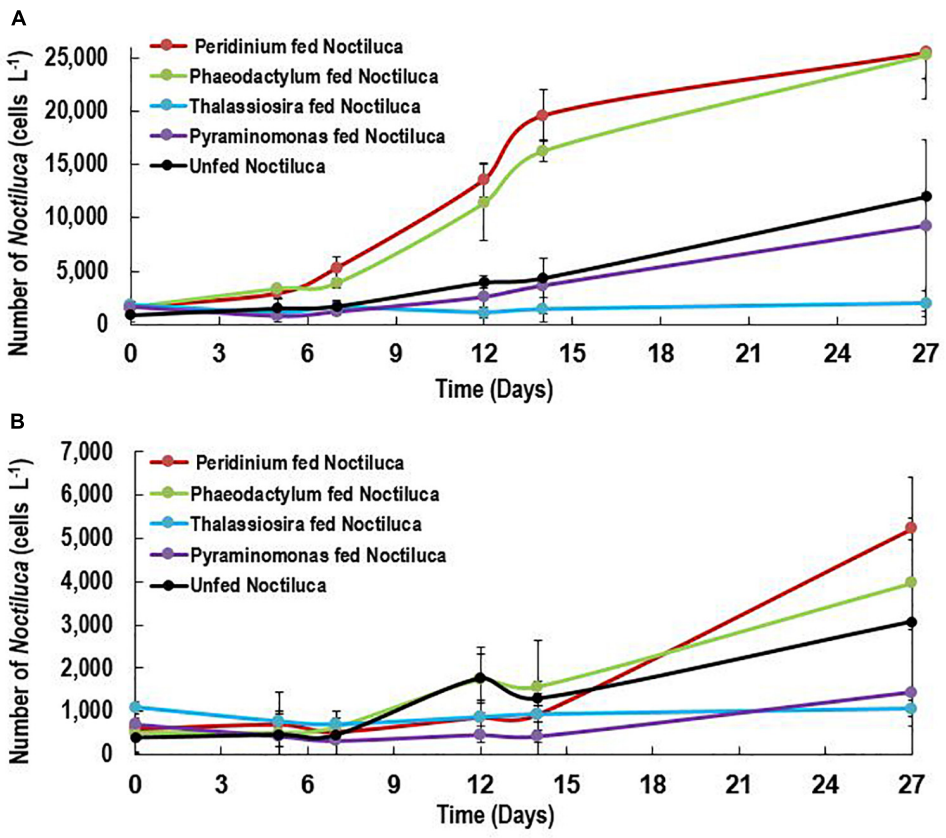

FIGURE 2 | (A,B) Growth response (Cells L^{-1}) of unfed *Noctiluca* and *Noctiluca* fed with prey and exposed to **(A)** optimal light (250 μE m^{-2} s^{-1}, HL) **(B)** low light (10 μE m^{-2} s^{-1}, LL). Data points represent means ± SE (n = 2).

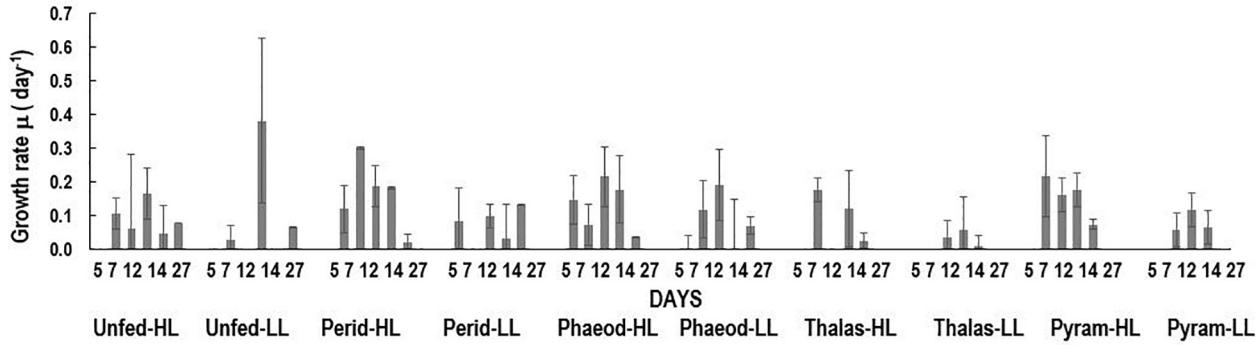

FIGURE 3 | Growth rates (day^{-1}) over the course of the experiment for unfed *Noctiluca* and for *Noctiluca* fed *P. foliaceum* (Perid), *P. tricornutum* (Phaeod), *T. weissflogii* (Thalas), and *Pyramimonas* sp. (Pyram) and exposed to optimal (250 μE m^{-2} s^{-1}, HL) and low light (10 μE m^{-2} s^{-1}, LL). Data points represent means ± SE (n = 2) (day^{-1}).

parameters of the ETR-E curves were performed using JMP 9® software.

RESULTS

Growth of Noctiluca With and Without Food

Of the four phytoplankton species provided as food and exposed to HL and LL conditions, the green *Noctiluca* culture currently growing in our laboratory, showed a distinct preference for the diatom *P. tricornutum* and the dinoflagellate *P. foliaceum* (**Figure 2A**). Conversely, it grew very slowly when fed the small celled *Pyramimonas* sp. while no growth was observed with the chain forming diatom *T. weissflogii*. Statistically significant differences (Paired t-test, $p < 0.05$, **Supplementary Table 1**) were observed between the number of cells in control samples with only *Noctiluca* and *Noctiluca* cells fed either *P. foliaceum* or *P. tricornutum* but this was not the case with cells feed either *T. weisflogii* or *Pyramimonas* sp. LL exposed *Noctiluca* cells (**Figure 2B**) showed similar food preferences after 14 days but growth was much slower and maximum number of cells was about 5233 cells L^{-1} in *Peridinium* fed cultures compared to 25,500 cells L^{-1} in HL with the same food. A comparison of all *Noctiluca* cells grown with prey in HL vs. LL, showed a statistically significant difference (Paired t-test, $p < 0.05$, **Supplementary Table 1**) for all four prey cultures indicating the importance of light for endosymbiont photosynthesis and growth of *Noctiluca*. Growth rates for the preferred food *Peridinium* increased from 0.1 to 0.3 day^{-1} after 2 days (**Figure 3**), the latter being the maximum growth rate achieved during the experiment in HL conditions. When *Noctiluca* was fed *Phaeodactylum*, the other preferred food, growth rates increased gradually with a maximum growth rate of 0.22 day^{-1} after 14 days. HL exposed *Thalassiosira* fed *Noctiluca* did not show any growth for 5 days but a growth rate of 0.17 was observed after 2 days. Although HL *Pyramimonas* sp. fed *Noctiluca*, showed an increased growth rate of 0.2 day^{-1} after 7 days, growth rates tapered off and *Noctiluca* cells did not show increases as observed for the preferred cultures (**Figure 2A**). Unfed *Noctiluca* achieved a maximal growth rate achieved of 0.17 day^{-1} after 12 days but tapered off to almost negligible by end of the experiment. Growth rates were lower in the LL regime than in the HL regime (Paired t-test, $p < 0.01$), except in the case of unfed *Noctiluca* (after 12 days) wherein a highly inflated growth rate of almost 0.4 day^{-1} was observed. We think this may have been a counting artifact because our duplicate counts after 7 days were highly disparate (67 vs. 1067). Average growth rate of fed cells (all foods) in HL was 0.12 day^{-1} and for LL (all foods) it was 0.05 day^{-1}. In the case of HL exposed *Peridinium* and *Phaeodactylum* fed cultures, it should be noted that in spite of a decrease in growth rates between 14 and 27 days (**Figure 3**), the number of *Noctilucacells* still increased from about 19,600 to 25,500 cells L^{-1} in the case of *Peridinium* fed *Noctiluca* and from 16,270 to 28,600 cells L^{-1} in the case of *Phaeodactylum* fed *Noctiluca* (**Figure 2**). From day 14 to 21, in some cases LL adapted cells, also showed a small increase in growth rates (negligible to ∼0.10 day^{-1}) which led to an increase in the number of cells by the end of the experiment (**Figure 2B**) and which could possibly be from acclimatization by endosymbionts to light levels which initially had been severely limiting.

Chl *a* Concentrations of Noctiluca's Endosymbionts

A slightly different pattern emerged when *Noctiluca*'s intracellular Chl *a* concentrations per cell were estimated (**Figures 4A,B**). Intracellular concentrations in cells fed with the two preferred foods increased in the first 7 days but gradually decreased to concentrations approximating those at the start of the experiment. Almost invariant intracellular Chl *a* concentrations were measured in *Pyramimonas* sp. fed cells over the experimental period.

After 14 days, when intracellular Chl *a* concentrations of HL exposed cells began to decrease subsequent to a peak of 0.6–2.0 μg cell^{-1}, a reverse situation was observed in LL light adapted cells where intracellular Chl *a* increased almost twofold especially in *Noctiluca* fed the two preferred foods and fourfold

with the other two foods as well as in the unfed *Noctiluca* (**Figures 4A,B**). One reason for this is that higher growth, cell division and an increase in cell numbers in the HL grown cells compared to those in LL, resulted in smaller cells in HL exposed cultures which contained less endosymbionts and consequently lower intracellular Chl *a*. The other, probably relates to pigment packaging invariably observed in phytoplankton cells growing under low light. When exposed for prolonged periods to low light, phytoplankton cells usually increase their pigment concentration and change the organization of pigments within their photosynthetic units to aid in harvesting light (Falkowski and Owens, 1980). However, pigment molecules, when tightly packed instead of being uniformly distributed within the cell, lessen the overall effectiveness in collecting photons from the prevailing irradiance field, lowering their efficiency of light absorption and consequently the amount of carbon fixation (Morel and Bricaud, 1981; Sosik and Mitchell, 1994). We believe that the increase in Chl *a* in *Noctiluca* cells growing under LL conditions is akin to pigment packaging in phytoplankton cells.

ETR vs. E Curves and Model Derived Photosynthetic Parameters

Figures 5A–F compares ETR vs. E curves in HL (**Figures 5A–C**) and LL (**Figures 5D–F**) regimes for *Noctiluca* cells grown with the two preferred foods *P. foliaceum* and *P. tricornutum* and unfed *Noctiluca*. All curves are an average of four replicate measurements. Both the light limited (initial) and light saturated parts of the curves from HL and LL exposed cells responded markedly to changes in irradiances. Maximum ETR (ETR_{max}) or the maximum photosynthetic capacity was clearly higher in HL exposed cells than in LL cells. Average ETR_{max} was 236 electrons s^{-1} RC^{-1} (electrons s^{-1} Reaction $Center^{-1}$) in HL exposed cells as opposed to 154 electrons s^{-1} RC^{-1} in LL exposed cells. The differences in ETR_{max} between HL and LL exposed cells were statistically significant (Paired *t*-test, $p < 0.001$; **Supplementary Table S1**). The rate of increase of light-limited ETR (α), which is the slope of the initial part of the curve and quantifies the efficiency of light capture averaged 2.0 electrons m^2 RC^{-1} μmole $quanta^{-1}$ compared to 1.5 electrons m^2 RC^{-1} μmole $quanta^{-1}$ for LL exposed cells. The differences in α, derived from curves of HL and LL exposed cells was also statistically significant (Paired *t*-test, $p < 0.005$; **Supplementary Table S1**). The saturating irradiance for ETR (E_k) which represents the optimal irradiance for photosynthesis was lower (average 380 μmole $quanta^{-1}$ s^{-1}) in LL exposed cells compared to that of cells exposed to HL (124 390 μmole $quanta^{-1}$ s^{-1}) although this difference was not statistically significant.

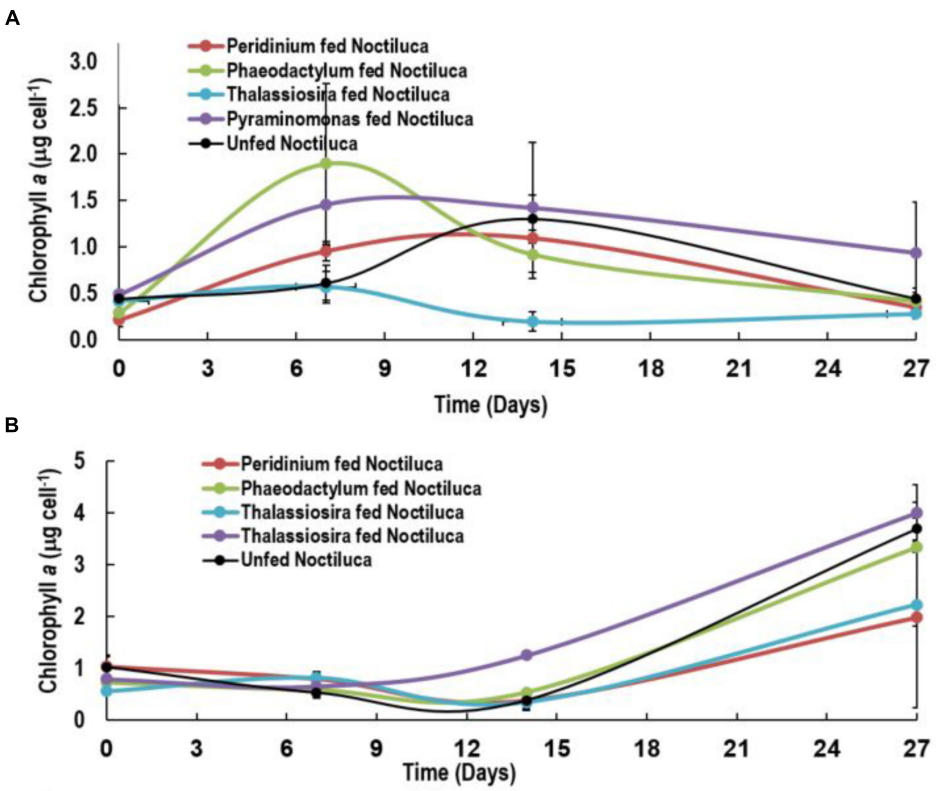

FIGURE 4 | Intracellular Chlorophyll *a* concentrations of *Noctiluca* (μg *Noctiluca* $cell^{-1}$) for unfed *Noctiluca* and for *Noctiluca* fed with *P. foliaceum*, *P. tricornutum*, *T. weissflogii*, and *Pyraminomonas* sp. for **(A)** optimal (250 μE m^{-2} s^{-1}, HL) and **(B)** low light (10 μE m^{-2} s^{-1}, LL) exposed cultures. Data points represent means ± SE ($n = 2$).

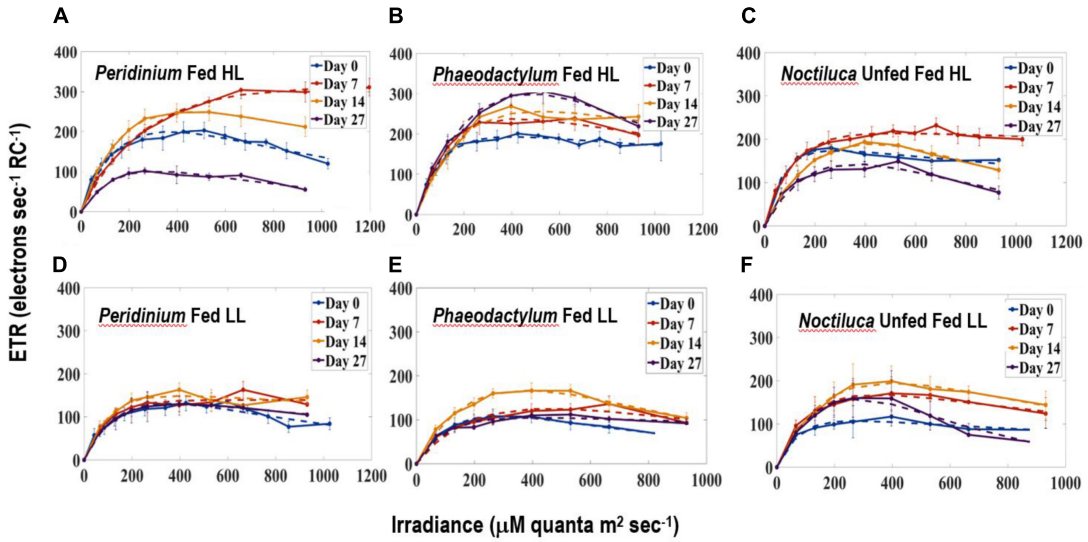

FIGURE 5 | Electron Transport Rates-Irradiance (ETR-E) curves for **(A)** *P. foliaceum* fed *Noctiluca* cells in HL **(B)** *P. tricornutum* fed *Noctiluca* cells in HL **(C)** Unfed *Noctiluca* cells in HL (250 μE m^{-2} s^{-1}) fitted to the function of Platt et al. (1980), as described in Section "Materials and Methods." ETR is expressed as electrons s^{-1} Reaction $Center^{-1}$. **(D–F)** are for the same but exposed to LL (10 μE m^{-2} s^{-1}). Data points represent means ± SE (n = 4).

Comparison of the parameters of the ETR vs. E curves obtained from fed and unfed cultures in HL exposed cells, provides us with information on whether food enhances the photosynthetic activity of the endosymbionts. Neither ETR_{max}, the maximum photosynthetic capacity nor α, the maximum rate of increase of light-limited photosynthesis, from both *P. foliaceum* and *P. tricornutum* fed cultures of *Noctiluca* in HL, were statistically different from those derived from unfed *Noctiluca* in the same light regime. This indicates that the endosymbionts in both fed and unfed cultures were not under any nutrient stress.

Intracellular Concentrations of NH_4^+

Although there are several reports on the accumulation of NH_4^+ in red *Noctiluca* (Okaichi and Nishio, 1976; Zhang et al., 2017) no such exist for green *Noctiluca*. This first report on the per cell intracellular concentrations of NH_4^+ in green *Noctiluca* in HL exposed cells (**Figure 6A**) show that highest NH_4^+ accumulation occurred on day 14 but decreased to undetectable concentrations 4 days later. This indicates rapid uptake of NH_4^+ by the green endosymbionts. NH_4^+ concentrations below detection levels were observed in cells fed the preferred food, *P. foliaceum* while the second lowest (0.0025 μM NH_4^+ $cell^{-1}$) concentration was found in *P. tricornutum* fed cells. The highest accumulation (0.01 μM NH_4^+ $cell^{-1}$) was observed in cells fed the least preferred food, *Pyramimonas* sp. This can tentatively suggest higher uptake of NH_4^+ by the green endosymbionts in cells that were fed the favored foods. Highest NH_4^+ accumulation of 0.006 NH_4^+ μM $cell^{-1}$ was measured in unfed samples. In contrast, LL exposed cells intracellular NH_4^+ concentrations were almost an order higher than those in HL exposed cells (**Figure 6B**). This is an indication that nutrient uptake by endosymbionts was lower when photosynthesis was light limited.

DISCUSSION

The strain of green *Noctiluca* from the Arabian Sea showed a distinct preference for *P. foliaceum* and *P. tricornutum*. Although it also grew without food especially in HL exposed cells, growth rates were almost half of that in the fed cultures and cell counts were five-fold higher in the latter after 14 days of feeding. The only other study on feeding and food preference in green *Noctiluca* (Hansen et al., 2004) isolated from the Manila Bay, Philippines showed a preference for two dinoflagellates *Pyrodinium bahamense* and *Akashiwo sanguinea*. The difference between these two studies is that irrespective of food type, food concentration, and irradiance, the *Noctiluca* culture in the study of Hansen et al. (2004) lost its endosymbionts after about 3 weeks and became colorless and died. This was not the case with the Arabian Sea *Noctiluca* culture which continued to grow albeit slowly even after the end of the experiment. Both, the current study and our previous one conducted in the Arabian Sea (Gomes et al., 2014) where natural populations of *Noctiluca* were fed a mixed phytoplankton bloom predominated by diatoms showed similar results to those obtained by Hansen et al. (2004) in that growth rates were higher for fed cultures than for unfed *Noctiluca*.

Our recalculated growth rates are concurrent with those of Hansen et al. (2004), which were 0.14 day^{-1} for HL and 0.058 day^{-1} for LL at comparable irradiances.

Our study clears shows that irrespective of the quality of food provided, adequate light is required for green *Noctiluca* to grow which reiterates findings from the earlier two studies

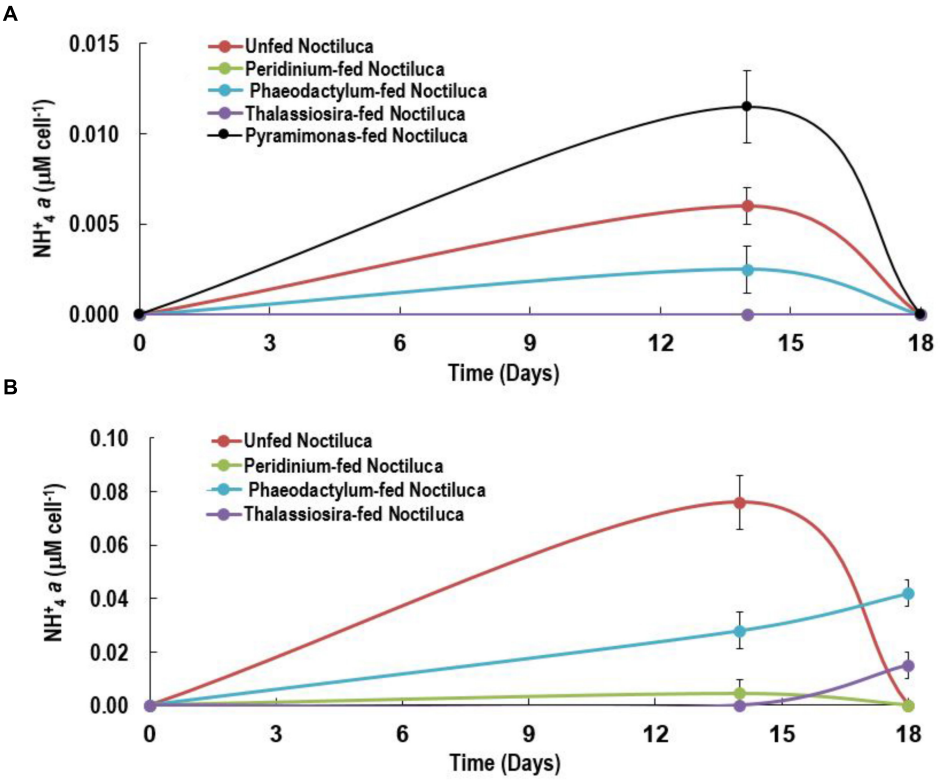

FIGURE 6 | Intracellular NH^{+}_{4} concentrations of *Noctiluca* (µg *Noctiluca* cell^{-1}) for unfed *Noctiluca* and for *Noctiluca* fed with *P. foliaceum, P. tricornutum*, *T. weissflogii*, and *Pyramimonas sp.* for **(A)** optimal (HL) and **(B)** low light (LL) exposed cultures. Data points represent means ± SE (n = 2).

(Hansen et al., 2004; Gomes et al., 2014). This is also clearly observed is in the ETR vs. E curves where higher ETR_{max} or maximum photosynthetic capacity was observed in HL exposed cells. Beyond this maxima, the rate of photosynthesis is limited by the activity of the electron transport chain or Calvin cycle (Serôdio et al., 2005).

The non-intrusive technique of ETR vs. E curves which we utilized yielded an interesting result in that the type of food provided did not change the photosynthetic response of the endosymbionts as there was no statistically significant relationship in the ETR vs. E parameters of fed (including the two preferred foods) and unfed *Noctiluca* cells. In addition to responding to variations in irradiance, both P-E curves and variable fluorescence are sensitive to changes in nutrient and trace metal concentrations (Falkowski and Kolber, 1995; Behrenfeld and Kolber, 1999; Bouman et al., 2005). The similarity in photosynthetic parameters between fed and unfed *Noctiluca* indicates that endosymbionts did not experience nutrient variations especially nutrient limitation in either of the two treatments. Using two types of cultures, one that required feeding to survive and the other which like our culture survived for extended periods without food, Saito et al. (2006) performed P-E curves where photosynthesis was measured using oxygen concentrations. They too observed no significant differences in gross photosynthetic rate between the feeding and non-feeding rate but net photosynthesis was higher in the non-feeding strain because feeding strains showed higher rates of respiration. Our ETRs (normalized to PSII reaction center content and expressed as electrons s^{-1} RC^{-1}), generated from active fluorescent measurements are being recognized as superior, instantaneous and non-intrusive alternatives to the traditional methods of oxygen evolution or assimilation of CO_2 especially in controlled experiments such as those undertaken here where the photophysiology of phytoplankton subjected to different treatments is being examined (Silsbe et al., 2015; Schuback et al., 2016).

Our current experiments suggest that NH_4^+ accumulation prevents endosymbiont nutrient limitation which we evidenced from the invariant parameters of the ETR-E curves for both fed and non-fed cells. This is indicated by higher accumulation of NH_4^+ in LL exposed vs. HL exposed cells suggesting higher uptake rates of NH_4^+ when light levels were more conducive for NH_4^+ uptake and phytoplankton growth (MacIsaac and Dugdale, 1972). Although it is likely that the endosymbionts benefited from the accumulation of NH_4^+ in *Noctiluca* cells we have to approach this conclusion with caution as we presently do not have the NH_4^+ concentrations in the treatment bottles which would have provided us with information as to whether ammonia could have been excreted into the media. Excretion of NH_4^+ by blooms of red *Noctiluca* has been documented (Okaichi and Nishio, 1976; Montani et al., 1998; Ara et al., 2013) which in times of bloom can enhance growth of other phytoplankton (Ara et al., 2013). We have however

not observed enhanced nutrients from the large scale blooms of green *Noctiluca* that we have reported previously in the Arabian Sea (Gomes et al., 2008, 2009, 2014). The fact that our culture of *Noctiluca* can survive for several months without food nor replenishment of nutrients in the media suggests a tight recycling of nutrients which allow endosymbionts to grow as well as support the growth of the host *Noctiluca* (Furuya et al., 2006a). Using an algal culture with differing N and P elemental composition Zhang et al. (2017) showed that the heterotrophic red *Noctiluca* strictly regulates its stoichiometry which allows it to tide over when resources are scarce. Total cellular elemental ratios of this red *Noctiluca* strain were nearly homeostatic, although its intracellular pools of NH_4^+ and PO_4^+ were weakly regulated. Additionally, this strain of red *Noctiluca*, was found to regulate its internal N more strongly and efficiently than its P content making it more vulnerable to P limitation. If this is also the case with green *Noctiluca*, it can explain its predominance in the Arabian Sea (Gomes et al., 2008, 2009) which is severely N but not P limited (Morrison et al., 1999). Future studies such as that of Zhang et al. (2017) with green *Noctiluca* will better enable us to understand what has triggered the recent and pervasive annual blooms of *Noctiluca* in the Arabian Sea which portend to cause severe repercussion for the marine resources of great economic and cultural significance to the more than 86 million people living along the coast. In the Arabian Sea, *Noctiluca* does not appear to be a preferred food source for common mesozooplankton and instead appears to be consumed by jellyfish and salps potentially casing disruptions to the traditional diatom-sustained food chain (Gomes et al., 2014).

More studies such as these are required to better understand the interplay between autotrophy and heterotrophy in the green Noctiluca so that mixotrophy can be included in conceptual and mathematical models. The current exclusion of mixotrophy misrepresents the functioning of the biological pump with important implications for our understanding of the influence of climate change on aquatic ecosystems (Mitra et al., 2014).

CONCLUSION

The recently isolated mixotrophic strain of green *Noctiluca* which harbors large populations of the Chlorophyte *P. noctilucae* yielded some interesting results on its mode of nutrition that could complicate the description and modeling of food web structures in pelagic ecosystems. The green *Noctiluca* showed a definite preference for certain algal foods preferring the dinoflagellate *P. foliaceum* and the pennate diatom *P. tricornutum* to another diatom *T. weissflogii* and the chlorophyte *Pyramimonas sp*. However, regardless of the food provided, light was necessary for *Noctiluca* to grow and growth was severely diminished at low irradiances of around 10 $\mu E\ m^{-2}\ s^{-1}$. This was confirmed by the instantaneous and non-intrusive measurements of variable fluorescence derived ETRs. However, when exposed to adequate light levels, however, ETR did not show any change in cells that were fed the preferred foods and those that were not indicating that the green endosymbionts were not nutritionally starved. The tight recycling of nutrients internally is indicated by the fact that our *Noctiluca* culture is able to sustain itself for several months without extraneous food or nutrients. Our first of their kind albeit preliminary measurements on the intracellular concentration of ammonia suggests that in the presence of adequate light, ammonia which accumulated early in the experiment decreased to undetectable levels soon after indicating uptake by the green endosymbionts.

AUTHOR CONTRIBUTIONS

HG and JG conceived and planned the experiments. HG processed the data and wrote the paper. KM planned and conducted the experiments. AM and ST conducted the experiments. KA-H provided insights on *Noctiluca*'s physiology from field studies for growing it in culture. XJ processed the data.

FUNDING

This work was supported in part by grants from Gordon Betty Moore Foundation, United States, the Sultan Qaboos Culture Center, United States and from NASA (NNX17AG66G-ECO4CAST) to JG and HG. AM acknowledges support from the NSF program "Research Experience for Undergraduates." ST acknowledges the support of Peddie School, Hightstown, NJ, United States where she was a High School student when this work was undertaken. XJ was supported by the Chinese Scholarship Council.

ACKNOWLEDGMENTS

We thank Dr. Daniel Kaufman, Chesapeake Research Consortium, MD for providing the curve fitting MATLAB code. We are grateful to our colleague, Prof. O. Roger Anderson, Columbia University for his insights and support for this and related work.

SUPPLEMENTARY MATERIAL

The Supplementary Material for this article can be found online at: https://www.frontiersin.org/articles/10.3389/fmars.2018.00374/full#supplementary-material

FIGURE S1 | Schematic of experimental set-up of *Noctiluca* cells fed with four types of algal food as well as unfed cells all exposed to optimal light (250 $\mu E\ m^{-2}\ s^{-1}$, HL). A similar and parallel experiment was set up under low light (10 $\mu E\ m^{-2}\ s^{-1}$, LL).

TABLE S1 | Statistically significant levels for comparison of HL vs. LL ($n = 25$), fed and unfed *Noctiluca* cell counts ($n = 7$) and for the parameters of the ETR-E curves ($n = 4$). P values were obtained using a two-sample *t*-test. All statistically significant levels ($p < 0.05$) for *p*-values are denoted by *.

REFERENCES

Al-Azri, A., Piontkovski, S., Al-Hashmi, K., Al-Gheilani, H., Al-Habsi, H., Al-Khusaibi, S., et al. (2012). The occurrence of algal blooms in Omani coastal waters. *Aquat. Ecosyst. Health Manage.* 15, 56–63. doi: 10.1080/14634988.2012.672151

Al-Hashmi, K. A., Smith, S. L., Claereboudt, M., Piontkovski, S. A., and Al-Azri, A. (2015). Dynamics of potentially harmful phytoplankton in a semi-enclosed bay in the Sea of Oman. *Bull. Mar. Sci.* 91, 141–166. doi: 10.5343/bms.2014.1041

Ara, K., Nakamura, S., Takahashi, R., Shiomoto, A., and Hiromi, J. (2013). Seasonal variability of the red tide-forming heterotrophic dinoflagellate *Noctiluca scintillans* in the neritic area of Sagami Bay, Japan: its role in the nutrient-environment and aquatic ecosystem. *Plankton Benthos Res.* 8, 9–30. doi: 10.3800/pbr.8.9

Banse, K., and McClain, C. R. (1986). Winter blooms of phytoplankton in the Arabian Sea as observed by the Coastal Zone Color Scanner. *Mar. Ecol. Prog. Ser.* 34, 201–211. doi: 10.3354/meps034201

Behrenfeld, M. J., and Kolber, Z. S. (1999). Widespread iron limitation of phytoplankton in the South Pacific Ocean. *Science* 283, 840–843. doi: 10.1126/science.283.5403.840

Bibby, T. S., Gorbunov, M. Y., Wyman, K. W., and Falkowski, P. G. (2008). Photosynthetic community responses to upwelling in mesoscale eddies in the subtropical North Atlantic and Pacific Oceans. *Deep Sea Res. Part II* 55, 1310–1320. doi: 10.1016/j.dsr2.2008.01.014

Bouman, H., Platt, T., Sathyendranath, S., and Stuart, V. (2005). Dependence of light-saturated photosynthesis on temperature and community structure. *Deep Sea Res. Part I* 52, 1284–1299. doi: 10.1016/j.dsr.2005.01.008

Breitburg, D., Levin, L. A., Oschlies, A., Grégoire, M., Chavez, F. P., Conley, D. J., et al. (2018). Declining oxygen in the global ocean and coastal waters. *Science* 359:eaam7240. doi: 10.1126/science.aam7240

Caron, D. A. (2016). Mixotrophy stirs up our understanding of marine food webs. *Proc. Natl. Acad. Sci. U.S.A.* 113, 2806–2808. doi: 10.1073/pnas.1600718113

Caron, D. A. (2017). Acknowledging and incorporating mixed nutrition into aquatic protistan ecology, finally. *Environ. Microbiol. Rep.* 9, 41–43. doi: 10.1111/1758-2229.12514

Elbrachter, M., and Qi, Y.-Z. (1998). "Aspects of *Noctiluca* (Dinophyceae) population dynamics," in *Physiological Ecology of Harmful Algal Blooms*, eds D. M. Andersen, A. Cembella and G. M. Hallegraeff. (Berlin: NATO ASI Series), 315–335.

Falkowski, P., and Kolber, Z. (1995). Variations in chlorophyll fluorescence yields in phytoplankton in the world oceans. *Funct. Plant Biol.* 22, 341–355.

Falkowski, P. G., Owens, T. H. G., Ley, A. C., and Mauzerall, D. C. (1981). Effects of growth irradiance levels on the ratio of reaction centers in two species of marine phytoplankton. *Plant Physiol.* 68, 969–973. doi: 10.1104/pp.68.4.969

Falkowski, P. G., and Owens, T. G. (1980). Light—shade adaptation. two strategies. *Mar. Phytoplankton* 66, 592–595.

Furuya, K., Saito, H., Rujinard, S., Vijayan, A. K., Omura, T., Furio, E. E., et al. (2006a). Persistent whole-bay red tide of *Noctiluca scintillans* in Manila Bay, Philippines. *Coast. Mar. Sci.* 30, 74–79.

Furuya, K., Saito, H., Sriwoon, R., Omura, T., Furio, E., Borja, V., et al. (2006b). Vegetative growth of *Noctiluca scintillans* containing the endosymbiont *Pedinomonas noctilucae*. *Afr. J. Mar. Sci.* 28, 305–308. doi: 10.2989/18142320609504167

Goes, J. I., and Gomes, H. D. R. (2016). "An ecosystem in transition: the emergence of mixotrophy in the Arabian Sea", in *Aquatic Microbial Ecology and Biogeochemistry: A Dual Perspective*, eds P. Glibert and T. Kana (Newyork, NY: Springer International Publishing), 245.

Goes, J. I., Prasad, T. G., Gomes, H. D. R., and Fasullo, J. T. (2005). Warming of the Eurasian landmass is making the Arabian Sea more productive. *Science* 308, 545–547. doi: 10.1126/science.1106610

Goes, J. I., Gomes, H. D. R., Al-Hashimi, K., and Buranapratheprat, A. (2018). "Ecological drivers of green *Noctiluca* blooms in two monsoonal-driven ecosystems," in *Global Ecology and Oceanography of Harmful Algal Blooms*, eds P. M. Glibert, E. Berdalet, M. A. Burford, G. C. Pitcher and M. Zhou (Cham: Springer International Publishing), 327–336. doi: 10.1007/978-3-319-70069-4_17

Gomes, H., Goes, J. I., Matondkar, S. G. P., Parab, S. G., Al-Azri, A., and Thoppil, P. G. (2009). "Unusual blooms of the green *Noctiluca miliaris* (Dinophyceae) in the Arabian Sea during the winter monsoon," in *Indian Ocean: Biogeochemical Processes and Ecological Variability*, eds J. D. Wiggert, R. R. Hood, S. W. A. Naqvi, S. L. Smith and K. H. Brink (Washington, DC: American Geophysical Union), 347–363. doi: 10.1029/2008GM000831

Gomes, H. D. R., Goes, J. I., Matondkar, S. G. P., Buskey, E. J., Basu, S., Parab, S., et al. (2014). Massive outbreaks of *Noctiluca scintillans* blooms in the Arabian Sea due to spread of hypoxia. *Nat. Commun.* 5:4862. doi: 10.1038/ncomms5862

Gomes, H. D. R., Goes, J. I., Matondkar, S. G. P., Parab, S. G., Al-Azri, A. R. N., and Thoppil, P. G. (2008). Blooms of *Noctiluca miliaris* in the Arabian Sea - An *in situ* and satellite study. *Deep Sea Res. Part I* 55, 751–765. doi: 10.1016/j.dsr.2008.03.003

Gorbunov, M. Y., and Falkowski, P. G. (2004). "Fluorescence Induction and Relaxation (FIRe) technique and instrumentation for monitoring photosynthetic process and primary production in aquatic ecosystems," in *Photosynthesis: Fundamental Aspects to Global Perspectives*, eds A. V. D. Est and D. Bruce (Lawrence, KS: Allen Press), 1029–1031.

Hansen, P. J., Miranda, L., and Azanza, R. (2004). Green *Noctiluca scintillans*: a dinoflagellate with its own greenhouse. *Mar. Ecol. Prog. Ser.* 275, 79–87. doi: 10.3354/meps275079

Harrison, P. J., Furuya, K., Glibert, P. M., Xu, J., Liu, H. B., Yin, K., et al. (2011). Geographical distribution of red and green *Noctiluca scintillans*. *Chin. J. Oceanol. Limnol.* 29, 807–831. doi: 10.1007/s00343-011-0510-z

Henley, W. J. (1993). Measurement and interpretation of photosynthetic light-response curves in algae in the context of photoinhibition and diel changes. *J. Phycol.* 29, 729–739. doi: 10.1111/j.0022-3646.1993.00729.x

Holmes, R. M., Aminot, A., Kérouel, R., Hooker, B. A., and Peterson, B. J. (1999). A simple and precise method for measuring ammonium in marine and freshwater ecosystems. *Can. J. Fish. Aquat. Sci.* 56, 1801–1808. doi: 10.1139/f99-128

Holm-Hansen, O., and Riemann, B. (1978). Chlorophyll a determination: improvements in methodology. *Oikos* 30, 438–447. doi: 10.2307/3543338

Houliez, E., Lefebvre, S., Lizon, F., and Schmitt, F. G. (2017). Rapid light curves (RLC) or non-sequential steady-state light curves (N-SSLC): which fluorescence-based light response curve methodology robustly characterizes phytoplankton photosynthetic activity and acclimation status? *Mar. Biol.* 164:175. doi: 10.1007/s00227-017-3208-8

Kolber, Z. S., Prášil, O., and Falkowski, P. G. (1998). Measurements of variable chlorophyll fluorescence using fast repetition rate techniques: defining methodology and experimental protocols. *Biochim. Biophys. Acta* 1367, 88–106. doi: 10.1016/S0005-2728(98)00135-2

Lachkar, Z., Lévy, M., and Smith, S. (2017). Intensification and deepening of the Arabian Sea oxygen minimum zone in response to increase in Indian monsoon wind intensity. *Biogeosciences* 15, 159–186. doi: 10.5194/bg-15-159-2018

Leles, S. G., Mitra, A., Flynn, K. J., Stoecker, D. K., Hansen, P. J., Calbet, A., et al. (2017). Oceanic protists with different forms of acquired phototrophy display contrasting biogeographies and abundance. *Proc. R. Soc. B Biol. Sci.* 284:20170664 doi: 10.1098/rspb.2017.0664

MacIsaac, J. J., and Dugdale, R. C. (1972). Interactions of light and inorganic nitrogen in controlling nitrogen uptake in the sea. *Deep Sea Res. Oceanogr. Abstr.* 19, 209–232. doi: 10.1016/0011-7471(72)90032-0

Mitra, A., Flynn, K. J., Burkholder, J. M., Berge, T., Calbet, A., Raven, J. A., et al. (2014). The role of mixotrophic protists in the biological carbon pump. *Biogeosciences* 11, 995–1005. doi: 10.5194/bg-11-995-2014

Mitra, A., Flynn, K. J., Tillmann, U., Raven, J. A., Caron, D., Stoecker, D. K., et al. (2016). Defining planktonic protist functional groups on mechanisms for energy and nutrient acquisition: incorporation of diverse mixotrophic strategies. *Protist* 167, 106–120. doi: 10.1016/j.protis.2016.01.003

Montani, S., Pithakpol, S., and Tada, K. (1998). Nutrient regeneration in coastal seas by *Noctiluca scintillans*, a red tide-causing dinoflagellate. *J. Mar. Biotechnol.* 6, 224–228.

Morel, A., and Bricaud, A. (1981). Theoretical results concerning light absorption in a discrete medium, and application to specific absorption of phytoplankton. *Deep Sea Res. Part A* 28, 1375–1393. doi: 10.1016/0198-0149(81)90039-X

Morrison, J. M., Codispoti, L. A., Smith, S. L., Wishner, K., Flagg, C., Gardner, W. D., et al. (1999). The oxygen minimum zone in the Arabian Sea during 1995. *Deep Sea Res. II* 46, 1903–1931. doi: 10.1016/S0967-0645(99)00048-X

Okaichi, T., and Nishio, S. (1976). Identification of ammonia as the toxic principle of red tide *Noctiluca miliaris*. *Bull. Plankton Soc. Japan* 23, 75–80.

Park, J., Park, T., Yang Eun, J., Kim, D., Gorbunov Maxim, Y., Kim, H. C., et al. (2013). Early summer iron limitation of phytoplankton photosynthesis in the Scotia Sea as inferred from fast repetition rate fluorometry. *J. Geophys. Res. Oceans* 118, 3795–3806. doi: 10.1002/jgrc.20281

Platt, T., Gallegos, C. L., and Harrison, W. G. (1980). Photoinhibition of photosynthesis in natural assemblages of marine phytoplankton. *J. Mar. Res.* 38, 103–111.

Platt, T., and Jassby, A. D. (1976). The relationship between photosynthesis and light for natural assemblages of coastal marine phytoplankton. *J. Phycol.* 12, 421–430. doi: 10.1111/j.1529-8817.1976.tb02866.x

Platt, T., and Sathyendranath, S. (1988). Oceanic primary production: estimation by remote sensing at local and regional scales. *Science* 241, 1613–1620. doi: 10.1126/science.241.4873.1613

Poulton, N. J. (2016). "FlowCam: quantification and classification of phytoplankton by imaging flow cytometry," in *Imaging Flow Cytometry: Methods and Protocols*, eds N. S. Barteneva and I. A. Vorobjev (New York, NY: Springer), 237–247.

Saito, H., Furuya, K., and Lirdwitayaprasir, T. (2006). Photoautotrophic growth of *Noctiluca scintillans* with the endosymbiont *Pedinomonas noctilucae*. *Plankton Benthos Res.* 1, 97–101. doi: 10.3800/pbr.1.97

Schuback, N., Flecken, M., Maldonado, M. T., and Tortell, P. D. (2016). Diurnal variation in the coupling of photosynthetic electron transport and carbon fixation in iron-limited phytoplankton in the NE subarctic Pacific. *Biogeosciences* 13, 1019–1035. doi: 10.5194/bg-13-1019-2016

Serôdio, J., Vieira, S., Cruz, S., and Barroso, F. (2005). Short-term variability in the photosynthetic activity of microphytobenthos as detected by measuring rapid light curves using variable fluorescence. *Mar. Biol.* 146, 903–914. doi: 10.1007/s00227-004-1504-6

Silsbe, G. M., Oxborough, K., Suggett, D. J., Forster, R. M., Ihnken, S., Komárek, O., et al. (2015). Toward autonomous measurements of photosynthetic electron transport rates: an evaluation of active fluorescence-based measurements of photochemistry. *Limnol. Oceanogr. Methods* 13:e10014. doi: 10.1002/lom3.10014

Sosik, H. M., and Mitchell, B. G. (1994). Effects of temperature on growth, light absorption, and quantum yield in *Dunaliella tertiolecta* (Chlorophycea). *J. Phycol.* 30, 833–840. doi: 10.1111/j.0022-3646.1994.00833.x

Sriwoon, R., Pholpunthin, P., Lirdwitayaprasit, T., Kishino, M., and Furuya, K. (2008). Population dynamics of green *Noctiluca scintillans* (Dinophyceae) associated with the monsoon cycle in the upper Gulf of Thailand. *J. Phycol.* 44, 605–615. doi: 10.1111/j.1529-8817.2008.00516.x

Stoecker, D. K., Hansen, P. J., Caron, D. A., and Mitra, A. (2017). Mixotrophy in the marine plankton. *Annu. Rev. Mar. Sci.* 9, 311–335. doi: 10.1146/annurev-marine-010816-060617

Stoecker, D. K., Johnson, M. D., Devargas, C., and Not, F. (2009). Acquired phototrophy in aquatic protists. *Aquat. Microb. Ecol.* 57, 279–310. doi: 10.3354/ame01340

Suggett, D. J., Moore, C. M., Hickman, A. E., and Geider, R. J. (2009). Interpretation of fast repetition rate (FRR) fluorescence: signatures of phytoplankton community structure versus physiological state. *Mar. Ecol. Prog. Ser.* 376, 1–19. doi: 10.3354/meps07830

Sweeney, B. M. (1971). Laboratory studies of a Green *Noctiluca* from New Guinea. *J. Phycol.* 7, 53–58. doi: 10.1111/j.1529-8817.1971.tb01478.x

Sweeney, B. M. (1976). *Pedinomonas noctilucae* (Prasinophyceae) the flagellate symbiotic in *Noctiluca* (Dinophyceae) in Southeast Asia. *J. Phycol.* 12, 460–464.

Wang, L., Lin, X., Goes, J. I., and Lin, S. (2016). Phylogenetic analyses of three genes of *Pedinomonas noctilucae*, the green Endosymbiont of the marine Dinoflagellate *Noctiluca scintillans*, reveal its affiliation to the order Marsupiomonadales (Chlorophyta, Pedinophyceae) under the reinstated name Protoeuglena noctilucae. *Protist* 167, 205–216. doi: 10.1016/j.protis.2016.02.005

Zhang, S., Liu, H., Glibert, P. M., Guo, C., and Ke, Y. (2017). Effects of prey of different nutrient quality on elemental nutrient budgets in *Noctiluca scintillans*. *Sci. Rep.* 7:7622. doi: 10.1038/s41598-017-05991-w

Zhang, S., Liu, H., Guo, C., and Harrison, P. J. (2016). Differential feeding and growth of *Noctiluca scintillans* on monospecific and mixed diets. *Mar. Ecol. Prog. Ser.* 549, 27–40. doi: 10.3354/meps11702

Conflict of Interest Statement: The authors declare that the research was conducted in the absence of any commercial or financial relationships that could be construed as a potential conflict of interest.

frontiers in Marine Science

ORIGINAL RESEARCH
published: 12 June 2018
doi: 10.3389/fmars.2018.00205

Strombidium rassoulzadegani: A Model Species for Chloroplast Retention in Oligotrich Ciliates

George B. McManus[1], Weiwei Liu[1,2], Rachel A. Cole[1], Daniel Biemesderfer[1] and Jennifer L. Mydosh[1]*

[1] Department of Marine Sciences, University of Connecticut, Groton, CT, United States, [2] Key Laboratory of Tropical Marine Bio-Resources and Ecology, South China Sea Institute of Oceanology, Chinese Academy of Science, Guangzhou, China

Strombidium rassoulzadegani is a planktonic ciliate that retains chloroplasts from its food and uses them to obtain a nutritional supplement from photosynthesis. Unlike most members of the Oligotrichia, it is not difficult to grow in culture and thus it can serve as an experimental model for this kind of mixotrophy. We report here on its distribution, seasonal pattern of occurrence in the western North Atlantic, and on experiments to elucidate patterns of encystment and excystment, preferred food algae, and heterotrophic growth. Among ten different microalgae, including members of the Dinophyceae, Chlorophyceae, Haptophyceae, Cryptophyceae, and Bacillariophyceae, only four could support growth for more than 1 week, and only the chlorophyte *Tetraselmis chui* (PLY 429) could consistently support sustained growth in the dark. Of the four algae that supported growth, three also resulted in longer survival when the ciliate was subsequently starved in the light, compared to the dark, suggesting that all of them provided some photosynthetic benefit to the ciliate. The dinoflagellate *Prorocentrum minimum* (JA) supported similar survival in the light and dark and likely does not undergo chloroplast retention in the ciliate.

Keywords: mixotrophy, kleptoplasty, oligotrich, encystment, chloroplast

OPEN ACCESS

Edited by:
Matthew D. Johnson, Woods Hole Oceanographic Institution, United States

Reviewed by:
Sai Elangovan S, National Institute of Oceanography (CSIR), India
Miran Kim, Chonnam National University, South Korea

****Correspondence:***
George B. McManus
george.mcmanus@uconn.edu

Specialty section:
This article was submitted to Marine Ecosystem Ecology, a section of the journal Frontiers in Marine Science

Received: *28 March 2018*
Accepted: *25 May 2018*
Published: *12 June 2018*

Citation:
McManus GB, Liu W, Cole RA, Biemesderfer D and Mydosh JL (2018) Strombidium rassoulzadegani: A Model Species for Chloroplast Retention in Oligotrich Ciliates. Front. Mar. Sci. 5:205. doi: 10.3389/fmars.2018.00205

INTRODUCTION

The widespread application of fluorescence microscopy in plankton studies during the 1980s resulted in the observation of chloroplasts in many marine ciliates, a group that had previously been considered wholly heterotrophic (the sole exception being the remarkably unique *Mesodinium rubrum*) (Laval-Peuto et al., 1986; McManus and Fuhrman, 1986; Stoecker et al., 1987). Plastids appeared to be "arranged" around the periphery of the cell in some cases, and could be distinguished clearly from ingested food algae in vacuoles. Some observations of chloroplasts in ciliates had been made earlier (e.g., Blackbourn et al., 1973), but these came before it was widely appreciated that ciliates are abundant and ecologically important members of marine plankton communities. Subsequent lab and field work indicated that chloroplast retention by ciliates was widespread, comprising up to half of the assemblage, and that the chloroplasts were physiologically functional within the ciliates (Stoecker and Silver, 1987; Stoecker et al., 1987; Putt, 1990).

The capacity of some ciliates to both eat and photosynthesize with retained chloroplasts has been referred to as a kind of mixotrophy. The overall prevalence of mixotrophy in the protist plankton has come to be better appreciated in recent years. Phytoplankton that can eat and

microzooplankton that can photosynthesize are probably the rule rather than the exception, and efforts are underway to quantify mixotrophy and incorporate it into models of the ocean's food web (Flynn and Mitra, 2009). To this end, a new lexicon of terms describing mixotrophy has been created to categorize organisms according to whether they have permanent photosynthetic capability (constitutive mixotrophs) or acquire this capacity from other organisms, either through symbiosis or retention of chloroplasts from algal food, and further, whether the mixotrophy is acquired from only one or multiple algal species (Flynn et al., 2013; Mitra et al., 2016). In this context, the organism that is the subject of this paper, *Strombidium rassoulzadegani*, is a "non-constitutive generalist" mixotrophic ciliate that can use plastids from multiple prey (Schoener and McManus, 2012; see also McManus et al., 2004, reported as *S. stylifer*). Other terms for this form of mixotrophy include "kleptoplastidy/kleptoplasty" and "chloroplast symbiosis", as reviewed in Stoecker (1998), Stoecker et al. (2009), and Johnson (2011).

We first observed *S. rassoulzadegani* by its DNA signature as a member of a cryptic species complex related to *S. oculatum*. The latter had long been studied from tide pools in Europe, where it apparently has a tidal period of encystment/excystment (Faure-Fremiet, 1948; Jonsson, 1994; Montagnes et al., 2002b). In 2003, we isolated *S. rassoulzadegani* from a tide pool in Connecticut, USA, brought it into culture, and described it as a new species (McManus et al., 2010). Since that time, we have isolated it more than a dozen times and maintained individual isolates for up to 6 years. A number of papers have described its growth, photosynthesis, and nutrient utilization (McManus et al., 2012; Schoener and McManus, 2012, 2017). Its transcriptome was obtained recently through the Marine Microbial Eukaryote Transcriptome Sequencing Project (Santoferrara et al., 2014). The practice of retaining chloroplasts from ingested food appears to be widespread in the ciliate subclass Oligotrichia, of which the Strombidiidae comprise a family, but progress in understanding the physiology and ecological importance of this phenomenon has been hampered by the difficulty of cultivating these ciliates (cf. Montagnes et al., 1996). Because *S. rassoulzadegani* is an easily-cultivated exception to this rule, it can serve as a good model organism for studying chloroplast retention, in particular the costs and benefits of this nutritional mode. The purpose of the present paper is to discuss what we have learned from field and culture studies about the global distribution of *S. rassoulzadegani*, its encystment/excystment patterns, utilization of different algal foods, and heterotrophic growth, and to recommend procedures for its isolation and maintenance in culture.

METHODS

Distribution

We previously designed primers specific to *S. rassouzadegani* for the ITS region of the ribosomal operon (ITS1-5.8S-ITS2; GenBank DQ241747), and tested them for specificity against DNAs from tide pools where multiple members of the cryptic species cluster were known to be present (McManus et al., 2010). Using this primer set (F1: TGCTAATCCAATCCA ACTCAACCA; R1: GAGCCCAGATACGATTCCAAAGT), we documented presence/absence of *S. rassoulzadegani* in tidepool samples from the North and South Atlantic and Pacific Oceans (Table S1), and in a time series of samples collected weekly or biweekly over an annual cycle from two shore sites in Connecticut, USA (March 2009–May 2010). Samples of 60 ml were collected by us or colleagues, filtered through cellulose nitrate filters (Whatman, 3.0 μm pore-size) and stored in lysis buffer prior to extraction and amplification. PCR methods were as described in Katz et al. (2005), including both positive and negative controls. Cycling conditions were: initial 95°C for 2 min, followed by 35 cycles of 95°C for 0.5 min, 55°C for 0.5 min, 72°C for 1.5 min, then a final 72°C for 2 min and hold at 4°C. Presence on a gel of the appropriate-sized PCR product was interpreted as presence of the ciliate. Ten percent of positive results were cut from gels and sequenced for verification.

Isolation and Cultivation

S. rassoulzadegani is readily found in tide pools at mid-latitudes in the North Atlantic. It is often abundant enough to pick directly from unconcentrated water samples using a drawn capillary and exploiting its strong positive phototaxis, or it can be harvested a few days later from samples enriched with the green alga *Tetraselmis chui* (PLY 429). Although we have sometimes picked its congener *S. apolatum* from the same samples (verified by ITS sequence), we have never been able to successfully keep the latter in culture. All experiments reported here were performed using an isolate from Appledore Island, ME, USA, collected in August 2016.

Cultures of *S. rassoulzadegani* are routinely maintained in the lab at 20°C, salinity 28, on a 12:12 L:D photoperiod at c. 70–100 μmol m^{-2} s^{-1}. They grow best on the green alga *Tetraselmis chui* (PLY 429), and under those conditions, growth saturates at a food concentration of about 2.5×10^4 cells ml^{-1} and light at 50 μmol m^{-2} s^{-1} (McManus et al., 2012). We have had the most success growing cultures in f/2 medium (Guillard and Ryther, 1962) in six-well plastic culture plates, though larger cultures can be successful when more material is needed for molecular or physiological studies and more dilute medium (f/20) is sometimes used to slow down the growth of the food algae (Schoener and McManus, 2017). Culture maintenance and temperature-controlled experiments were done in a reach-in incubator (Thermo Scientific) with controlled temperature and light (using 60 watt cool-white fluorescent bulbs).

Microscopy

Light microscope images were taken with bright-field or differential interference contrast illumination on an Olympus BX50 compound microscope, using either an Olympus Magna-Fire (color) or Hammamatsu C11440 (monochrome) digital camera. For transmission electron microscopy, cultures of *S. rassoulzadegani* (approximately 100 ml) were concentrated to 1 ml over a 25 mm diameter 0.45 μm pore size filter. Concentrated samples were fixed for 30 min by mixing 1:1 with 2.5% glutaraldehyde and 2.5% paraformaldehyde buffered with 0.1 M Na cacodylate (pH 7.4) in sterile seawater. Fixed samples were pelleted by centrifugation and prepared for electron

microscopy as described previously (Stanton et al., 1981). Ultrathin sections were examined and photographed using a FEI Biotwin (LaB6, 80 kv) transmission electron microscope.

Sizes of plastids in light- and dark-grown cells were measured on live cells suspended in a drop of 0.4 M sucrose (isotonic to the chloroplasts) and squashed between cover slip and slide to release the plastids. Plastid dimensions in digital images were measured with NIS Elements software and volumes calculated assuming either spherical or prolate spheroid shape.

Encystment/Excystment

New ciliate cultures generally produce cysts during the first few weeks of cultivation, but long-term cultures seem to lose this habit, possibly due to selection for only active trophic cells during culture transfers because the cysts adhere to the culture well bottoms. Encystment experiments were conducted in six-well plates in triplicate, with triplicate controls, using relatively new cultures from which cells had recently excysted. For salinity shock experiments, cells were suspended in f/2 medium at salinities of 5, 10, 15, 20, 30, 45, or 60 (practical salinity scale), with controls at the standard culture salinity of 28. Other treatments included presence/absence of predators (copepods), evaporation to dryness, cold (4°C) and darkness, and starvation. We also compared cyst formation in control cultures (20°C 12:12 L:D) with those exposed to shortened photoperiod (12:12 L:D to 9.5:14.5 over 12 days), gradual temperature reduction (20°−10°C over 12 days), or both photoperiod and temperature reduction at the same time. Comparison of treatments was done by *t*-test.

To attempt to induce excystment, culture wells containing cysts adhering to the bottom were treated with additions of dried macroalgae (*Ulva* sp.), filtered medium in which *T. chui* had been grown, additions of *S. rassoulzadegani* trophic cells from other cultures, or rinses of fresh autoclaved f/2 medium. The cysts are very sticky and cannot be picked up by drawn capillary, the way trophic cells can, so we just waited until enough cysts had accumulated in the culture wells to start an experiment by removing all trophic cells. Although we did not quantify them precisely, there were hundreds of cysts per well and they accumulated in the cultures over several weeks. Thus, we did not test for emergence from cysts that had been encysted for months or years. However, given the very short duration of encystment in congener *S. oculatum* (tidal cycle of encystment/excystment) we considered that short-term experiments were appropriate.

Food Preference Experiments

Ten different algal strains were tested for the ability to support survival and growth in light (12:12 L:D cycle at 70 μmol m^{-2} s^{-1}) or dark (24 D, inside an insulated styrofoam container) conditions (**Table 1**). *S. rassoulzadegani* cells were picked from cultures growing on PLY 429 and placed, 20 per well, into six-well plates containing the different food algae and f/2 medium. Because no quantitative statistical results were produced in these initial tests, the treatments were not replicated. All algae were obtained from the National Marine Fisheries Service/NOAA Laboratory collection in Milford CT, except for ISO SP. The latter was isolated by us from our ciliate cultures. Using universal primers (Medlin et al., 1988), we sequenced the small-subunit (SSU) and used BLAST at the NCBI website to identify it as 99% similar to *Isochrysis* sp. strain CCAP 927/14 (NCBI accession number DQ079859). The latter is synonymous with the TISO strain, according to the culture data in the National Center for Marine Algae. The amount of food algae was judged by eye and adjusted each day to avoid over- or under-feeding (growth is saturated above 10^4 cells ml^{-1}; McManus et al., 2004). Initially, wells were observed every day for 6 days (short-term experiments). After 6 days, the wells with 100% mortality were emptied and those treatments were restarted with the same algae and 20 new *S. rassouladegani* cells. Those, and the wells in which ciliates were still alive, were followed for a further 4 weeks, with growth and survival monitored in the same way (long-term experiments).

TABLE 1 | Microalgae tested as food for *S. rassoulzadegani* in light vs. dark experiments.

Food tested	Strain	Class
Isochrysis galbana	TISO	Haptophyte
Isochrysis sp.	ISO SP	Haptophyte
Tetraselmis chui	PLY429	Chlorophyte
Rhodomonas lens	RHODO	Cryptophyte
Thalassiosira weissflogii	TWEISS	Diatom
Amphidinium carterae	AMP	Dinoflagellate
Prorocentrum minimum	EXUV	Dinoflagellate
Prorocentrum minimum	JA	Dinoflagellate
Alexandrium minutum	ALEX	Dinoflagellate
Scrippsiella lachrymosa	SCRIPPS	Dinoflagellate

All cultures were obtained from the culture collection of the US National Marine Fisheries Service, NOAA, except for Isochrysis sp.*, which was isolated by us from local waters.*

Heterotrophic vs. Mixotrophic Growth

After we had established that *S. rassoulzadegani* could be grown heterotrophically in darkness if sufficient care was given to ensure saturating concentrations of fresh PLY 429 were added daily, we performed 5 separate experiments to measure growth under light (12:12 L:D) or dark (24 D) conditions. Cultures were started in f/2 medium in well-plates with 10–30 ciliates per triplicated well and fed abundant PLY 429. Plates were either kept in darkness (24 D, inside an insulated styrofoam container) or light (12:12 L:D at 70 μmol m^{-2} s^{-1}). Light, or lack thereof, was measured with an Apogee model MQ-200 quantum light meter. After 5–8 days, well contents were preserved with lugols iodine solution and ciliates were counted with an inverted microscope. Growth rates were calculated assuming exponential growth, in units of d^{-1}, as $\mu = \ln(N_t/N_0)/\Delta t$, where N_0 and N_t are ciliate abundances at the beginning and end of the experiment, respectively, and Δt is the experimental duration in days.

Starvation Experiments

Ciliates grown out in each of the four most suitable algal foods (PLY 429, RHODO, JA, and ISO SP) were rinsed and placed, 20 per well, in triplicate wells in 12-well plates with 4 ml of filtered,

autoclaved f/2 medium and no food. Plates were placed in light (12:12 L:D) or darkness and monitored for survivors until all were dead (3–8 d, depending on treatment).

RESULTS

Distribution

We have isolated cultures of *S. rassoulzadegani* from tide pools in Dunbar, Scotland, the northeast USA (Maine and Connecticut), and from open water nearshore in Sao Sebastiao, Brazil (CEBIMAR marine laboratory, U. Sao Paolo). We have found it reliably during summer in the relatively pristine tide pools of Shoals Marine Lab (Appledore Island, Maine), and have sometimes observed it co-occurring with its close congener *S. apolatum*, though we have never succeeded in keeping the latter under cultivation for more than a day or so. Based on finding its ITS sequence in filtered water samples, we conclude that it is globally distributed (**Figure 1**; Table S1).

At two shore sites on Long Island Sound, USA, we sampled 41 (Groton, CT) and 32 (Madison, CT) times over a 14-month period, collecting water from three different tide pools each time. At Groton, *S. rassoulzadegani* rDNA was present in at least one pool on all sampling dates from May through October and on a few dates in March and April. It was never detected from November through February. In Madison, which is 45 km closer to the eutrophic western end of the Sound, *S. rassoulzadegani* rDNA signature was seen in at least one pool in every month except December.

Isolation and Cultivation

Although it was initially cultured on "swarmer cells" (zoospores or gametes) of a green macroalga, *Ulva* sp. (McManus et al., 2004), we have subsequently isolated and maintained *S. rassoulzadegani* primarily on the green microalga *Tetraselmis chui* (strain PLY 429), a common food in aquaculture applications. In culture, the cells are grass-green, with a prominent reddish eyespot consisting of a cluster of pigment granules that appear to originate in the food alga. They show strong positive phototaxis, swimming in a helical pattern toward the light, which can help to concentrate them from natural populations for isolation. In culture, they can achieve densities of $>10^3$ cells/ml.

Encystment/Excystment

S. rassoulzadegani produces a typical oligotrich cyst, consisting of a roughly spherical body, with a short neck and a frothy-looking plug (Montagnes et al., 2002a; **Figure 2**). The cysts appear to be surrounded with a sticky organic layer to which bacteria and algae in the cultures adhere. It does

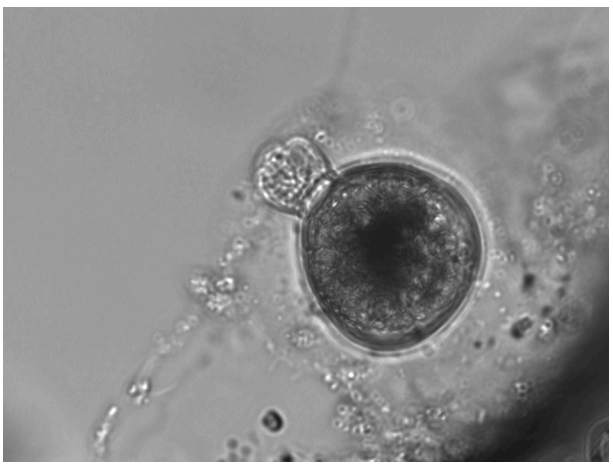

FIGURE 2 | Typical *S. rassoulzadegani* cyst, with "frothy plug" at top left, and adhering organic layer. Cyst diameter is c. 40 μm.

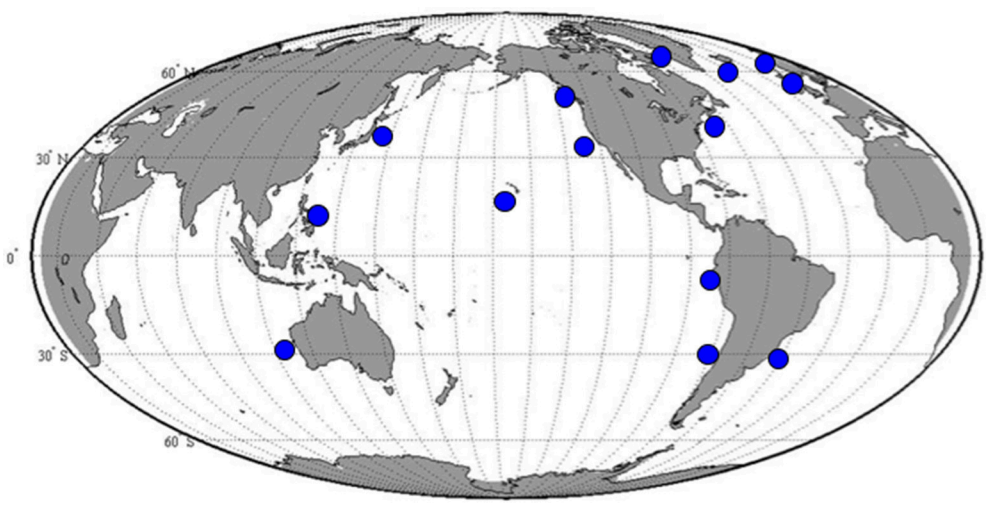

FIGURE 1 | Positive results for amplification with *S. rassoulzadegani* species-specific ITS-region PCR primers.

not appear to encyst/excyst on a tidal cycle, as described for its tidepool congener *S. oculatum*. We did not observe any other distinct periodicity to the cyst cycle. Trophic cells did not encyst in response to sudden changes in salinity (range 5–60, with no survival at the highest and lowest salinities), the presence of predators (copepods), evaporation of the medium to dryness, starvation, or cold/dark (4°C) conditions. A gradual reduction in temperature, from 20° to 10°C over 12 days under constant light conditions (12:12 photoperiod at c. 70 μmol m^{-2} s^{-1}) did not induce encystment. Neither did a gradual decrease in the light period (from 12:12 to 9.5:14.5) at constant 20°C. However, simultaneous reductions in temperature and light did result in significantly more cysts, compared to controls at 20°C and 12:12 (**Figure 3A**).

Excystment was not induced by additions of algal exudates (*T. chui* spent medium), dried *Ulva* sp., or trophic cells of *S. rassoulzadegani*. Rinsing cysts with fresh medium (filtered, autoclaved f/2 seawater) was the only treatment with which we successfully stimulated excystment (**Figure 3B**).

Microscopy

Plastids within the ciliate appear to be free in the cytoplasm (not surrounded by ciliate vacuolar membrane), and are found in various shapes and sizes, even when derived from a single food alga (**Figures 4A,B**). Under the light microscope, some plastids are smaller, rounder, and darker (color changes from green to dark green), possibly with age (**Figure 5**). When ciliates were grown on *Tetraselmis chui* (PLY 429) in light (12:12) or dark conditions, the cells still contained abundant chloroplasts, but the plastids were much smaller in dark-grown cells (mean volume per plastid of 107 vs. 37 μm^3 in light vs. dark, respectively; $P < 0.001$ *t*-test).

Food Preference and Heterotrophic Growth Experiments

In short-term experiments (6 d), *S. rassoulzadegani* achieved positive growth when fed *Tetraselmis chui* (PLY 429), *Rhodomonas lens* (RHODO), *Isochrysis* sp. (ISO SP), and *Prorocentrum minimum* (JA) (**Figure 6**). On all other foods (the

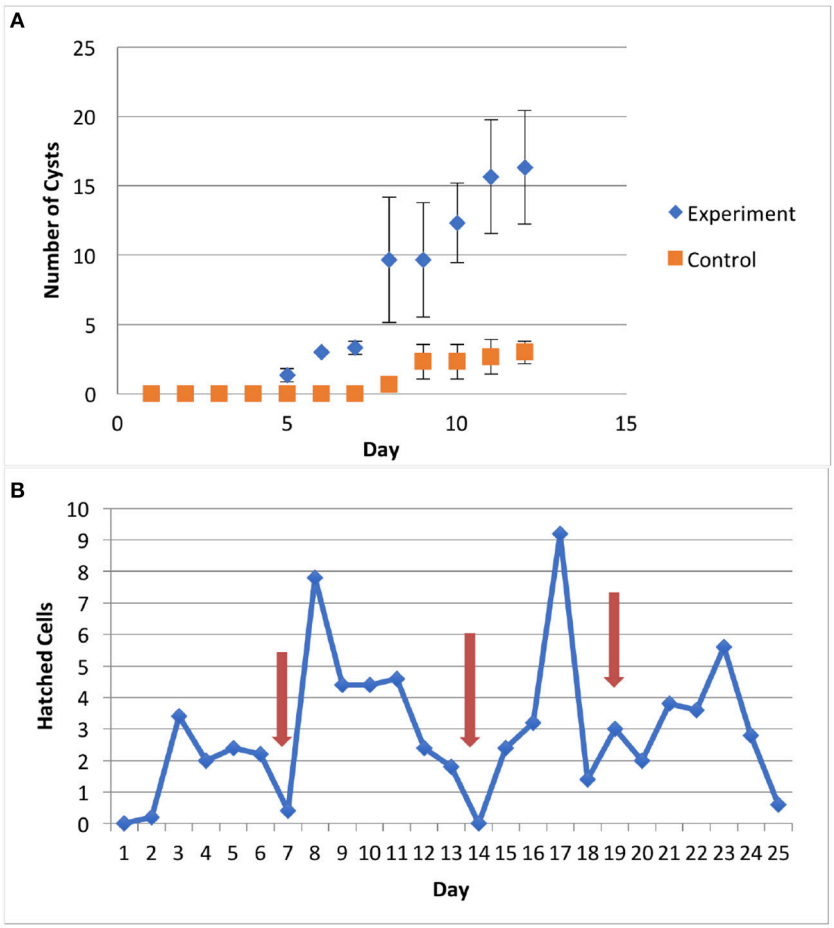

FIGURE 3 | (A) Results of encystment experiment. Shortened photoperiod (12:12–9.5:14.5) and decrease in temperature (20°-10°C) over 12 days induced formation of more cysts, compared to controls (12:12, 20°C); error bars are one standard deviation ($n = 3$). **(B)** Excystment was stimulated by rinsing cysts with fresh medium (arrows).

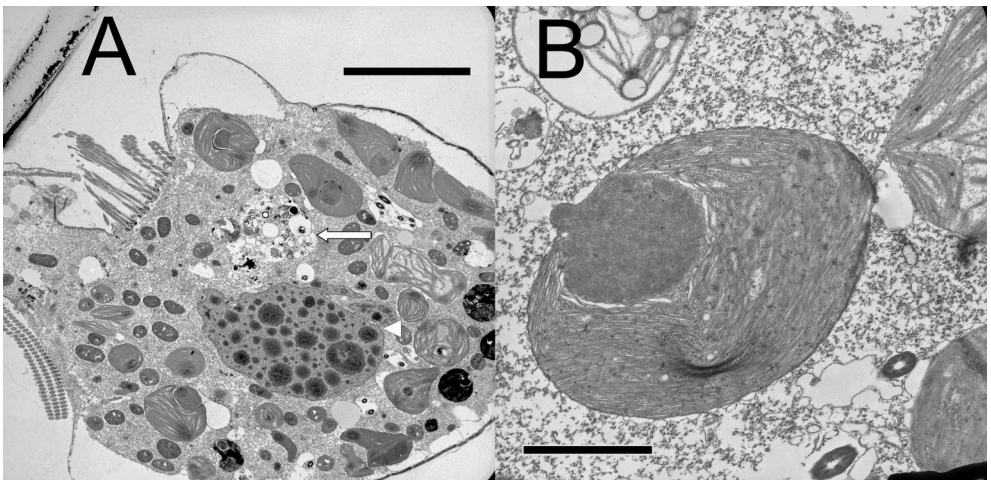

FIGURE 4 | (A) Lower magnification thin section of *S. rassoulzadegani* cell with chloroplasts in varying shapes and sizes, digestive vacuole (long arrow), and the ciliate macronucleus (arrowhead); scale bar = 10 μm. **(B)** Individual *Tetraselmis chui* chloroplast retained within *S. rassoulzadegani*; scale bar = 2 μm.

FIGURE 5 | Micrograph of *S. razoulzadegani* fed *Tetraselmis chui* (PLY 429), showing variety of shapes and sizes of retained chloroplasts, including smaller dark green and brownish ones (arrow) that may be older than the larger "grass-green" ones.

diatom *T. weissflogii*, the haptophyte *I. galbana* TISO, and the dinoflagellates *P. minimum* EXUV, *A. carterae*, *A. minutum*, and *S. lachrymosa*; **Table 1**) the ciliates were all dead by the end of the experiment. In each case of successful growth, cells that were grown on PLY 429 and switched to another food replaced the PLY 429 chloroplasts almost completely by the end of the experiment. As with PLY 429, the chloroplasts of the other algae appeared under light microscopy to be free in the cytoplasm (**Figures 6A–C**). A caveat is that this can only be verified with electron microscopy, whereas we have only observed PLY 429 and RHODO (data not shown) by transmission electron microscopy. In the dinoflagellate JA, on the other hand, the algae appear to be digested in vacuoles (**Figure 6D**). When held in darkness for 6 d with ample food, only *Tetraselmis chui* (PLY 429) and *Isochrysis galbana* (TISO) supported net positive growth in the ciliate, though we have observed short-term positive growth in both light and darkness on *Rhodomonas lens* (RHODO) and *Prorocentrum minimum* (EXUV) as well (unpublished data and McManus et al., 2012).

In longer-term experiments (5 weeks), PLY 429, RHODO, ISO SP, and JA supported survival of the ciliate under 12:12 L:D conditions. We had noticed that in RHODO, ISO SP, and JA treatments, the algae sometimes overgrew the ciliates, causing cultures to crash, so sustained growth could only be obtained by carefully controlling the algal abundance. Only PLY 429 supported long-term growth even at very high algal densities, and only PLY 429 supported long-term growth (several months) in darkness. Even after 4 weeks of cultivation in darkness on PLY 429, the ciliates continued to retain some chloroplasts from their food (**Figures 7A,D**). The ciliates died within 3 weeks in the dark in all other food treatments. One issue we faced in trying to grow the mixotrophic ciliate on these foods even for PLY 429 in the dark is that fresh algal food had to be added daily or every second day because the algae appeared to become less motile in the dark, possibly declining in nutritional value. This may have been a factor leading to the earlier conclusion that mixotrophy was "obligate" (no growth in darkness even with abundant food) in plastid-retaining ciliates (McManus et al., 2004, reported as *S. stylifer*).

When fed with fresh PLY 429 every day at saturating concentrations, *S. rassoulzadegani* could achieve growth rates 55–78% as great as those in the light (**Figure 8**). In five short-term

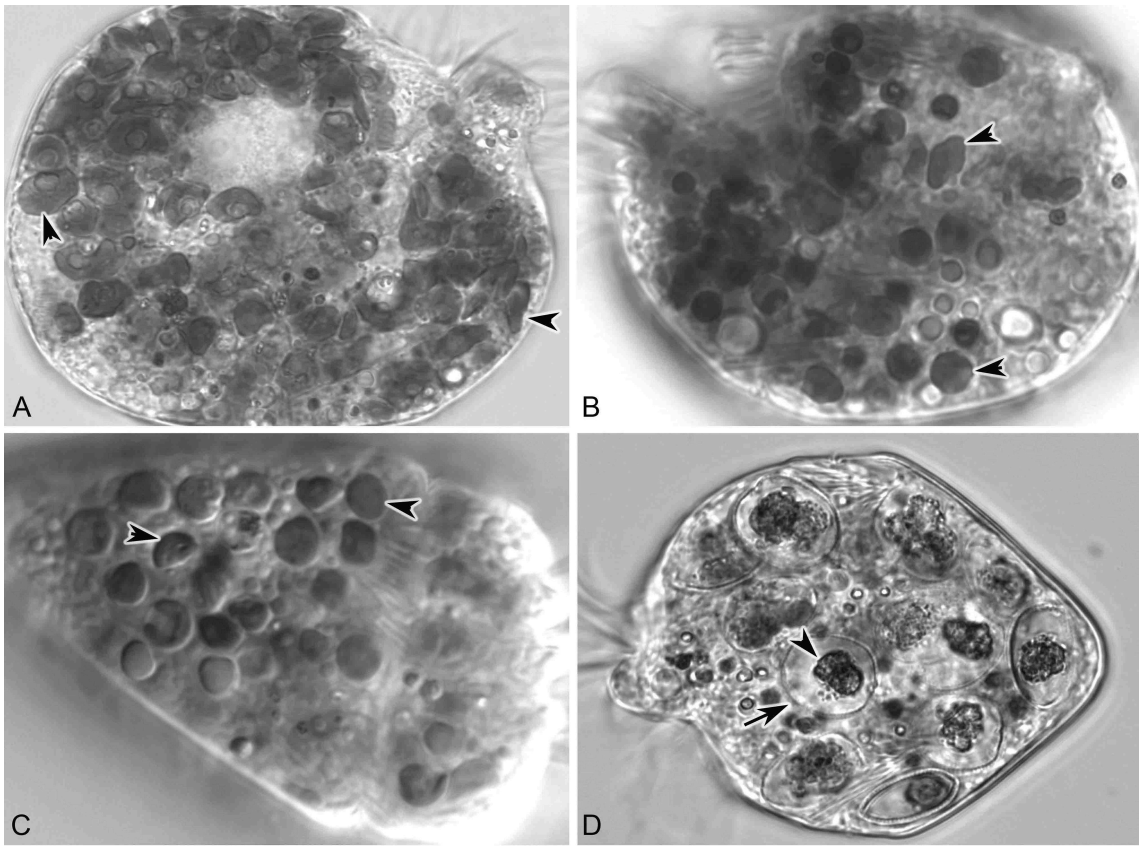

FIGURE 6 | *S. rassoulzadegani* fed four food algae that supported positive growth in the light (12:12 L:D). **(A)** *S. rassoulzadegani* fed *T. chui* PLY429; arrowheads indicate different shapes and sizes of retained chloroplasts; **(B)** *S. rassoulzadegani* fed *R. lens* RHODO; arrowheads as in **A**; **(C)** *S. rassoulzadegani* fed *Isochrysis* sp. ISO SP; arrowheads as in **A**; **(D)** *S. rassoulzadegani* fed *P. minimum* JA; note that no retained plastids appear in the cell. Arrow marks the rigid wall of the algal cell and arrowhead marks the partially-digested algal cytoplasm.

experiments (5–8 day), growth on PLY 429 in the light (12:12 L:D at c. 70 μmol m^{-2} s^{-1}) ranged from 0.75 to 1.19 d^{-1}; that in the dark ranged from 0.58 to 0.82 d^{-1} (**Figure 8**).

Ciliates fed any of the four food algae that supported net positive growth in the 6 day experiments (PLY 429, RHODO, ISO SP, or JA) survived longer in the light than the dark when subsequently starved, with the exception of JA, where survival was nearly identical in light and dark (**Figure 9**). Live observation on ciliates fed PLY 429 showed that the chloroplasts declined in size and number when cell were starved under both 12:12 L:D and 24 D (**Figures 7B,E**). After algal food was added to starved cultures, new chloroplasts were quickly retained as with non-starved cultures (**Figures 7C,F**).

DISCUSSION

We have found *S. rassoulzadegani* by its rDNA signature nearly everywhere we have looked for it, including shore samples from Greenland, Iceland, Ireland, Scotland, Norway, the east and west coasts of North and South America, Hawaii, Japan, the Philippines, and western Australia. In northwest Atlantic tide pools, it is detectable almost all year, except for winter. Its apparent disappearance in winter may be related to the encystment pattern we observed, which is related to seasonal changes in light and temperature, if the cysts are in the benthos or otherwise unrepresented in our DNA samples from the tide pools. Even when it is low in abundance, the ciliate can easily be concentrated by placing a sample in a darkened volumetric flask and placing a light near the top of the neck, where the ciliates will aggregate by phototaxis (cf. Faure-Fremiet, 1948 for *S. oculatum*). Thus, this ciliate should be available for study almost anywhere in the world and could become a model for mixotrophs, and ciliates in general, in aquaculture or ecological studies.

Although we often observed cysts in culture, we never observed the full processes of encystment or excystment. The cysts are clear enough to allow observation of the developing trophic cells tumbling about inside (**Figure 2**), and we have seen the frothy plug being pushed out, but were not able to document emergence. Likewise, although we could cause relatively new cysts (weeks old) to hatch in response to flushing with fresh growth medium, older cysts stored >6 months in darkness at 4°C could not be induced to excyst. Thus, we have not developed any methods for longer-term storage of the resting stage, and we do

not know how long the cysts may remain viable in nature. The only treatment we found that successfully stimulated encystment was simultaneous stepdown in temperature and light to levels the ciliates would experience during Autumn at mid-latitudes. This suggests that encystment is a seasonal response in this ciliate. Although our time series samples were collected from surface water in the tide pools, whereas cysts would be expected to be at the bottom or attached to macroalgae or other substrates (cf. Montagnes et al., 2002b), we cannot rule out that some of the positive results for presence of *S. rassoulzadegani* may have been due to cysts, especially in winter.

The apparent loss of the encystment habit in older cultures is interesting. It may be that long-term cultivation in abundant food and light at constant temperature places the mechanism for encystment in an inactive state. Since most of our cultures have been started from several individuals, we cannot rule out that selection for rapidly-growing non-encysting cell lines during culture transfers is responsible for the loss of the encystment habit. Further experimental work or transcriptomic studies on encysting/excysting cells may shed light on this in the future.

Between the present and previous work (McManus et al., 2012), we have tested 15 different strains of microalgae as food for *S. rassoulzadegani*. Although results have sometimes been inconsistent, a few general conclusions can be made. First, the best food giving the most consistent positive growth is *Tetraselmis chui* (PLY 429). In the light, exponential growth on PLY 429 was consistently about 1 d^{-1} (doubling time of 0.7 day; **Figure 8**). Growth in the light on *Rhodomonas lens* (RHODO) was about the same, but care had to be taken not to overfeed with RHODO, whereas the ciliates still grew well even at PLY 429 concentrations well above 10^5 cells ml^{-1}.

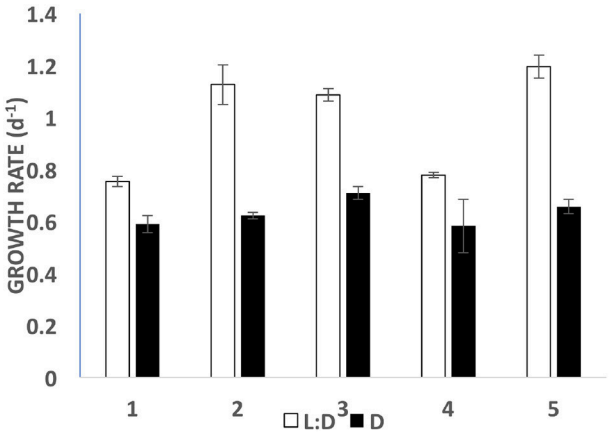

FIGURE 8 | Growth rates in light (open bars; 12:12 photoperiod at c. 70 μmol m^{-2} s^{-1}) vs. dark (filled bars) for five short term (5–8 day) experiments. Error bars are standard deviations ($n = 3$).

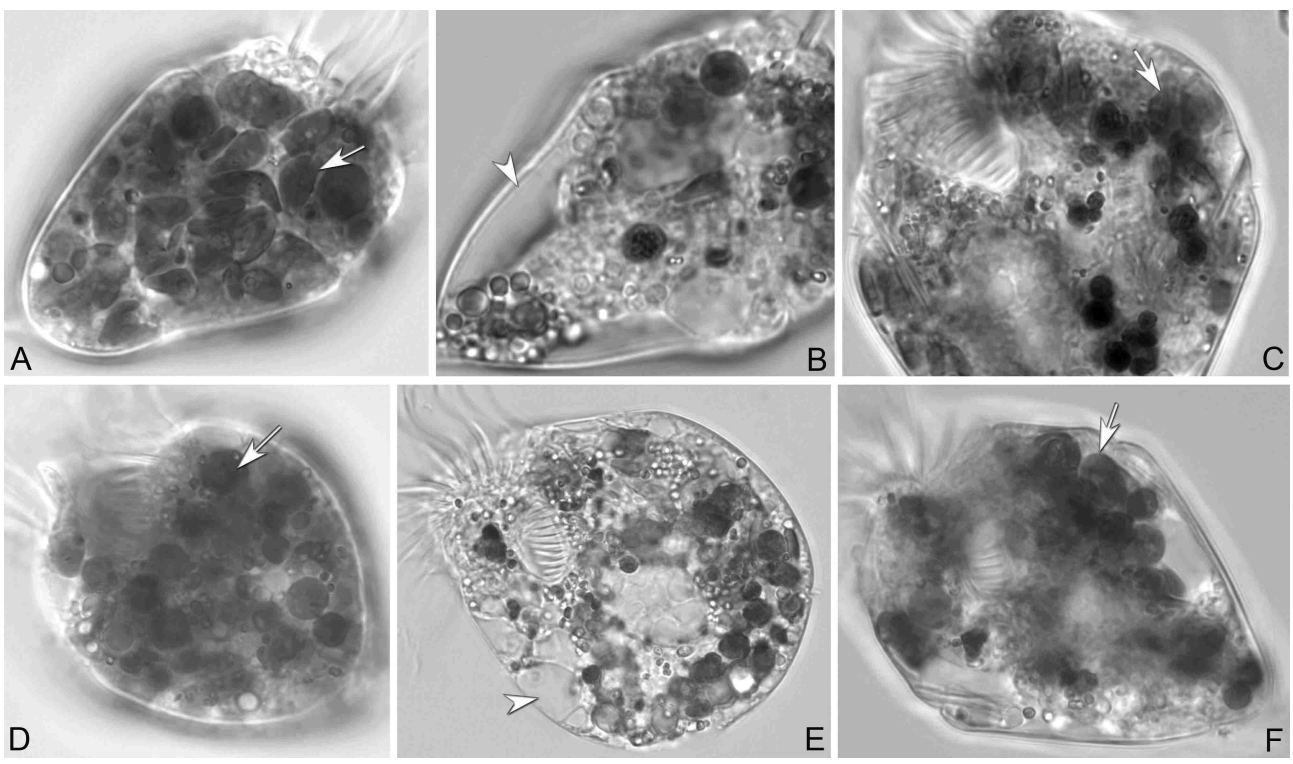

FIGURE 7 | *S. rassoulzadegani* from cultures grown on *T. chui* PLY429 at 12:12 L:D **(A–C)** or 24 D **(D–F)**. **(A,D)** Cells with adequate algae food (arrows). **(B,E)** Cells starved for 72 h; arrowheads mark empty vacuoles. **(C,F)** Algae were taken up again (arrows) after new algal food was added. Even in complete darkness **(F)**, fed cells retain some chloroplasts.

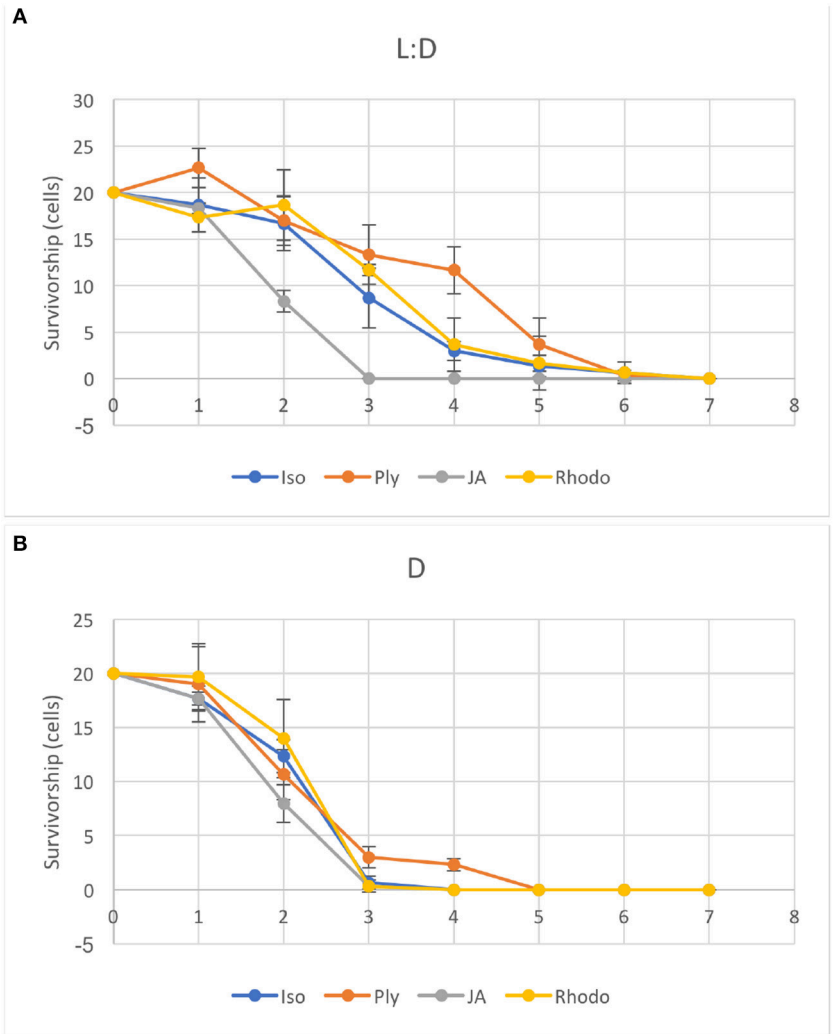

FIGURE 9 | Ciliates were starved under light (**A**, 12:12 L:D photoperiod at c. 70 μmol $m^{-2}s^{-1}$) or dark **(B)** conditions after growth on four different food algae (see **Table 1** for algal abbreviations). Error bars are standard deviations ($n = 3$).

Poor growth at high algal concentrations is likely due to the accumulation of metabolites or other changes in the medium (e.g., pH; Pedersen and Hansen, 2003) from the microalgae. Growth was never successful with diatoms as the diet, while some dinoflagellates supported growth and others did not. Two haptophytes, *Isochrysis galbana* (TISO) and an *Isochrysis* sp. (ISO SP) that is 99% similar to TISO by SSU sequence but notably different in pigmentation and some culture habits, were able to support growth if cell concentrations were carefully controlled (e.g., the failure of TISO to support growth in the light in our experiments was probably due to overgrowth of the algae in the light treatment). To date, we have found no green alga besides PLY 429 that supports growth. It should be noted that absence of growth on a given food is not proof that growth is not possible, as slight changes in culture conditions can lead to success in some cases. Also, combinations of different unsuitable foods may themselves be suitable, though we have not found a mixed food that supports growth without one of its components being PLY 429 (cf. McManus et al., 2012).

We previously succeeded in achieving positive growth rates in light and dark for several weeks on the dinoflagellate *Prorocentrum minimum* (EXUV; McManus et al., 2012). In the present study, EXUV did not support growth in light or dark, whereas a different strain of *P.minimum*, JA, only supported growth in the light, including long-term growth (5 weeks). In darkness or light, cultures eventually died out when feeding on *P. minimum* (both strains). Given the vagaries of establishing and maintaining ciliate cultures, we think the only supportable conclusion is that heterotrophic growth in *S. rassoulzadegani* is possible on a variety of foods, but difficult to maintain due to possible overgrowth or food quality issues with the algae.

In contrast to earlier results, in the present study we were able to sustain growth in darkness on *T. chui* (PLY 429) by adding fresh algae several times per week. We observed that in

dark-grown ciliate cultures, these small flagellates became less motile, possibly also declining in food quality. Prey properties including swimming motility and nutritional quality are regarded as having important effects on grazing selectivity of ciliates (Chen et al., 2010; Yang et al., 2015). Thus, previous failure of cultures to grow in darkness may have been due to food issues rather than the metabolism of the ciliate itself.

When ciliates are grown in the dark, chloroplasts are still retained from food, though they are distinctly smaller and seem darker than when they are grown in the light. Chloroplasts decline in size and number but are still present when ciliates are starved as well, suggesting that there is some process whereby chloroplasts are partly or wholly "immunized" from digestion by the ciliate. It is still not known whether plastids are egested from the ciliate when no longer functional or digested by them. As they appear to be free in the cytoplasm of the ciliate, it would require autophagous vacuoles to digest them. The latter are not seen in mixotrophic ciliates (Laval-Peuto and Febvre, 1986), so it may be difficult for the ciliates to eliminate the plastids and this may impose a cost on growth in the dark. Others have speculated that space taken up by retained chloroplasts imposes a "cost" on digestion and hence growth in the dark (Raven, 1997), but we found that growth in the dark, while significantly slower than in the light, was still in the range of 0.5–0.6 d^{-1}, so the cost may not be as great as previously thought (**Figure 8**).

The only available evidence on functioning of chloroplasts in *S. rassoulzadegani* comes from $^{14}CO_2$ uptake observations. Schoener and McManus (2017) showed net incorporation of ^{14}C into organic matter in the light, and found that this gave this mixotrophic ciliate a growth efficiency advantage in comparison to a strict heterotroph, primarily at growth-limiting food concentrations. Our light vs. dark starvation experiment showed that survival was enhanced in the light for three of the four microalgae (ISO SP, PLY 429, and RHODO) that were capable of supporting short-term growth in the dark. This suggests that retained chloroplasts from ISO SP and RHODO remained functional as well. Only the dinoflagellate *Prorocentrum minimum* (JA) had equivalent survival in light and dark, supporting earlier conjectures that growth by *S. rassoulzadegani* on dinoflagellates is wholly heterotrophic. Possibly, digestion of the cellulosic cell wall of these armored dinoflagellates makes it difficult preserve and retain the chloroplasts, or dinoflagellate chloroplasts may not have a sufficient genome to function independently inside the ciliate.

The new observations on culture conditions and food preferences from this study raise questions about the nature of mixotrophy in *S. rassoulzadegani*. Although they always grow best in light, it is now clearly established that they can grow wholly heterotrophically in the dark over at least several months. We also found that multiple algal species can support mixotrophic growth in this species, though the green *Tetraselmis chui* was clearly the best food. The ability to grow on diverse foods and potentially to use multiple different chloroplasts for mixotrophy indicates a level of nutritional plasticity that may contribute to their widespread distribution in the ocean. Future work on how food quality affects mixotrophic metabolism should shed more light on this.

Given that plastids are retained from food even in darkness and that they endure within the cells when starved, it is important to know how photosynthetic performance varies over time and whether the ciliate exerts any genetic control over the plastids. Host nucleus-encoded genes that target retained chloroplasts have been found in *Dinophysis acuminata*, a mixotrophic dinoflagellate that uses plastids retained from the ciliate *Mesodinium rubrum*, which itself retains plastids from cryptophyte algae (Wisecaver and Hackett, 2010). We have not found similar transcripts in *S. rassoulzadegani* so far (Santoferrara et al., 2014), but new methods in transcriptomics are making an experimental approach to mixotrophy more tractable. In the remarkable mixotrophic ciliate *Mesodinium rubrum*, both nuclei and plastids of prey are retained (Johnson et al., 2007) and trancriptomics has been used to elucidate how the ciliate/prey chimera functions as an integrated organism (Lasek-Nesselquist et al., 2015; Kim et al., 2016).

CONCLUSION

S. rassoulzadegani is a widely-distributed, easily cultivable mixotrophic oligotrich ciliate. It should be isolated from more regions of the world and used as a model for mixotrophs, and oligotrichs in general, in ecological, aquaculture, and physiological studies. In particular, its ability to grow on a variety of foods and to survive under light and dark conditions raises the possibility that it can provide insight into the costs and benefits of kleptoplastic mixotrophy in marine ciliates.

AUTHOR CONTRIBUTIONS

All authors listed have made a substantial, direct and intellectual contribution to the work, and approved it for publication.

ACKNOWLEDGMENTS

We thank Gary Wikfors (NOAA National Marine Fisheries Service Laboratory, Milford CT) for algal cultures; Laura Katz (Smith College) for help with sequencing and primer design; Wen Song, Susan Smith, and Luciana Santoferrara for help with experiments; and Paul Renaud, Leo Blanco-Bernal, Barbara Costas, Andrew Payson, and Joseph Eslao for sample collection. We thank Sueann Mentone, Department of Cellular and Molecular Physiology, Yale School of Medicine for technical help with the electron microscopy. Support was provided by the US National Science Foundation (grant OCE 1435515), the Natural Science Foundation of China (No. 41576124), Shoals Marine Lab, and the University of Connecticut.

SUPPLEMENTARY MATERIAL

The Supplementary Material for this article can be found online at: https://www.frontiersin.org/articles/10.3389/fmars.2018.00205/full#supplementary-material

REFERENCES

Blackbourn, D. J., Taylor, F. J. R., and Blackbourn, J. (1973). Foreign organelle retention by ciliates. *J. Protozool.* 20, 286–288. doi: 10.1111/j.1550-7408.1973.tb00877.x

Chen, B., Liu, H., and Lau, M. T. S. (2010). Grazing and growth responses of a marine oligotrichous ciliate fed with two nanoplankton: does food quality matter for micrograzers? *Aquatic Ecol.* 44, 113–119. doi: 10.1007/s10452-009-9264-5

Faure-Fremiet, E. (1948). Le rythme de maree du *S. oculatum* Gruber. *Bull. Biol. France Belgique* 82, 3–23.

Flynn, K. J., and Mitra, A. (2009). Building the "perfect beast": modelling mixotrophic plankton. *J. Plankton Res.* 31, 965–992. doi: 10.1093/plankt/fbp044

Flynn, K. J., Stoecker, D. K., Mitra, A., Raven, J. A., Glibert, P. M., Hansen, P. J., et al. (2013). Misuse of the phytoplankton–zooplankton dichotomy: the need to assign organisms as mixotrophs within plankton functional types. *J. Plankton Res.* 35, 3–11. doi: 10.1093/plankt/fbs062

Guillard, R. R., and Ryther, J. H. (1962). Studies of marine planktonic diatoms. I. Cyclotella nana Hustedt, and Detonula confervacea (cleve). *Gran. Can. J. Microbiol.* 8, 229–239. doi: 10.1139/m62-029

Johnson, M. D., (2011). Acquired phototrophy in ciliates: a review of cellular interactions and structural adaptations. *J. Eukaryot. Microbiol.* 58, 185–195. doi: 10.1111/j.1550-7408.2011.00545.x

Johnson, M. D., Oldach, D., Delwiche, C. F., and Stoecker, D. K. (2007). Retention of transcriptionally active cryptophyte nuclei by the ciliate *Myrionecta rubra*. *Nature* 445, 426–428. doi: 10.1038/nature05496

Jonsson, P. R. (1994). Tidal rhythm of cyst formation in the rock pool ciliate *Strombidium-oculatum* Gruber (*Ciliophora*, Oligotrichida) - a description of the functional biology and an analysis of the tidal synchronization of encystment. *J. Exp. Mar. Biol. Ecol.* 175, 77–103. doi: 10.1016/0022-0981(94)90177-5

Katz, L. A., McManus, G. B., Snoeyenbos-West, O. L. O., Griffin, A., Pirog, K., Costas, B. et al. (2005). Reframing the "Everything is everywhere" debate: evidence for high gene flow and diversity in ciliate morphospecies. *Aquat. Microbial Ecol.* 41, 55–65. doi: 10.3354/ame041055

Kim, G. H., Han, J. H., Kim, B., Han, J. W., Nam, S. W., Shin, W., et al. (2016). Cryptophyte gene regulation in the kleptoplastidic, karyokleptic ciliate Mesodinium rubrum. *Harmful Algae* 52, 23–33. doi: 10.1016/j.hal.2015.12.004

Lasek-Nesselquist, E., Wisecaver, J. H., Hackett, J. D., and Johnson, M. D. (2015). Insights into transcriptional changes that accompany organelle sequestration from the stolen nucleus of *Mesodinium rubrum*. *BMC Genomics* 16:805. doi: 10.1186/s12864-015-2052-9

Laval-Peuto, M., and Febvre, M. (1986). On plastid symbiosis in *Tontonia appendiculariformis* (Ciliophora, Oligotrichina). *Biosystems* 19, 137–158. doi: 10.1016/0303-2647(86)90026-2

Laval-Peuto, M., Salvano, P., Gayol, P., and Greuet, C. (1986). Mixotrophy in marine planktonic ciliates: ultrastructural study of *Tontonia appendiculariformis* (*Ciliophora*, Oligotrichina). *Mar. Microb. Food Webs.* 1, 81–104.

McManus, G. B., and Fuhrman, J. A. (1986). Photosynthetic pigments in the ciliate *Laboea strobila* from Long Island Sound, USA. *J. Plankton Res.* 8, 317–327. doi: 10.1093/plankt/8.2.317

McManus, G. B., Schoener, D. M., and Haberlandt, K. (2012). Chloroplast symbiosis in a marine ciliate: ecophysiology and the risks and rewards of hosting foreign organelles. *Front. Microbiol.* 3:321. doi: 10.3389/fmicb.2012.00321

McManus, G. B., Xu, D., Costas, B. A., and Katz, L. A. (2010). Genetic identities of cryptic species in the *Strombidium stylifer/apolatum/oculatum* cluster, including a description of *Strombidium rassoulzadegani* n. *sp. J. Euk. Microbiol.* 57, 369–378. doi: 10.1111/j.1550-7408.2010.00485.x

McManus, G. B., Zhang, H., and Lin, S. (2004). Marine planktonic ciliates that prey on macroalgae and enslave their chloroplasts. *Limnol. Oceanogr.* 49, 308–313. doi: 10.4319/lo.2004.49.1.0308

Medlin, L., Elwood, H. J., Stickel, S., and Sogin, M. L. (1988). The characterization of enzymatically amplified eukaryotic 16S-like rRNA-coding regions. *Gene* 71, 491–499. doi: 10.1016/0378-1119(88)90066-2

Mitra, A., Flynn, K. J., Tillmann, U., Raven, J. A., Caron, D., Stoecker, D. K., et al. (2016). Defining planktonic protist functional groups on mechanisms for energy and nutrient acquisition: incorporation of diverse mixotrophic strategies. *Protist* 167, 106–120. doi: 10.1016/j.protis.2016.01.003

Montagnes, D. J. S., Berger, J. D., and Taylor, F. J. R. (1996). Growth rate of the marine planktonic ciliate *Strombidinopsis cheshiri* Snyder and Ohman as a function of food concentration and interclonal variability. *J. Exp. Mar. Biol. Ecol.* 206, 121–132. doi: 10.1016/S0022-0981(96)02626-3

Montagnes, D. J., Lowe, C. D., Poultonb, A., and Jonsson, P. R. (2002a). Redescription of *Strombidium oculatum* Gruber 1884 (*Ciliophora,* Oligotrichia). *J. Eukaryot. Microbiol.* 49, 329–337. doi: 10.1111/j.1550-7408.2002.tb00379.x

Montagnes, D. J. S., Wilson, D., Brooks, S. J., Lowe, C., and Campey, M. (2002b). Cyclical behaviour of the tide-pool ciliate *Strombidium oculatum*. *Aquat. Microbial. Ecol.* 28, 55–68. doi: 10.3354/ame028055

Pedersen, M. F., and Hansen, P. J. (2003). Effects of high pH on the growth and survival of six marine heterotrophic protists. *Mar. Ecol. Prog. Ser.* 260, 33–41. doi: 10.3354/meps260033

Putt, M. (1990). Abundance, chlorophyll content and photosynthetic rates of ciliates inthe Nordic Seas during summer. *Deep Sea Res.* 37, 1713–1731. doi: 10.1016/0198-0149(90)90073-5

Raven, J. A. (1997). Phagotrophy in phototrophs. *Limnol. Oceanogr.* 42, 198–205. doi: 10.4319/lo.1997.42.1.0198

Santoferrara, L. F., Guida, S., Zhang, H., and McManus, G. B. (2014). *De Novo* transcriptomes of a mixotrophic and a heterotrophic ciliate from marine plankton. *PLoS ONE* 9:e101418. doi: 10.1371/journal.pone.0101418

Schoener, D. M., and McManus, G. B. (2012). Plastid retention, use, and replacement in a kleptoplastidic ciliate. *Aquat. Microb. Ecol.* 67, 177–187. doi: 10.3354/ame01601

Schoener, D. M., and McManus, G. B. (2017). Growth, grazing, and inorganic C and N uptake in a mixotrophic and a heterotrophic ciliate. *J. Plankton Res.* 39, 379–391. doi: 10.1093/plankt/fbx014

Stanton, B. A., Biemesderfer, D., Wade, J. B., and Giebisch, G. (1981). Structural and functional study of the rat distal nephron: effects of potassium adaptation and depletion. *Kidney Int.* 19, 36–48. doi: 10.1038/ki.1981.5

Stoecker, D. K. (1998). Conceptual models of mixotrophy in planktonic protists and some ecological and evolutionary implications. *Eur. J. Protistol.* 34, 281–290. doi: 10.1016/S0932-4739(98)80055-2

Stoecker, D. K., and Silver, M. W. (1987). Chloroplast retention by marine planktonic ciliates. *Ann. N. Y. Acad. Sci.* 503, 562–565. doi: 10.1111/j.1749-6632.1987.tb40646.x

Stoecker, D. K., Johnson, M. D., de Vargas, C., and Not, F. (2009). Acquired phototrophy in aquatic protists. *Aquat. Microbial Ecol.* 57, 279–310. doi: 10.3354/ame01340

Stoecker, D. K., Michaels, A. E., and Davis, L. H. (1987). Large proportion of marine planktonic ciliates found to contain functional chloroplasts. *Nature* 326, 790–792. doi: 10.1038/326790a0

Wisecaver, J. H., and Hackett, J. D. (2010). Transcriptome analysis reveals nuclear-encoded proteins for the maintenance of temporary plastids in the dinoflagellate *Dinophysis acuminata*. *BMC Genomics* 11:366. doi: 10.1186/1471-2164-11-366

Yang, J., Löder, M. G. J., Boersma, M., and Wiltshire, K.H. (2015). Factors influencing the grazing response of the marine oligotrichous ciliate *Strombidium cf. sulcatum*. *Aquat. Microb. Ecol.* 74, 59–71. doi: 10.3354/ame01729

Conflict of Interest Statement: The authors declare that the research was conducted in the absence of any commercial or financial relationships that could be construed as a potential conflict of interest.

The handling Editor declared a past co-authorship with one of the authors, GM.

frontiers in Marine Science

ORIGINAL RESEARCH
published: 14 August 2018
doi: 10.3389/fmars.2018.00273

Evaluation of Mixotrophy-Associated Gene Expression in Two Species of Polar Marine Algae

Zaid M. McKie-Krisberg[1]*, *Robert W. Sanders*[2] *and Rebecca J. Gast*[3]

[1] Department of Biology, Brooklyn College, City University of New York, Brooklyn, NY, United States, [2] Department of Biology, Temple University, Philadelphia, PA, United States, [3] Woods Hole Oceanographic Institution, Woods Hole, MA, United States

Mixotrophic flagellates can comprise significant proportions of plankton biomass in marine ecosystems. Despite the growing recognition of the importance of this ecological strategy, and the identification of major environmental factors controlling phagotrophic behavior (light and nutrients), the physiological and molecular mechanisms underlying mixotrophic behavior are still unclear. In this study, we performed RNA-Seq transcriptomic analysis for two mixotrophic prasinophytes, *Micromonas polaris* and *Pyramimonas tychotreta,* under dissolved nutrient regimes that altered their ingestion of bacteria prey. Though the strains examined were polar isolates, both belong to genera with widespread distribution. Our aim was to characterize the transcriptomes of these two non-model phytoflagellates, identify transcripts consistent with phagotrophic activity and assess their differential expression in response to nutrient stress. *De novo* assembly of the transcriptomes yielded large numbers of novel coding transcripts with no known match within public databases. A summary of the transcripts by Gene Ontology terms showed many expected expression patterns, including genes involved in photosynthetic pathways and enzymes implicated in nutrient uptake pathways. Searches of KEGG databases identified several genes associated with intra-cellular digestive pathways actively transcribed in both prasinophytes. Differential expression analysis showed a larger response in *P. tychotreta*, where 23,373 genes were up-regulated and 1,752 were down-regulated in the low nutrient treatment when phagotrophy was enhanced. In contrast, in *M. polaris*, low nutrient treatments resulted in up-regulation of 314 transcripts while down-regulating 371. With respect to phagotrophic-related expression, 37 genes were co-expressed in both *P. tychotreta* and *M. polaris*, and although the response was less pronounced in *M. polaris,* it is consistent with differences in observed ingestion behavior. This study presents the first genomic data for *Pyramimonas tychotreta,* and also contributes to the limited available data for *Micromonas polaris*. Furthermore, it provides insight into the presence of genes associated with phagocytosis within the Prasinophyceae and contributes to the understanding of potential target genes required for the construction of a complete model of gene regulation of phagocytic behavior in algae.

Keywords: mixotrophy, *Pyramimonas*, *Micromonas*, RNA-Seq, transcriptomics, phagotrophy

OPEN ACCESS

Edited by:
Holly V. Moeller, University of California, Santa Barbara, United States

Reviewed by:
Jelena Godrijan, Bigelow Laboratory For Ocean Sciences, United States
Suzanne Jane Painting, Centre for Environment, Fisheries and Aquaculture Science (CEFAS), United Kingdom

***Correspondence:**
Zaid M. McKie-Krisberg
Zaid.mk@brooklyn.cuny.edu

Specialty section:
This article was submitted to Marine Ecosystem Ecology, a section of the journal Frontiers in Marine Science

Received: *01 March 2018*
Accepted: *18 July 2018*
Published: *14 August 2018*

Citation:
McKie-Krisberg ZM, Sanders RW and Gast RJ (2018) Evaluation of Mixotrophy-Associated Gene Expression in Two Species of Polar Marine Algae. Front. Mar. Sci. 5:273. doi: 10.3389/fmars.2018.00273

INTRODUCTION

The traditional view of protistan species is that they can be defined in terms of a single trophic mode, either photo- or hetero-trophic (Azam et al., 1983). However, more recently, a greater recognition of the impact of photosynthetic protists with the ability to ingest prey has been growing (Pomeroy, 1974; Flynn et al., 2012). Ingestion of prey by phytoplankton is found to occur in both freshwater and marine environments, ranging from tropical to polar ecosystems (Boraas et al., 1988; Sanders, 1991; Pålsson and Granéli, 2004; Moorthi et al., 2009; Hartmann et al., 2013). This ecological strategy can account for significant impact with regard to the movement of nutrients and carbon, as well as through substantial reintroduction of immobilized carbon back into the food web (Boraas et al., 1988; Sanders, 2011; Unrein et al., 2014). Mixotrophic behavior has also been demonstrated to satisfy organismal requirements for macro- and micro-nutrient deficiencies, and ingestion behavior is often a response to these limiting conditions (Nygaard and Tobiesen, 1993; Maranger et al., 1998). Mixotrophic phytoflagellates can comprise a considerable proportion of planktonic communities and potentially graze large proportions of bacterial standing stock daily in both freshwater and marine planktonic food webs (Bird and Kalff, 1986; Sanders et al., 1989; Sanders, 2011), accounting for a majority of the bacterial mortality (Hitchman and Jones, 2000; Zubkov and Tarran, 2008; Sanders and Gast, 2012).

Despite the growing recognition of predatory behavior in photosynthetic protists, and the substantial collection of physiological measurements of mixotrophic behavior (e.g., predation rates and conversion efficiencies), the regulatory controls at the genetic level are still poorly understood. This is, in part, a result of the broad spectrum of mixotrophic organisms representing diverse evolutionary lineages, many of which lack established and well-curated model organisms for use in genetic and molecular studies (Sherr and Sherr, 2002). This area is of importance because phagotrophic behavior provides evidence of the mechanisms underlying the endosymbiotic theory, which unites all eukaryotic lineages, and all plastid containing organisms in particular (Burns et al., 2015). Some molecular targets involved in the process of cellular phagotrophy have been previously identified, including receptors associated with phagocytosis, actin filament remodeling and regulatory gene families (Yutin et al., 2009). Liu et al. (2016) also identified genes potentially associated with mixotrophy, however, the details in terms of regulation and biochemical controls need further study.

Within the Archeaplastida, also referred to as the green algae, the Prasinophyta represent an ancient group of plastid containing eukaryotes that are widely distributed in both freshwater and marine environments, and have been found to make up significant portions of the standing biomass in polar microbial communities (Moro et al., 2002; Lovejoy et al., 2007; Li et al., 2009; Gast et al., 2014). Green algae were long thought to be a wholly autotrophic lineage of organisms, but recent observations have shown ingestion behavior in several green algal species, including several Prasinophytes (Maruyama and Kim, 2013; Raven, 2013; McKie-Krisberg and Sanders, 2014; McKie-Krisberg et al., 2015). Within the Prasinophyceae, genomic data is available for a limited number of species, including *Ostreococcus tauri*, an isolate of *Micromonas pusilla* and *Cymbomonas tetramitiformis* (Derelle et al., 2006; Worden et al., 2009; Tirichine and Bowler, 2011; Burns et al., 2015). Of these prasinophytes, aside from *C. tetramitiformis*, none have been positively identified as mixotrophs. The recent advancements in genomic technologies, particularly RNA-Seq and related computational analysis, provide efficient, cost effective methods to gain a deeper understanding of the changes at the molecular level, particularly in non-model organisms.

In this study, we examine the transcriptional profiles of two polar mixotrophic prasinophytes representing different phytoplankton size fractions (pico- vs. nano-flagellates). We investigate the response at the molecular level, in terms of gene expression, to changes in nutrient availability previously shown to illicit changes in prey ingestion behavior in these two organisms. Our aims were to characterize the transcriptomes of these two non-model phytoflagellates, identify transcripts consistent with phagotrophic activity and assess their differential expression in response to stimulation of mixotrophy due to nutrient limitation. We hypothesize that nutrient availability is a major factor in driving ingestion behavior in polar mixotrophic algae, and that by using a comparative "-omics" approach, we can identify patterns of gene expression common among mixotrophic behavior in microbial eukaryotes. We obtained feeding activity and transcriptomic data simultaneously from an Arctic isolate of *Micromonas polaris*, and the Antarctic *Pyramimonas tychotreta*, and identified changes in transcript abundance in response to a reduction in nutrients. By comparing the transcriptomes of the two prasinophytes, we also attempt to identify genes linked to phagotrophic behavior shared by both organisms, which could be potential targets for the evaluation of mixotrophic activity in environmental samples.

MATERIALS AND METHODS

Culture Origin and Maintenance

Pyramimonas tychotreta (I-9 Pyram) was isolated from the Ross Sea, Antarctica in 1999 and maintained at Woods Hole Oceanographic Institution and at Temple University (http://www.whoi.edu/science/B/protists/). *Micromonas* isolate (CCMP 2099, Provasoli-Guillard National Center for Marine Algae and Microbiota), recently identified as *M. polaris* (Simon et al., 2017), was originally isolated from an Arctic polyna. The prasinophytes in the present study differ in terms of cell size (1.2 μm *M. polaris* vs. 5–7 μm average diameter for *P. tychotreta*). Experimental cultures of these algae were maintained at 4°C in 32 PSU f/2 + Si (Guillard, 1975; Caron, 1993). The cultures were non-axenic and grown under 14 h light/10 h dark irradiance from 50 W cool-white fluorescent bulbs at ∼50 μmol m^{-2} s^{-1}.

Experimental Setup

Previous studies have shown both *P. tychotreta* and *M. polaris* to ingest particles, and that ingestion rates are influenced by nutrient availability in the culture media (McKie-Krisberg and Sanders, 2014; McKie-Krisberg et al., 2015). Replicate flasks of *P. tychotreta* (2.5×10^3 cells ml^{-1}) and *M. polaris* ($1.44 \times$

10^5 cells ml^{-1}) were grown in either high- or reduced-nutrient conditions for 1 week for transcriptional analysis ($n = 4$ per treatment/species/time point; total 16 per species) and ingestion experiments ($n = 3$ per treatment/species/time point; total 12 per species) conducted at the time of whole cell collection for sequencing to confirm differences in feeding. The differences in cell abundances are reflective of the shorter doubling time and smaller size of *M. polaris* as compared to *P. tychotreta*. High-nutrient treatments were full strength f/2+Si (i.e., the maintenance media, 882 μM N, 36.2 μM PO_4^{3-}), while low-nutrient treatments were a 10-fold dilution of f/2 + Si culture media (88.2 μM N, 3.62 μM PO_4^{3-}) prepared with filter-sterilized seawater. The low-nutrient conditions were previously found to elicit increases in ingestion by these two species (McKie-Krisberg and Sanders, 2014; McKie-Krisberg et al., 2015) and the concentrations of nitrogen and phosphorous fall within the range observed in both the Artic and Antarctic environments (Wheeler et al., 1997; Smith et al., 2003). Illumination and temperature conditions were the same as used for culture maintenance (14 h light/10 h dark irradiance at ∼50 μmol m^{-2} s^{-1}).

RNA Extraction, Transcriptome Assembly and Differential Expression Analysis

Replicate cultures of *P. tychotreta* ($n = 4$) and *M. polaris* ($n = 4$) that had been incubated under high- and reduced-nutrient conditions known to affect ingestion were collected on 25 mm, 0.2 μm polycarbonate filters, frozen at −80°C, then extracted using the Qiagen Mini RNA kit, with confirmation of nucleic acid abundance and quality assessed by Bioanalyzer (Agilent Technologies, Santa Clara, CA). Replicate samples were sent to the Sulzberger Genome Center at Columbia University for poly-A selection, library construction and sequencing by Illumina Mi-Seq (150 bp paired-end reads, 30 million reads per sample). Raw reads have been deposited in the NCBI Sequence Read Archive under accession number SRP090401.

Overall quality of Illumina raw reads data was assessed using FastQC (Andrews, 2010). Poor quality reads and adapters were removed using Trimmomatic 0.32, with settings for removing seed mismatches = 2, palindrome clip threshold = 10, and a simple clip threshold = 30. Additional settings included removing leading and trailing bases below quality scores of 3 and excluding reads less than 36 bp (Bolger et al., 2014). Prior to assembly, FLASh (version 1.2.11) was used to find overlaps and merge read pairs to increase the quality of the transcript assembly (Magoc and Salzberg, 2011). Following these preparatory steps, all paired-end reads for each species were combined and assembled using Trinity (version 2.3.2), using default assembly settings (Grabherr et al., 2011) (**Table 1**). Following assembly, bacterial decontamination was performed by Deconseq (version 0.4.3) using the bacterial data base generated by the script designers (Schmieder and Edwards, 2011). Transcriptomes of each species were filtered through CD-hit to identify unique transcripts (Li and Godzik, 2006). This step clustered transcripts that were ≥90% similar. In the absence of sequenced genomes and proper functional annotation of either of these prasinophytes, this was a conservative approach that allowed for the occurrence of differential splicing of transcriptional products, but constrained computational artifacts from the *de novo* assembly that could not be validated. Transcript abundance from each replicate was determined by sequence-read alignment to transcriptomes with Bowtie2 (Langmead and Salzberg, 2012), followed by count estimation with eXpress (Roberts et al., 2011). Differential expression of *M. polaris* and *P. tychotreta* was determined using edgeR according to the experimental design, using the exact test based on quantile-adjusted conditional maximum likelihood (qCML) method (Robinson et al., 2010). Our threshold for differential regulation of Trinity "genes" was defined by transcript differences of at least 2 Log_2-fold (4-fold) increase/decrease in expression. Transcript assembly, differential expression analysis and gene annotation were all performed using computational resources available via the Owlsnest Super-Computing Cluster at Temple University, and the CUNY High Performance Computing Center at the CUNY College of Staten Island.

TABLE 1 | Summary statistics from Trinity *de novo* transcriptome assembly for two polar mixotrophic algae *Micromonas polaris* and *Pyramimonas tychotreta*.

Species	*Micromonas polaris*	*Pyramimonas tychotreta*
Illumina paired-end reads	3.59×10^8	3.07×10^8
Number of bases assembled	2.48×10^7	7.89×10^7
Number of transcripts	12,368	111,043
Mean contig length	2005.4	710
N50	4,021	1,074
GC content (%)	59.53	54.72

Functional Annotation

Functional annotation of assembled transcripts was performed with Trinotate 2.0 (Haas et al., 2013). Searches of several genomic databases, including Uniprot databases (http://www.uniprot.org/) and *nr* and *nt* (http://www.ncbi.nlm.nih.gov/) were performed using BLAST utility and employing Transdecoder to identify predicted Open Reading Frames (ORFs). ORFs were also queried using hmmscan, and rnammer for predictions of conserved domains with homology to protein families and domains found in the Pfam database (Lagesen et al., 2007; Eddy, 2011; Finn et al., 2015). Gene Ontology (GO) associated with identified genes obtained from Interproscan searches were grouped according to "Biological Process" (BP), "Cellular Component" (CC) or "Molecular Function" (MF) (Jones et al., 2014). Whole transcriptome Gene Ontologies were summarized with the goSlim function of the GSEABase package, within the R statistical environment using the plant ontology (http://www.plantontology.org) (Gentleman et al., 2004; Morgan et al., 2008; R Core Team, 2013). GO term information from transcript data was integrated into Gene Enrichment analysis. We obtained the ontology pathways that were enriched by the treatment conditions using the runTest function in the topGO package, performing a Fisher Exact test inputting normalized gene expression measurements along with differential expression analysis results (Alexa and Rahnenfuhrer, 2017). Assembled transcripts of both *M. polaris*

and *P. tychotreta* were submitted to the KAAS-KEGG Automatic Annotation Server provided by the Kyoto Encyclopedia of Genes and Genomes (http://www.genome.jp/tools/kaas/) for the identification of additional enzymes involved in primary nutrient metabolism (Carbon, Nitrogen), as well as phagotrophic related pathways, such as autophagy (Moriya et al., 2007). Additionally, genes found to be involved in phosophorus (P) limitation response in plants (Rouached et al., 2010) were identified by blast searches of *M. polaris* and *P. tychotreta* transcriptomes (**Supplementary Data Sheet 1**).

Ingestion Experiments

Both microspheres and fluorescently-labeled bacteria have been used to demonstrate ingestion behavior (Nygaard and Tobiesen, 1993), but the fluorescent particles employed in the present work were also used in previous studies of phagotrophy of both *P. tychotreta* and *M. polaris*, and therefore provide the most suitable comparison to the previous experimental work (McKie-Krisberg and Sanders, 2014; McKie-Krisberg et al., 2015). A total of 1×10^6 microspheres were added to each flask and the T_0 replicates (controls) were immediately fixed using the Lugol's/formaldehyde/$Na_2S_2O_3$ method that prevents egestion (Sherr et al., 1993). The remaining replicates were incubated under the same light and temperature used for culture maintenance for 20 min (T_f), after which they were fixed as for the T_0 samples. Previous studies indicate that 20 min is within the period of time when there is a linear uptake of microspheres for both *P. tychotreta, M. polaris* (McKie-Krisberg et al., McKie-Krisberg and Sanders). Ten milliliter of fixed sample were filtered onto 25 mm Poretics polycarbonate membranes (0.8 μm pore size for *M. polaris* and 3 μm pore size for *P. tychotreta*, GE Osmonics, Minnetonka MN, USA) and stained/mounted using VectaShield® with DAPI (Vector Laboratories Inc., Burlingame, CA). Epifluorescence microscopy was used to examine at least 500 cells per filter for *P. tychotreta,* while 10 fields per filter were counted for *M. polaris*. Mixotrophic behavior was identified as the ingestion of beads after background correction with the T_0 samples.

RESULTS

Under high nutrient treatment conditions, a low level of particle ingestion was observed for *M. polaris*, and undetectable for *P. tychotreta*. However, in the low nutrient treatments, the percent of cells that ingested microspheres increased by 69% for *M. polaris* and 31% for *P. tychotreta*. These observations are consistent with previous studies where grazing in both species was affected by concentrations of nutrients in the culture media, with *P. tychotreta* showing a particularly distinct response (McKie-Krisberg and Sanders, 2014; McKie-Krisberg et al., 2015).

Transcriptome Assembly and Functional Annotation

The *de novo* transcriptome assembly of RNA-Seq data identified ∼12,000 and ∼110,000 unique transcripts for *M. polaris* and *P. tychotreta*, respectively (**Table 1**). Current available genomic data for two isolates of *Micromonas* (CCMP1545 v3.0, and RCC299 v.3, Phytozome) include annotation of 10,660 and 10,103 genes, respectively (Goodstein et al., 2012). Therefore, even with our conservative approach, the transcriptome for *M. polaris* likely includes differential splicing products. The large transcriptome size of *P. tychotreta* was associated with a smaller N50 value, which may be due to a large portion of short length contigs (unique, consensus regions of RNA produced as a result of the *de novo* assembly) (**Table 1**). No genomic data is currently available for *P. tychotreta*, but annotation of the related prasinophyte, *Cymbomonas tetramitiformis* (Order Pyramimondales) was found to have almost 4 times the number of genes (∼37,000 genes) compared to the published *Micromonas pusilla* genomes (Burns et al., 2015).

The functional annotation of the transcriptomes for each species revealed a large number of novel transcripts that had no matches to previously identified genomic information in available databases. Functional annotation identified 64% of transcripts in *M. polaris*, while in *P. tychotreta*, only ∼24% of transcripts matched previously identified proteins in the SwissProt database, indicating a large proportion of the transcripts represented potential novel sequences (**Figure 1**). Regardless of the relatively small percentage of identified transcripts, 2.7×10^3 transcripts were matched to existing accessions and functional annotation via the KEGG database. Looking in detail at differential expression results for both *M. polaris* and *P. tychotreta*, we observed changes in mechanisms associated with acquisition for both light and nutrient uptake pathways (**Supplementary Table 1**). Not surprisingly, proteins involved in photosynthesis represented a large number of the GO terms associated with Biological Processes in both *M. polaris* and *P. tychotreta* (**Figure 2**, **Supplementary Data Sheet 2**). These include Light Harvesting Complex proteins (LHC) and Ribuose-1,5-Bisphosphate Carboxylase/Oxygenase (RUBISCO) (**Supplementary Table 1**).

Overall, the effect of lower concentrations of dissolved nutrients was less pronounced in *M. polaris*, resulting in fewer changes in gene expression as compared to *P. tychotreta*. In cultures of *M. polaris*, lower nutrient concentrations resulted in 314 up-regulated and 371 down-regulated, at least a Log_2-fold change of 2 (**Figure 2**). This response is less, but still comparable to, earlier studies of a tropical isolate of *Micromonas* (CCMP2709), which found up-regulation of 738 out of 960 differentially-expressed transcripts under of the effect of phosphorus limitation (Whitney and Lomas, 2016). In low-nutrient treatments of *P. tychotreta*, we found 23,373 up-regulated and 1,752 down-regulated at a 2 Log_2-fold change) (**Figure 3**). Reduction in nutrient availability resulted in up-regulation of genes related to carbon metabolism, and to some extent nitrogen metabolism, in both prasinophytes, although the response was more pronounced in cultures of *P. tychotreta* (**Figures 4**,**5**). Differential expression of genes associated with phosphorus limitation was greater in cultures of *P. tychotreta*, but *M. polaris* appears to constitutively express these genes, as they did not respond to the experimental conditions (**Figures 3**–**5**).

Specific to phagotrophy, low nutrient conditions resulted in up-regulation of 153 genes related to phagotrophic ingestion,

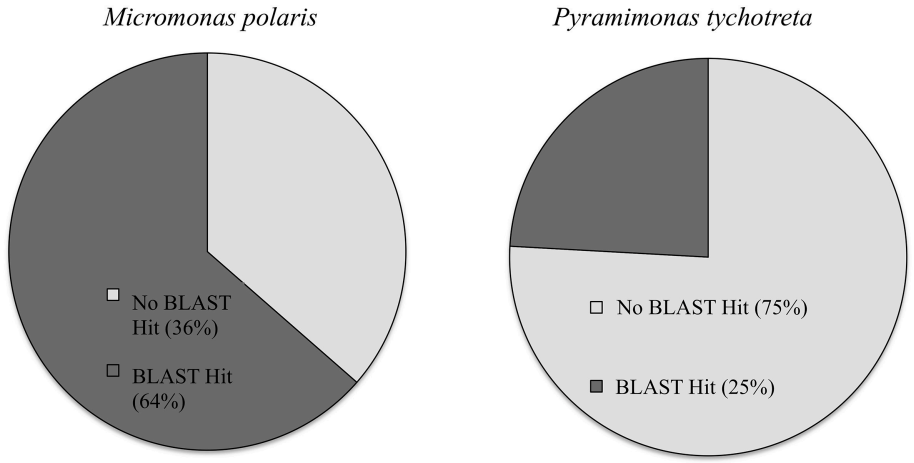

FIGURE 1 | Percentage of transcripts with BLAST matches in Uniprot database in *Micromonas polaris* and *Pyramimonas tychotreta*.

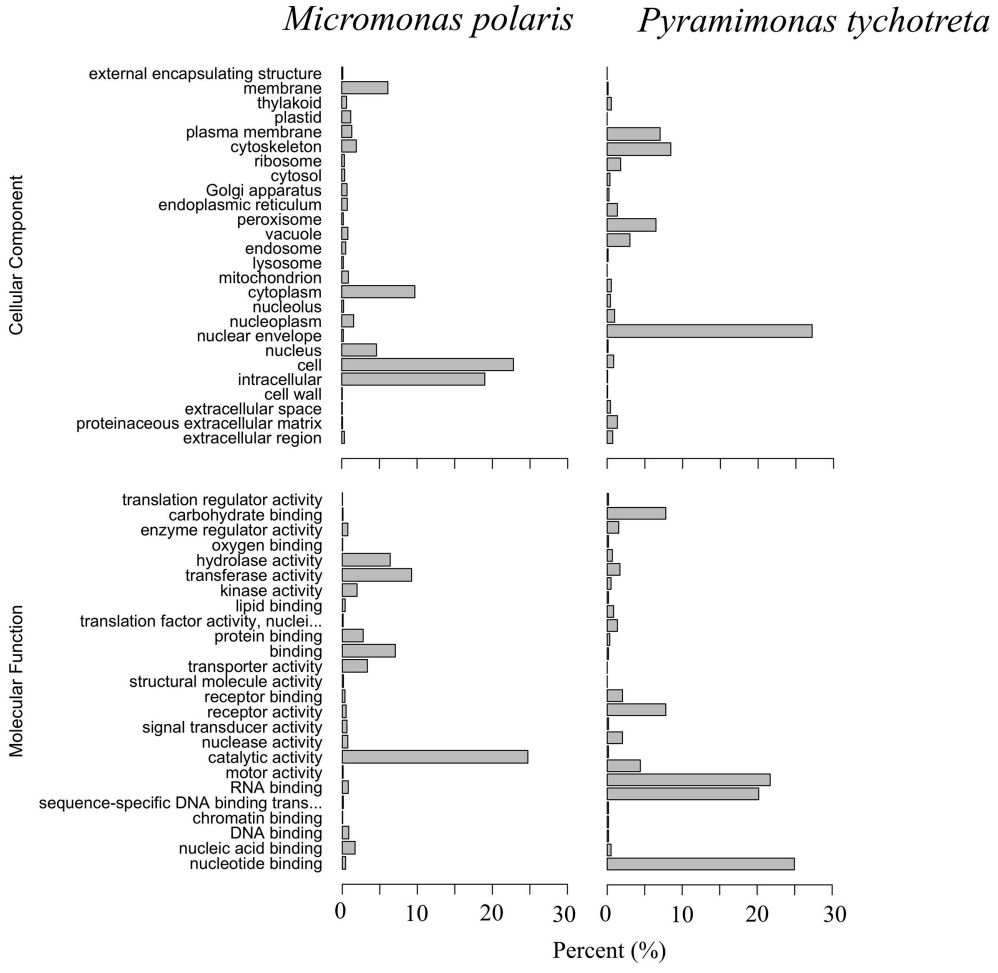

FIGURE 2 | Gene Ontology (GO) summaries of *M. polaris and P. tychotreta* transcriptomes as a percentage of total identified transcripts. GO terms were grouped by Molecular Function and Cellular Component.

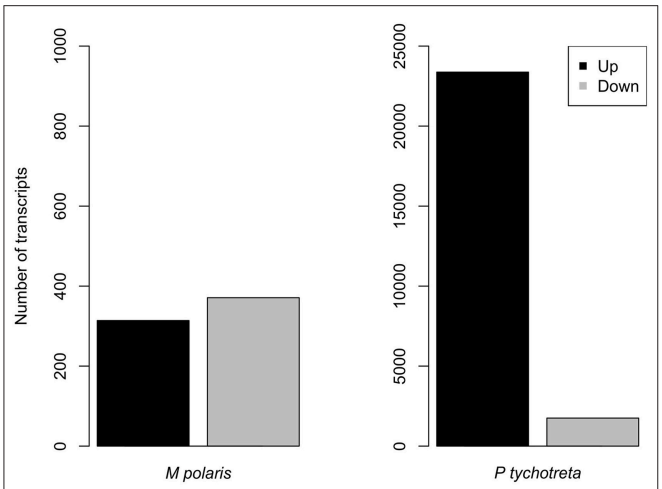

FIGURE 3 | Number or genes differentially expressed in *M. polaris and P. tychotreta*. The threshold for significant differential expression is defined as a 2 $\log_2$ fold-change in expression in response to changes in nutrient condition Note difference in scales.

as defined by KEGG (**Table 2**). We also found 37 genes (in some cases, with multiple transcript matches) to be present in both *M. polaris* and *P. tychotreta*. These include genes that function in endocytosis (20), formation of phagosome (8), lysosome production (11), and regulation of autophagy (7) (**Table 2**, **Supplementary Table 1**). Several transcripts in the transcriptome of both *M. polaris* and *P. tychotreta* contained predicted Ankyrin domains (identified by KEGG), which have been suggested to play a role in phagocytosis (Moffat et al., 1996; Grolleau et al., 2003; Nguyen et al., 2014). Many of these genes appear to be found across eukaryotic taxa and not only among prasinophytes (Yutin et al., 2009).

Although genes related to phagotrophic processes, as identified by KEGG, were represented in *M. polaris,* none of these genes were found to be differentially expressed at the defined threshold rate (at least 2 Log_2-fold change). The relatively constant level of expression of many of these genes may indicate the ubiquitous, though low, nature of ingestion behavior exhibited by *M. polaris*. Ingestion by this isolate has been found to be less responsive to media conditions than was the case for *P. tychotreta*, which was not phagotrophic in nutrient replete

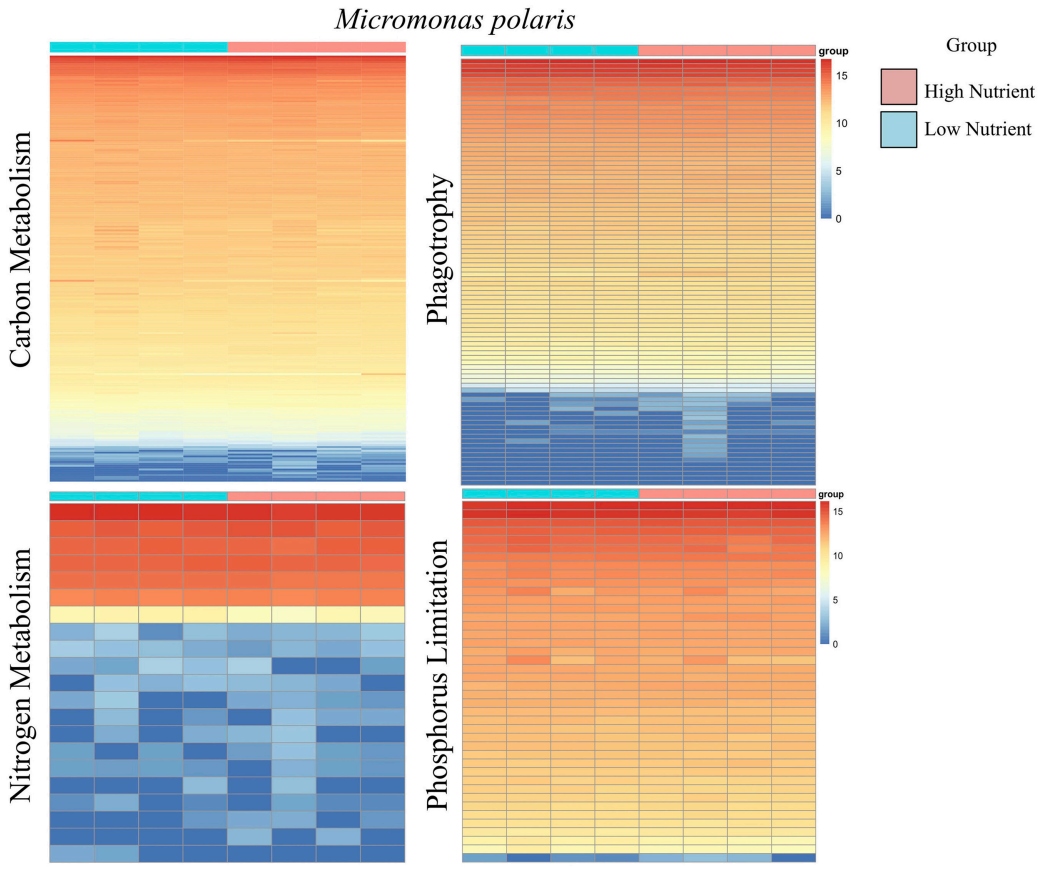

FIGURE 4 | A series of heatmaps for *Micromonas polaris* comparing gene expression associated with carbon (C) metabolism, nitrogen (N) metabolism, phagotrophy, and phosphorus (P) limitation, in cultures grown under high nutrient vs. low nutrient conditions. Tiles represent log-normalized count estimations of transcripts. Genes for C metabolism, N metabolism, and phagotrophy were identified by KEGG and categories were selected based on BRITE hierarchies, except P limitation genes, where genes were selected based on genes identified by Rouached et al. (2010).

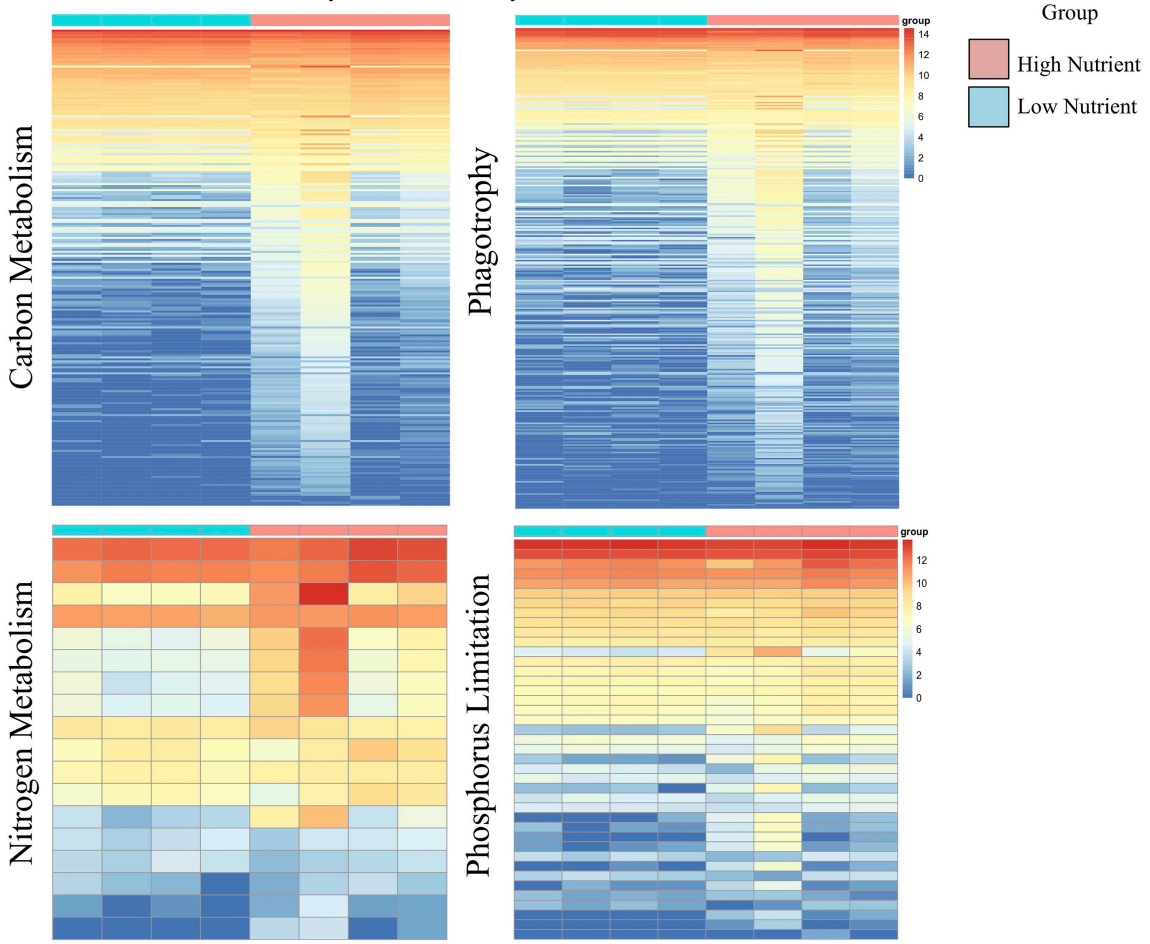

FIGURE 5 | A series of heatmaps for *Pyramimonas tychotreta* comparing gene expression associated with carbon (C) metabolism, nitrogen (N) metabolism, phagotrophy and phosphorus (P) limitation, in cultures grown under high nutrient vs. low nutrient conditions. Tiles represent log-normalized count estimations of transcripts. Genes for C metabolism, N metabolism, and phagotrophy were identified by KEGG and categories were selected based on BRITE hierarchies, except P limitation genes, where genes were selected based on genes identified by Rouached et al. (2010).

media (McKie-Krisberg and Sanders, 2014; McKie-Krisberg et al., 2015) (**Figure 4**, **Supplementary Table 1**, Normalized Transcript count data).

DISCUSSION

Light and dissolved nutrients are often considered to be the most important factors affecting phagotrophy in mixotrophs, as these environmental factors represent two significant resource pools required by obligate phototrophs and also used by mixotrophs. The degree to which these factors may induce changes in trophic plasticity (i.e., phagotrophic activity) in a given mixotroph will vary (Stoecker, 1998; Sanders et al., 2001; Liu et al., 2011). Liu et al. (2016) modified light levels when comparing the transcriptomes of three temperate mixotrophs and found significant differences in patterns of gene expression in response to those changes that were consistent with the degree of mixotrophic behavior. We did not include dark treatment here because previous work indicated that *P. tychotreta* populations decline in dark conditions, and that nutrient concentrations were the major driver of ingestion behavior in this organism (McKie-Krisberg et al., 2015). Both macro- and micro-nutrient concentrations have previously been shown to affect the ingestion rates of these and other mixotrophic phytoflagellates and, in some cases, can dictate whether flagellates will engage in phagotrophy at all (Nygaard and Tobiesen, 1993; Maranger et al., 1998; McKie-Krisberg and Sanders, 2014; McKie-Krisberg et al., 2015). Other factors can also affect ingestion in both mixotrophs and heterotrophs. For example, the differences in cell size between the prasinophytes in the present study (1.2 μm *M. polaris* vs. 5–7 μm average diameter for *P. tychotreta*) seems to constrain the number (and size) of bacteria that can be ingested, and prey size has been recognized as a factor limiting ingestion in various single-celled eukaryotes (Fenchel, 1986; Sanders and Gast, 2012; McKie-Krisberg and Sanders, 2014).

TABLE 2 | Functional annotation of transcripts encoding for enzymes associated with **(A)** Endocytosis, **(B)** Phagosome, **(C)** Lysozome, **(D)** Regulation of Autophagy, expressed in both *M. polaris* and *P. tychotreta* that as identified by the Kyoto Encyclopedia of Genes and Genomes.

KO	Gene symbol	Description	EC
(A) ENDOCYTOSIS			
K00889	PIP5K	1-phosphatidylinositol-4-phosphate 5-kinase	2.7.1.68
K12492	ARFGAP1	ADP-ribosylation factor GTPase-activating protein 1	–
K12200	PDCD6IP, ALIX, RIM20	Programmed cell death 6-interacting protein	–
K11824	AP2A	AP-2 complex subunit alpha	–
K12489	ACAP	Arf-GAP with coiled-coil ANK repeat and PH domain-containing protein	–
K18442	ARFGEF, BIG	Brefeldin A-inhibited guanine nucleotide-exchange protein	–
K12483	EHD1	EH domain-containing protein 1	–
K07901	RAB8A, MEL	Ras-related protein Rab-8A	–
K07889	RAB5C	Ras-related protein Rab-5C	–
K12194	CHMP4, SNF7, VPS32	Charged multivesicular body protein 4	–
K18464	RTSC, SPG8	WASH complex subunit strumpellin	–
K12198	CHMP5, VPS60	Charged multivesicular body protein 5	–
K12562	AMPH	Amphiphysin	–
K04646	CLTC	Clathrin heavy chain	–
K12471	EPN	Epsin	–
K13649	FOLR	Folate receptor	–
K18443	GBF1	Golgi-specific brefeldin A-resistance guanine nucleotide exchange factor 1	–
K03283	HSPA1_8	Heat shock 70kDa protein 1/8	–
K17917	SNX1_2	Sorting nexin-1/2	–
K12486	SMAP	Stromal membrane-associated protein	–
(B) PHAGOSOME			
K03661	ATPeV0B ATP6F	V-type H+-transporting ATPase 21kDa proteolipid subunit	–
K10414	DYNC2H DNCH2	dynein heavy chain 2 cytosolic	–
K00921	PIKFYVE FAB1	1-phosphatidylinositol-3-phosphate 5-kinase	2.7.1.150
K08054	CANX	Calnexin	–
K08057	CALR	Calreticulin	–
K01365	CTSL	Cathepsin L	3.4.22.15
K10956	SEC61A	Protein transport protein SEC61 subunit alpha	–
K07374	TUBA	Tubulin alpha	–
(C) LYSOZOME			
K02154	ATPeV0A ATP6N	V-type H+-transporting ATPase subunit a	–
K12391	AP1G1	AP-1 complex subunit gamma-1	–
K12396	AP3D1	AP-3 complex subunit delta-1	–
K12400	AP4E1	AP-4 complex subunit epsilon-1	–
K02146	ATPeV0D ATP6D	V-type H+-transporting ATPase subunit d	–
K03661	ATPeV0B ATP6F	V-type H+-transporting ATPase 21kDa proteolipid subunit	–
K02155	ATPeV0C ATP6L	V-type H+-transporting ATPase 16kDa proteolipid subunit	–
K05656	ABCB9 TAPL	ATP-binding cassette subfamily B (MDR/TAP) member 9	–
K04646	CLTC	Clathrin heavy chain	–
K01074	PPT	Palmitoyl-protein thioesterase	3.1.2.22
K02144	ATPeV1H	V-type H+-transporting ATPase subunit H	–
(D) REGULATION OF AUTOPHAGY			
K08269	ULK1_2_3, ATG1	serine/threonine-protein kinase ULK/ATG1	2.7.11.1
K07198	PRKAA, AMPK	5'-AMP-activated protein kinase catalytic alpha subunit	2.7.11.11
K08333	PIK3R4, VPS15	phosphoinositide-3-kinase regulatory subunit 4	2.7.11.1
K08334	BECN1, VPS30, ATG6	Beclin 1	–
K00914	PIK3C3, VPS34	Phosphatidylinositol 3-kinase	2.7.1.137
K08339	ATG5	Autophagy-related protein 5	–
K08342	ATG4	Cysteine protease ATG4	3.4.22.-

KO, KEGG Orthology number; EC, Commisson nomenclature number produced by the IUBMB/IUPAC Biochemical Nomenclature Committee.

M. pusilla (CCMP1545) has a relatively small genome (∼20 Mbp, Joint Genome Institute), certainly much smaller than its green algal counterpart, *P. tychotreta*. Although a sequenced genome of *P. tychotreta* is not yet available, a recent study of the alga *C. tetramitiformis*, which is from the same Order, identified a genome size of ∼250 Mbp, more than 10 times greater than that of *M. pusilla* (Worden et al., 2009). The contrasting size of the transcriptomes for *M. polaris* and *P. tychotreta* is likely a reflection of the diversity of genome size within the green algal clade. The extensive number of transcripts (over 100 K) found in *P. tychotreta* suggest additional functions present in this alga, compared to *M. polaris*, but it may also represent an increase in differential splicing, and/or alternative transcripts. These mechanisms have been shown to exist in other green algae such as *Chlamydomonas reinhardtii,* as well as in other algal groups including the cryptophytes and chlorarachniophyte algae (Curtis et al., 2012; Blaby et al., 2014). Understanding these types of regulatory mechanisms can only be resolved with additional genome sequencing and annotation efforts, creating a reference wherein the true number of genes and the relation of gene-to-transcript can be determined.

Previous work with marine mixotrophs indicated shifts in gene expression related to both nutrient metabolism and limitation in response to changes in light and nutrient conditions (Koid et al., 2014; Liu et al., 2016; Caron et al., 2017). The results presented here indicate a comparable, though lesser, response noted for a tropical isolate of *Micromonas* (CCMP2709), which found up-regulation of 738 out of 960 differentially-expressed transcripts under of the effect of phosphorus limitation (Whitney and Lomas, 2016). However, low phosphorus treatments in our present work are 4 times higher than the low nutrient treatments used by Whitney and Lomas (0.5 μM PO_4^{3-} vs. 1.81 μM PO_4^{3-} in our study). Furthermore, Whitney and Lomas (2016) identified the isolate as *M. pusilla*, but the current nomenclature for this isolate via CCMP, designates CCMP2709 as *M. commoda*, and was found to be evolutionarily distinct from our *M. polaris*, which may also contribute to the relative differences in patterns of transcriptional response to changes in nutrients (Worden et al., 2009). In addition, *M. polaris* may respond to fluctuations in nutrient concentration by employing alternative acquisition strategies, like mixotrophy, which have not been observed in *Micromonas* sp. (CCMP 2709) to date, and may not be consistent across the genus. In the case of *P. tychotreta*, we observed significant up regulation of at least one transcript identified as nitrate reductase (NR, EC 1.7.1.1, EC 1.7.1.2, EC 1.7.1.3) as well as ferredoxin-nitrite reductase (EC 1.7.7.1). These results are consistent with previous results of nutrient limitation responses in several non-phagotrophic types of algae from diverse evolutionary lineages, suggesting a basic algal response that is still consistent with a mixotroph that is primarily photosynthetic (Allen, 2003; Berg et al., 2008; Wurch et al., 2011; Dyhrman et al., 2012).

Koid et al. (2014) used the EuKaryotic Orthologous Groups (KOG) tool to compare functional categories in four prymnesiophyte algae, including three known mixotrophs, and found that the overall distributions were very similar. However, when data from an additional 37 protistan species were added to their analysis, the effects of both trophic mode and phylogenetic grouping were detected and non-alveolate mixotrophs formed a distinct cluster. The *Micromonas* strain CCMP2099 used in our study was also included in the broader analysis of Koid et al. (2014). The prasinophytes clustered together, but were distant from other known mixotrophs, so it may be that in this case the clustering more strongly reflected phylogeny than nutritional mode for the mixotrophs. Genome size may also have affected the analysis of Koid et al. (2014), as the three *Micromonas* strains and *Ostreococcus lucimarinus* that were included and clustered together are among the smallest eukaryotes with correspondingly small genomes.

Using the genes linked to phagotrophic behavior proposed by the work of Yutin et al. (2009), a recent genomic study of *Cymbomonas tetramitiformis* identified the presence of enzymes associated with phagotrophic pathways (Burns et al., 2015). Some of those phagotrophy-associated enzymes could also be identified in the current study. However, the majority of these enzymes were described in metazoan cell types, for example, in macrophages of the mouse, *Mus musculus*. Additionally, many of these associated genes may have multiple functions within a cell, which makes it difficult to determine the direct participation of a specific gene in cell phagocytosis based solely on the presence of the transcript coding for these enzymes. From an evolutionary perspective, dual function in genes creates the opportunity for conservation of these pathways among phyla containing phagotrophic and non-phagotrophic members, such as the Chlorophyceae. Conversely, it has been suggested that feeding behavior in algae may be associated with loss of biosynthetic pathways, which could drive mixotrophs to seek out prey to replace essential biomolecules—just as this loss is associated with obligatory phagotrophy (Swingley et al., 2007; Burns et al., 2015). Also, even for those genes able to be identified, the nucleotide sequence for a particular gene can vary among organisms from different evolutionary lineages. Depending on the limitations of genomic databases available for query, this variation in nucleotide sequence for a gene may limit reliable identification, even when genes are present in the subject organism.

The dearth of well-annotated reference genomes as well as transcriptomic data on a wide distribution of microbial eukaryotes, particularly within the Prasinophyceae, presents a challenge to interpreting these results. Despite this, the more pronounced response of ingestion-related genes in *P. tychotreta* as compared to *M. polaris* is consistent with previous work, which indicated that in *P. tychotreta* grazing activity is induced only under nutrient-limited conditions. In comparison, *M. polaris* grazing activity was found at low rates when nutrients were replete, and were only slightly further stimulated when nutrients were limited (McKie-Krisberg and Sanders, 2014; McKie-Krisberg et al., 2015). The results presented here also echo those of Liu et al. (2016), in which expression changes in phagotrophy-associated genes (specifically PEP carboxykinase and vacuolar ATPase) reflected the different ingestion behaviors of *Prymnesium parvum* and *Dinobryon*. Under dark conditions, the higher expression of PEP carboxykinase by *P. parvum* indicated that prey became

an important source of organic carbon. In contrast, *Dinobryon* did not increase PEP carboxykinase expression in the dark, and showed a decrease in vacuolar ATPase expression. This suggests that prey digestion is not active in the dark, and is also supported by the fact that *Dinobryon* prey ingestion dramatically decreased in the dark (Caron et al., 1993). An additional outcome of employing a comparative genomic approach in this study is the identification of 37 phagotrophy related genes that are shared, and expressed, between these two prasinophytes (Supplementary Information). These studies, and that of a mixotrophic oligotrich ciliate by Santoferrara et al. (2014), provide the basis for future multi-species comparative genomic studies of mixotrophic regulation at the genetic level. These efforts will yield greater understanding of whether the mechanisms regulating prey ingestion in mixotrophic protists are conserved across evolutionarily distinct groups.

The present work contributes to the limited, but growing, data set on the transcription dynamics of green algal lineages in contrasting nutrient regimes. We observed responses to reduction in nutrients consistent with predicted responses at the level of gene expression by photosynthetic marine microalgae. These results were obtained using RNA-Seq technology, and despite the presence of bacteria in these non-axenic conditions, we were able to obtain good quality transcriptomic data from target species using a sufficiently conservative bioinformatic analysis pipeline. In addition, we have identified genes in both organisms that are associated with phagotrophic activity, one of the main aims of the study, despite the fact that *M. polaris* and *P. tychotreta* are representatives of different phylogenetic Orders with a large difference in genome size. Additionally, several transcripts containing conserved domains associated with phagotrophic ingestion were found in both transcriptomes, further supporting that these processes are operating within otherwise photosynthetic organisms.

AUTHOR CONTRIBUTIONS

RG conducted grazing experiments and RNA isolation for sequencing. RG and ZM-K conducted the bioinformatic analysis of RNA-seq data including, *de novo* assembly, functional annotation, and differential expression analysis. ZM-K was the primary writer of the manuscript. RG and RS provided critical revision of the manuscript.

ACKNOWLEDGMENTS

The Owlsnest Super-Computing Cluster at Temple University is funded by a National Science Foundation Grant CNS-09-58854. The CUNY HPCC is operated by the College of Staten Island and funded, in part, by grants from the City of New York, State of New York, CUNY Research Foundation, and National Science Foundation Grants CNS-0958379, CNS-0855217, and ACI 1126113. Support for this work was also supplied by National Science Foundation grants PLR-1341362 (RG), PLR-1603538 (RS), and PLR-1603833 (RG).

SUPPLEMENTARY MATERIAL

The Supplementary Material for this article can be found online at: https://www.frontiersin.org/articles/10.3389/fmars.2018.00273/full#supplementary-material

REFERENCES

Alexa, A., and Rahnenfuhrer, J. (2017). *topGO: Enrichment Analysis for Gene Ontology*. R Package version 2.32.0. doi: 10.18129/B9.bioc.topGo

Allen, J. F. (2003). Cyclic, pseudocyclic and noncyclic photophosphorylation: new links in the chain. *Trend Plant Sci.* 8, 15–19. doi: 10.1016/S1360-1385(02)00006-7

Andrews, S. (2010). *FastQC A Quality Control tool for High Throughput Sequence Data*. Available online at: http://www.bioinformatics.babraham.ac.uk/projects/fastqc/

Azam, F., Fenchel, T., Field, J. G., Gray, J. S., Meyer-Reil, L. A., and Thingstad, F. (1983). The ecological role of water-column microbes in the sea. *Mar. Ecol. Prog. Ser.* 10, 257–263. doi: 10.3354/meps010257

Berg, G. M., Shrager, J., Glöckner, G., Arrigo, K. R., and Grossman, A. R. (2008). Understanding nitrogen limitation in *Aureococcus anophagefferens* (Pelagophyceae) through cDNA and qRT-PCR analysis. *J. Phycol.* 44, 1235–1249. doi: 10.1111/j.1529-8817.2008.00571.x

Bird, D. F., and Kalff, J. (1986). Bacterial grazing by planktonic lake algae. *Science* 231, 493–495. doi: 10.1126/science.231.4737.493

Blaby, I. K., Blaby-Haas, C. E., Tourasse, N., Hom, E. F., Lopez, D., Aksoy, M., et al. (2014). The *Chlamydomonas* genome project: a decade on. *Trends Plant Sci.* 19, 672–680. doi: 10.1016/j.tplants.2014.05.008

Bolger, A. M., Lohse, M., and Usadel, B. (2014). Trimmomatic: a flexible trimmer for Illumina sequence data. *Bioinformatics* 30, 2114–2120. doi: 10.1093/bioinformatics/btu170

Boraas, M. E., Estep, K. W., Johnson, P. W., and Sieburth, J. (1988). Phagotrophic phototrophs: the ecological significance of mixotrophy. *J. Protozool.* 35, 249–252. doi: 10.1111/j.1550-7408.1988.tb04336.x

Burns, J. A., Paasch, A., Narechania, A., and Kim, E. (2015). Comparative genomics of a bacterivorous green alga reveals evolutionary causalities and consequences of phago-mixotrophic mode of nutrition. *Genome Biol. Evol.* 7, 3047–3061. doi: 10.1093/gbe/evv144

Caron, D. A. (1993). "Enrichment, isolation, and culture of free-living heterotrophic flagellates," in *Handbook of Methods in Aquatic Microbial Ecology,* eds P. F. Kemp, B. F. Sherr, E. B. Sherr, and J. J. Cole (Boca Raton, FL: Lewis Publishers), 77–90.

Caron, D. A., Alexander, H., Allen, A. E., Archibald, J. M., Armbrust, E. V., Bachy, C., et al. (2017). Probing the evolution, ecology and physiology of marine protists using transcriptomics. *Nat. Rev. Microbiol.* 15, 6–20. doi: 10.1038/nrmicro.2016.160

Caron, D. A., Sanders, R. W., Lim, E. L., Marrasé, C., Amaral, L. A., Whitney, S., et al. (1993). Light-dependent phagotrophy in the freshwater mixotrophic chrysophyte *Dinobryon cylindricum*. *Microb. Ecol.* 25, 93–111. doi: 10.1007/BF00182132

Curtis, B. A., Tanifuji, G., Burki, F., Gruber, A., Irimia, M., Maruyama, S., et al. (2012). Algal genomes reveal evolutionary mosaicism and the fate of nucleomorphs. *Nature* 492, 59–65. doi: 10.1038/nature11681

Derelle, E., Ferraz, C., Rombauts, S., Rouzé, P., Worden, A. Z., Robbens, S., et al. (2006). Genome analysis of the smallest free-living eukaryote *Ostreococcus tauri* unveils many unique features. *Proc. Natl. Acad. Sci. U.S.A.* 103, 11647–11652. doi: 10.1073/pnas.0604795103

Dyhrman, S. T., Jenkins, B. D., Rynearson, T. A., Saito, M. A., Mercier, M. L., Alexander, H., et al. (2012). The transcriptome and proteome of the diatom *Thalassiosira pseudonana* reveal a diverse phosphorus stress response. *PLoS ONE* 7:e33768. doi: 10.1371/journal.pone.0033768

Eddy, S. R. (2011). Accelerated profile HMM searches. *PLoS Comput. Biol.* 7:e1002195. doi: 10.1371/journal.pcbi.1002195

Fenchel, T. (1986). "Protozoan filter feeding," in *Progress in Protistology,* eds J. O. Corliss and D. J. Patterson (Bristol: Biopress, Ltd.), 65–113.

Finn, R. D., Coggill, P., Eberhardt, R. Y., Eddy, S. R., Mistry, J., Mitchell, A. L., et al. (2015). The Pfam protein families database: towards a more sustainable future. *Nucleic Acids Res.* 44, D279–D285. doi: 10.1093/nar/gkv1344

Flynn, K. J., Stoecker, D. K., Mitra, A., Raven, J. A., Glibert, P. M., Hansen, P. J., et al. (2012). Misuse of the phytoplankton–zooplankton dichotomy: the need to assign organisms as mixotrophs within plankton functional types. *J. Plankton Res.* 35, 3–11. doi: 10.1093/plankt/fbs062

Gast, R. J., McKie-Krisberg, Z. M., Fay, S. A., Rose, J. M., and Sanders, R. W. (2014). Antarctic mixotrophic protist abundances by microscopy and molecular methods. *FEMS Microbiol. Ecol.* 89, 388–401. doi: 10.1111/1574-6941.12334

Gentleman, R. C., Carey, V. J., Bates, D. M., Bolstad, B., Dettling, M., Dudoit, S., et al. (2004). Bioconductor: open software development for computational biology and bioinformatics. *Genome Biol.* 5:R80. doi: 10.1186/gb-2004-5-10-r80

Goodstein, D. M., Shu, S., Howson, R., Neupane, R., Hayes, R. D., Fazo, J., et al. (2012). Phytozome: a comparative platform for green plant genomics. *Nucleic Acids Res.* 40, D1178–D1186. doi: 10.1093/nar/gkr944

Grabherr, M. G., Haas, B. J., Yassour, M., Levin, J. Z., Thompson, D. A., Amit, I., et al. (2011). Full-length transcriptome assembly from RNA-Seq data without a reference genome. *Nat. Biotechnol.* 29, 644–652. doi: 10.1038/nbt.1883

Grolleau, A., Misek, D. E., Kuick, R., Hanash, S., and Mulé, J. J. (2003). Inducible expression of macrophage receptor Marco by dendritic cells following phagocytic uptake of dead cells uncovered by oligonucleotide arrays. *J. Immunol.* 171, 2879–2888. doi: 10.4049/jimmunol.171.6.2879

Guillard, R. R. L. (1975). "Culture of phytoplankton for feeding marine invertebrates," in *Culture of Marine Invertebrate Animals,* eds W. L. Smith and M. H. Chanley (Boston, MA: Springer), 29–60.

Haas, B. J., Papanicolaou, A., Yassour, M., Grabherr, M., Blood, P. D., Bowden, J., et al. (2013). De novo transcript sequence reconstruction from RNA-seq using the Trinity platform for reference generation and analysis. *Nat. Protoc.* 8, 1494–1512. doi: 10.1038/nprot.2013.084

Hartmann, M., Zubkov, M. V., Scanlan, D. J., and Lepère, C. (2013). *In situ* interactions between photosynthetic picoeukaryotes and bacterioplankton in the Atlantic Ocean: evidence for mixotrophy. *Environ. Microbiol. Rep.* 5, 835–840. doi: 10.1111/1758-2229.12084

Hitchman, R. B., and Jones, H. L. (2000). The role of mixotrophic protists in the population dynamics of the microbial food web in a small artificial pond. *Freshw. Biol.* 43, 231–241. doi: 10.1046/j.1365-2427.2000.00541.x

Jones, P., Binns, D., Chang, H. Y., Fraser, M., Li, W., McAnulla, C., et al. (2014). InterProScan 5: genome-scale protein function classification. *Bioinformatics* 30, 1236–1240. doi: 10.1093/bioinformatics/btu031

Koid, A. E., Liu, Z., Terrado, R., Jones, A. C., Caron, D. A., and Heidelberg, K. B. (2014). Comparative transcriptome analysis of four prymnesiophyte algae. *PLoS ONE* 9:e97801. doi: 10.1371/journal.pone.0097801

Lagesen, K., Hallin, P., Rødland, E. A., Staerfeldt, H.-H., Rognes, T., and Ussery, D. W. (2007). RNAmmer: consistent and rapid annotation of ribosomal RNA genes. *Nucleic Acids Res.* 35, 3100–3108. doi: 10.1093/nar/gkm160

Langmead, B., and Salzberg, S. L. (2012). Fast gapped-read alignment with Bowtie 2. *Nat. Methods* 9, 357–359. doi: 10.1038/nmeth.1923

Li, W., and Godzik, A. (2006). Cd-hit: a fast program for clustering and comparing large sets of protein or nucleotide sequences. *Bioinformatics* 22, 1658–1659. doi: 10.1093/bioinformatics/btl158

Li, W. K., McLaughlin, F. A., Lovejoy, C., and Carmack, E. C. (2009). Smallest algae thrive as the Arctic Ocean freshens. *Science* 326, 539–539. doi: 10.1126/science.1179798

Liu, J., Huang, J., Sun, Z., Zhong, Y., Jiang, Y., and Chen, F. (2011). Differential lipid and fatty acid profiles of photoautotrophic and heterotrophic *Chlorella zofingiensis*: assessment of algal oils for biodiesel production. *Bioresour. Technol.* 102, 106–110. doi: 10.1016/j.biortech.2010.06.017

Liu, Z., Campbell, V., Heidelberg, K. B., and Caron, D. A. (2016). Gene expression characterizes different nutritional strategies among three mixotrophic protists. *FEMS Microbiol. Ecol.* 92:fiw106. doi: 10.1093/femsec/fiw106

Lovejoy, C., Vincent, W. F., Bonilla, S., Roy, S., Martineau, M.-J., Terrado, R., et al. (2007). Distribution, phylogeny, and growth of cold-adapted picoprasinophytes in arctic seas. *J. Phycol.* 43, 78–89. doi: 10.1111/j.1529-8817.2006.00310.x

Magoc, T., and Salzberg, S. L. (2011). FLASH: fast length adjustment of short reads to improve genome assemblies. *Bioinformatics* 27, 2957–2963. doi: 10.1093/bioinformatics/btr507

Maranger, R., Bird, D. F., and Price, N. M. (1998). Iron acquisition by photosynthetic marine phytoplankton from ingested bacteria. *Nature* 396, 248–251. doi: 10.1038/24352

Maruyama, S., and Kim, E. (2013). A modern descendant of early green algal phagotrophs. *Curr. Biol.* 23, 1081–1084. doi: 10.1016/j.cub.2013.04.063

McKie-Krisberg, Z. M., Gast, R. J., and Sanders, R. W. (2015). Physiological responses of three species of antarctic mixotrophic phytoflagellates to changes in light and dissolved nutrients. *Microb. Ecol.* 70, 21–29. doi: 10.1007/s00248-014-0543-x

McKie-Krisberg, Z. M., and Sanders, R. W. (2014). Phagotrophy by the picoeukaryotic green alga *Micromonas*: implications for Arctic Oceans. *ISME J.* 8, 1953–1961. doi: 10.1038/ismej.2014.16

Moffat, F. L., Han, T., Li, Z. M., Peck, M. D., Falk, R. E., Spalding, P. B., et al. (1996). Involvement of CD44 and the cytoskeletal linker protein ankyrin in human neutrophil bacterial phagocytosis. *J. Cell. Physiol.* 168, 638–647. doi: 10.1002/(SICI)1097-4652(199609)168:3<638::AID-JCP16>3.0.CO;2-V

Moorthi, S. D., Caron, D. A., Gast, R. J., and Sanders, R. W. (2009). Mixotrophy: a widespread and important ecological strategy for planktonic and sea-ice nanoflagellates in the Ross Sea, Antarctica. *Aquat. Microb. Ecol.* 54, 269–277. doi: 10.3354/ame01276

Morgan, M., Falcon, S., and Gentleman, R. (2008). *GSEABase: Gene Set Enrichment Data Structures and Methods.* R Package Version 1.42.0. doi: 10.18129/B9.bioc.GSEABase

Moriya, Y., Itoh, M., Okuda, S., Yoshizawa, A. C., and Kanehisa, M. (2007). KAAS: an automatic genome annotation and pathway reconstruction server. *Nucleic Acids Res.* 35, W182–W185. doi: 10.1093/nar/gkm321

Moro, I., La Rocca, N., Valle, L. D., Moschin, E., Negrisolo, E., and Andreoli, C. (2002). *Pyramimonas australis* sp. nov.(Prasinophyceae, Chlorophyta) from Antarctica: fine structure and molecular phylogeny. *Eur. J. Phycol.* 37, 103–114. doi: 10.1017/S0967026201003493

Nguyen, M. T., Liu, M., and Thomas, T. (2014). Ankyrin-repeat proteins from sponge symbionts modulate amoebal phagocytosis. *Mol. Ecol.* 23, 1635–1645. doi: 10.1111/mec.12384

Nygaard, K., and Tobiesen, A. (1993). Bacterivory in algae: a survival strategy during nutrient limitation. *Limnol. Oceanogr.* 38, 273–279. doi: 10.4319/lo.1993.38.2.0273

Pålsson, C., and Granéli, W. (2004). Nutrient limitation of autotrophic and mixotrophic phytoplankton in a temperate and tropical humic lake gradient. *J. Plankton Res.* 26, 1005–1014. doi: 10.1093/plankt/fbh089

Pomeroy, L. R. (1974). The ocean's food web, a changing paradigm. *Bioscience* 24, 499–504.

R Core Team (2013). R: A Language and Environment for Statistical Computing. Available online at: http://www.R-project.org/

Raven, J. A. (2013). Cells inside cells: symbiosis and continuing phagotrophy. *Curr. Biol.* 23, R530–R531. doi: 10.1016/j.cub.2013.05.006

Roberts, A., Trapnell, C., Donaghey, J., Rinn, J. L., and Pachter, L. (2011). Improving RNA-Seq expression estimates by correcting for fragment bias. *Genome Biol.* 12:R22. doi: 10.1186/gb-2011-12-3-r22

Robinson, M. D., McCarthy, D. J., and Smyth, G. K. (2010). edgeR: a bioconductor package for differential expression analysis of digital gene expression data. *Bioinformatics* 26, 139–140. doi: 10.1093/bioinformatics/btp616

Rouached, H., Arpat, A. B., and Poirier, Y. (2010). Regulation of phosphate starvation responses in plants: signaling players and cross-talks. *Mol. Plant* 3, 288–299. doi: 10.1093/mp/ssp120

Sanders, R. W. (1991). Mixotrophic protists in marine and freshwater ecosystems. *J. Protozool.* 38, 76–81. doi: 10.1111/j.1550-7408.1991.tb04805.x

Sanders, R. W. (2011). Alternative nutritional strategies in protists: symposium introduction and a review of freshwater protists that combine

photosynthesis and heterotrophy. *J. Eukaryot. Microbiol.* 58, 181–184. doi: 10.1111/j.1550-7408.2011.00543.x

Sanders, R. W., Caron, D. A., Davidson, J. M., Dennett, M. R., and Moran, D. M. (2001). Nutrient acquisition and population growth of a mixotrophic alga in axenic and bacterized cultures. *Microb. Ecol.* 42, 513–523. doi: 10.1007/s00248-001-1024-6

Sanders, R. W., and Gast, R. J. (2012). Bacterivory by phototrophic picoplankton and nanoplankton in Arctic waters. *FEMS Microbiol. Ecol.* 82, 242–253. doi: 10.1111/j.1574-6941.2011.01253.x

Sanders, R. W., Porter, K. G., Bennett, S. J., and DeBiase, A. E. (1989). Seasonal patterns of bacterivory by flagellates, ciliates, rotifers, and cladocerans in a freshwater planktonic community. *Limnol. Oceanogr.* 34, 673–687. doi: 10.4319/lo.1989.34.4.0673

Santoferrara, L. F., Guida, S., Zhang, H., and McManus, G. B. (2014). *De novo* transcriptomes of a mixotrophic and a heterotrophic ciliate from marine plankton. *PLoS ONE* 9:e101418. doi: 10.1371/journal.pone.0101418

Schmieder, R., and Edwards, R. (2011). Fast identification and removal of sequence contamination from genomic and metagenomic datasets. *PLoS ONE* 6:e17288. doi: 10.1371/journal.pone.0017288

Sherr, E. B., Caron, D. A., and Sherr, B. F. (1993). "Staining of heterotrophic protists for visualization via epifluorescence microscopy," in *Handbook of Methods in Aquatic Microbial Ecology,* eds P. F. Kemp, B. F. Sherr, E. B. Sherr, and J. J. Cole (New York, NY: Lewis Publishers), 213–227.

Sherr, E. B., and Sherr, B. F. (2002). Significance of predation by protists in aquatic microbial food webs. *Antonie Van Leeuwenhoek* 81, 293–308. doi: 10.1023/A:1020591307260

Simon, N., Foulon, E., Grulois, D., Six, C., Desdevises, Y., Latimier, M., et al. (2017). Revision of the genus Micromonas Manton et Parke (Chlorophyta, Mamiellophyceae), of the type species *M. pusilla* (Butcher) Manton and Parke and of the species *M. commoda* van Baren, Bachy and Worden and description of two new species based on the genetic and phenotypic characterization of cultured isolates. *Protist* 168, 612–635. doi: 10.1016/j.protis.2017.09.002

Smith, W. O., Dinniman, M. S., Klinck, J. M., and Hofmann, E. (2003). Biogeochemical climatologies in the Ross Sea, Antarctica: seasonal patterns of nutrients and biomass. *Deep Sea Res. Part II Top. Stud. Oceanogr.* 50, 3083–3101. doi: 10.1016/j.dsr2.2003.07.010

Stoecker, D. K. (1998). Conceptual models of mixotrophy in planktonic protists and some ecological and evolutionary implications. *Eur. J. Protistol.* 34, 281–290. doi: 10.1016/S0932-4739(98)80055-2

Swingley, W. D., Sadekar, S., Mastrian, S. D., Matthies, H. J., Hao, J., Ramos, H., et al. (2007). The complete genome sequence of *Roseobacter denitrificans* reveals a mixotrophic rather than photosynthetic metabolism. *J. Bacteriol.* 189, 683–690. doi: 10.1128/JB.01390-06

Tirichine, L., and Bowler, C. (2011). Decoding algal genomes: tracing back the history of photosynthetic life on Earth. *Plant. J.* 66, 45–57. doi: 10.1111/j.1365-313X.2011.04540.x

Unrein, F., Gasol, J. M., Not, F., Forn, I., and Massana, R. (2014). Mixotrophic haptophytes are key bacterial grazers in oligotrophic coastal waters. *ISME J.* 8, 164–176. doi: 10.1038/ismej.2013.132

Wheeler, P. A., Watkins, J. M., and Hansing, R. L. (1997). Nutrients, organic carbon and organic nitrogen in the upper water column of the Arctic Ocean: implications for the sources of dissolved organic carbon. *Deep Sea Res. Part II Top. Stud. Oceanogr.* 44, 1571–1592. doi: 10.1016/S0967-0645(97)00051-9

Whitney, L. P., and Lomas, M. W. (2016). Growth on ATP elicits a P-stress response in the picoeukaryote *Micromonas pusilla*. *PLoS ONE* 11:e0155158. doi: 10.1371/journal.pone.0155158

Worden, A. Z., Lee, J. H., Mock, T., Rouzé, P., Simmons, M. P., Aerts, A. L., et al. (2009). Green evolution and dynamic adaptations revealed by genomes of the marine picoeukaryotes *Micromonas*. *Science* 324, 268–272. doi: 10.1126/science.1167222

Wurch, L. L., Bertrand, E. M., Saito, M. A., Van Mooy, B. A., and Dyhrman, S. T. (2011). Proteome changes driven by phosphorus deficiency and recovery in the brown tide-forming alga *Aureococcus anophagefferens*. *PLoS ONE* 6:e28949. doi: 10.1371/journal.pone.0028949

Yutin, N., Wolf, M. Y., Wolf, Y. I., and Koonin, E. V. (2009). The origins of phagocytosis and eukaryogenesis. *Biol. Direct* 4, 6150–6154. doi: 10.1186/1745-6150-4-9

Zubkov, M. V., and Tarran, G. A. (2008). High bacterivory by the smallest phytoplankton in the North Atlantic Ocean. *Nature* 455, 224–226. doi: 10.1038/nature07236

Conflict of Interest Statement: The authors declare that the research was conducted in the absence of any commercial or financial relationships that could be construed as a potential conflict of interest.

frontiers in Marine Science

ORIGINAL RESEARCH
published: 11 May 2018
doi: 10.3389/fmars.2018.00157

Single-Cell View of Carbon and Nitrogen Acquisition in the Mixotrophic Alga *Prymnesium parvum* (Haptophyta) Inferred From Stable Isotope Tracers and NanoSIMS

Kevin J. Carpenter[1]*, *Maitrayee Bose*[2], *Lubos Polerecky*[3], *Alle A. Y. Lie*[1], *Karla B. Heidelberg*[1] and *David A. Caron*[1]

[1] Department of Biological Sciences, University of Southern California, Los Angeles, CA, United States, [2] School of Molecular Sciences, Arizona State University, Tempe, AZ, United States, [3] Department of Earth Sciences – Geochemistry, Utrecht University, Utrecht, Netherlands

OPEN ACCESS

Edited by:
Matthew D. Johnson, Woods Hole Oceanographic Institution, United States

Reviewed by:
Robert Fischer, Wasser Cluster Lunz, Austria
Akkur Vasudevan Raman, Andhra University, India

***Correspondence:**
Kevin J. Carpenter
kevin@kevinjcarpenter.com

Specialty section:
This article was submitted to Marine Ecosystem Ecology, a section of the journal Frontiers in Marine Science

Received: *13 January 2018*
Accepted: *19 April 2018*
Published: *11 May 2018*

Citation:
Carpenter KJ, Bose M, Polerecky L, Lie AAY, Heidelberg KB and Caron DA (2018) Single-Cell View of Carbon and Nitrogen Acquisition in the Mixotrophic Alga Prymnesium parvum (Haptophyta) Inferred From Stable Isotope Tracers and NanoSIMS. Front. Mar. Sci. 5:157. doi: 10.3389/fmars.2018.00157

Nutritional modes of unicellular eukaryotes range from pure photoautotrophy of some phytoplankton to pure heterotrophy of species typically called protozoa. Between these two extremes lies a functional continuum of nutrient and energy acquisition modes termed mixotrophy. *Prymnesium parvum* is an ecologically important mixotrophic haptophyte alga that can produce toxins and form ecosystem disruptive blooms that result in fish kills and changes in planktonic food web structure. We investigated carbon and nitrogen acquisition strategies of single cells of *P. parvum* using a combined experimental-imaging approach employing labeling of live cells with stable isotope tracers (^{13}C and ^{15}N) followed by measurement of cellular isotopic ratios using nanometer-scale secondary ion mass spectrometry (NanoSIMS). With this method, we were able to quantify the relative contributions of photosynthesis and heterotrophy to the nutrition of the alga. Our results suggest that *P. parvum* relies on predation primarily for nitrogen, while most carbon for cellular building blocks is obtained from inorganic sources. Our analysis further revealed that nitrogen assimilation can vary up to an order of magnitude among individual cells, a finding that would be difficult to determine using other methods. These results help to improve our understanding of mixotrophy across the enormous diversity of eukaryotes, one cell and one species at a time.

Keywords: algae, haptophyte, mixotrophy, NanoSIMS, protist, predation, *Prymnesium parvum*, stable isotope tracers

INTRODUCTION

It is often assumed that the vast diversity of the eukaryotic domain can be neatly divided into plant-like (exclusively photoautotrophic) or animal-like (exclusively heterotrophic) categories, with the few taxa that combine both capabilities (i.e., mixotrophy) viewed as curiosities. However, accumulating research and recent reviews on protists offer a strikingly different view of our domain

(Raven et al., 2009; Mitra et al., 2016; Caron, 2017; Stoecker et al., 2017). Mixotrophy is very common across the eukaryotic tree (Raven et al., 2009), is ubiquitous in aquatic ecosystems, and is of great importance in aquatic biogeochemical cycles where it influences carbon and energy flow in food webs (e.g., Sanders, 2011; Mitra et al., 2014; Ward and Follows, 2016). In recent attempts to include mixotrophy in marine global biogeochemical models, mixotrophy has been shown to increase primary productivity where inorganic nutrients are limiting, to result in larger average cell size of plankton (diameter), and to increase the proportion of carbon exported into the deep ocean (Mitra et al., 2014; Ward and Follows, 2016). Further, mixotrophy is a key strategy influencing the distributions and abundances of planktonic protistan taxa (Jones, 1994, 2000; Hartmann et al., 2013; Leles et al., 2017), including many harmful algal bloom (HAB) species (Tillmann, 2003; Burkholder et al., 2008).

The term mixotrophy has been broadly applied to protists that combine photoautotrophic with heterotrophic nutrition (primarily phagotrophy) (Flynn et al., 2013; Mitra et al., 2016). Far from a curiosity, many phytoplankton taxa have phagotrophic members, including numerous dinoflagellates, chrysophytes, cryptophytes, prasinophytes, and haptophytes (Sanders and Porter, 1988; Raven et al., 2009; Flynn et al., 2013). The great abundances of mixotrophs in most aquatic systems suggest this nutritional mode should be considered the rule rather than the exception (Matantseva and Skarlato, 2013).

The range of energy and nutrient acquisition strategies exhibited by three mixotrophic algae was recently illustrated by a comparative analysis of gene expression under different light regimes and prey availabilities for cultures of the haptophyte, *Prymnesium parvum,* and two chrysophyte algae (*Dinobryon* sp. and *Ochromonas* sp., strain CCMP1393). *P. parvum* and *Dinobryon* sp. showed differential expression of thousands of genes between light and dark regimes, while *Ochromonas* sp. showed differential expression of only ∼50 genes between the two regimes (Liu et al., 2016). These observations led to the conclusion that *P. parvum* and *Dinobryon* sp. are both predominantly photosynthetic, but the study also revealed subtle differences in nutritional strategy between those two algae (Liu et al., 2016). *Ochromonas* strain 1393, on the other hand, is more heterotrophic as shown by a less dramatic response of gene expression to the light regime. A study of another *Ochromonas* species (strain BG-1) also demonstrated the predominantly heterotrophic nature of the alga by showing that the availability of bacterial prey led to the differential expression of >7X more genes than the availability of light (Lie et al., 2017).

The mixotrophic alga *P. parvum* (Carter, 1937) is a member of the Haptophyta (prymnesiophytes), a large and extremely abundant group of photosynthetic plankton including coccolithophorids (e.g., *Emiliania huxleyi*), whose chloroplasts arose via endosymbiosis with a red alga (Yoon et al., 2002; Burki et al., 2016). *P. parvum* is a small (8–16 μm), ellipsoid cell with phagotrophic ability assisted by a tube-like feeding appendage (the haptonema) emerging between two anterior flagella. It occurs in freshwater, brackish, and coastal marine waters worldwide (Green et al., 1982; Moestrup, 1994; Barkoh and Fries, 2010), and is classified as an Ecosystem Disruptive Algal Bloom (EDAB) species (Sunda et al., 2006), due to its production of a variety of potent toxins (e.g., prymnesins) (Rasmussen et al., 2016). Some of these blooms result in massive fish kills and deaths of other gill-breathing organisms as well as other algae, protists, and bacteria (Tillmann, 2003; Hambright et al., 2015; Roelke et al., 2016). Such devastating harmful blooms have undergone a dramatic range expansion in recent decades, especially in western North America freshwater systems (Sallenave, 2010; Roelke et al., 2016).

P. parvum appears to rely on phagotrophy to supplement a predominantly photoautotrophic nutritional mode (Carvalho and Granéli, 2010; Granéli et al., 2012; Liu et al., 2016). The alga is capable of photosynthetic growth in axenic culture but cannot maintain growth or survival in continuous darkness, even with an abundance of prey (Brutemark and Granéli, 2011). Experimental and observational studies have indicated that mixotrophy and toxin production in this species may be particularly important under inorganic nutrient limitation (Granéli et al., 2012; Liu et al., 2015b; Roelke et al., 2016). Tillmann (2003) provided evidence that *P. parvum* toxins are crucial to its mixotrophic strategy, and are used to immobilize and kill prey prior to ingestion. Recent transcriptomic evidence has supported the contention that inorganic nutrient limitation stimulates toxin production in *P. parvum* (Manning and La Claire, 2010). Based on comparison of gene expression under different growth conditions, such work has also intimated that *P. parvum* may take up organic carbon from both ciliate and bacterial prey for energy and carbon skeletons (fatty acids), and obtain nitrogen (amino acids) from ciliate prey and iron from bacteria (Liu et al., 2015a). Transcriptomic evidence also suggests that *P. parvum* may supplement energy from photosynthesis with organic carbon from prey capture, especially when grown under light limitation (Liu et al., 2016).

These studies have provided insight into the general trophic activities of *P. parvum*, but a complementary line of evidence quantifying the behavior of individual cells is needed to test and further refine our understanding of the specific contributions of mixotrophy for this species and to serve as a source of new hypotheses generated at the single-cell level. The experimental-imaging approach combining exposure of live cells to substrates enriched in stable isotope tracers followed by nanometer-scale secondary ion mass spectrometry (NanoSIMS) imaging of the cells is now well-established as a powerful tool in microbial ecology, offering the unique capability of imaging and quantifying isotopic ratios at very high spatial resolution (up to 50 nm lateral resolution). This technique has been successfully applied in numerous studies to investigate uptake, metabolism, and transfer of various isotopically labeled substances in individual cells, symbiotic consortia, and complex natural microbial communities (Orphan et al., 2001; Lechene et al., 2007; Carpenter et al., 2013; Kopp et al., 2013; Bonnet et al., 2016; Tai et al., 2016). This approach was recently applied for the first time to the study of a chrysophyte mixotrophic alga (*Ochromonas* sp. strain BG-1) to demonstrate that this species relies heavily on carbon and nitrogen uptake from prey for energy and nutrients, while photosynthesis represents a minor contribution to its overall nutrition (Terrado et al., 2017).

We investigated the mixotrophic potential of *P. parvum* at the single cell level by comparing carbon and nitrogen uptake from prey and inorganic nutrients using stable isotope tracers and imaging of cells with NanoSIMS. The primary goal of this study was to quantify and compare the amounts of carbon and nitrogen that *P. parvum* obtains from inorganic sources (using ^{13}C-bicarbonate and ^{15}N-nitrate) vs. nutrients obtained from live prey (using a ^{13}C- and ^{15}N-labeled ciliate protist, *Uronema marina*, ranging from 18 to 25 μm in length). Variability among *P. parvum* cells with respect to C and N uptake within each experimental treatment was also examined to gain insight on potential variability in natural populations. Whole *P. parvum* cells were imaged using NanoSIMS at time zero and 48 h, shortly after all prey were killed by the alga. We also imaged cells in an unlabeled control treatment to assess the effects of cell topography on the measured isotopic fractionation. This study provides important insights into how mixotrophy contributes to energy and nutrient budgets in *P. parvum*, an organism of considerable ecological interest.

MATERIALS AND METHODS

Organisms and Cultures

Prymnesium parvum strain UOBS-LP0109 (Texoma1) was isolated from Lake Texoma, Oklahoma, USA, and rendered axenic by repetitively micropipetting single cells through rinses of sterile medium. The alga was grown in sterile L1 medium without silica following the recipe of the Provasoli-Guillard National Center for Marine Algae and Microbiota protocol (see https://ncma.bigelow.org/algal-recipes) at 18‰ (1:1 0.2 μm-filtered, aged natural seawater: ultrapure water (Barnstead GenPure xCAD Plus, Thermo Fisher Scientific, Waltham, USA). *P. parvum* is a euryhaline alga, but has been demonstrated to be most toxic at low-to-intermediate salinities (Roelke et al., 2016). For that reason we chose to conduct all experimental work at 18‰. The axenicity of the *P. parvum* culture used for the experiment was confirmed by the lack of bacterial or fungal growth after inoculating 3 ml of the culture into 7 ml of 0.5% yeast extract broth at 18‰ and observing for 2 weeks.

The bacterivorous ciliate *U. marina* was originally isolated from Buzzards Bay, Massachusetts, USA, and was used as prey for *P. parvum*. It is also a relatively euryhaline species, and was chosen as prey because it grows readily at 18‰ and has been previously shown to be suitable prey item for *P. parvum* (Liu et al., 2015a). The ciliate was maintained on its attendant bacterial flora by periodic subculturing into the same medium used to culture *P. parvum,* with addition of yeast extract (∼0.02% final concentration) and a sterilized rice grain to promote bacterial growth.

Ciliate prey for the NanoSIMS experiments were grown by subculturing ciliates in a medium designed to promote the growth of their attendant bacteria (final concentrations: 362 μM $NaH_2PO_4{\cdot}H_2O$; 501 μM NH_4Cl; 0.04% glucose; 18‰). Labeled ciliates (^{13}C and ^{15}N) were grown with labeled bacteria in medium made with $^{15}NH_4Cl$ (98 atom % ^{15}N; Sigma-Aldrich, St. Louis, USA) and D-glucose-1-^{13}C (99 atom % ^{13}C, Sigma-Aldrich). Both labeled and unlabeled ciliates were cleaned of remaining attendant bacteria, and concentrated prior to use as prey in the NanoSIMS experiment through 3 rounds of centrifugation (1,500 g for 5 min at 4°C; Sorvall RC5C plus, Thermo Fisher) and rinsed using sterilized 18‰ water (Liu et al., 2015a). Ciliates remained alive and highly motile following this procedure.

Stable Isotope Labeling Experiments

Experiments were designed to determine the degree to which *P. parvum* acquired carbon and nitrogen directly from the ciliate prey, relative to these elements from the dissolved inorganic pools. This was done by comparing reciprocal labeling of the carbon and nitrogen pools (inorganic pools of carbon and nitrogen, or these elements contained in ciliate prey). Predator (*P. parvum*) and prey (*U. marina*) abundances were chosen based on preliminary studies of the ability of the smaller alga (cell volume ∼200 μm^3) to attack and subdue the larger ciliate prey (cell volume ∼800–1,000 μm^3). Our observations in the laboratory revealed that several *P. parvum* are required to immobilize and kill a ciliate, therefore we conducted simple bioassay experiments with a set number of algae ($\sim 2 \times 10^5$ ml^{-1}) but varying abundances of ciliates in order to determine the optimal ratio of *P. parvum* to *U. marina* that led to the complete elimination of ciliates within 48–72 h (unpublished data). We chose this time frame to ensure that all prey would be killed by the time of stable isotope analysis. Based on that work, we chose starting concentrations of *P. parvum* and ciliates of $\sim 2 \times 10^5$ ml^{-1} and $\sim 1 \times 10^4$ ml^{-1}, respectively. Furthermore, to our knowledge, cannibalism is not known in *P. parvum*. We have grown it to very high abundances (>10^6/ml) and we have not witnessed it, even after extensive behavioral monitoring with microscopy.

Batch (50 ml) cultures of *P. parvum* were grown in 125 ml Erylenmeyer flasks at 18°C and 200 μE m^{-2} s^{-1} light intensity (12:12 h light:dark cycle) on an orbital shaker (60 rpm), and was used in all experiments while still in exponential growth. Cultures were grown in the same medium for maintaining *P. parvum*, with an addition of 95 μM $NaHCO_3$. No attempt was made to limit inorganic nutrients in the experiments for three reasons. First, in order to directly compare the outcomes of the treatments with labeled inorganic carbon and nitrogen to treatments with labeled ciliate carbon and nitrogen, it was necessary to provide the same amounts of inorganic nutrient or ciliates in all treatments (labeled or unlabeled). Second, release of inorganic carbon or nitrogen when isotope-labeled ciliate prey are killed could be confounded by subsequent uptake (i.e., erroneously attributed to direct uptake from prey). Maintaining high concentrations of unlabeled inorganic carbon and nitrogen in the medium at all times minimized this potential artifact. Finally, our preliminary work (noted above) demonstrated that our strain of *P. parvum* remained toxic in the presence of inorganic nutrients and therefore there was no reason to limit nutrients to stimulate predation.

Four experimental treatments were carried out. These included two unlabeled treatments and two combining ^{13}C and ^{15}N labeled inorganics or ^{13}C and ^{15}N labeled prey. Treatments 1–3 were performed in triplicates:

- Treatment 1 used labeled ciliates (as described above) + unlabeled inorganics.
- Treatment 2 used unlabeled ciliates + labeled inorganics [$NaH^{13}CO_3$ (98 atom % ^{13}C, Sigma-Aldrich) was added as 100% of the total bicarbonate (95 μM) while $Na^{15}NO_3$ (98 atom % ^{15}N, Sigma-Aldrich) was added as 50% of the total nitrate (441 μM $Na^{15}NO_3$ and 441 μM $NaNO_3$)].
- Treatment 3 used unlabeled ciliates + unlabeled inorganics. Material from this treatment was not imaged in NanoSIMS but was included in a comparison of growth rates across the first three treatments.
- Treatment 4 used unlabeled ciliates + unlabeled inorganics. This treatment was run for a duration of 30 min, and was included to ensure sufficient material to test sample preparation procedures for field emission scanning electron microscope (FESEM) and NanoSIMS, and to quantify the effects of topography on isotopic fractionation. Based on evidence that *P. parvum* attacks prey very quickly (Tillmann, 2003), we confirmed beforehand that this was a suitable duration to observe predation, but not so long that ciliates would be completely consumed.

Treatments 1–3 were sampled every 24 h for the determination of *P. parvum* and ciliate densities. Aliquots for cell counts (3 ml) were preserved with Lugol's solution (final concentration 2.5%) and enumerated using a Palmer-Maloney counting chamber at 200 x on a compound light microscope (BX51; Olympus, Waltham, USA). The growth rate of *P. parvum* was calculated as the slope of natural log algal abundance against time (72 h).

NanoSIMS samples (5 ml aliquots) were taken from Treatment 1 and Treatment 2 immediately after the addition of labeled inorganics or labeled ciliates to *P. parvum* cultures (T0) and 48 h later (T48). The samples were preserved with glutaraldehyde at a final concentration of 1% and stored at 4°C.

Hence, five samples were prepared for analysis using NanoSIMS: Treatments 1 and 2, each at time zero (T0) and 48 h (T48) time points, and Treatment 4 (unlabeled control):

1) T0 labeled ciliates
2) T0 labeled inorganics
3) T48 labeled ciliates
4) T48 labeled inorganics
5) Treatment 4 (unlabeled control)

Specimen Fixation and Preparation for NanoSIMS

Fixed subsamples were pipetted onto 13 mm diam., 1.2 μm pore size Millipore polycarbonate filters (Billerica, MA, USA) held in Millipore Swinnex cartridges between two Teflon gaskets. Three of these filter-cartridge assemblies were affixed to 10 ml plastic syringes to process material from each sample. Approximately 500 μl of material was pipetted onto each filter to ensure deposition of enough *P. parvum* and *U. marina* cells without clogging the filters. Material on filters was then rinsed three times in PBS buffer to remove excess glutaraldehyde, and dehydrated in a series of 50, 70, 90, and 3X 100% ethanol. Rinses and dehydration were carried out by removing the cartridge from the syringe at the end of each step, quickly drawing the next solution into the syringe, reattaching it to the cartridge, and pushing the liquid through the filter using the syringe plunger (i.e., not by gravity filtration). Filters were then removed from the cartridges while immersed in 100% ethanol and dried in a Tousimis Autosamdri 815 carbon dioxide critical point dryer (Rockville, MD, USA). Dried filters were affixed to 12.5 mm aluminum pin mount stubs with conductive carbon double-stick tape and coated with ∼5–10 nm of platinum in a Cressington 108 sputter coater (Watford, UK). Prepared material on stubs was examined with a JEOL 7001 FESEM (Tokyo, Japan) to ensure adequate cellular preservation and abundance prior to NanoSIMS measurements. This sample preparation method has previously been shown to be suitable for preserving cell ultrastructure and retaining ^{13}C and ^{15}N signal within fixed cells (Carpenter et al., 2013; Tai et al., 2016).

NanoSIMS Measurements and Image Analysis

Measurements of carbon and nitrogen isotopes in *P. parvum* and *U. marina* were carried out using a Cameca 50L NanoSIMS high resolution imaging mass spectrometer (Gennevilliers, France) at Arizona State University. The instrument was operated in Cesium mode (Cs+ primary ion beam), which maximizes yield of negatively charged secondary ions from the sample surface. Electron multiplier detectors 1–5 were set to collect the following species: $^{12}C^-$, $^{13}C^-$, $^{12}C^{14}N^-$, $^{12}C^{15}N^-$, and $^{31}P^-$. For each session, prior to collection of data from samples, tuning, and measurements were made on a cyanoacrylate standard. Target cells for NanoSIMS imaging were selected by using the CCD camera to navigate to areas on the specimen mount surface with abundant cells and a minimal filter topography. This preliminary observation was followed by higher magnification observation and final selection using the secondary electron image and/or the $^{12}C^{14}N^-$ secondary ion image. For imaging of the two T0 samples, care was taken to image *P. parvum* and *U. marina* in separate fields of view (FOV), to ensure that isotopically enriched material from labeled ciliates did not become redeposited upon nearby *P. parvum* cells, thus affecting measurements of those cells.

Data from samples were collected using a 75 nm diameter primary beam with 2–4 pA current measured at the sample (FC0 Faraday cup). Images ranged from 5–40 μm rasters, with dwell times of 10,000 to 15,000 μs/pixel and 2–40 planes. Upon selecting each FOV, secondary ion beam centering and focusing of secondary and primary ion beams with EOS and EOP (immersion lenses) were carried out. Mass peaks on each of the five electron multiplier detectors were checked in High Mass Resolution (HMR) scans. Prior to data collection, presputtering was conducted on an area slightly larger than the selected FOV using high L1 lens setting, and D1-0 aperture for a beam current of a few nA.

Images were analyzed using Look@NanoSIMS (Polerecky et al., 2012) and Cameca WinImage (Gennevilliers, France). Corrections for dead time and quasi-simultaneous arrival (QSA) were applied and drift-corrected planes were accumulated (combined into a single image) for further analysis. Regions of interest (ROIs) were hand-drawn around individual *P. parvum* cells, or portions of *U. marina* cells in the accumulated

images, and ^{13}C and ^{15}N abundances in individual cells were quantified using the secondary ion counts accumulated over all pixels in the respective ROI as $^{13}C/(^{12}C+^{13}C)$ and $^{12}C^{15}N/(^{12}C^{14}N+^{12}C^{15}N)$, respectively. Statistical tests comparing isotopic ratios in various pairs of samples [e.g., $^{13}C/(^{12}C+^{13}C)$] in T48 labeled inorganic vs. T0 labeled inorganic) were conducted in Look@NanoSIMS. Data were first analyzed with Levene's test to check for equal variances (homoscedasticity). Those with equal variances were analyzed with ANOVA, while the others were analyzed with the Kruskal-Wallis test.

RESULTS

Growth of *P. parvum* and Ciliate Abundances

The growth rates of *P. parvum* over the 72 h period were similar among the different treatments ($p > 0.05$ One-way ANOVA), yielding averages of 0.48 ± 0.02 d^{-1}, 0.57 ± 0.14 d^{-1}, and 0.54 ± 0.05 d^{-1} for Treatment 1, 2, and 3, respectively. The predation of ciliates occurred rapidly. The abundances of ciliates were reduced by 70% after 24 h, and no ciliates were observed after 48 h.

Field Emission Scanning Electron Microscope (FESEM) Imaging

Chemically fixed, critical point dried, and sputter coated *P. parvum* cells, and those of its prey, *U. marina*, from each of the four isotopically labeled samples, plus an unlabeled control (Treatment 4; see Methods), were observed with FESEM prior to NanoSIMS imaging. Cellular preservation of both species was observed to be generally good, with most cells remaining intact, and retaining good membrane integrity and good overall shape, including cilia or flagella (**Figure 1**). Both species were abundant in the two T0 samples, and in the unlabeled control. However, *U. marina* was not observed in either of the two T48 samples with FESEM, nor in NanoSIMS secondary electron or ion images, due to predation by *P. parvum*.

NanoSIMS imaging—T0 and Unlabeled Control Samples

Because the *P. parvum* cells are relatively large, 20 whole *P. parvum* cells from the unlabeled control (Treatment 4) were imaged using NanoSIMS to assess the effect of topography on the measured $^{13}C/C$ and $^{15}N/N$ ratios. The effect was relatively minor for ^{13}C, with the $^{13}C/C$ ratio varying by about 5% (mean = 0.0112, $SD = 0.0005$), whereas it was substantial for ^{15}N, with the $^{15}N/N$ ratio varying by about 55% (mean = 0.00367, $SD = 0.00200$) (**Figure 2**). This variation was taken into account when comparing enrichments in samples incubated with the label.

Four to five whole *P. parvum* cells were imaged in each of the two T0 samples (T0 labeled inorganics and T0 labeled ciliates). All of these cells fell within the ranges for both isotopes obtained from the unlabeled control sample with the exception of a single cell from the T0 labeled ciliate sample, which was slightly above this range for both ratios (1.21×10^{-2} for $^{13}C/C$ and 8.49×10^{-3} for $^{15}N/N$) (**Figure 3**). However, statistical analysis showed no significant difference in $^{13}C/C$ in *P. parvum* between the T0 inorganic labeled and unlabeled samples, or between T0 ciliate labeled and unlabeled samples (**Table 1**). However, the $^{15}N/N$ ratios in *P. parvum* cells from the T0 ciliate labeled treatment were significantly, although only slightly, larger than in the unlabeled control (**Table 1**).

Two *U. marina* cells were imaged in the T0 labeled inorganic sample, and their $^{13}C/C$ and $^{15}N/N$ ratios fell within the range of values obtained for the unlabeled control (**Figure 3**). In contrast, two *U. marina* cells imaged for the T0 labeled ciliate treatment showed a relatively small but significant enrichment in ^{13}C (mean $^{13}C/C$ of 0.0185) and a substantial enrichment in ^{15}N (mean $^{15}N/N$ of 0.386).

NanoSIMS Imaging—T48 Samples

Twenty-five whole *P. parvum* cells were imaged with NanoSIMS for the T48 labeled inorganic sample, while 22 whole *P. parvum* cells were imaged for the T48 labeled ciliate sample (no ciliates remained in either T48 sample). Carbon and nitrogen isotopic ratios from the two T48 samples and the unlabeled control are plotted in **Figure 4**, while representative NanoSIMS images are shown in **Figure 5**.

The ^{13}C enrichment in the *P. parvum* cells from the T48 labeled inorganic sample was relatively low and variable (mean $^{13}C/C$ ratio of 0.0172, $SD = 0.003$; **Figure 4**). Nevertheless, it was significant when compared to the T0 labeled inorganic sample as well as to the unlabeled control (**Table 1**). In contrast, most of the *P. parvum* cells from the T48 labeled ciliate sample had $^{13}C/C$ ratios within the range defined by the T0 labeled ciliate sample or the unlabeled control, with only 3 out of 22 exhibiting significant enrichment ($^{13}C/C$ ratios in the range 0.0119–0.0127). Overall, *P. parvum* cells from the T48 labeled ciliate sample had no significant ^{13}C enrichment (**Table 1**).

Irrespective of the N source, the ^{15}N enrichment in the *P. parvum* cells from the T48 samples was relatively high and variable (**Figure 4**). For the T48 labeled inorganic sample, the average $^{15}N/N$ ratio was 0.093 ($SD = 0.051$), whereas it was 0.089 ($SD = 0.054$) for the T48 labeled ciliate sample. Both of these values were significantly larger than the values in the corresponding T0 samples as well as in the unlabeled control samples, but not significantly different from each other (**Table 1**).

To estimate the importance of the different C and N sources in the nutrition of *P. parvum*, we calculated the relative amounts of C and N assimilated by the *P. parvum* cells during the incubation interval of $\Delta t = 2$ days as

$$r_C = [(^{13}C/C)_{T48} - (^{13}C/C)_{T0}]/[(^{13}C/C)_{SRC} - (^{13}C/C)_{T0}]/\Delta t, \quad (1)$$

$$r_N = [(^{15}N/N)_{T48} - (^{15}N/N)_{T0}]/[(^{15}N/N)_{SRC} - (^{15}N/N)_{T0}]/\Delta t. \quad (2)$$

This calculation takes into account both the measured enrichment in the *P. parvum* cells (subscripts T48 and T0) as well as the enrichment of the corresponding assumed C and N source (subscript SRC).

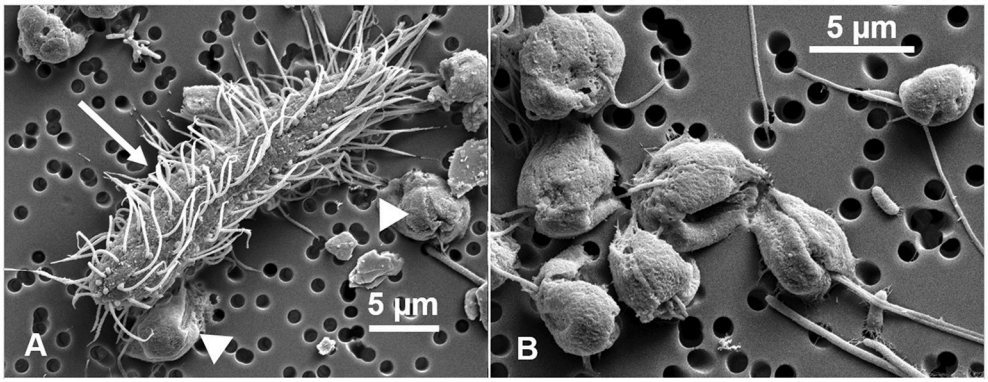

FIGURE 1 | Scanning electron micrographs of the organisms used in these experimental treatments. Cells shown here were sampled from the unlabeled control treatment (see Methods). **(A)** *Uronema marina* (arrow), used as prey for *Prymnesium parvum* (arrow heads). **(B)** *P. parvum* cells.

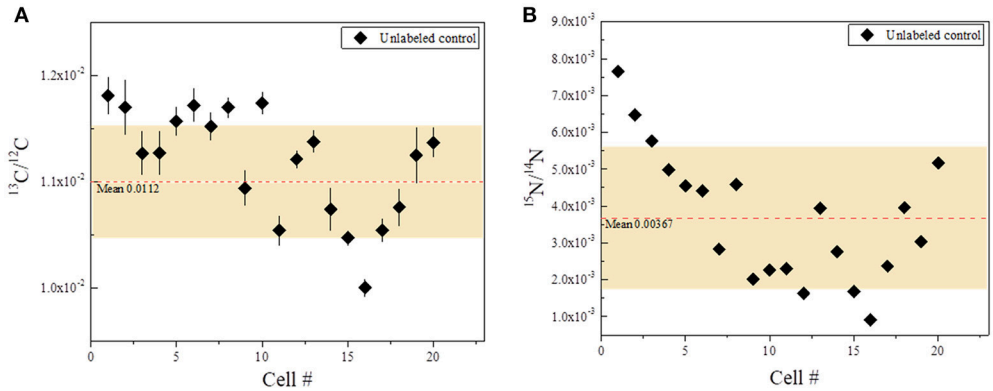

FIGURE 2 | Carbon and nitrogen isotopic ratios from the unlabeled control (Treatment 4), showing effects of topography on isotopic fractionation. Each data point represents a single, whole *P. parvum* cell (20 cells total). Red dashed lines indicate the mean value for each ratio. The shaded area indicates one standard deviation for all data points. Bars represent standard errors. Where bars are not visible, it indicates that the error is smaller than the data point. **(A)** $^{13}C/^{12}C$ ratios. Mean ratio (red dashed line) = 0.0112. **(B)**. $^{15}N/^{14}N$ ratios. Mean ratio (red dashed line) = 0.00367.

For the labeled inorganic incubation (Treatment 2), we assumed that the DIC and nitrate were the only labeled C and N sources, and hence used $(^{13}C/C)_{SRC} = 0.99$ and $(^{15}N/N)_{SRC} = 0.49$ (see Methods). Using the average isotopic ratios measured in the *P. parvum* cells, we obtained $r_C = 0.0033$ mol C (mol C)$^{-1}$ d^{-1} and $r_N = 0.092$ mol N (mol N)$^{-1}$ d^{-1}; i.e., a roughly 30-fold lower value of r_C relative to r_N.

For the labeled ciliate incubation (Treatment 1), we assumed that the ciliates were the only labeled source of C and N, and hence used the average values measured by NanoSIMS $(^{13}C/C)_{SRC} = 0.0185$ and $(^{15}N/N)_{SRC} = 0.386$ (see Results above). For the *P. parvum* cells whose values of $(^{13}C/C)_{T48}$ and $(^{13}C/C)_{T0}$ were not significantly different, we obtained $r_C = 0$ and $r_N = 0.11$ mol N (mol N)$^{-1}$ d^{-1}, whereas for the three *P. parvum* cells that showed significant ^{13}C enrichment we obtained $r_C = 0.094$ mol C (mol C)$^{-1}$ d^{-1} and $r_N = 0.20$ mol N (mol N)$^{-1}$ d^{-1}. This suggests that while most of the *P. parvum* cells preyed on the ciliates to gain nitrogen, a few of them likely used them as a significant source of both C and N. Additionally, because the r_N values estimated for the inorganic and ciliate labeled treatments were similar *P. parvum* appears to exhibit no preference for nitrogen assimilation from inorganic nutrients (nitrate) vs. predation on *U. marina*.

DISCUSSION

Prior to this study of *P. parvum*, the only previous application of stable isotope tracers and NanoSIMS to investigate protistan mixotrophy was completed by Terrado et al. (2017) on the chrysophyte alga *Ochromonas* sp. strain BG-1. That study showed that strain BG-1 relied heavily on heterotrophy (predation on bacteria) for acquisition of both carbon and nitrogen (84–99 and 88–95% of total uptake respectively). Uptake of inorganic forms of these elements from photoautotrophy occurred only after prey were depleted, and was insufficient to support population growth (Terrado et al., 2017). The inferred strategy of *P. parvum* determined in the present study stands in marked contrast to those findings. Our results suggest that *P. parvum* relied

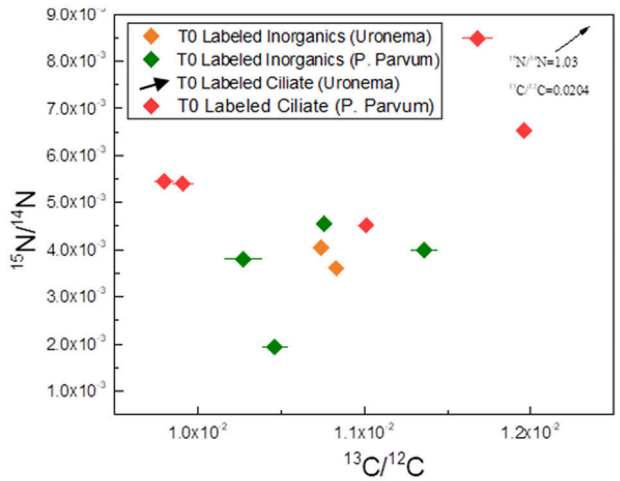

FIGURE 3 | Carbon and nitrogen isotopic ratios measured from treatments 2 and 3—Labeled Inorganics and Labeled Ciliates, respectively—at Time point zero (T0). Each data point represents a single, whole *P. parvum* cell, or an approximate half of a *U. marina* cell. The arrow indicates a single *U. marina* cell from T0 Labeled Ciliate sample with a $^{15}N/^{14}N$ ratio exceeding the range of the graph. This ratio is indicated, and the position of the point along the X-axis ($^{13}C/^{12}C$) is indicated by the arrow. Note that the range for each ratio is the same as in **Figure 2** to illustrate that the T0 samples are similar to the unlabeled controls in their isotopic composition (except for the *U. marina* cell indicated by the arrow).

mostly on photoautotrophy for carbon assimilation into cellular biomass, while predation served as a strategy to supplement energy and nitrogen, but much less for carbon integrated into cellular building blocks. However, no preference was demonstrated for nitrogen uptake from prey vs. inorganic sources (nitrate) when both were available. Hence, in the spectrum of strategies exhibited by mixotrophic protists, *P. parvum* lies close to the pure phototrophy end of the spectrum (also supported by data from Carvalho and Granéli, 2010; Brutemark and Granéli, 2011), while *Ochromonas* strain BG-1 lies much closer to the pure heterotrophy end of the mixotrophic spectrum.

Previous NanoSIMS imaging of protists has demonstrated that their large cell topography can have a significant influence on isotopic fractionation, and that this effect must be quantified through measurement of unlabeled cells (Carpenter et al., 2013; Kopp et al., 2015). Hence, we imaged 20 whole *P. parvum* cells from the unlabeled control sample to assess the effects of topography on fractionation of both carbon and nitrogen isotopes ($^{13}C/C$ and $^{15}N/N$). This was done to ensure that we could unequivocally detect enrichments in our labeled treatments (i.e., T48 labeled ciliate and T48 labeled inorganic samples)—i.e., whether these putative enrichments fall outside the range of variability caused by topography. Although the values for both isotopic ratios as measured from the unlabeled control sample show a fairly wide range (**Figure 2**), our statistical tests revealed significant differences in $^{15}N/N$ in both T48 samples compared to the unlabeled control, and in $^{13}C/C$ in the labeled T48 inorganic sample compared to the unlabeled control (**Table 1**; **Figure 4**). This analysis confirmed that the level of precision achieved here was sufficient to meet the goals of the study.

As expected, the $^{13}C/C$ and $^{15}N/N$ ratios measured from whole *P. parvum* cells of our two T0 samples (T0 inorganic labeled and T0 ciliate labeled) showed ranges that were not significantly different from the unlabeled control (**Table 1**; **Figure 3**), with the exception of ^{15}N in the T0 ciliate labeled sample. We suggest this signal is attributable to some assimilation of the ^{15}N label after immediate feeding while we were sampling T0 samples. For the prey ciliate cells (*U. marina*), those from the T0 labeled inorganics sample fell in the center of the ranges for *P. parvum* cells from the unlabeled control for both isotopes ($^{13}C/C$ and $^{15}N/N$), but the T0 labeled ciliates were significantly enriched in both isotopes as expected (**Figure 3**).

We found no significant difference in $^{13}C/C$ between the T48 labeled ciliate sample and the unlabeled control, or between the former and the T0 labeled ciliate sample. We conclude that, in our experimental design, *P. parvum* cells overall obtained no detectable carbon (i.e., for anabolic integration into cellular biomass) from ingestion of labeled ciliates after 48 h. However, three of the 22 imaged *P. parvum* cells did exhibit small but significant ^{13}C enrichment (**Figure 4** and Results). Hence, it appears that a small amount of carbon assimilation for integration into cellular biomass does occur through predation for some individual *P. parvum*, although this source appears to be a less important carbon source overall than photoautotrophy. That no significant difference in ^{13}C enrichment between T48 labeled inorganic and T48 labeled ciliate samples was observed is due to the few data points that overlap between the two data sets (**Figure 4**), while the *p*-value of 0.06 is close to significance (**Table 1**). No significant difference in ^{15}N enrichment between the two T48 samples was observed (**Table 1**; **Figure 4**), indicating that *P. parvum* had no preference for assimilation of nitrogen from inorganic nutrients (nitrate) or live prey when both are available.

Our results after 48 h (T48 labeled ciliate and T48 labeled inorganics treatments) demonstrated a much greater assimilation of prey nitrogen than prey carbon (**Figure 4**). A roughly 30-fold greater assimilation of ^{15}N than ^{13}C was observed in the treatment with labeled ciliates, although there was considerable variability among individual cells, as would be expected (see next paragraph). This was surprising in that we expected nitrogen and carbon assimilation would be more closely in balance. Specifically, the assimilation of nitrogen from prey by the alga was consistent with our expectation (i.e., prey can be a significant source of nitrogen for the mixotroph), but the low level of carbon assimilation was unexpected. A previous transcriptomic study of *P. parvum* (Liu et al., 2015a) indicated that the availability of ciliate prey had a clear effect on gene expression in the alga, resulting in increased expression of genes involved in fatty acid oxidation compared to treatments lacking prey (Liu et al., 2015a). These prior results seemed to imply that carbon from prey was readily utilized (and presumably assimilated) by *P. parvum*. However, given that fatty acid oxidation can result in either complete breakdown to CO_2 via the TCA cycle (i.e., for energy production), or anabolic processes (conversion to

TABLE 1 | Results of statistical tests (ANOVA or Kruskal-Wallis) for comparisons of different experimental treatments.

Treatments compared	Test	*P*-value	Conclusion
T0 Inorganic labeled vs. Unlabeled Control for 13C/12C	ANOVA	0.145	No significant difference
T0 Inorganic labeled vs. Unlabeled Control for 15N/14N	ANOVA	0.92	No significant difference
T0 Ciliate labeled vs. Unlabeled Control for 13C/12C	ANOVA	0.36	No significant difference
T0 Ciliate labeled vs. Unlabeled Control for 15N/14N	ANOVA	0.011	Significant difference
T48 Inorganic labeled vs. T0 Inorganic labeled for 13C/12C	ANOVA	0.0012	Significant difference
T48 Ciliate labeled vs. T0 Ciliate labeled for 13C/12C	ANOVA	0.152	No significant difference
T48 Ciliate labeled vs. T48 inorganic labeled for 13C/12C	ANOVA	0.06	No significant difference
T48 Inorganic labeled vs. T0 Inorganic labeled for 15N/14N	ANOVA	0.0023	Significant difference
T48 Ciliate labeled vs. T0 Ciliate labeled for 15N/14N	ANOVA	0.013	Significant difference
T48 Ciliate labeled vs. T48 inorganic labeled for 15N/4N	ANOVA	0.83	No significant difference
T48 Inorganic labeled vs. Unlabeled Control for 13C/12C	Kruskal-Wallis	1E-08	Significant difference
T48 Inorganic labeled vs. Unlabeled Control for 15N/14N	Kruskal-Wallis	1E-08	Significant difference
T48 Ciliate labeled vs. Unlabeled Control for 13C/12C	ANOVA	0.25	No significant difference
T48 Ciliate labeled vs. Unlabeled Control for 15N/14N	ANOVA	2.2E-06	Significant difference

succinate through the glyoxylate cycle), our NanoSIMS data help to clarify which of the two pathways are favored for prey-derived fatty acids. Specifically, our data suggest that *P. parvum* utilizes fatty acids derived from ciliate prey mostly for energy generation and to a lesser extent, in some individuals, for anabolic processes. Thus, our data further refine the picture of *P. parvum* as a predominantly photoautotrophic species that can rely on predation to supplement its nitrogen requirements. In a similar NanoSIMS-tracer study of the cellulolytic protist *Oxymonas* sp.—a gut symbiont of the termite *Paraneotermes*—Carpenter et al. (2013) found a roughly two order of magnitude enrichment in ^{13}C, but no detectable enrichment in ^{15}N after a 6-week labeling experiment, thus providing another example of unbalanced uptake of C and N.

The high levels of variability in isotopic enrichment—up to an order of magnitude for ^{15}N, but also wide for ^{13}C—among *P. parvum* cells in each of the two T48 treatments (**Figure 4**) appears to indicate that individual cells of *P. parvum* within a natural population encompass a correspondingly wide range of carbon and nitrogen uptake from various sources. This is possibly a function of cell size, point in the cell cycle, or—in the case of the T48 ciliate labeled sample—proximity to freshly killed prey. (This latter possibility makes sense because the ratio of predator to prey was 20:1.) We believe that assessment of such cell-to-cell variability, which is not possible to infer from molecular or other standard approaches, is an important outcome of this study. With such data in hand, it becomes possible to estimate averages for populations with much greater accuracy. It also becomes possible to then ask why such variability exists, and what effect the variation may have for populations, predator-prey relationships, production of toxins/harmful blooms, ecosystems, and biogeochemical cycles. In any case, it illustrates that in addition to the great diversity of mixotrophic strategies across higher taxa, evaluating the diversity across cells of a given species and/or population can refine our understanding of mixotrophy.

Our stable isotope labeling and NanoSIMS imaging analysis of single cells yields new insights on the cell physiology and ecology of *P. parvum*. It offers evidence that *P. parvum* relies on photoautotrophy for the production of cellular carbon, but uses predation mostly as a supplemental source of nitrogen and perhaps an energy source from carbon. It also shows *P. parvum* displays no preference for uptake of the nitrogen from prey or inorganic nutrients (nitrate) when both sources are available. One might conclude, however, that nitrogen derived from prey could be important when inorganic nitrogen sources are limiting. In addition, our study reveals a wide range of cell physiologies with respect to uptake of carbon and nitrogen across

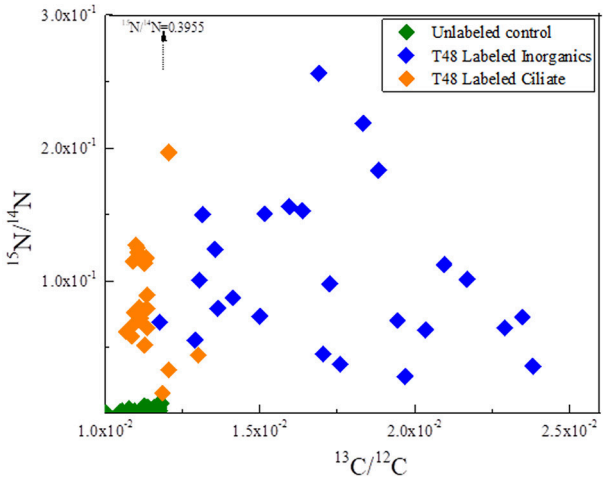

FIGURE 4 | Carbon and nitrogen isotopic ratios from the two T48 samples and the unlabeled control. Each data point represents a single, whole *P. parvum* cell (Ciliates were not observed in T48 samples.) The arrow indicates a single *P. parvum* cell from T48 Labeled Ciliate sample with a $^{15}N/^{14}N$ ratio exceeding the range of the graph. This ratio is indicated, and the position of the point along the X-axis ($^{13}C/^{12}C$) is indicated by the arrow. The X-axis intersects the Y-axis at the mean $^{15}N/^{14}N$ ratio, while the Y-axis intersects the X-axis at the mean $^{13}C/^{12}C$ ratio. Some points from the unlabeled control are thus not visible and lie below the Y-axis boundary.

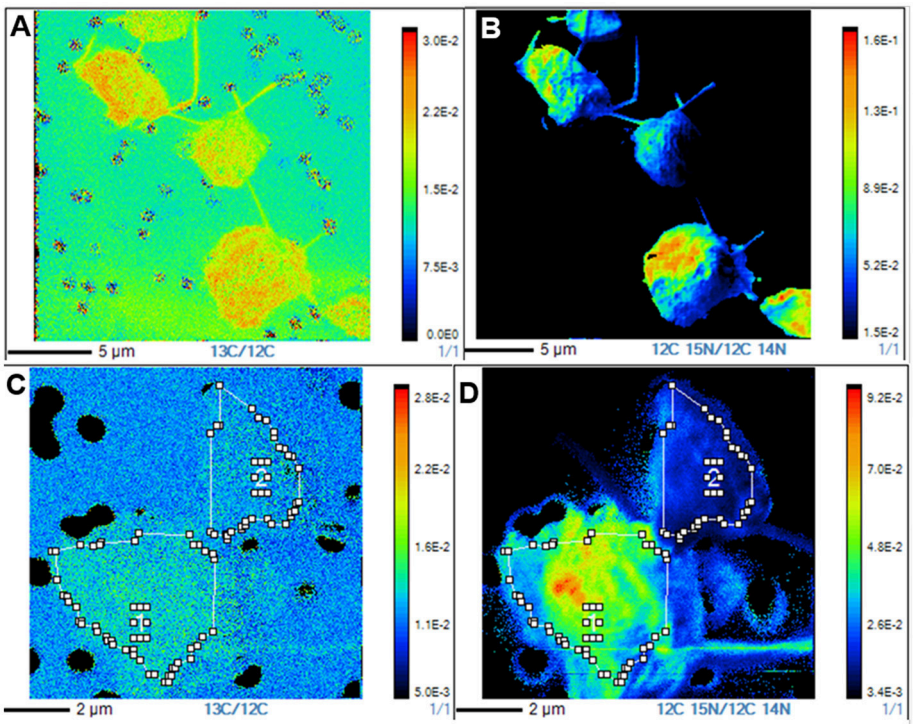

FIGURE 5 | NanoSIMS $^{13}C/^{12}C$ and $^{15}N/^{14}N$ isotope ratio images of representative *P. parvum* cells from the two T48 experiments. **(A)** $^{13}C/^{12}C$ isotope ratio image from a T48 labeled inorganic nutrients sample. **(B)** $^{15}N/^{14}N$ ratio image from a T48 labeled inorganic nutrients sample. **(C)** $^{13}C/^{12}C$ isotope ratio image from a T48 labeled ciliate sample. **(D)** $^{15}N/^{14}N$ isotope ratio image from a T48 labeled ciliate sample.

this population, perhaps reflecting the opportunistic nature of individual cells encountering (and utilizing) prey biomass, thus highlighting the capability to make far more accurate estimates of population level processes and the activity of an average cell within it. Future studies using methods such as the one presented here will continue to yield important insight into the vast and largely unexplored range of nutrient and energy acquisition strategies that fall under the very broad umbrella of mixotrophy—a strategy that is only very recently gaining recognition as one of enormous importance in biogeochemical cycles.

AUTHOR CONTRIBUTIONS

KC designed the experiments, fixed and prepared the samples, imaged the samples with FESEM and NanoSIMS, analyzed and interpreted the data, and led the development of the manuscript; MB imaged the samples with NanoSIMS and analyzed the data; LP analyzed and interpreted the data and contributed to the development of the manuscript; AL designed and carried out stable isotope tracer experimental treatments and measured *P. parvum* growth rates; KH and DC designed the experiments, interpreted the data and contributed to the development of the manuscript.

ACKNOWLEDGMENTS

The authors wish to thank the Moore Foundation (Grant GBMF3299 to DC and KH) for funding and Peter Williams (Arizona State University) for helpful discussions on NanoSIMS analysis. Electron micrographs presented in this article were acquired at the Center for Electron Microscopy and Microanalysis at the University of Southern California with technical assistance from John Curulli and Casey Barr.

REFERENCES

Barkoh, A., and Fries, L. T. (2010). Aspects of the origins, ecology, and control of Golden Alga *Prymnesium parvum*: introduction to the featured collection. *J. Am. Water Resour. Assoc.* 46, 1–5. doi: 10.1111/j.17521688.2009.00394.x

Bonnet, S., Berthelot, H., Turk-Kubo, K., Cornet-Bartaux, V., Fawcett, S. E., Berman-Frank, I., et al.. (2016). Diazotroph derived nitrogen supports diatoms growth in the South West Pacific: a quantitative study using nanoSIMS. *Limnol. Oceanogr.* 61, 1549–1562. doi: 10.1002/lno.10300

Brutemark, A., and Granéli, E. (2011). Role of mixotrophy and light for growth and survival of the toxic haptophyte *Prymnesium parvum*. *Harmful Algae* 10, 388–394. doi: 10.1016/j.hal.2011.01.005

Burkholder, J. M., Glibert, P. M., and Skelton, H. M. (2008). Mixotrophy, a major mode of nutrition for harmful algal species in eutrophic waters. *Harmful Algae* 8, 77–93. doi: 10.1016/j.hal.2008.08.010

Burki, F., Kaplan, M., Tikhonenkov, D. V., Zlatogursky, V., Minh, B. Q., Radaykina, L. V., et al. (2016). Untangling the early diversification of eukaryotes: a phylogenomic study of the evolutionary origins of Centrohelida, Haptophyta and Cryptista. *Proc. R. Soc. B* 283:20152802. doi: 10.1098/rspb.2015.2802

Caron, D. (2017). Acknowledging and incorporating mixed nutrition into aquatic protistan ecology, finally. *Environ. Microbiol. Rep.* 9, 41–43. doi: 10.1111/1758-2229.12514

Carpenter, K. J., Weber, P. K., Davisson, M. L., Pett-Ridge, J., Haverty, M. I., and Keeling, P. J. (2013). Correlated SEM, FIB-SEM, TEM, and nanoSIMS imaging of microbes from the hindgut of a lower termite: methods for *in situ* functional and ecological studies of uncultivable microbes. *Microsc. Microanal.* 19, 1490–1501. doi: 10.1017/S1431927613013482

Carter, N. (1937). New or interesting algae from brackish water. *Arch. Protistenk.* 90, 1–68.

Carvalho, W. F., and Granéli, E. (2010). Contribution of phagotrophy versus autotrophy to *Prymnesium parvum* growth under nitrogen and phosphorus sufficiency and deficiency. *Harmful Algae* 9, 105–115. doi: 10.1016/j.hal.2009.08.007

Flynn, K. J., Stoecker, D. K., Mitra, A., Raven, J. A., Glibert, P. M., Hansen, P. J., et al. (2013). Misuse of the phytoplankton-zooplankton dichotomy: the need to assign organisms as mixotrophs within plankton functional types. *J. Plankton Res.* 35, 3–11. doi: 10.1093/plankt/fbs062

Granéli, E., Edvardsen, B., Roelke, D. L., and Hagström, J. A. (2012). The ecophysiology and bloom dynamics of *Prymnesium* spp. *Harmful Algae* 14, 260–270. doi: 10.1016/j.hal.2011.10.024

Green, J. C., Hibberd, D. J., and Pienaar, R. N. (1982). The taxonomy of *Prymnesium* (Prymnesiophyceae) including a description of a new cosmopolitan species, *P. patellifera* sp. nov., and further observations on *P. parvum* N. Carter. *Br. Phycol. J.* 17, 363–382.

Hambright, D. K., Beyer, J. E., Easton, J. D., Zamor, R. M., Easton, A. C., Hallidayschult, T. C. (2015). The niche of an invasive marine microbe in a subtropical freshwater impoundment. *ISME J.* 9, 256–264. doi: 10.1038/ismej.2014.103

Hartmann, M., Zubkov, M. V., Scanian, D. J., and Lepère, C. (2013). *In situ* interactions between photosynthetic picoeukaryotes and bacterioplankton in the Atlantic Ocean: evidence for mixotrophy. *Environ. Microbiol. Rep.* 5, 835–840. doi: 10.1111/1758-2229.12084

Jones, R. I. (1994). Mixotrophy in planktonic protists as a spectrum of nutritional strategies. *Mar. Microb. Food Webs* 8, 87–96.

Jones, R. I. (2000). Mixotrophy in planktonic protists: an overview. *Freshw. Biol.* 45, 219–226. doi: 10.1046/j.1365-2427.2000.00672.x

Kopp, C., Pernice, M., Domart-Coulon, I., Djediat, C., Spangenberg, J., Alexander, D. T. L., et al. (2013). Highly dynamic cellular-level response of symbiotic coral to a sudden increase in environmental nitrogen. *mBio* 4, e00052–e00013. doi: 10.1128/mBio.00052-13

Kopp, C., Wisztorski, M., Revel, J., Mehiri, M., Dani, V., Capron, L., et al. (2015). MALDI-MS and NanoSIMS imaging techniques to study cnidarian–dinoflagellate symbioses. *Zoology* 118, 125–131. doi: 10.1016/j.zool.2014.06.006

Lechene, C. P., Luyten, Y., McMahon, G., and Distel, D. L. (2007). Quantitative imaging of nitrogen fixation by individual bacteria within animal cells. *Science* 317, 1563–1566. doi: 10.1126/science.1145557

Leles, S., Mitra, A., Flynn, K. J., Stoecker, D. K., Hansen, P. J., Calbet, A., et al. (2017). Oceanic protists with different forms of acquired phototrophy display diverse biogeographies and abundance. *Proc. Biol. Sci.* 284:20170664. doi: 10.1098/rspb.2017.0664

Lie, A. A. Y., Liu, Z., Terrado, R., Tatters, A. O., Heidelberg, K. B., and Caron, D. C. (2017). Effect of light and prey availability on gene expression of the mixotrophic chrysophyte, *Ochromonas sp*. *BMC Genomics* 18:163. doi: 10.1186/s12864-017-3549-1

Liu, Z., Jones, A. C., Campbell, V., Hambright, K. D., Heidelberg, K., Caron, D. A. (2015a). Gene expression in the mixotrophic prymnesiophyte, *Prymnesium parvum*, responds to prey availability. *Front. Microbiol.* 6:319. doi: 10.3389/fmicb.2015.00319

Liu, Z., Jones, A. C., Campbell, V., Heidelberg, K. B., and Caron, D. A. (2016). Gene expression characterizes different nutritional strategies among three mixotrophic protists. *FEMS Microbiol. Ecol.* 92, 1–11. doi: 10.1093/femsec/fiw106

Liu, Z., Koid, A. E., Terrado, R., Campbell, V., Caron, D. A., Heidelberg, K. B. (2015b). Changes in gene expression of *Prymnesium parvum* induced by nitrogen and phosphorus limitation. *Front. Microbiol.* 6:631. doi: 10.3389/fmicb.2015.00631

Manning, S. R., and La Claire, J. W. (2010). Prymnesins: toxic metabolites of the golden alga, *prymnesium parvum* carter (Haptophyta). *Mar. Drugs* 8, 678–704. doi: 10.3390/md8030678

Matantseva, O. V., and Skarlato, S. O. (2013). Mixotrophy in microorganisms: ecological and cytophysiological aspects. *J. Evol. Biochem. Phys.* 49, 377–388. doi: 10.1134/S0022093013040014

Mitra, A., Flynn, K. J., Burkholder, J. M., Berge, T., Calbet, A., Raven, J. A., et al. (2014). The role of mixotrophic protists in the biological carbon pump. *Biogeosciences* 11, 995–1005. doi: 10.5194/bg-11-995-2014

Mitra, A., Flynn, K. J., Tillmann, U., Raven, J. A., Caron, D., Stoecker, D. K., et al. (2016). Defining planktonic protist functional groups on mechanisms for energy and nutrient acquisition: incorporation of diverse mixotrophic strategies. *Protist* 167, 106–120. doi: 10.1016/j.protis.2016.01.003

Moestrup, O. (1994). "Economic aspect of 'blooms', nuisance species, and toxins," in *The Haptophyte Algae*, eds J. C. Green and B. S. C. Leadbeater (New York, NY: Oxford University Press), 265–285.

Orphan, V. J., House, C. H., Hinrichs, K.-U., McKeegan, K. D., and DeLong, E. F. (2001). Methane-consuming Archaea revealed by directly coupled isotopic and phylogenetic analysis. *Science* 293, 484–487. doi: 10.1126/science.1061338

Polerecky, L., Adam, B., Milucka, J., Musat, N., Vagner, T., and Kuypers, M. M. (2012). Look@NanoSIMS - a tool for the analysis of nanoSIMS data in environmental microbiology. *Environ. Microbiol.* 14, 1009–1023. doi: 10.1111/j.1462-2920.2011.02681.x

Rasmussen, S. A., Meier, S., Andersen, N. G., Blossom, H. E., Duus, J. Ø., Nielsen, K. F., et al. (2016). Chemodiversity of ladder-frame prymnesin polyethers in *Prymnesium parvum*. *J. Nat. Prod.* 79, 2250–2256. doi: 10.1021/acs.jnatprod.6b00345.

Raven, J. A., Beardall, J., Flynn, K. J., and Maberly, S. C. (2009). Phagotrophy in the origins of photosynthesis in eukaryotes and as a complementary mode of nutrition in phototrophs:relation to Darwin's insectivorous plants. *J. Exp. Bot.* 60, 3975–3987. doi: 10.1093/jxb/erp282

Roelke, D. L., Barkoh, A., Brooks, B. W., Grover, J. P., Hambright, D., LaClaire, J. W. II., et al. (2016). A chronicle of a killer alga in the west: ecology, assessment, and management of *Prymnesium parvum* blooms. *Hydrobiologia* 764, 29–50. doi: 10.1007/s10750-015-2273-6

Sallenave, R. (2010). *Toxic Golden Algae (Prymnesium parvum), Circular 647*. Cooperative extension service, New Mexico State University, NM.

Sanders, R. W. (2011). Alternative nutritional strategies in protists: symposium introduction and a review of freshwater protists that combine photosynthesis and heterotrophy. *J. Euk. Microbiol.* 58, 181–184. doi: 10.1111/j.1550-7408.2011.00543.x

Sanders, R. W., and Porter, K. G. (1988). Phagotrophic phytoflagellates. *Adv. Microb. Ecol.* 10, 167–192. doi: 10.1007/978-1-4684-5409-3_5

Stoecker, D. K., Hansen, P. J., Caron, D. A., and Mitra, A. (2017). Mixotrophy in the marine plankton. *Ann. Rev. Mar. Sci.* 9, 331–335. doi: 10.1146/annurev-marine-010816-060617

Sunda, W. G., Granelli, E., and Gobler, C. J. (2006). Positive feedback and the development and persistence of ecosystem disruptive algal blooms. *J. Phycol.* 42, 963–974. doi: 10.1111/j.1529-8817.2006.00261.x

Tai, V., Carpenter, K. J., Weber, P. K., Nalepa, C. A., Perlman, S. J., Keeling, P. J. (2016). Genome evolution and nitrogen fixation in bacterial ectosymbionts of a protist inhabiting wood-feeding cockroaches. *Appl. Environ. Microbiol.* 82, 4682–4695. doi: 10.1128/AEM.00611-16

Terrado, R., Pasulka, A. L., Lie, A. A., Orphan, V. J., Heidelberg, K. B., Caron, D. A. (2017). Autotrophic and heterotrophic acquisition of carbon and nitrogen by a mixotrophic chrysophyte. *ISME J.* 11, 2022–2034. doi: 10.1038/ismej.2017.68

Tillmann, U. (2003). Kill and eat your predator: a winning strategy of the planktonic flagellate *Prymnesium parvum*. *Aquat. Microgiol. J.* 32, 73–84. doi: 10.3354/ame032073

Ward, B. A., and Follows, M. J. (2016). Marine mixotrophy increases trophic transfer efficiency, mean organism size, and vertical carbon flux. *Proc. Nat. Acad. Sci. U.S.A.* 113, 2958–2963. doi: 10.1073/pnas.1517118113

Yoon, H. S., Hackett, J. D., Pinto, G., and Bhattacharya, D. (2002). The single, ancient origin of chromist plastids. *Proc. Natl. Acad. Sci. U.S.A.* 99, 15507–15512. doi: 10.1073/pnas.242379899

Conflict of Interest Statement: The authors declare that the research was conducted in the absence of any commercial or financial relationships that could be construed as a potential conflict of interest.

frontiers in Marine Science

ORIGINAL RESEARCH
published: 25 July 2018
doi: 10.3389/fmars.2018.00241

High Grazing Rates on Cryptophyte Algae in Chesapeake Bay

Matthew D. Johnson[1], David J. Beaudoin[1], Miguel J. Frada[2], Emily F. Brownlee[3] and Diane K. Stoecker[3]*

[1] Woods Hole Oceanographic Institution, Woods Hole, MA, United States, [2] Interuniversity Institute for Marine Sciences in Eilat, Alexander Silberman Institute of Life Sciences, Hebrew University of Jerusalem, Eilat, Israel, [3] Horn Point Laboratory, University of Maryland Center for Environmental Science, Cambridge, MD, United States

Cryptophyte algae are globally distributed photosynthetic flagellates found in freshwater, estuarine, and neritic ecosystems. While cryptophytes can be highly abundant and are consumed by a wide variety of protistan predators, few studies have sought to quantify *in situ* grazing rates on their populations. Here we show that autumnal grazing rates on *in situ* communities of cryptophyte algae in Chesapeake Bay are high throughout the system, while growth rates, particularly in the lower bay, were low. Analysis of the genetic diversity of cryptophyte populations within dilution experiments suggests that microzooplankton may be selectively grazing the fastest-growing members of the population, which were generally *Teleaulax* spp. We also demonstrate that potential grazing rates of ciliates and dinoflagellates on fluorescently labeled (FL) *Rhodomonas salina, Storeatula major*, and *Teleaulax amphioxeia* can be high (up to 149 prey predator^{-1} d^{-1}), and that a *Gyrodinium* sp. and *Mesodinium rubrum* could be selective grazers. Potential grazing was highest for heterotrophic dinoflagellates, but due to its abundance, *M. rubrum* also had a high overall impact. This study reveals that cryptophyte algae in Chesapeake Bay can experience extremely high grazing pressure from phagotrophic protists, and that this grazing likely shapes their community diversity.

Keywords: cryptophytes, mixotrophy, grazing, Chesapeake Bay, dinoflagellates, *Mesodinium rubrum*

OPEN ACCESS

Edited by:
Stelios Katsanevakis, University of the Aegean, Greece

Reviewed by:
Kalle Olli, University of Tartu, Estonia
Sai Elangovan S, National Institute of Oceanography (CSIR), India
George B. McManus, University of Connecticut Groton, United States

****Correspondence:***
Matthew D. Johnson
mattjohnson@whoi.edu

Specialty section:
This article was submitted to Marine Ecosystem Ecology, a section of the journal Frontiers in Marine Science

Received: *27 March 2018*
Accepted: *25 June 2018*
Published: *25 July 2018*

Citation:
Johnson MD, Beaudoin DJ, Frada MJ, Brownlee EF and Stoecker DK (2018) High Grazing Rates on Cryptophyte Algae in Chesapeake Bay. Front. Mar. Sci. 5:241. doi: 10.3389/fmars.2018.00241

INTRODUCTION

Cryptophyte algae are predominantly a photosynthetic lineage of flagellated protists in aquatic ecosystems (Mallin et al., 1991; Gervais, 1997; Marshall et al., 2005), capable of thriving in turbid and low light environments due to their highly efficient green light harvesting phycobiliproteins (Spear-Bernstein and Miller, 1989). Several species have been shown to use dissolved organic carbon (DOC) to supplement their growth requirements (Lewitus et al., 1991; Lewitus and Kana, 1995; Gervais, 1997), while others, particularly in freshwater and polar habitats, ingest bacterial prey (Marshall and Laybourn-Parry, 2002; Yoo et al., 2017). Collectively, these traits allow cryptophytes to thrive in diverse environmental conditions.

Cryptophyte algae are either preferred or optimal prey for numerous protist and mesozooplankton grazers. Most non-constitutive mixotrophic (i.e., acquired phototrophic or kleptoplastidic) dinoflagellates selectively graze on cryptophytes for their plastids, in both marine (Larsen, 1988; Skovgaard, 1998) and freshwater (Fields and Rhodes, 1991; Onuma and Horiguchi, 2016) environments. Many constitutively mixotrophic (i.e., phagotrophic phototrophs) and heterotrophic dinoflagellates have also been shown to selectively graze cryptophyte algae (Li et al., 1999; Jeong et al., 2007; Johnson, 2015). Numerous studies have also demonstrated that

heterotrophic and mixotrophic ciliates are important grazers of cryptophyte algae (Stoecker and Silver, 1990; Jakobsen and Hansen, 1997; Weisse and Kirchhoff, 1997). Several studies have also shown that certain mesozooplankton grazers may also selectively graze cryptophyte algae (Liu et al., 2010; Tõnno et al., 2016).

In Chesapeake Bay the cryptophyte pigment alloxanthin peaks within the southern Bay during autumn, but is present throughout the Bay year-round (Adolf et al., 2006). High concentrations of cryptophyte algae are commonly found in many of the tidal regions of Chesapeake Bay tributaries (Marshall et al., 2005), and are sometimes associated with blooms of the organelle stealing ciliate *Mesodinium rubrum* (Johnson et al., 2013) or the mixotrophic dinoflagellate *Karlodinium veneficum* (Li et al., 2000; Adolf et al., 2008). While cryptophytes are known to be ecologically important in estuarine ecosystems, few studies have directly measured their *in situ* growth rates or grazing pressure on their populations. Here we provide estimates of growth and grazing rates of *in situ* cryptophyte communities, the effects of grazing on community diversity, as well as potential loss rates on fluorescently labeled cryptophyte prey added to natural samples.

METHODS

Study Sites, Sampling, and Sample Processing

All research occurred within the main stem of Chesapeake Bay and three of its tributaries (**Table 1**, **Figure 1**). In Chesapeake Bay and the Potomac River, all sampling was conducted during October 2011 on the R/V Sharp. Otherwise tributary sampling was conducted from small boats and occurred in the Choptank River in April 2012 and in the Pocomoke River during May, June, and October 2001–2002 (**Table 1**). Station sampling within the main stem of Chesapeake Bay and the Potomac River was conducted during a cruise that surveyed much of the Bay system, and is part of a series of long-term monitoring locations visited in previous studies (Johnson et al., 2003).

Water was collected from Chesapeake Bay and Potomac River stations at 1 m depth from R/V Sharp using Niskin bottles attached to a rosette equipped with a CTD probe (Seabird 911 plus, conductivity, temperature and density). Water was kept in carboys within a flow-through incubator until used for "on-deck" experiments. From the Choptank River, water was obtained from 1 m depth, using a small boat and a single Niskin bottle affixed to a CTD probe cage. Surface water was collected from the Pocomoke River using small boats and a bucket. Water collected using small boats was stored in carboys on deck or in bottles in coolers until returned to the lab for experiments.

Dilution Experiments

Dilution experiments were used to measure *in situ* cryptophyte community growth (μ) and mortality (g) rates due to grazing by microzooplankton. Pre-screened ($<200\,\mu m$) whole seawater (WSW), containing phytoplankton and microzooplankton, was prepared by gently passing water through a $200\,\mu m$ mesh filter and particle free filtered seawater (FSW) was prepared by filtering water through Pall $0.2\,\mu m$ vented sterile filter capsule. A three-point dilution method was used to create 100, 20, and 5% WSW, diluted with FSW, and all treatments were measured in triplicate bottles (Landry, 1993). All dilution bottles were incubated on deck at *in situ* surface temperature and at ∼50% surface irradiance. Sampling for enumeration of cryptophytes and assessment of cryptophyte diversity was conducted at time 0 and 24 h. Cryptophyte populations from dilution experiments were counted using a BD Accuri C6 flow cytometer equipped with a 488 nm laser. Cryptophyte cells were differentiated based on their autofluorescence properties using bivariate scatter plots of orange (585/40 nm emission filter) for high phycoerythrin and red fluorescence (>670 nm emission filter) for chlorophyll against side scatter. Cultures of the cryptophytes *Teleaulax amphioxeia* (strain GCEP01), *Storeatula major* (strain SM), and *Rhodomonas salina* (strain Q) were used as standards for

TABLE 1 | Station locations, conditions, and experiments conducted.

System	Date	Station	Latitude	Longitude	Sal (PSU)	Temp (°C)	Experiment
Chesapeake Bay	10/17/11	845	38.749667	−76.433167	6.7	18.8	DIL
Chesapeake Bay	10/17/11	834	38.567333	−76.433500	7.1	19.1	DIL
Chesapeake Bay	10/19/11	724	37.400667	−76.082500	19.8	19.3	DIL
Choptank River	4/24/12	S13	38.682000	−75.970000	3.8	16.4	FLC
Choptank River	4/24/12	S11	38.611000	−75.982333	6.3	16	FLC
Choptank River	Various	HPLD	38.593333	−76.128833	NA	NA	FLC
James River	10/19/11	JR6	37.030000	−76.523500	6.7	18.8	DIL
Potomac River	5/1/11	P5	38.03266	−76.38696	6.5	16	FLC
Potomac River	5/1/11	P34	38.03266	−76.38696	3	17.7	FLC
Potomac River	5/1/11	P8	38.07154	−76.47446	6.5	16.5	FLC
Pocomoke River	Various	Poc1	37.985833*	−75.632833*	5*	NA	FLC
Pocomoke River	Various	Poc2	37.961759*	−75.667818*	10*	NA	FLC

*DIL, dilution experiment; FLC, fluorescently labeled cryptophyte experiment; NA, not available; *Approximate value.*

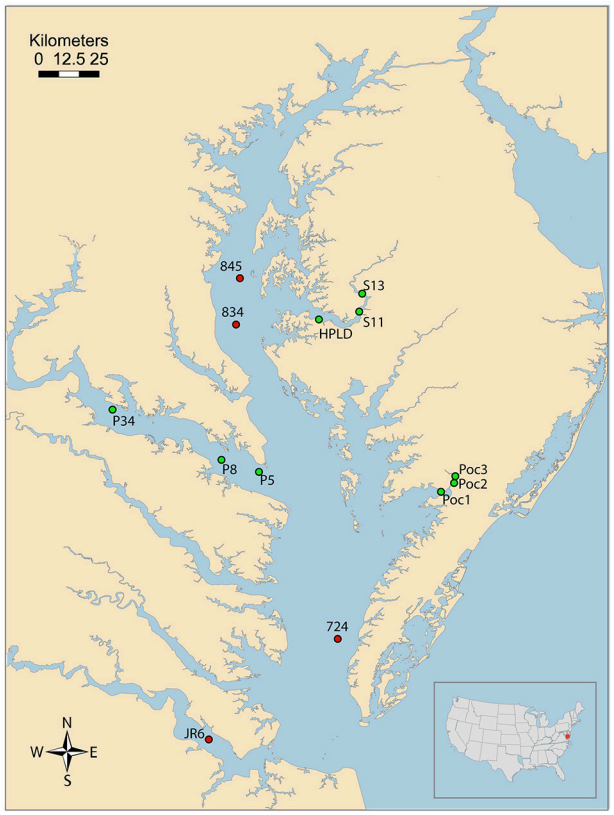

FIGURE 1 | Map of Chesapeake Bay Ecosystem with approximate location of all sampling stations. Stations where dilution experiments were performed are marked with a red circle and experiments where fluorescently labeled cryptophytes were used are marked with a green circle. Map edited from original source: Saxby, T. and Boicourt, K., Integration and Application Network, University of Maryland Center for Environmental Science (ian.umces.edu/imagelibrary/).

establishing "ballpark" settings for assessing field populations. However, the acquisition gates used on the flow cytometer did not exactly correspond to these species. The *T. amphioxeia* culture was almost exclusively in gate G3 (97%), while *R. salina* and *S. major* cultures were in gates G1 (19 and 26%) and G2 (81 and 74%).

Genetic Diversity of Cryptophyte Community Within Dilution Experiments

DNA was extracted from filter-collected samples using the DNeasy Plant Mini Kit (Qiagen) following the manufacturer's recommendations. Ribulose-1,5-bisphosphate carboxylase oxygenase (RuBisCO) gene fragments were PCR amplified from DNA extracts using the cryptophyte plastid-targeting primers L2F (Hoef-Emden, 2005) and crypt_rbcLR2 (Johnson et al., 2016). PCR conditions were: 95°C for 5 min followed by 40 cycles of 95°C for 60 s, 55°C for 60 s, and 72°C for 90 s followed by 72°C for 7 min. PCR products were visualized by agarose gel electrophoresis and later excised and purified from the gels using the Zymoclean Gel DNA Recovery Kit (Zymo Research). Clone libraries were constructed from gel purified fragments using the pGEM-T Easy Vector in the pGEM-T Easy Vector System II cloning kit (Promega Corporation) according to the manufacturer's protocol. A clone library was constructed for each sample and time point used in this study. For each library, ∼45 clones were submitted for Sanger sequencing with a single primer to the W.M. Keck Ecological and Evolutionary Genetics Facility at the MBL as directed. Sequences were edited and assembled into contigs using Sequencher (Gene Codes Corporation). All sequence data were submitted to Genbank (NCBI) under accession numbers MH488130-MH488710.

Grazing on Fluorescently Labeled Cryptophytes

Cultures of the cryptophytes *R. salina*, *Stoeratula major*, and *T. amphioxeia* were grown in F/2-Si media at 15, 10, and 5 PSU salinity, in order to have a range of options for field conditions in Chesapeake Bay. All cultures were grown at 18–20°C and in 14:10 L:D and maintained in log growth phase during field experiments. In order to stain cryptophytes for grazing experiments, a final concentration of 2 μg ml^{-1} proflavine was added to 10–20 ml of cryptophyte culture and cells were allowed to take up the dye for 30 min in darkness. Proflavine is a protein stain that is typically not used for labeling living cells, however, it has been used previously on *Isochrysis galbana* (Dupuy et al., 1999) and marine ciliates (Vincent and Hartmann, 2001) with no short-term mortality. Proflavine was used to stain cryptophyte algae after failed attempts to stain them with Cell-Tracker Green CMFDA (5-chloromethylfluorescein diacetate), a more commonly employed stain (Li et al., 1996). Stained cells were then added to a 15 ml 25 mm diameter glass tower with a 2.0 μm polycarbonate (PC) filter membrane and attached to a side arm flask. Using gentle pressure applied to a hand pump, culture media was slowly removed over 20–30 min, until cells were concentrated down to 2-3 ml. After concentrating the cells, they were washed with F/2-Si media by returning cells to their original volume, and the concentrating and wash step was repeated. When finished, cells were observed live under a dissecting microscope to verify that they were still motile. A small aliquot was then preserved with 1% glutaraldehyde and after 15 min filtered onto a 2 μm PC membrane filter and observed with a Zeiss Axio Scope A1 fluorescence microscope using an excitation BP filter of 450–490 nm in order to verify they were sufficiently stained with proflavine, as well as to count the stock culture. Success of this method depended greatly on how carefully the cells could be concentrated and washed, and the failure rate of the procedure was close to 20%. However, the protocol was considered successful when cryptophyte prey remained motile and all cells were apparently fluorescently stained.

Stained cryptophyte cells were added to Chesapeake Bay or tributary water samples at a final concentration of between ∼1,000 and 10,000 cells ml^{-1}. In most cases these concentrations were substantially higher than *in situ* levels of cryptophytes and likely resulted in estimates of saturated grazing rates. Therefore, these estimates of potential grazing rates are probably akin to

maximum rates (but see discussion). Samples were first screened with a 200 μm mesh in order to remove copepods and other mesozooplankton. Samples (10 ml) were taken and preserved with glutaraldehyde, at time 0, 10, 20, 40, and 120 min, as well as 24 h and stored at 4°C in darkness until filtered (5 ml) onto a PC membrane as described above, and mounted on a glass microscope slide as described previously (Johnson et al., 2013). All species of protist that were observed to have ingested fluorescently labeled cryptophytes (FLC) were counted across all time points and instantaneous ingestion rates (IIR) were determined by taking the slope of ingested FLC cell^{-1} vs. time in hours, and multiply by 24 for prey cells ingested grazer^{-1} day^{-1}. Clearance rates were calculated using the formula $C = IIR/N_{prey}$, where N_{prey} is the concentration of FLC (Rublee and Gallegos, 1989).

Statistical Analysis

Differences in growth and grazing rates across different experiments were determined using a one-way ANOVA, and comparisons between treatments were clarified using a Tukey HSD test. All statistics were calculated using the R statistical function "AOV" (R Core Team, 2013).

RESULTS

In Situ Growth and Grazing Rates of Cryptophyte Algae

During a cruise in October 2011 we ran dilution experiments in Chesapeake Bay, and measured dynamics of cryptophyte populations within the experiments using flow cytometry. At each station 2–3 subpopulations of cryptophytes could be discerned using flow cytometry and analyzing forward scatter and orange fluorescence (i.e., phycoerythrin) as well as orange vs. red fluorescence. Growth and grazing rates on these cryptophyte subpopulations varied greatly both within and between stations. Growth rates of *in situ* populations of cryptophytes were higher in the upper Bay (mean: 0.47 d^{-1}) than in the lower Bay and the mouth of the James River Estuary (mean: 0.13 d^{-1}). Grazing rates on cryptophytes were generally high, exceeding combined population growth rates at all stations (**Table 2**). Only 2 of the 12 subpopulations analyzed in these experiments had positive net population growth, G1 at station 845 and G3 at 834. In the lower Bay and James River station, grazing was 3.2–10.3x (mean: 6.5x) that of growth rates, while in the upper Bay it was 0.3–3.6x (mean: 1.9) greater (**Table 2**).

Except for *M. rubrum*-like ciliates, potential grazers were not counted at every station where dilution experiments were performed. The concentration of *M. rubrum* at stations 845, 834, and 724 were 7.7, 23.1, and 3.8 cells ml^{-1}, respectively. Cell counts for microzooplankton groups that may have been potential grazers of cryptophytes were only made for one lower and one upper Chesapeake Bay station, which was similar to the location of stations 724 and 845/834, respectively. In lower Chesapeake Bay, potential grazers included oligotrich ciliates at 3.1 cells ml^{-1}, tintinnid ciliates at 6.6 cells ml^{-1}, and naked heterotrophic dinoflagellates (NHD) at 1.2 cells ml^{-1}. The upper Chesapeake Bay station had 1.9 tintinnids ml^{-1}, 8.1 oligotrichs ml^{-1}, and 26 NHDs ml^{-1}. Counts of tintinnid and oligotrich ciliates only included cells >30 μm.

Impact of Grazing on Cryptophyte Diversity

The impact of grazing on cryptophyte community diversity was assessed from dilution experiments at 4 stations during a cruise in October, by clone library sequencing of cryptophyte 18S rDNA

TABLE 2 | Population-specific apparent growth and grazing rates for cryptophyte algae during dilution experiments in Chesapeake Bay.

Station	Date	Population	Cells ml^{-1}	Growth (d^{-1})	Grazing (d^{-1})	Net
845	10/17/11	G1	564	0.97 (0.32)	0.30 (0.37)	0.67
		G2	1108	0.46 (0.17)	1.39 (0.20)	−0.94
		G3	1005	0.55 (0.22)	1.42 (0.03)	−0.87
		Total	2779	0.60 (0.01)	1.17 (0.28)	−0.57
834	10/17/11	G1	673	−0.18 (0.41)	0.65 (0.52)	−0.82
		G2	418	0.97 (0.15)	1.06 (0.20)	−0.09
		G3	582	0.48 (0.12)	0.35 (0.08)	0.13
		Total	1755	0.34 (0.16)	0.65 (0.08)	−0.31
724	10/19/11	G2	899	0.14 (0.50)	1.42 (0.99)	−1.28
		G3	1937	0.12 (0.35)	0.73 (0.23)	−0.62
		G4	2626	0.39 (0.35)	1.25 (0.10)	−0.86
		Total	5221	0.25 (0.09)	1.09 (0.21)	−0.84
J6	10/19/11	G1	53	−0.07 (0.38)	0.72 (0.52)	−0.79
		G2	315	−0.39 (0.06)	1.76 (0.36)	−2.15
		G3	289	0.47 (0.43)	2.16 (0.84)	−1.69
		Total	656	0.01 (0.20)	1.85 (0.49)	−1.84

Size of cryptophyte cells decreases with increasing population (G) number.

amplicons. The cryptophyte clone libraries were dominated by *Teleaulax* spp. (72%), followed by *Rhodomonas* spp. (17%) and *Hemiselmis* spp. (11%). A *Teleaulax gracilis* phylotype was one of the largest constituents (34.5% of clones) of the cryptophyte communities measured in this study and increased with dilution at all stations (**Figure 2**). A phylotype of *T. amphioxeia* was also a dominant species within the clone libraries (32% of all clones), but only revealed increases in the 20% whole seawater dilution at 3 of the stations, and not in 5% dilution treatments (**Figure 2**). In the upper and mid Bay stations (845, 834), *Rhodomonas* spp. were a major component of clone libraries, but were nearly absent from lower Bay samples. At both the upper and mid-bay stations, a *Rhodomonas* sp. phylotype also revealed increases with dilution, consistent with net growth following the dilution of grazing pressure. No data are available for cryptophyte diversity for the 5% dilution at station 845 because no samples were taken for DNA.

Grazing on Fluorescently Labeled Cryptophytes

In order to estimate potential grazing rates of protistan predators on specific cryptophyte algae, we tracked the ingestion of fluorescently labeled prey added to natural samples in three Chesapeake tributaries (**Tables 3–5**). The mixotrophic ciliate *M. rubrum* was the most persistent grazer of fluorescently labeled (FL) cryptophytes (**Figure 3**), being present in all samples, and sometimes at high concentrations (**Table 3**). Within the Pocomoke River experiments ($n = 14$), only grazing by *M. rubrum* was enumerated, and only *R. salina* was used as prey. The highest ingestion rates for *M. rubrum* were observed for *T. amphioxeia* prey (5.4–18.3 prey pred^{-1} d^{-1}), with grazing on *S. major* and *R. salina* being lower (0.17–6.53 prey pred^{-1} d^{-1}). Grazing by *M. rubrum* on FL *R. salina* and *S. major* was statistically lower than on *T. amphioxeia* [ANOVA, $F_{(2, 19)} = 7.85$, $p = 0.003$; **Figure 4A**]. Potential grazing impact on cryptophyte populations by *M. rubrum* alone, a function of both ingestion rate and abundance, varied across all experiments from consumption of 0.14–25.8% of the population d^{-1}.

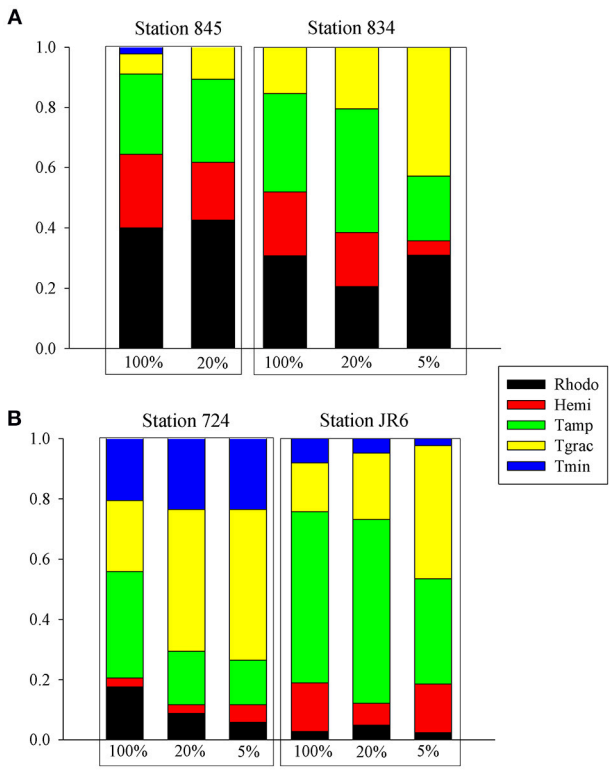

FIGURE 2 | Genetic diversity of cryptophytes in dilution experiments during October 2011 in Chesapeake Bay. Dilution experiment treatment is shown on the x-axis, % clone library composition on the y-axis. **(A)** Results for Stations 845 and 834; **(B)** Results for stations 724 and James River station 6. Rhodo: *Rhodomonas* sp., Hemi: *Hemiselmis* sp., Tamp: *Teleaulax amphioxeia*; Tgrac: *T. gracilis*; Tmin: *T. minuta*.

Grazing on cryptophytes was also documented for various heterotrophic and mixotrophic dinoflagellates. In an experiment within the Potomac River grazing was assessed on all three cryptophyte species, while only *T. amphioxeia* was used in two experiments in the Choptank River. Ingestion rates by dinoflagellates were high, averaging 28 prey pred^{-1} d^{-1} across all dinoflagellate and prey types. Highest grazing rates on cryptophytes were by heterotrophic species (**Table 4**, **Figure 4A**), however, many dinoflagellate species did not ingest cryptophytes during experiments. Generally only small or medium (20–40 μm) naked heterotrophic species and small plastid-containing mixotrophic dinoflagellates were observed to graze cryptophytes. High ingestion rates were measured for both *Prorocentrum cordatum (=P. minimum)* on *T. amphioxeia* prey and for a *Karlodinum veneficum*-like mixotrophic dinoflagellate (referred to hereafter as "*K. veneficum*") on all three species (**Table 4**). Grazing by these mixotrophic dinoflagellates was high in the Choptank River at station S11, which was downriver from a small *P. cordatum* bloom (6,900 cells ml^{-1}) at station S13. No grazing was observed by *P. cordatum* on labeled cryptophytes from within the bloom at S13. For one location we measured grazing on multiple cryptophyte cultures, and therefore could determine if certain prey species are grazed more than others. At station P8 in the Potomac River, no differences were observed for grazing rates on three cryptophyte prey species by the mixotroph "*K. veneficum*" or the heterotrophs *O. marina* and an unidentified naked heterotrophic dinoflagellate, while the heterotrophic *Gyrodinium* sp. had significantly lower grazing on *T. amphioxeia* compared to the other two species [ANOVA, $F_{(2, 3)} = 39.68$, $p = 0.007$; HSD $P < 0.05$; **Figure 4A**]. The overall potential grazing impact on cryptophyte populations by dinoflagellates varied between 0.7 and 15.5% of any one species of labeled cryptophytes d^{-1}.

Since we evaluated relatively small volumes of water for estimating potential ingestion rates, only species that were present at high abundances could be measured. Thus, grazing rates were obtained for only two heterotrophic ciliate species. Both a *Eutintinnus* sp. and an unidentified heterotrophic oligotrich ciliate were found to ingest *T. amphioxeia* at two stations in the Choptank River, and ingestion rates for both ciliate species were high. The heterotrophic oligotrich ciliate had the

TABLE 3 | Grazing rates of *Mesodinium rubrum* (MR)-like ciliates in Chesapeake Bay Tributaries on fluorescently labeled (FL) cryptophyte algae.

Date	Station	FL-Prey	FL-prey Cells ml^{-1}	MR Cells ml^{-1}	FL-prey: MR (ratio)	MR* counted	IR cells MR-$^{-1}$ d^{-1}	C µl MR^{-1} d^{-1}	GP % pop d^{-1}
POCOMOKE RIVER									
5/20/02	Poc2	*R. salina*	1,550	106	14.6	212	3.28 (1.12)	2.12 (0.72)	22.4
5/20/02	Poc1	*R. salina*	1,226	17.9	68.6	71.5	3.24 (1.02)	2.64 (0.84)	4.72
10/10/01	Poc2	*R. salina*	1,192	75.9	15.8	152	0.47 (0.04)	0.39 (0.04)	2.98
10/10/01	Poc1	*R. salina*	1,036	1551	0.67	163	0.17 (0.03)	0.17 (0.03)	25.8
5/28/02	Poc2	*R. salina*	4,223	27.6	153	110	6.53 (0.35)	1.55 (0.08)	4.26
6/26/02	Poc3	*R. salina*	2,128	99.7	21.3	199	0.98 (0.26)	0.46 (0.12)	4.56
6/26/02	Poc2	*R. salina*	2,062	31.6	65.2	63.3	1.93 (0.58)	0.94 (0.28)	2.97
CHOPTANK RIVER									
5/24/02	13	*R. salina*	3,848	14.2	271	56.9	1.55 (1.58)	0.40 (0.41)	0.57
9/7/02	HPLD	*R. salina*	3,059	5.28	579	26.4	0.79 (1.10)	0.26 (0.36)	0.14
9/7/02	HPLP	*R. salina*	2,417	17.2	140	86.1	1.66 (0.56)	0.69 (0.23)	1.18
9/25/02	HPLD	*R. salina*	1,345	16.6	81.2	82.8	0.39 (0.00)	0.29 (0.00)	0.48
9/25/02	HPLP	*R. salina*	958	12.7	75.6	63.3	0.73 (0.41)	0.77 (0.43)	0.97
9/23/02	HPLD	*R. salina*	730	12.8	56.9	64.1	0.64 (0.21)	0.88 (0.28)	1.12
9/23/02	HPLP	*R. salina*	1,085	20.1	52.6	100	0.68 (0.01)	0.64 (0.01)	1.28
4/24/12	S13	*T. amphioxeia*	10,000	29.3	341.3	87.4	5.4 (0.11)	0.54 (0.01)	1.82
4/24/12	S11	*T. amphioxeia*	10,000	15.8	632.9	47.3	4.61 (0.74)	0.46 (0.07)	0.85
4/25/12	S13	*T. amphioxeia*	10,000	39.0	256.4	57.3	18.3 (2.5)	1.83 (0.25)	8.41
POTOMAC RIVER									
5/1/11	P5	*S, major*	10,000	4.3	2325	22.6	BD	BD	BD
5/1/11	P5	*T. amphioxeia*	10,000	–	–	–	BD	BD	BD
5/1/11	P8	*S, major*	10,000	4.0	2484	10.1	BD	BD	BD
5/1/11	P8	*T. amphioxeia*	10,000	–	–	–	BD	BD	BD
5/1/11	P34	*S, major*	10,000	31	328	147	2.79 (0.82)	0.28 (0.08)	0.83
5/1/11	P34	*T. amphioxeia*	10,000	–	–	–	8.5 (0.12)	0.85 (0.01)	2.59

All numbers are means with standard deviations in parentheses; MR, average number of cells counted during experiment across all samples; IR, ingestion rate; C, Clearance rate; GP, Grazing potential; pop, population (labeled cryptophytes); BD, below detection.*

highest grazing rate of any species observed, at 149 ± 20 prey pred^{-1} d^{-1}. Potential impact on *T. amphioxeia* populations for these ciliates varied from 1.3 to 4.2% of the population d^{-1}.

DISCUSSION

While numerous laboratory studies have demonstrated that cryptophyte algae are consumed at high rates by a variety of heterotrophic and mixotrophic protists (Jeong et al., 2005; Lewitus et al., 2006; Adolf et al., 2008), fewer studies have sought to document their grazing losses *in situ*. Cryptophytes are abundant in coastal marine and estuarine ecosystems (Mallin et al., 1991; Jeong et al., 2013; Johnson et al., 2013), and while they may form blooms (Laza-Martínez, 2012; Šupraha et al., 2014), such events are rare and generally short lived. More typically, cryptophytes form multiple seasonal peaks of sustained abundance, but remain in the planktonic community year round (Mallin et al., 1991; Adolf et al., 2006). Here we provide evidence that *in situ* grazing pressure on cryptophyte algae is high in Chesapeake Bay, and that variability among cryptophyte species in growth rates and susceptibility to grazing may help explain their persistence within the plankton.

In Situ Growth and Grazing Rates

Several previous studies using the dilution technique coupled with either flow cytometry (Paterson et al., 2008) or quantitative pigment analyses (Burkill et al., 1987; McManus and Ederington-Cantrell, 1992; Suzuki et al., 1998; Lie and Wong, 2010) have also measured growth and grazing rates on *in situ* cryptophyte populations. The use of quantitative pigment analysis to monitor *in situ* population dynamics can be problematic due to regulatory changes in cellular pigment levels during experiments (e.g., photoacclimation) as well as incorrect assignment of pigments to taxonomic groups. In the case of the carotenoid alloxanthin, one cannot differentiate between cryptophyte algae *per se* and protists that steal their plastids (e.g., *M. rubrum*), which can be abundant in estuarine and coastal ecosystems (Stoecker et al., 2009). Despite these caveats, such studies are valuable for their potential to estimate group-specific *in situ* population dynamics. Previous studies that have traced the concentration of alloxanthin within dilution experiments suggest that cryptophyte algal populations are dynamic, with high growth and grazing rates. In one such study using mesocosm enclosures within Saanich Inlet, Canada, alloxanthin-based estimates of cryptophyte growth were >1.0 (max 1.7) d^{-1} and grazing >0.5 (max 0.9) d^{-1} during the first 4

TABLE 4 | Grazing rates of dinoflagellates (DINO) in Chesapeake Bay Tributaries on the fluorescently labeled (FL) cryptophytes *Storeatula major*, *Rhodomonas salina*, and *Teleaulax amphioxeia*.

Grazer	Prey	DINO (cells/ml)	FL-prey: DINO (ratio)	DINO* counted	IR cells DINO $^{-1}$ d^{-1}	C µl DINO $^{-1}$ d^{-1}	GP % pop d^{-1}
POTOMAC RIVER, 5/1/11, STATION P8							
Gyro	*S. major*	27.8	360	63.4 (13.7)	36.6 (8.37)	3.66 (0.84)	9.66
	R. salina				58.6 (3.19)	5.86 (0.32)	15.5
	T. amphioxeia				9.9 (2.91)	0.99 (0.29)	2.62
Omar	*S. major*	32.5	308	67.1 (19.3)	6.1 (1.83)	0.61 (0.18)	1.95
	R. salina				3.1 (0.65)	0.31 (0.07)	0.98
	T. amphioxeia				2.2 (2.93)	0.22 (0.29)	0.70
Kvene	*S. major*	12.3	813	30.4 (6.2)	23.1 (4.88)	2.31 (0.48)	2.63
	R. salina				15.0 (3.80)	1.50 (0.38)	1.71
	T. amphioxeia				26.1 (5.97)	2.61 (0.60)	2.97
NHD	*S. major*	7.5	1333	15.5 (6.4)	40.8 (7.26)	4.08 (0.73)	3.59
	R. salina				67.3 (13.6)	6.73 (1.36)	5.93
	T. amphioxeia				67.8 (46.6)	6.78 (4.66)	5.97
CHOPTANK RIVER, 4/24/12, STATION S11							
Pcord	*T. amphioxeia*	30.6	327	103 (18.4)	23.7 (0.1)	2.37 (0.01)	7.23
Kvene	*T. amphioxeia*	9.8	1020	29.5 (2.1)	13.8 (1.0)	1.38 (0.10)	1.35

Prey was added at 10,000 cells ml^{-1}; DINO* is the average dinoflagellate concentration during experiment across all samples; IR, ingestion rate; C, clearance rate; GP, grazing potential; pop, population (labeled cryptophytes); Gyro, Gyrodinium sp.; Omar, Oxyrrhis marina; Kvene, Karlodinium veneficum; NHD, naked heterotrophic dinoflagellate; Pcord, Prorocentrum cordatum.

TABLE 5 | Grazing rates of heterotrophic ciliates in the Choptank River on fluorescently labeled (FL) *Teleaulax amphioxeia*.

Date	Site	Ciliate	Ciliate* (cells/ml)	FL-prey: Ciliate (ratio)	Ciliates counted	IR cells ciliate^{-1} d^{-1}	C µl ciliate^{-1} d^{-1}	GP % pop d^{-1}
4/25/12	S13	Unid. tintinnid	5.3	1875	9.28 (3.45)	26.4 (4.1)	2.64 (0.41)	1.34
4/24/12	S11	*Eutintinnus* sp.	5.0	2000	15.0 (3.65)	67.1 (18.0)	6.7(1.8)	3.35
4/24/12	S11	Oligotrich	2.8	3529	9.50 (1.29)	149 (20.3)	14.9 (2.0)	4.17

Prey was added at 10,000 cells ml^{-1}; Ciliate is the average ciliate concentration during experiment across all samples; IR, ingestion rate; C, clearance rate; GP, grazing potential; pop, population (labeled cryptophytes).*

days of the experiment (Suzuki et al., 2002). In contrast, another study found that microzooplankton within the coastal seas of Eastern Hong Kong selectively grazed alloxanthin-containing populations, with grazing rates 1–45 times that of growth rates (Lie and Wong, 2010). In a Western Australia study that also measured growth and grazing rates using flow cytometry with dilution experiments, the percent of cryptophyte production grazed varied seasonally and over 3 sites between ∼30 and 120% (Paterson et al., 2008).

In Chesapeake Bay, one study found high growth (1.22–2.23 d^{-1}) and grazing (1.08–1.22 d^{-1}) rates based on alloxanthin during spring, becoming lower in August (with net population loss), with both rates becoming negligible during fall (McManus and Ederington-Cantrell, 1992). In our study growth rates of cryptophyte populations measured using flow cytometry during October revealed moderate rates in the upper Bay with net population loss due to grazing, and very low growth rates in the Southern Bay and James River that were greatly exceeded by grazing rates. The James River population had the highest concentrations of *M. rubrum*-like ciliates encountered during the October Chesapeake Bay cruise (Supplemental Table 1). Such high differences between measurements of growth and grazing rates of a phytoplankton population is not uncommon in dilution experiments, and suggests a decoupling of these processes. In an estuarine or productive coastal environment grazing responses may be greater at times, due to higher standing stocks of microzooplankton from greater overall ecosystem productivity and biomass (Calbet and Landry, 2004). Previous studies have shown that cryptophyte populations in Chesapeake Bay peak in fall (McManus and Ederington-Cantrell, 1992), and that blooms of diatoms or cryptophytes appear to alternate within the southern regions (Adolf et al., 2006). Our measurements appear to capture a period of demise for rich cryptophyte populations in these regions, with growth rates being low or negative and decoupled from intense grazing pressure.

The Effects of Grazing on Cryptophyte Community Diversity

Relatively little is known regarding the genetic diversity of cryptophyte algae in marine ecosystems. Several studies

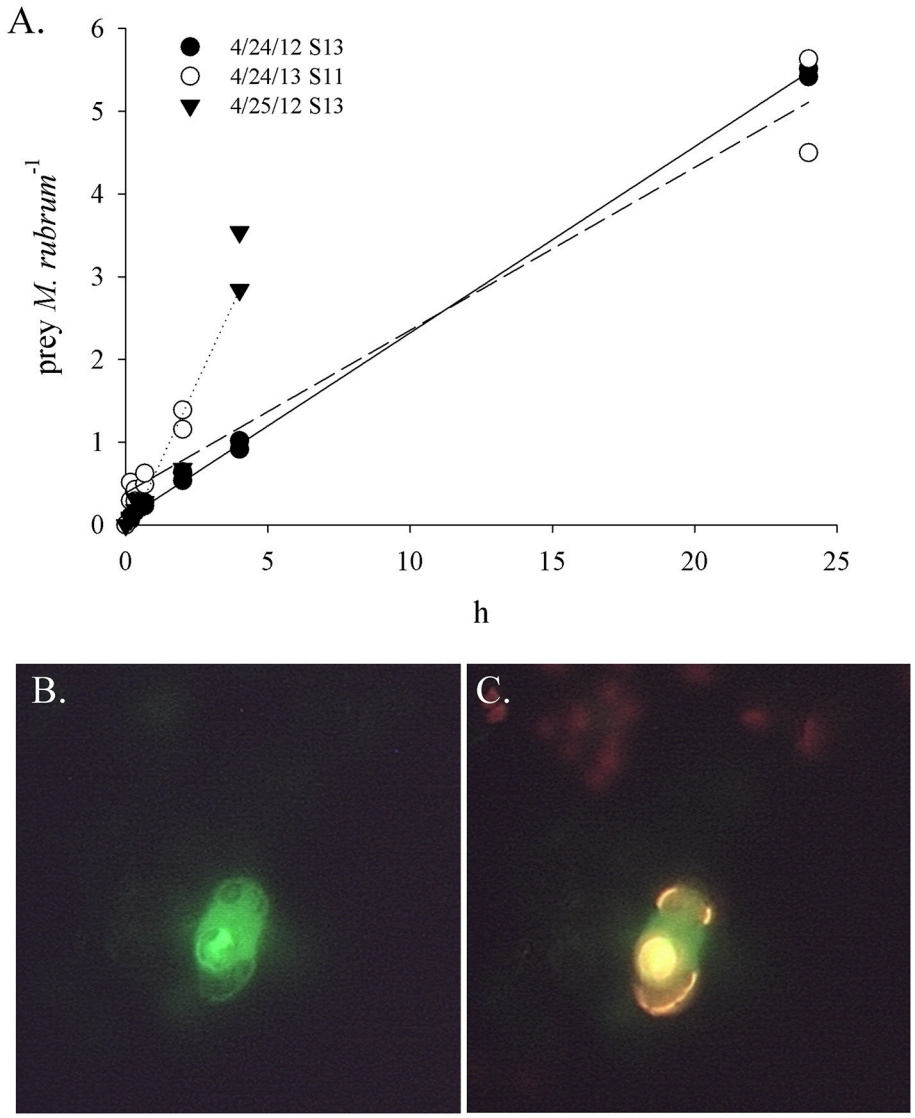

FIGURE 3 | Ingestion of fluorescently labeled cryptophytes (FLC) by *Mesodinium rubrum* in the Choptank River. **(A)** Examples of ingested FL *Teleaulax amphioxeia* over time. Regression equations for each experiment are as follows: 4/24/12 station 13, $y = 0.225x + 0.072$, $R^2 = 0.999$; 4/24/12 station 11, $y = 0.567x + 0.160$, $R^2 = 0.908$; 4/25/12 station 13, $y = 0.748x + 0.156$, $R^2 = 0.888$; **(B)** An *M. rubrum* cell with an ingested FL *Rhodomonas salina* under green emission (BP 515–565 nm); **(C)** Same *M. rubrum* cell as in **(B)** with an ingested FL *R. salina* under a dichromatic long pass emission (>515 nm).

using microscopy or molecular approaches have found that *Teleaulax*/*Plagioselmis*/*Geminigera* (TPG) and *Hemiselmis* cryptophytes are abundant in marine ecosystems (Hill et al., 1992; Cerino and Zingone, 2007; Metfies et al., 2010; Johnson et al., 2016; Luo et al., 2016). However, these studies are somewhat limited in scope due to their regional specificity. While the study of Johnson et al. (2016) included a broad geographic sampling for cryptophyte genetic diversity, many of the samples were from red tides of the ciliate *M. rubrum* and therefore were likely skewed toward *Teleaulax*-dominated communities. While the present study doesn't provide a comprehensive assessment of cryptophyte diversity in Chesapeake Bay, it reveals relative changes in genetic diversity of their communities when grazers are diluted. In this study *Teleaulax* cryptophytes were dominant in the Southern Bay and James River, comprised about 50% of the population in the middle Bay (834), and were between 35 and 40% in the upper Bay (845). During every experiment, a *T. gracilis* phylotype increased in response to dilution, suggesting that grazing pressure on this species is high. However, interpreting the observed dynamics of other taxa in these experiments was more complicated. In experiments at stations 834 and JR6, we observed increases in *T. amphioxeia* only at 20% dilution, but a decline in the proportion of this phylotype within the clone library at 5%. This result suggests that as grazing pressure is diluted, species with higher growth rates are better able to capitalize and grow (e.g., *T. gracilis*). At station

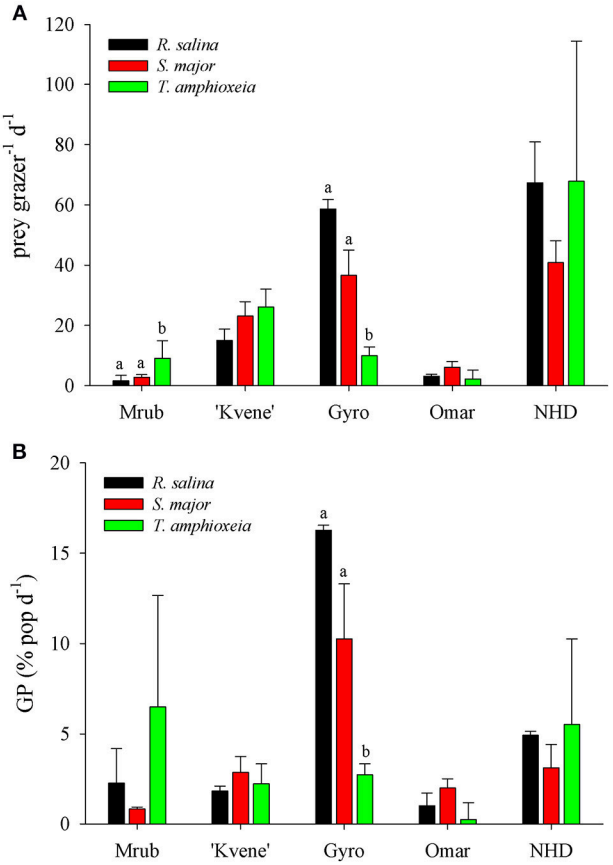

FIGURE 4 | Grazing by phagotrophic protists on three species of cryptophytes. **(A)** Ingestion rates (IR) of *Mesodinium rubrum* (Mrub), a *Karlodinium veneficum*-like dinoflagellate ("Kvene"), a *Gyrodinium* sp. (Gyro), *Oxyrrhis marina* (Omar), and an unidentified naked heterotrophic dinoflagellate (NHD) on *Rhodomonas salina*, *Storeatula major* and *Teleaulax amphioxeia*. **(B)** Grazing potential (GP) on cryptophyte populations. Same information as in **(A)**. Significant differences between IR and GP on different prey indicated by letters.

845 a phylotype of *Rhodomonas* sp. increased with dilution, suggesting that it too had high grazing pressure and *in situ* growth rates. *Rhodomonas* tends to be larger than many other marine cryptophyte species (Johnson, 2015) and station 845 was the only sample where the largest population of cryptophytes measured by flow cytometry had the highest growth rate (**Table 2**). Our observations of changes in cryptophyte diversity in response to protistan predation is not surprising, as selection or preference for certain species has been observed among various mixotrophs. Acquired phototrophic predators such as *M. rubrum* (Park et al., 2007; Hansen et al., 2012; Peltomaa and Johnson, 2017), *M. chamaeleon* (Moeller and Johnson, 2017), and the dinoflagellate *Nusuttodinium aeruginosum* (Onuma and Horiguchi, 2016) have all been shown to select certain cryptophyte species as prey and/or selectively retain plastids from certain species. Selective grazing on cryptophyte species by constitutive mixotrophic protists, i.e., that possess their own plastids (Mitra et al., 2016), is more rare, but has been demonstrated in the dinoflagellate *P. cordatum* (Johnson, 2015). Other mixotrophic dinoflagellates, such as *K. veneficum*, are known to graze on a variety of cryptophytes (Adolf et al., 2008). Less is known regarding selective grazing by heterotrophic protists on cryptophytes.

Grazing on Fluorescently Labeled Cryptophytes

The majority of our grazing experiments using fluorescently labeled prey were conducted using 10,000 cells ml^{-1}, which is at or near saturating levels of cryptophyte prey for most protist grazers. Saturation of ingestion rate varies with predator type and concentration, but in general dinoflagellates have lower saturation levels then ciliates, occurring in the mixotrophic *Prorocentrum donghaiense* around 5,000 cells ml^{-1} (Jeong et al., 2005) and in a small heterotrophic *Gyrodinium* sp. at around 2,000 cells ml^{-1} (Jakobsen and Hansen, 1997) when feeding on cryptophytes. For the ciliate *M. rubrum* saturation of ingestion rate when feeding on *T. amphioxeia* occurred in a Danish strain (variant F) between 3,000 and 7,000 cells ml^{-1} (Smith and Hansen, 2007), while in a Chesapeake Bay strain (Variant G) it occurred between 5,000 and 7,000 cells ml^{-1} (Peltomaa and Johnson, 2017). In contrast ingestion rate of the medium sized mixotrophic oligotrich ciliate, *Strombidium rassoulzadegani*, saturated around 15,000 cells ml^{-1} when fed *Rhodomonas lens* (Schoener and McManus, 2012). While many of our experiments using *R. salina* prey to measure grazing by *M. rubrum* were probably below concentrations (i.e., 730–4,223 cells ml^{-1}) that would have saturated grazing using *T. amphioxeia* as prey, its functional response to *Rhodomonas* spp. has not been determined.

Another important consideration when adding labeled prey to natural assemblages is the concentration of similar species preexisting within the community. Unfortunately we do not have cell count data for cryptophytes within these samples prior to adding labeled prey, but the mean and range concentrations of cryptophytes observed in Chesapeake Bay are 1,432 and 15,720 cells ml^{-1}, respectively (Johnson et al., 2013).

Previous studies have measured high potential grazing rates by mixotrophic dinoflagellates on cryptophyte algae added to natural samples in Chesapeake Bay (Li et al., 1996), and many cultured mixotrophic dinoflagellates have also been shown to have high grazing rates for cryptophytes (Jeong et al., 2005; Adolf et al., 2008). In Chesapeake Bay, both *K. veneficum* and *P. cordatum* have been observed to possess phycoerythrin-containing food vacuoles (Li et al., 1996, 2000, 2001; Stoecker et al., 1997). Predation on cryptophyte populations in Chesapeake Bay is thought to play an important role in bloom initiation of *K. veneficum* due to the stimulation of its growth rate by mixotrophy (Adolf et al., 2008). Mixotrophic grazing by a *P. cordatum* culture isolated from the James River region of Chesapeake Bay was induced under N and P limitation and was almost exclusively limited to ingestion of the cryptophyte *T. amphioxeia* (Johnson, 2015). Consistent with these previous studies, here we found that both "*K. veneficum*" and *P. cordatum* ingested *T. amphioxeia* prey at high rates while "*K. veneficum*" also readily ingested *R. salina* and *S. major*.

In our samples, heterotrophic dinoflagellates were the greatest consumers of labeled cryptophyte prey, due to both their high abundance and ingestion rates (**Figure 4B**). Small (∼20–25 μm) naked heterotrophic dinoflagellates (e.g., *Amphidinium* sp., *Gyrodinium, Oxyrrhis, Pfiesteria*) are known to graze voraciously upon cryptophyte algae (Jakobsen and Hansen, 1997; Strom et al., 1998; Eriksen et al., 2002; Jeong et al., 2010), in addition to other prey. In this study, small naked heterotrophic dinoflagellates, consistent in size and shape with *Gyrodinium* sp., were observed to consume large quantities of *R. salina* and *S. major*, but not *T. amphioxeia*. A microcosm study of natural communities from the Southern Ocean rich in cryptophyte algae also found that cryptophytes are consumed at high rates by heterotrophic *Gyrodinium*-like dinoflagellates (Bjørnsen and Kuparinen, 1991). While we found *O. marina*-like cells consumed fluorescently labeled cryptophytes, their rates were lower than co-occurring mixotrophic and other heterotrophic dinoflagellates. Previous studies on cultures of *O. marina* suggest that it prefers to ingest slightly larger prey than cryptophytes, such as raphidophytes and dinoflagellates (Jeong et al., 2003, 2010).

The highest cell-specific grazing rates that we observed were by large heterotrophic ciliates, including two tintinnid species and an oligotrich. While the grazing rate of the oligotrich ciliate was extremely high, it was comparable to previous rates measured for other large species grazing on cryptophytes (Müller and Schlegel, 1999). In contrast, maximum ingestion rates of *S. rassoulzadegani* on *R. lens* were ∼10 cells ciliate^{-1} d^{-1}, (Schoener and McManus, 2012). While this was an order of magnitude lower than our observed rate for an unidentified oligotrich species (**Table 5**), the species that we observed was larger than *S. rassoulzadegani* (not shown). The mixotrophic oligotrich ciliate *Laboea strobila* is known to ingest and steal plastids from cryptophyte prey (Stoecker et al., 1988), and natural populations of the ciliate have been reported to have predominantly cryptophyte plastids (McManus and Fuhrman, 1986).

Acquired phototrophs, or non-constitutive mixotrophs (NCMs), which steal plastids from algal prey, are one of the main consumers of cryptophyte algae in marine ecosystems (Stoecker et al., 2009). In particular *M. rubrum* and *M. major* are known to selectively graze cryptophytes from the *Teleaulax/Plagioselmis/Geminigera* (TPG) group (Park et al., 2007; Myung et al., 2011; Hansen et al., 2012; Peltomaa and Johnson, 2017). In the Columbian River Estuary, *M. rubrum/major* have been observed to rapidly ingest large quantities of cryptophytes by "gathering" prey cells in their feeding tentacles and possibly their cirri as well as cytoplasmic protrusions from their oral region (Peterson et al., 2013). This novel observation needs to be validated under laboratory conditions in order to determine the mechanism of this unusual feeding behavior. Garcia-Cuetos et al. (2012) observed a "medusa" form of *M. major* that had cytoplasmic projections from its oral regions, and a similar phenotype has been observed in blooms from the Southampton estuary (Crawford, 1993), however feeding events were not observed. We observed the highest grazing rates by *Mesodinium* spp. on *T. amphioxeia*, however, moderate grazing rates were also observed on *R. salina* and *S. major* in several experiments (**Table 3**). While previous studies have demonstrated that *M. rubrum* will ingest non-*Teleaulax/Geminigera/Plagioselmis* (TGP) cryptophytes (Myung et al., 2011; Hansen et al., 2012), these species have not been shown to support sustained growth. One recent study that used an *M. rubrum* isolate from the James River in Chesapeake Bay, found that the ciliate ingested and sequestered plastids from *T. acuta* and *T. amphioxeia* equally, but found no evidence for ingesting *S. major* (Peltomaa and Johnson, 2017). This result contrasts with our observations of *in situ* populations of *M. rubrum* ingesting fluorescently labeled *S. major*. Our average grazing rates measured for *M. rubrum* on *T. amphioxeia* in this study (9.3 prey MR^{-1} d^{-1}) were consistent with rates measured previously for a culture from the James River (10–13 prey MR^{-1} d^{-1}) (Peltomaa and Johnson, 2017). In comparison, the average grazing rates on *R. salina* and *S. major* for *M. rubrum* in Chesapeake Bay were about an order of magnitude lower, both only 1.65 prey MR^{-1} d^{-1}. While *M. rubrum* had lower ingestion rates on non-*Teleaulax* cryptophytes, our experiments demonstrated that it could still have a profound effect on cryptophyte populations (**Table 3**, **Figure 4B**). In two cases, the potential impact on cryptophyte populations was >20% of the population d^{-1}, caused in one case by elevated *M. rubrum* concentrations and ingestion rates, and in another case by low ingestion rates but very high ciliate concentrations (**Table 3**). These data suggest that when *M. rubrum* is abundant, they may clear cryptophyte populations, even if they are not their preferred TGP prey. Causes of variation observed here in grazing rates by *M. rubrum* on fluorescently labeled cryptophytes obviously depend upon the prey species offered, however other factors such as feeding history, the variant(s) of *M. rubrum* present, and the makeup and abundance of *in situ* cryptophyte populations are other possible sources.

CONCLUSIONS

Our findings demonstrate that cryptophyte populations in Chesapeake Bay are heterogeneous in their species composition, cell size, and growth rates, and experience high *in situ* grazing pressure. During October 2011 in Chesapeake Bay, cryptophyte populations had high grazing pressure due to protistan predators throughout the system, but the impact was particularly severe in the southern regions where growth rates were very low. Our experiments using fluorescently labeled cryptophyte prey, which were conducted primarily during spring, demonstrated high species-specific grazing rates for various dinoflagellates and ciliates that sometimes varied with prey species. The combined potential impact of various grazers on fluorescently labeled cryptophytes ranged between 19 and 50% of the population d^{-1}, which was lower than our community loss rates estimated from dilution experiments for cryptophyte populations (44–313% d^{-1}). However, direct comparisons between methods are problematic since the experiments were run in different seasons and locations and conducted over different time scales. Further, not all grazers of fluorescently labeled cryptophytes were enumerated, since many predators were at concentrations that were too low to include. Future experiments

with fluorescently labeled cryptophytes could be improved by processing larger fixed sample volumes for cell counts. In summary, our findings are the first to demonstrate species-specific selection of cryptophyte prey by natural communities of protist grazers. Observed changes in cryptophyte diversity in dilution experiments combined with high ingestion rates on labeled *T. amphioxeia*, suggest that *Teleaulax* cryptophytes generally dominate this ecosystem, possess high growth rates, and are heavily grazed. These results help to explain why certain mixotrophs that select *Teleaulax* as prey, such as *M. rubrum* and *P. cordatum*, are able to maintain high abundance within coastal ecosystems. Further, since heterotrophic protists in our labeled cryptophyte experiments showed either no preference for *T. amphioxeia* or grazed them at lower rates, competition with these mixotrophic predators for cryptophyte prey may be somewhat alleviated, thus facilitating overlapping niches for phagotrophic protists.

AUTHOR CONTRIBUTIONS

MJ designed and performed experiments, analyzed data, and wrote the manuscript. DB and MF helped with experiments, sample analysis, and in preparing the manuscript. EB helped with experiments and in preparing the manuscript. DS helped in designing and performing experiments, analyzing data, and in preparing the manuscript.

FUNDING

The authors thank the National Science Foundation (OCE 1031718 and 1436169) for providing support for this research.

ACKNOWLEDGMENTS

The authors would like to thank the captain and crew of the R/V Hugh R. Sharp for their assistance and support during our cruises in May and October of 2011. We also thank Drs. Don Anderson and Mengmeng Tong for kindly providing *T. amphioxeia* culture GCEP01.

SUPPLEMENTARY MATERIAL

The Supplementary Material for this article can be found online at: https://www.frontiersin.org/articles/10.3389/fmars.2018.00241/full#supplementary-material

REFERENCES

Adolf, J., Yeager, C. L., Miller, W. D., Mallonee, M., and Harding, L. Jr. (2006). Environmental forcing of phytoplankton floral composition, biomass, and primary productivity in Chesapeake Bay, USA. *Estuar. Coast. Shelf Sci.* 67, 108–122. doi: 10.1016/j.ecss.2005.11.030

Adolf, J. E., Bachvaroff, T., and Place, A. R. (2008). Can cryptophyte abundance trigger toxic *Karlodinium veneficum* blooms in eutrophic estuaries? *Harmful Algae* 8, 119–128. doi: 10.1016/j.hal.2008.08.003

Bjørnsen, P., and Kuparinen, J. (1991). Growth and herbivory by heterotrophic dinoflagellates in the Southern Ocean, studied by microcosm experiments. *Mar. Biol.* 109, 397–405. doi: 10.1007/BF01313505

Burkill, P., Mantoura, R., Llewellyn, C., and Owens, N. (1987). Microzooplankton grazing and selectivity of phytoplankton in coastal waters. *Mar. Biol.* 93, 581–590. doi: 10.1007/BF00392796

Calbet, A., and Landry, M. R. (2004). Phytoplankton growth, microzooplankton grazing, and carbon cycling in marine systems. *Limnol. Oceanogr.* 49, 51–57. doi: 10.4319/lo.2004.49.1.0051

Cerino, F., and Zingone, A. (2007). "Decrypting cryptomonads: a challenge for molecular taxonomy," in *Unravelling the Algae: the Past, Present, and Future of Algal Systematics,* eds J. Brodie and J. Lewis (Boca Raton, FL: CRC Press), 197–214. doi: 10.1201/9780849379901.ch11

Crawford, D. W. (1993). Some observations on morphological variation in the red-water ciliate *Mesodinium rubrum*. *J. Mar. Biol. Assoc. U.K.* 73, 975–978. doi: 10.1017/S002531540003486X

Dupuy, C., Le Gall, S., Hartmann, H. J., and Bréret, M. (1999). Retention of ciliates and flagellates by the oyster *Crassostrea gigas* in French Atlantic coastal ponds: protists as a trophic link between bacterioplankton and benthic suspension-feeders. *Mar. Ecol. Prog. Ser.* 177, 165–175. doi: 10.3354/meps177165

Eriksen, N. T., Hayes, K. C., and Lewitus, A. J. (2002). Growth responses of the mixotrophic dinoflagellates, *Cryptoperidiniopsis* sp. and *Pfiesteria piscicida,* to light under prey-saturated conditions. *Harmful Algae* 1, 191–203. doi: 10.1016/S1568-9883(02)00011-2

Fields, S. D., and Rhodes, R. G. (1991). Ingestion and retention of *Chroomonas* spp. (Cryptophyceae) by *Gymnodinium acidotum* (Dinophyceae). *J. Phycol.* 27, 525–529. doi: 10.1111/j.0022-3646.1991.00525.x

Garcia-Cuetos, L., Moestrup, Ø., and Hansen, P. J. (2012). Studies on the genus Mesodinium II. Ultrastructural and molecular investigations of five marine species help clarifying the taxonomy. *J. Eukaryot. Microbiol.* 59, 374–400. doi: 10.1111/j.1550-7408.2012.00630.x

Gervais, F. (1997). Light-dependent growth, dark survival, and glucose uptake by cryptophytes isolated from a freshwater chemocline. *J. Phycol.* 33, 18–25. doi: 10.1111/j.0022-3646.1997.00018.x

Hansen, P. J., Moldrup, M., Tarangkoon, W., Garcia-Cuetos, L., and Moestrup, Ø. (2012). Direct evidence for symbiont sequestration in the marine red tide ciliate *Mesodinium rubrum*. *Aquat. Microb. Ecol.* 66, 63–75. doi: 10.3354/ame01559

Hill, D. R., Moestrup, Ø., and Vørs, N. (1992). "Rekylalger (Cryptophyceae)," in *Plankton i de Indre Danske Farvande*, ed H. A. Thompson (Havforskning fra Miljøstyrelsen), 251–265.

Hoef-Emden, K. (2005). Multiple independent losses of photosynthesis and differing evolutionaryrates in the genus *Cryptomonas* (Cryptophyceae): combined phylogenetic analyses of DNA sequences of the nuclear and the nucleomorph ribosomal operons. *J. Mol. Evol.* 60, 183–195. doi: 10.1007/s00239-004-0089-5

Jakobsen, H. H., and Hansen, P. J. (1997). Prey size selection, grazing and growth response of the small heterotrophic dinoflagellate *Gymnodinium* sp. and the ciliate Balanion comatum—a comparative study. *Mar. Ecol. Prog. Ser.* 158, 75–86.

Jeong, H., Yoo, Y., Kim, J., Seong, K., Kang, N., and Kim, T. (2010). Growth, feeding and ecological roles of the mixotrophic and heterotrophic dinoflagellates in marine planktonic food webs. *Ocean Sci. J.* 45, 65–91. doi: 10.1007/s12601-010-0007-2

Jeong, H. J., Du Yoo, Y., Lee, K. H., Kim, T. H., Seong, K. A., Kang, N. S., et al. (2013). Red tides in Masan Bay, Korea in 2004–2005: I. Daily variations in the abundance of red-tide organisms and environmental factors. *Harmful Algae* 30, S75–S88. doi: 10.1016/j.hal.2013.10.008

Jeong, H. J., Ha, J. H., Yoo, Y. D., Park, J. Y., Kim, J. H., Kang, N. S., et al. (2007). Feeding by the *Pfiesteria*-like heterotrophic dinoflagellate *Luciella masanensis*. *J. Eukaryot. Microbiol.* 54, 231–241. doi: 10.1111/j.1550-7408.2007.00259.x

Jeong, H. J., Kim, J. S., Yoo, Y. D., Kim, S. T., Kim, T. H., Park, M. G., et al. (2003). Feeding by the heterotrophic dinoflagellate *Oxyrrhis marina* on the red-tide raphidophyte *Heterosigma akashiwo*: a potential biological method to control

red tides using mass-cultured grazers. *J. Eukaryot. Microbiol.* 50, 274–282. doi: 10.1111/j.1550-7408.2003.tb00134.x

Jeong, H. J., Yoo, Y. D., Park, J. Y., Song, J. Y., Kim, S. T., Lee, S. H., et al. (2005). Feeding by phototrophic red-tide dinoflagellates: five species newly revealed and six species previously known to be mixotrophic. *Aquat. Microb. Ecol.* 40, 133–150. doi: 10.3354/ame040133

Johnson, M., Rome, M., and Stoecker, D. (2003). Microzooplankton grazing on *Prorocentrum minimum* and *Karlodinium micrum* in Chesapeake Bay. *Limnol. Oceanogr.* 48, 238–248. doi: 10.4319/lo.2003.48.1.0238

Johnson, M. D. (2015). Inducible mixotrophy in the dinoflagellate Prorocentrum minimum. *J. Eukaryot. Microbiol.* 62, 431–443. doi: 10.1111/jeu.12198

Johnson, M. D., Beaudoin, D. J., Laza-Martinez, A., Dyhrman, S. T., Fensin, E., Lin, S., et al. (2016). The genetic diversity of *Mesodinium* and associated cryptophytes. *Front. Microbiol.* 7:2017. doi: 10.3389/fmicb.2016.02017

Johnson, M. D., Stoecker, D. K., and Marshall, H. G. (2013). Seasonal dynamics of *Mesodinium rubrum* in Chesapeake Bay. *J. Plankton Res.* 35, 877–893. doi: 10.1093/plankt/fbt028

Landry, M. (1993). *Estimating Rates of Growth and Grazing Mortality of Phytoplankton by the Dilution Method*. Boca Raton, FL: Lewis Publishers.

Larsen, J. (1988). An ultrastructural-study of *Amphidinium poecilochroum* (Dinophyceae), a phagotrophic dinoflagellate feeding on small species of cryptophytes. *Phycologia* 27, 366–377. doi: 10.2216/i0031-8884-27-3-366.1

Laza-Martínez, A. (2012). *Urgorri complanatus* gen. et sp. nov.(cryptophyceae), a red-tide-forming species in brackish waters. *J. Phycol.* 48, 423–435. doi: 10.1111/j.1529-8817.2012.01130.x

Lewitus, A. J., Caron, D. A., and Miller, K. R. (1991). Effects of light and glycerol on the organization of the photsyntehtic apparatus in the faculatative heterotroph *Pyrenomonas salina* (cryptophyceae).1. *J. Phycol.* 27, 578–587. doi: 10.1111/j.0022-3646.1991.00578.x

Lewitus, A. J., and Kana, T. M. (1995). Light respiration in six estuarine phytoplankton species: contrasts under photoautotrophic and mixotrophic growth conditions. *J. Phycol.* 31, 754–761. doi: 10.1111/j.0022-3646.1995.00754.x

Lewitus, A. J., Wetz, M. S., Willis, B. M., Burkholder, J. M., Parrow, M. W., and Glasgow, H. B. (2006). Grazing activity of *Pfiesteria piscicida* (Dinophyceae) and susceptibility to ciliate predation vary with toxicity status. *Harmful Algae* 5, 427–434. doi: 10.1016/j.hal.2006.04.012

Li, A., Stoecker, D. K., and Adolf, J. E. (1999). Feeding, pigmentation, photosynthesis and growth of the mixotrophic dinoflagellate *Gyrodinium galatheanum*. *Aquat. Microb. Ecol.* 19, 163–176. doi: 10.3354/ame019163

Li, A., Stoecker, D. K., and Coats, D. W. (2000). Spatial and temporal aspects of *Gyrodinium galatheanum* in Chesapeake Bay: distribution and mixotrophy. *J. Plankton Res.* 22, 2105–2124. doi: 10.1093/plankt/22.11.2105

Li, A., Stoecker, D. K., and Coats, D. W. (2001). Use of the 'food vacuole content' method to estimate grazing by the mixotrophic dinoflagellate *Gyrodinium galatheanum* on cryptophytes. *J. Plankton Res.* 23, 303–318. doi: 10.1093/plankt/23.3.303

Li, A., Stoecker, D. K., Coats, D. W., and Adam, E. J. (1996). Ingestion of fluorescently labeled and phycoerythrin-containing prey by mixotrophic dinoflagellates. *Aquat. Microb. Ecol.* 10, 139–147. doi: 10.3354/ame010139

Lie, A. A., and Wong, C. K. (2010). Selectivity and grazing impact of microzooplankton on phytoplankton in two subtropical semi-enclosed bays with different chlorophyll concentrations. *J. Exp. Mar. Biol. Ecol.* 390, 149–159. doi: 10.1016/j.jembe.2010.05.001

Liu, H., Chen, M., Suzuki, K., Wong, C. K., and Chen, B. (2010). Mesozooplankton selective feeding in subtropical coastal waters as revealed by HPLC pigment analysis. *Mar. Ecol. Prog. Ser.* 407, 111–123. doi: 10.3354/meps08550

Luo, W., Li, H., Gao, S., Yu, Y., Lin, L., and Zeng, Y. (2016). Molecular diversity of microbial eukaryotes in sea water from Fildes Peninsula, King George Island, Antarctica. *Polar Biol.* 39, 605–616. doi: 10.1007/s00300-015-1815-8

Mallin, M. A., Paerl, H. W., and Rudek, J. (1991). Seasonal phytoplankton composition, productivity and biomass in the Neuse River estuary, North Carolina. *Estuar. Coast. Shelf Sci.* 32, 609–623. doi: 10.1016/0272-7714(91)90078-P

Marshall, H. G., Burchardt, L., and Lacouture, R. (2005). A review of phytoplankton composition within Chesapeake Bay and its tidal estuaries. *J. Plankton Res.* 27, 1083–1102. doi: 10.1093/plankt/fbi079

Marshall, W., and Laybourn-Parry, J. (2002). The balance between photosynthesis and grazing in Antarctic mixotrophic cryptophytes during summer. *Freshw. Biol.* 47, 2060–2070. doi: 10.1046/j.1365-2427.2002.00950.x

McManus, G. B., and Ederington-Cantrell, M. C. (1992). Phytoplankton pigments and growth rates, and microzooplankton grazing in a large temperate estuary. *Mar. Ecol. Prog. Ser.* 87, 77–85. doi: 10.3354/meps087077

McManus, G. B., and Fuhrman, J. A. (1986). Photosynthetic pigments in the ciliate *Laboea strobila* from Long Island Sound, USA. *J. Plankton Res.* 8, 317–327. doi: 10.1093/plankt/8.2.317

Metfies, K., Gescher, C., Frickenhaus, S., Niestroy, R., Wichels, A., Gerdts, G., et al. (2010). Contribution of the class cryptophyceae to phytoplankton structure in the German Bight. *J. Phycol.* 46, 1152–1160. doi: 10.1111/j.1529-8817.2010.00902.x

Mitra, A., Flynn, K. J., Tillmann, U., Raven, J. A., Caron, D., Stoecker, D. K., et al. (2016). Defining planktonic protist functional groups on mechanisms for energy and nutrient acquisition: incorporation of diverse mixotrophic strategies. *Protist* 167, 106–120. doi: 10.1016/j.protis.2016.01.003

Moeller, H. V., and Johnson, M. D. (2017). Preferential plastid retention by the acquired phototroph *Mesodinium chamaeleon*. *J. Eukaryot. Microbiol.* 65, 148–158. doi: 10.1111/jeu.12446

Müller, H., and Schlegel, A. (1999). Responses of three freshwater planktonic ciliates with different feeding modes to cryptophyte and diatom prey. *Aquat. Microb. Ecol.* 17, 49–60. doi: 10.3354/ame017049

Myung, G., Kim, H. S., Park, J. S., Park, M. G., and Yih, W. (2011). Population growth and plastid type of *Myrionecta rubra* depend on the kinds of available cryptomonad prey. *Harmful Algae* 10, 536–541. doi: 10.1016/j.hal.2011.04.005

Onuma, R., and Horiguchi, T. (2016). Specificity of *Chroomonas* (Cryptophyceae) as a source of kleptochloroplast for *Nusuttodinium aeruginosum* (Dinophyceae). *Phycol. Res.* 64, 35–43. doi: 10.1111/pre.12117

Park, J. S., Myung, G., Kim, H. S., Cho, B. C., and Yih, W. (2007). Growth responses of the marine photosynthetic ciliate *Myrionecta rubra* to different cryptomonad strains. *Aquat. Microb. Ecol.* 48, 83–90. doi: 10.3354/ame048083

Paterson, H., Knott, B., Koslow, A., and Waite, A. (2008). The grazing impact of microzooplankton off south west Western Australia: as measured by the dilution technique. *J. Plankton Res.* 30, 379–392. doi: 10.1093/plankt/fbn004

Peltomaa, E., and Johnson, M. D. (2017). *Mesodinium rubrum* exhibits genus-level but not species-level cryptophyte prey selection. *Aquat. Microb. Ecol.* 78, 147–159. doi: 10.3354/ame01809

Peterson, T. D., Golda, R. L., Garcia, M. L., Li, B., Maier, M. A., Needoba, J. A., et al. (2013). Associations between *Mesodinium rubrum* and cryptophyte algae in the Columbia River estuary. *Aquat. Microb. Ecol.* 68, 117–130. doi: 10.3354/ame01598

R Core Team (2013). *R: A Language and Environment for Statistical Computing*. Vienna: R Foundation for Statistical Computing. Available online at: http://www.R-project.org/

Rublee, P. A., and Gallegos, C. L. (1989). Use of fluorescently labelled algae (FLA) to estimate microzooplankton grazing. *Mar. Ecol. Prog. Ser.* 51, 221–227. doi: 10.3354/meps051221

Schoener, D., and McManus, G. (2012). Plastid retention, use, and replacement in a kleptoplastidic ciliate. *Aquat. Microb. Ecol.* 67:177. doi: 10.3354/ame01601

Skovgaard, A. (1998). Role of chloroplast retention in a marine dinoflagellate. *Aquat. Microb. Ecol.* 15, 293–301. doi: 10.3354/ame015293

Smith, M., and Hansen, P. J. (2007). Interaction between *Mesodinium rubrum* and its prey: importance of prey concentration, irradiance and pH. *Mar. Ecol. Progr. Ser.* 338, 61–70. doi: 10.3354/meps338061

Spear-Bernstein, L., and Miller, K. R. (1989). Unique location of the phycobiliprotein light-harvesting pigment in the Cryptophyceae. *J. Phycol.* 25, 412–419. doi: 10.1111/j.1529-8817.1989.tb00245.x

Stoecker, D., Li, A., Coats, D., Gustafson, D., and Nannenl, M. (1997). Mixotrophy in the dinoflagellate *Prorocentrum minimum*. *Mar. Ecol. Prog. Ser.* 152, 1–12. doi: 10.3354/meps152001

Stoecker, D. K., Johnson, M. D., de Vargas, C., and Not, F. (2009). Acquired phototrophy in aquatic protists. *Aquat. Microb. Ecol.* 57, 279–310. doi: 10.3354/ame01340

Stoecker, D. K., and Silver, M. W. (1990). Replacement and aging of chloroplasts in *Strombidium capitatum* (Ciliophora, Oligotrichida). *Mar. Biol.* 107, 491–502. doi: 10.1007/BF01313434

Stoecker, D. K., Silver, M. W., Michaels, A. E., and Davis, L. H. (1988). Obligate mixotrophy inLaboea strobila, a ciliate which retains chloroplasts. *Mar. Biol.* 99, 415–423.

Strom, S. L., Morello, T. A., and Bright, K. J. (1998). Protozoan size influences algal pigment degradation during grazing. *Mar. Ecol. Prog. Ser.* 164, 189–197. doi: 10.3354/meps164189

Šupraha, L., Bosak, S., Ljubešić, Z., Mihanović, H., Olujić, G., Mikac, I., et al. (2014). Cryptophyte bloom in a Mediterranean estuary: high abundance of *Plagioselmis* cf. prolonga in the Krka River estuary (eastern Adriatic Sea). *Sci. Mar.* 78, 329–338. doi: 10.3989/scimar.03998.28C

Suzuki, K., Tsuda, A., Kiyosawa, H., Takeda, S., Nishioka, J., Saino, T., et al. (2002). Grazing impact of microzooplankton on a diatom bloom in a mesocosm as estimated by pigment-specific dilution technique. *J. Exp. Mar. Biol. Ecol.* 271, 99–120. doi: 10.1016/S0022-0981(02)00038-2

Suzuki, T., Yamada, N., and Taniguchi, A. (1998). Standing crops of planktonic ciliates and nanoplankton in oceanic waters of the western Pacific. *Aquat. Microb. Ecol.* 14, 49–58. doi: 10.3354/ame014049

Tõnno, I., Agasild, H., Kõiv, T., Freiberg, R., Nõges, P., and Nõges, T. (2016). Algal diet of small-bodied crustacean zooplankton in a cyanobacteria-dominated Eutrophic Lake. *PLoS ONE* 11:e0154526. doi: 10.1371/journal.pone.0154526

Vincent, D., and Hartmann, H. J. (2001). Contribution of ciliated microprotozoans and dinoflagellates to the diet of three copepod species in the Bay of Biscay. *Hydrobiologia* 443, 193–204. doi: 10.1023/A:10175028 13154

Weisse, T., and Kirchhoff, B. (1997). Feeding of the heterotrophic freshwater dinoflagellate *Peridiniopsis berolinense* on cryptophytes: analysis by flow cytometry and electronic particle counting. *Aquat. Microb. Ecol.* 12, 153–164. doi: 10.3354/ame012153

Yoo, Y. D., Seong, K. A., Jeong, H. J., Yih, W., Rho, J.-R., Nam, S. W., et al. (2017). Mixotrophy in the marine red-tide cryptophyte *Teleaulax amphioxeia* and ingestion and grazing impact of cryptophytes on natural populations of bacteria in Korean coastal waters. *Harmful Algae* 68, 105–117. doi: 10.1016/j.hal.2017.07.012

Conflict of Interest Statement: The authors declare that the research was conducted in the absence of any commercial or financial relationships that could be construed as a potential conflict of interest.

The reviewer GM declared a past co-authorship with several of the authors DS and MJ to the handling Editor.

frontiers in Marine Science

ORIGINAL RESEARCH
published: 19 June 2018
doi: 10.3389/fmars.2018.00217

Genetic Analyses of the *rbc*L and *psa*A Genes From Single Cells Demonstrate a Rhodophyte Origin of the Prey in the Toxic Benthic Dinoflagellate *Ostreopsis*

*Bora Lee and Myung G. Park**

LOHABE, Department of Oceanography, Chonnam National University, Gwangju, South Korea

OPEN ACCESS

Edited by:
Matthew D. Johnson, Woods Hole Oceanographic Institution, United States

Reviewed by:
Jelena Godrijan, Bigelow Laboratory for Ocean Sciences, United States
Punyasloke Bhadury, Indian Institute of Science Education and Research Kolkata, India

****Correspondence:***
Myung G. Park
mpark@chonnam.ac.kr

Specialty section:
This article was submitted to Marine Ecosystem Ecology, a section of the journal Frontiers in Marine Science

Received: *13 February 2018*
Accepted: *31 May 2018*
Published: *19 June 2018*

Citation:
Lee B and Park MG (2018) Genetic Analyses of the rbcL and psaA Genes From Single Cells Demonstrate a Rhodophyte Origin of the Prey in the Toxic Benthic Dinoflagellate Ostreopsis. Front. Mar. Sci. 5:217. doi: 10.3389/fmars.2018.00217

Phagotrophy of the harmful benthic dinoflagellates of the genus *Ostreopsis* has long been inferred based on observations of food particles present inside cells, but the prey has not yet been identified. This study aimed to investigate the seasonal dynamics of benthic dinoflagellates *Ostreopsis* spp. in temperate Korean coastal sites, with special emphasis on their phagotrophy. Further, prey species were identified by extracting the ingested food particles from single *Ostreopsis* cells and determining their *rbc*L and *psa*A gene sequences. High concentration of *Ostreopsis* cells was observed between June and October at all sites, when the water temperatures were higher than 19°C, exhibiting a marked temporal seasonality. The percentage of *Ostreopsis* cells containing ingested food particles exhibited large spatial and temporal variations among sampling sites, ranging from undetectable level to 29.5%, and was not always associated with *Ostreopsis* cell abundance. Phylogenetic analyses performed using both plastid-encoded *rbc*L and *psa*A genes revealed that all sequences obtained from the ingested food particles of *Ostreopsis* cells grouped within the class Florideophyceae, Rhodophyta. Our result clearly demonstrates that *Ostreopsis* species consume various macroalgae from Rhodophyta, but not protists, which have long been thought to be the potential prey. The results of this study provide a basis for better understanding the mixotrophic behavior and nutritional ecology of the harmful benthic dinoflagellate *Ostreopsis* species.

Keywords: mixotroph, phagotrophy, red algae, phylogeny, seasonality

INTRODUCTION

The genus *Ostreopsis* belonging to the family Ostreopsidaceae (Dinophyceae) has a worldwide distribution from tropical to temperate marine waters (Rhodes, 2011; Parsons et al., 2012; Accoroni and Totti, 2016). At present, the genus *Ostreopsis* includes 11 species with type species of *O. siamensis* (Schmidt, 1901; Parsons et al., 2012; Accoroni et al., 2016; Verma et al., 2016), of which

several species are known to produce toxins of the palytoxin group that could cause serious human and environmental health problems (e.g., Yasumoto et al., 1987; Ukena et al., 2001; Tichadou et al., 2010). *Ostreopsis* species have been found in various of habitats, including on macroalgae, hard substrates (e.g., rocks, sand, and mollusk shells), and in the water column (Schmidt, 1901; Faust et al., 1996; Vila et al., 2001; Laza-Martinez et al., 2011). They often occur in association with other toxic or potentially toxic benthic dinoflagellates *Gambierdiscus* spp., *Amphidinium* spp., *Prorocentrum* spp., and *Coolia monotis* (Penna et al., 2005; Aligizaki and Nikolaidis, 2006; Parsons et al., 2012).

Although great progress has been made in the study of *Ostreopsis* biology, ecology, and toxicology over the past several years, some aspects about the nutritional ecology associated with this genus still remain unclear. For example, Faust and her colleagues (Faust and Morton, 1995; Faust et al., 1996; Faust, 1998) reported reddish round inclusions inside *Ostreopsis* cells collected in Belize through light microscopic observations and speculated that they were the ingested prey that might originate from cyanobacteria, centric diatoms, ciliates, and small microalgae, although the feeding behavior was not reported. Since then, some studies (e.g., Aligizaki and Nikolaidis, 2006; Selina and Orlova, 2010; Accoroni et al., 2014) also observed the presence of red bodies in *Ostreopsis* cells collected in field samples, and Fraga et al. (2012) suggested that the presence of these red bodies might be related to the mixotrophic behavior of *Ostreopsis* species. Very recently, Almada et al. (2017) also reported that only a small percentage (0.4%) of *O.* cf. *ovata* cells in Brazil showed evidence of phagotrophy by using epifluorescence microscopy with DAPI and LysoSensor staining, although the prey inside the cells were not discernible.

The present study aimed to investigate the seasonal dynamics of the benthic dinoflagellates *Ostreopsis* spp.in temperate Korean coastal waters, with special emphasis on their phagotrophy. To further identify the prey, the ingested food particles were extracted from single *Ostreopsis* cells and their *rbc*L and *psa*A genes sequences were determined. These chloroplast-encoded genes have often been used to identify food particles inside protists such as dinoflagellates and ciliates (e.g., Hackett et al., 2003; McManus et al., 2004; Nishitani et al., 2010; Kim et al., 2012; Fawcett and Parrow, 2014). For example, McManus et al. (2004) found through *rbc*L gene sequencing from chloroplasts found in the marine ciliates *Strombidium oculatum* and *S. stylifer* that the ciliates ingest ulvaceous green macroalgal swarmers and retain their chloroplasts. The *psb*A gene has also been applied to infer the origin and diversity of chloroplasts found in the mixotrophic dinoflagellate *Dinophysis* (e.g., Hackett et al., 2003; Nishitani et al., 2010; Kim et al., 2012). Thus, the application of these chloroplast-encoded gene sequences on red bodies found in *Ostreopsis* would be expected to provide a clue about the identity of prey.

MATERIALS AND METHODS

Sampling and Sample Treatment

Macroalgal samples were collected monthly from August 2016 to December 2017 during low tide from 4 sites on the Korean

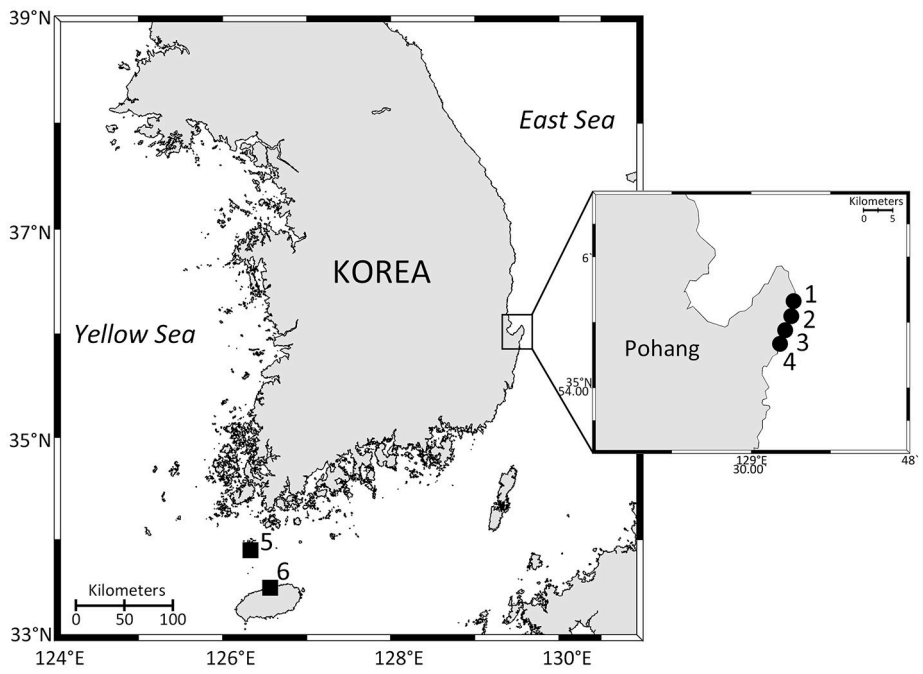

FIGURE 1 | Map of the study area showing the sampling sites. 1, Gangsa; 2, Samjeong; 3, Guryongpo; 4, Hajeong; 5, Chuja Island; 6, Jeju harbor. Closed circles are monitoring sites. Closed squares are sites where additional *Ostreopsis* cells were isolated from the concentrated planktonic samples.

TABLE 1 | Summary of sampling sites, dates, and plastid genes sequenced for the ingested food particles within *Ostreopsis* cells isolated from field samples during this study.

Sampling site	Date	Species	Abbreviation	*rbc*L	*psa*A
Samjeong	June-09-2017	*Ostreopsis* sp.	OSsj0609-1	+	+
		Ostreopsis sp.	OSsj0609-2	+	+
		Ostreopsis sp.	OSsj0609-3	+	
		Ostreopsis sp.	OSsj0609-4	+	+
		Ostreopsis sp.	OSsj0609-7	+	+
		Ostreopsis sp.	OSsj0609-23		+
		Ostreopsis sp.	OSsj0609-24	+	+
		Ostreopsis sp.	OSsj0609-33	+	+
	July-05-2017	*Ostreopsis* sp.	OSsj0705-20	+	+
		Ostreopsis sp.	OSsj0705-22	+	+
	August-31-2017	*Ostreopsis* sp.	OSsj0831-2		+
		Ostreopsis sp.	OSsj0831-5	+	
		Ostreopsis sp.	OSsj0831-10		+
		Ostreopsis sp.	OSsj0831-14	+	
		Ostreopsis sp.	OSsj0831-15	+	
		Ostreopsis sp.	OSsj0831-16		+
		Ostreopsis sp.	OSsj0831-20	+	
	November-3-2017	*Ostreopsis* sp.	OSsj1103-1	+	+
		Ostreopsis sp.	OSsj1103-2		+
		Ostreopsis sp.	OSsj1103-3	+	+
		Ostreopsis sp.	OSsj1103-4	+	
		Ostreopsis sp.	OSsj1103-5	+	+
		Ostreopsis sp.	OSsj1103-6	+	
		Ostreopsis sp.	OSsj1103-7	+	+
		Ostreopsis sp.	OSsj1103-8	+	
		Ostreopsis sp.	OSsj1103-9	+	+
		Ostreopsis sp.	OSsj1103-10	+	+
		Ostreopsis sp.	OSsj1103-11	+	+
		Ostreopsis sp.	OSsj1103-12	+	+
Guryongpo	October-21-2017	*Ostreopsis* sp.	OSgp1021-2	+	
		Ostreopsis sp.	OSgp1021-3	+	
		Ostreopsis sp.	OSgp1021-6	+	
		Ostreopsis sp.	OSgp1021-16	+	
Hajeong	June-09-2017	*Ostreopsis* sp.	OShj0609-12	+	+
		Ostreopsis sp.	OShj0609-14	+	+
	July-05-2017	*Ostreopsis* sp.	OShj0705-2	+	+
		Ostreopsis sp.	OShj0705-3	+	+
		Ostreopsis sp.	OShj0705-5	+	+
		Ostreopsis sp.	OShj0705-7	+	+
		Ostreopsis sp.	OShj0705-8	+	+
		Ostreopsis sp.	OShj0705-10	+	+
		Ostreopsis sp.	OShj0705-13	+	+
		Ostreopsis sp.	OShj0705-15	+	+
		Ostreopsis sp.	OShj0705-17	+	+
		Ostreopsis sp.	OShj0705-18	+	+
		Ostreopsis sp.	OShj0705-19	+	+
	September-21-2017	*Ostreopsis* sp.	OShj0921-04	+	
		Ostreopsis sp.	OShj0921-07	+	
		Ostreopsis sp.	OShj0921-08	+	
		Ostreopsis sp.	OShj0921-09	+	
		Ostreopsis sp.	OShj0921-11	+	
		Ostreopsis sp.	OShj0921-12	+	
		Ostreopsis sp.	OShj0921-14	+	
		Ostreopsis sp.	OShj0921-15	+	
Chuja Is.	September-14-2017	*Ostreopsis* sp.	OScj0914-12	+	
		Ostreopsis sp.	OScj0914-16	+	
		Ostreopsis sp.	OScj0914-22	+	
		Ostreopsis sp.	OScj0914-23	+	
Jeju Is.	November-21-2017	*Ostreopsis* sp.	OSjj1121-1	+	+
		Ostreopsis sp.	OSjj1121-2	+	+
Number of total cells		60	55	36	

southeastern coast (**Figure 1**). The study area is among the regions within the Korean peninsula, where the benthic and epiphytic dinoflagellate *Ostreopsis* has been previously reported to occur (Baek, 2012), and is known to be seasonally affected by the Tsushima Warm Current (Park et al., 2013), which could be responsible for introduction of the species. Therefore, the area was considered as appropriate sampling sites for monitoring the seasonal dynamics of the species and its phagotrophy. Additional planktonic *Ostreopsis* cells were collected using a plankton net (20 μm) from Chuja Island on September 14, 2017 and Jeju Island on November 21, 2017. During the sampling, surface water temperature and salinity were measured using a Yellow Spring Instrument (YSI, Ohio, USA). Two macroalgae of the most common macroalgal species at each sampling time were chosen; each was collected in duplicate (**Table S1**) and transferred to a zip lock bag along with some adjacent seawater. After the samples were transported to the laboratory, they were vigorously shaken to detach the epiphytic *Ostreopsis* cells, filtered through a 200 μm mesh to remove large particles, and then concentrated using a 20 μm mesh. The concentrates on the second mesh were resuspended in filtered seawater (50 ml volume). The aliquots (5 ml) of the 50 ml volume were fixed with glutaraldehyde (final 1%) to determine the abundance of *Ostreopsis* cells. Macroalgal thalli were weighed to determine fresh weight (g fw).

Determination of *Ostreopsis* Abundance

The cell abundance was determined by scanning all cells in a Sedgwick-Rafter counting chamber in duplicate at 100x magnification using a light microscope (Axiostar plus, Carl Zeiss Inc., Hallbergmoos, Germany). For determination of *Ostreopsis* cells containing the ingested food particles, all *Ostreopsis* cells encountered in the chamber were scored as cells containing food

particles or those without food particles. Cell abundance was expressed as the number of cells per gram of fresh weight of macrophyte (cells g^{-1} fw).

Light Microscopy

Live *Ostreopsis* cells with ingested prey were individually isolated using a drawn Pasteur glass pipette and loaded on a slide glass. Light micrographs were taken at 1000 × magnification by using an AxioCam HRc (Carl Zeiss Inc., Hallbergmoos, Germany) photomicrographic system coupled to the Axio Imager A2 equipped with differential interference contrast.

DNA Extraction and PCR Amplification

A total of 60 *Ostreopsis* cells containing the ingested prey were isolated from the remaining 45 ml concentrated samples by using drawn Pasteur glass pipettes under an inverted microscope (AX10, Carl Zeiss Inc., Hallbergmoos, Germany) or a stereoscope (Discovery. V8, Carl Zeiss Inc., Hallbergmoos, Germany) (**Table 1**). First, the isolated single cells were cleaned using filtered seawater several times (at least five times) and then soaked in distilled water in order to break the cells. Shortly after cell breakage, only food particles were picked and placed into a PCR tube and stored at a −80°C for 1 day. The samples were thawed at room temperature for 10 min, and DNA was extracted using Chelex 100 resin (100–200 mesh, sodium form; Bio-Rad Laboratories, Hercules, CA, USA). Next, 20 μl of 10% Chelex solution was added to the samples and incubated at 95°C for 1 h. Subsequently, the PCR tubes were centrifuged at 8,000 rpm at 4°C for 1 min, and then the supernatant in the PCR tube was transferred to a new tube and was used as a template. Polymerase chain reaction (PCR) amplifications were performed using some primers for *psa*A and *rbc*L genes. Primer pairs for amplification and sequencing of each gene were as follows: for *psa*A, psaA130F-psaA1600R (Yoon et al., 2002); and for *rbc*L, two primer sets F57-R753 and F321-RrbcS start (Freshwater and Rueness, 1994). Each gene was amplified using Diastar^{TM} Taq DNA polymerase (SolGent Co., Daejeon, Korea) in the following reaction mixture: 2.5 μl of 10X *Taq* reaction buffer (containing 25 mM $MgCl_2$), 0.5 μl of dNTP mix (10 mM), 1 μl of each primer (10 pmole μl^{-1}), 0.125 μl of *Taq* DNA polymerase (5 U μl^{-1}), and 3 μl genomic DNA for a 25 μl reaction. The PCR for *psa*A was run as follows: 2 min at 95°C, followed by 39 cycles of 20 s at 95°C, 40 s at 50°C, 1 min 30 s at 72°C, and a final incubation for 5 min at 72°C. The PCR for *rbc*L was run as above, except for 1 min (for primer set F57-R753) and 1 min 40 s (for primer set F321-RrbcS start set) instead of 1 min 30 s at 72°C. The PCR products were analyzed using electrophoresis on 1% agarose gels and visualized under UV illumination. Subsequently, amplified PCR products were purified using a PCR purification kit (Bioneer, Daejeon, Korea) and sequenced with primers (psaA130F and psaA1600R for *psa*A gene, F57, F321, R753, and RrbcS start for *rbc*L gene) by using a Big-Dye Terminator v3.1 Cycle Sequencing Kit (Applied Biosystems, Foster City, CA, USA) and an ABI PRISM 3730xl Analyzer (Applied Biosystems, Foster City, CA, USA), according to manufacturer's protocols at Cosmogenetech Corp. in Seoul, Korea. The amplicons were sequenced until at least double stranded coverage was reached. ContigExpress (Vector NTI version 10.1, Invitrogen, NY, USA) was used to assemble the individual sequence reads and edit out low quality regions. The assembled sequences were verified by comparison by using BLASTN search in the NCBI database and deposited in GenBank under the accession numbers MH200821-MH200875 for *rbc*L and MH200876-MH200911 for *psa*A.

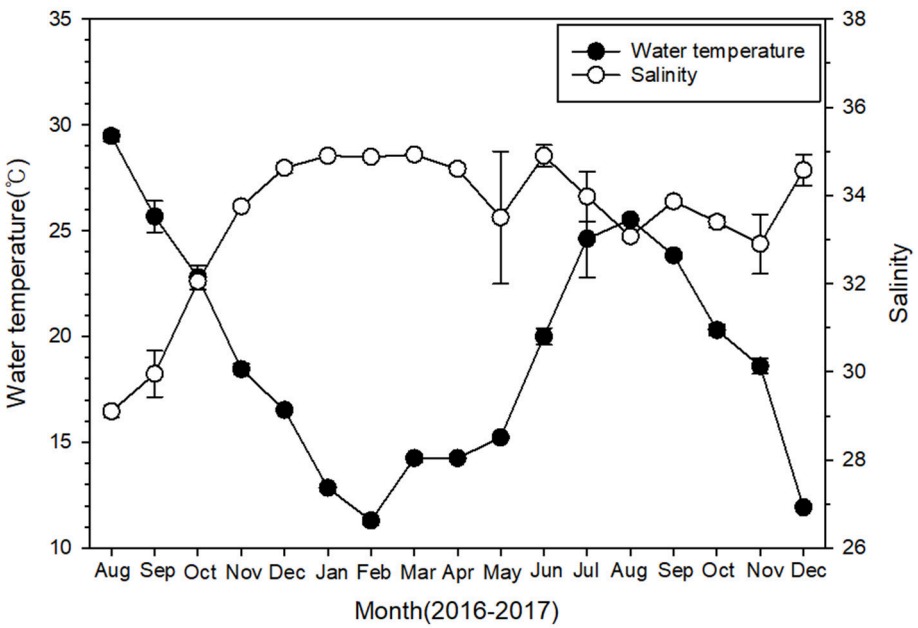

FIGURE 2 | Temporal variations of surface water temperature and salinity at four monitoring sites near Pohang during 2016–2017. Data are given as mean ± SE.

Phylogenetic Analysis

The sequences of *psa*A and *rbc*L genes of food particles were aligned with those of Rhodophyta, Cryptophyta, Stramenopiles, Haptophyta, Chlorophyta, and Glaucophyta obtained from GenBank database by using ClustalW 1.6 (Thompson et al., 1994) and were manually refined using MacGDE 2.4 (Linton, 2005). The final alignments of 2,200 positions for the *psa*A region and 1,390 positions for the *rbc*L region were selected. Phylogenies of the *psa*A and *rbc*L regions were inferred using the maximum likelihood (ML) and Bayesian inference methods. Modeltest v.3.7 (Posada and Crandall, 1998) was used to select the most appropriate model of substitution for the ML method in PAUP. The GTRGAMMA evolution model was selected from MODELTEST by using RAxML (Stamatakis, 2006), with the rapid bootstrapping option and 2,000 replicates. Bayesian analyses were run using MrBayes v.3.1.1 (Ronquist et al., 2012). GTR + I + G (-lnL= 37064.0586) and GTR + I + G (-lnL= 29063.3262) models were selected for *psa*A and *rbc*L datasets, respectively (Posada and Crandall, 1998). Bayesian analysis was performed using MrBayes 3.1.1 (Ronquist et al., 2012) running four simultaneous Monte Carlo Markov Chains for 2,000,000 generations and sampling every 100 generations, following a burn in of 2,000 generations.

RESULTS

Temporal Variations in Total *Ostreopsis* Abundance and Cells With Ingested Food Particles

During the sampling period, sea surface temperature showed a large temporal variation at 4 sampling sites, ranging from 11.3°C in February 2017 to 29.5°C in August 2016 (**Figure 2**). Salinity remained relatively constant (34.1 ± 0.2) throughout the study period, except for the first 3 months, when salinity ranged from 29.1 to 32.1.

The abundance of the epiphytic dinoflagellate *Ostreopsis* showed spatial and temporal variations during the study period among sampling sites (**Figure 3**). Nonetheless, a repeated marked temporal pattern of *Ostreopsis* abundance was observed at each sampling site, coinciding with warm temperatures. High concentration of *Ostreopsis* cells was observed between June and October at all sites, when water temperatures were higher than 19°C. The highest cell abundance (1,588 cells g^{-1} fw) during this study was recorded in July 2017 at Samjeong site, where water temperature was 25°C (**Figure 4**). Between November and May, when the water temperatures ranged from 11.3° to 18.6°C, *Ostreopsis* cells were not detected or were present at low concentration less than 80 cells g^{-1} fw at all sites.

Ostreopsis cells that contained the ingested food particles were frequently encountered at all sampling sites during this study. The ingested food particles were almost reddish brown (**Figures 5A,B**). In planktonic *Ostreopsis* cells isolated from Chuja Island in September 2017, however, food particles having either blue-green or purple color were also observed (**Figures 5C,D**). The size of the ingested food particles was highly

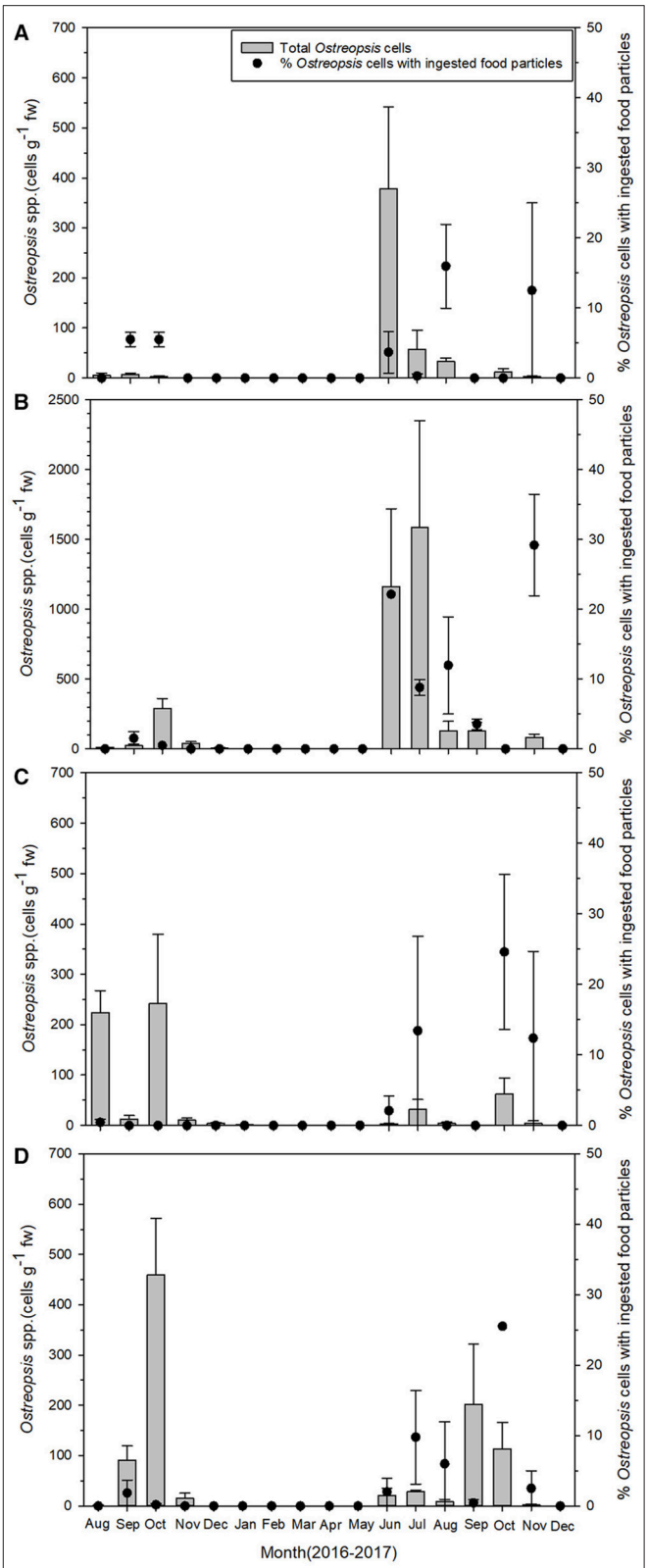

FIGURE 3 | Temporal pattern of total *Ostreopsis* spp. abundance (gray bars) on macrophytes and the percentage of *Ostreopsis* cells with ingested food particles (closed circles) during the study period at **(A)** Gangsa, **(B)** Samjeong, **(C)** Guryongpo, and **(D)** Hajeong. Data are given as mean ± SE.

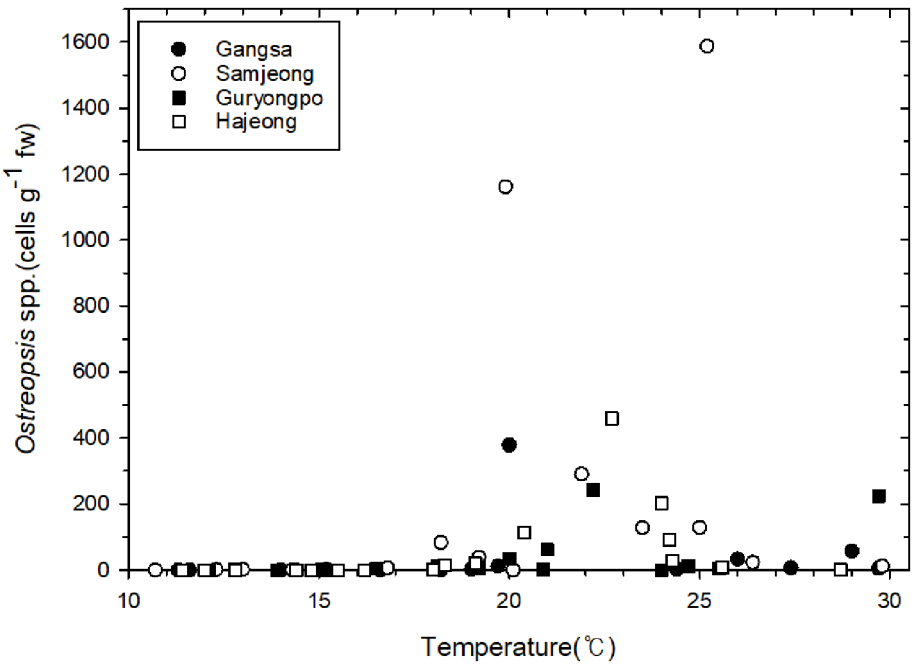

FIGURE 4 | Epiphytic *Ostreopsis* abundance depending on the water temperature.

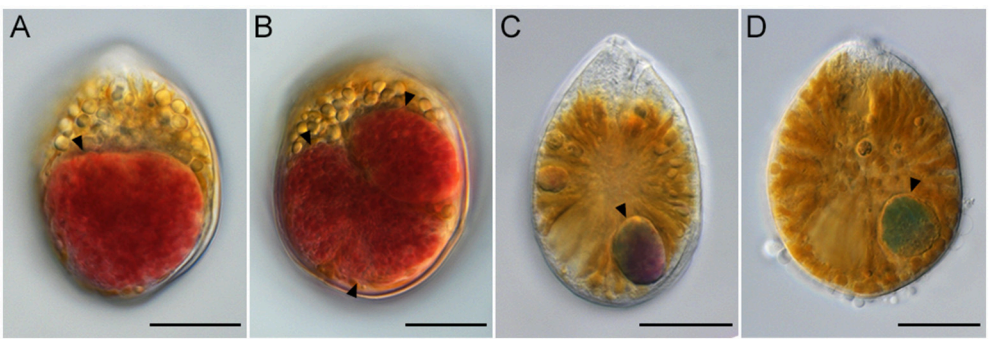

FIGURE 5 | Light micrographs of *Ostreopsis* cells with the ingested food particles (arrowheads) from field samples. In **(B)** three food particles are visible inside an *Ostreopsis* cell. The ingested food particles within *Ostreopsis* cells were reddish brown **(A,B)**, purple **(C)**, and blue-green **(D)**. Scale bars = 20 μm.

variable; in some cells, the food particles occupied half or two-thirds of *Ostreopsis* cytoplasm (**Figures 5A,B**). Occasionally, an *Ostreopsis* cell with more than two food particles was observed (**Figure 5B**).

The percentage of *Ostreopsis* cells containing ingested food particles also exhibited large spatial and temporal variations among sampling sites (**Figure 3**). The percentage of *Ostreopsis* with ingested food particles was highly variable, ranging from undetectable level to 29.5% (in November 2017 at Samjeong site), and was not always associated with *Ostreopsis* cell abundance. For example, in July 2017 at Samjeong site, where the highest cell abundance (1,588 cells g^{-1} fw) was observed, the percentage of *Ostreopsis* cells with ingested food particles was 8.8%. In contrast, the highest percentage of Ostreopsis cells with ingested food particles was recorded in November 2017 at Samjeong site where relatively low cell density (83 cells g^{-1} fw) was observed.

Phylogenetic Analyses of the Food Particles Within *Ostreopsis* Cells

The sequences of the D8-D10 region of LSU rDNA suggested that all *Ostreopsis* species in our study area were *Ostreopsis* sp.1 (data not shown). A total of 36 plastid *psa*A and 55 *rbc*L sequences were determined from the food particles within 60 *Ostreopsis* cells (**Table 1**). Phylogenetic analyses inferred from *psa*A alignment of 2,200 sites for 80 taxa and *rbc*L alignment of 1,390 sites of 115 taxa showed overall similar topologies (**Figures 6**, **7**). Phylogenetic analyses revealed that all sequences obtained from the food particles grouped within Rhodophyta,

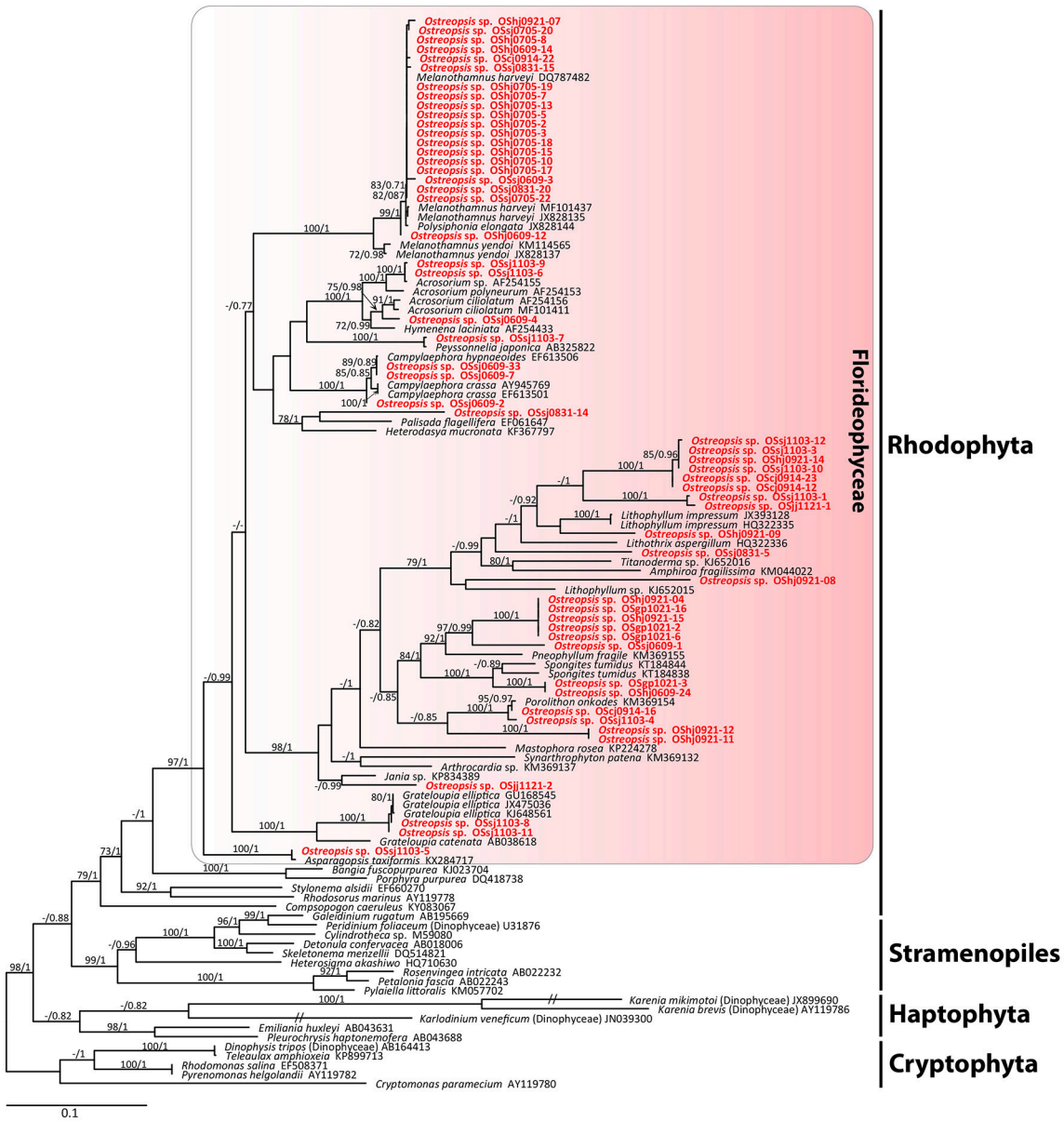

FIGURE 6 | RAxML tree inferred from *rbc*L sequences of 1,390 sites and representing 115 taxa including Rhodophyta, Cryptophyta, Stramenopiles, and Haptophyta. Sequences from the ingested food particles of *Ostreopsis* cells isolated from this study are indicated in bold face. Bootstrap value (>70%) from maximum likelihood and a Bayesian posterior probability of 0.7 or greater are indicated at nodes. Double slash marks indicate shrink nodes length (70%).

more specifically class Florideophyceae. The phylogenetic tree based on *rbc*L amino acid sequences also showed the same result, although the resolution was not better than the tree based on nucleotide sequences (**Figure S1**). Among 55 *rbc*L sequences, a total of 20 sequences were closely related to *Melanothamnus harveyi* (99% similarity), which was the most commonly detected food algal species in July 2017. Seventeen *rbc*L sequences were related to species belonging to the genera *Lithophyllum* and *Pneophyllum* although the sequence similarities were relatively low (86 and 88%, respectively). In addition, several sequences obtained from the food particles were related to various genera and/or species within Florideophyceae, including *Acrosorium* sp., *Campylaephora* sp., *Peyssonnelia japonica*, *Spongites* sp., *Grateloupia* sp., and *Asparagopsis taxiformis*. The *rbc*L sequence (cell ID OScj0914-16) obtained from blue-green food particle inside an *Ostreopsis* cell isolated from Chuja Island in September 2017 was closely related to *Porolithon onkodes* with 99% similarity. Two *rbc*L sequences (cell ID OScj0914-12 and OScj0914-23) obtained from purple colored food particles inside two *Ostreopsis* cells isolated from Chuja Island in September 2017 were related to *Lithophyllum impressum*, but their sequence similarities were relatively low (88%).

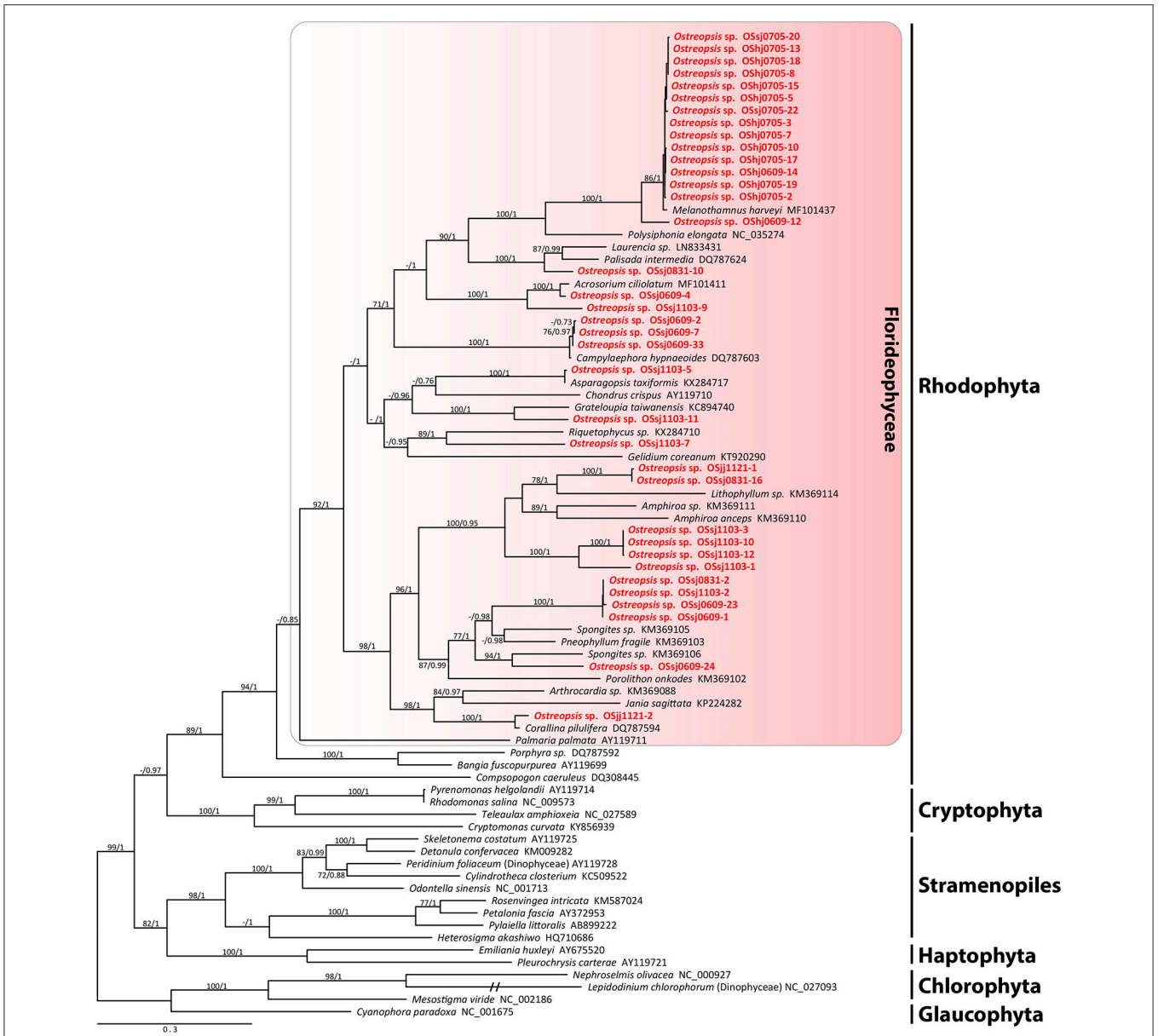

FIGURE 7 | RAxML tree inferred from *psa*A sequences of 2,200 sites and representing 80 taxa including Rhodophyta, Cryptophyta, Stramenopiles, Haptophyta, Chlorophyta, and Glaucophyta. Sequences from the ingested food particles of *Ostreopsis* cells isolated from this study are indicated in bold face. Bootstrap value (>70%) from maximum likelihood and a Bayesian posterior probability of 0.7 or greater are indicated at nodes. Double slash marks indicate shrink nodes length (70%).

DISCUSSION

The major findings from this study were that (1) while the total *Ostreopsis* cell abundance exhibited a marked temporal seasonality, mostly coinciding with warm temperatures, phagotrophy of the dinoflagellate (i.e., the percentages of cells containing ingested food particles) did not, and (2) all the ingested food particles originated from species belonging to class Florideophyceae.

While the seasonality of the epiphytic dinoflagellates *Ostreopsis* species has been reported in temperate waters, including the Mediterranean areas and Peter the Great Bay (NW Sea of Japan) (e.g., Aligizaki and Nikolaidis, 2006; Selina et al., 2014; Carnicer et al., 2015), their seasonal pattern seems to be highly study site-specific as well as year-specific as the peak abundances can occur from spring to autumn (Accoroni and Totti, 2016). In the present study, the *Ostreopsis* bloom onset was always observed at all sites in June when the water temperature reached more than 19°C, and the bloom persisted until October. Nonetheless, the bloom peak occurred at different times between June and October depending on the study sites. As in other temperate waters, the present study sites also followed a general

temporal trend that *Ostreopsis* blooms are summer events in temperate areas although the peak can occur at different months of the year (Carnicer et al., 2015; Accoroni and Totti, 2016).

Faust (1998) reported that the abundance of *Ostreopsis* species with prey ranged from 7 to 55% of all specimens examined from Belize. Very recently, Almada et al. (2017) reported only a small percentage (0.4%) of *O.* cf. *ovata* containing prey from Brazil. In the present study conducted in temperate waters, the percentages (0∼30%) of *Ostreopsis* cells with ingested food particles were in the range reported by previous studies. Further, despite the marked seasonality of *Ostreopsis* abundance, no pronounced seasonality of their phagotrophy was observed in the present study. For example, in July 2017 at Samjeong site, where the highest cell abundance (1,588 cells g^{-1} fw) was observed, the percentage of *Ostreopsis* cells with ingested food particles was at most 8.8%. In contrast, the highest percentage (about 30%) of *Ostreopsis* cells with ingested food particles was recorded in November 2017 at Samjeong site where relatively low cell density (83 cells g^{-1} fw) was observed. In dinoflagellates, several potential factors, including light and nutrient limitations, organic growth factors, organic carbon, and even plastid retention, have been reported to be linked with their mixotrophic strategy (Stoecker, 1998; Mitra et al., 2016). Unfortunately, data presented from this study could not clearly explain the occurrence of phagotrophy and its role in nutritional ecology of the benthic dinoflagellate *Ostreopsis*. Further studies, including well-designed laboratory experiments, are necessary to assess the role of mixotrophy in benthic dinoflagellates, including *Ostreopsis*.

Faust and Morton (1995) reported for the first time the presence of ingested food particles with an intense red color within the cytoplasm of *Ostreopsis labens* cells, indicating its phagotrophic behavior, and speculated that the dinoflagellate might prey on ciliates. Faust et al. (1996) and Faust (1998) subsequently found several *Ostreopsis* species with ingested food particles, which were hypothesized to be centric diatoms, ciliates, and small microalgae. In the present study, we frequently observed *Ostreopsis* cells containing reddish brown, blue-green, or purple colored food particles, all of which corresponded to species belonging to the class Florideophyceae, Rhodophyta.

Notably, all the ingested food particles originated from species belonging to the class Florideophyceae, although red algae did not always dominate macroalgal community of the study area. For example, in July 2017 at Samjeong site, where brown (*Sargassum* sp.) and green (*Ulva* sp.) algae were dominant and collected, all *Ostreopsis* cells with ingested prey had reddish brown colored food particles of the Florideophyceae origin, more specifically from *Melanothammus harveyi*. Thus, molecular data from this study raise questions as to why and/or how the dinoflagellate *Ostreopsis* prefers or feeds on only species belonging to the Florideophyceae as prey among various macroalgal species. There might be several possibilities to answer these questions. First, the preferred nutritional values of red algae as prey for *Ostreopsis* could be attributed to the difference in cell covering between red algae and other macroalgae. While green and brown macroalgae have hard cell wall composed of cellulose, red algal cell wall is relatively flexible and is composed of extracellular matrix, which typically consists of microfibrillar and sulfated galactans (Craigie, 1990; Delattre et al., 2011). The sulfated galactans include agars and carrageenans (Domozych, 2011). Because red algae have more gelatinous material than other algae, they might be more preferable as food for the epiphytic *Ostreopsis* than green/brown macroalgae. This difference in cell covering might allow *Ostreopsis* to easily penetrate and suck out the cell material of red algae. Nonetheless, this possibility seems not always to be the case in our study because many sequences of food particles were also related to species from the order Corallinales within the class Florideophyceae, such as *Lithophyllum impressum*, *Pneophyllum fragile*, *Spongites tumidus*, and *Porolithon onkodes*. Alternatively, *Ostreopsis* might directly ingest carpospores, which are produced after fertilization by red algae and germinated from their carposporophyte, provided red algae are abundant or the dinoflagellate is epiphytic on red algae (West and Mcbride, 1999). Diploid carpospores are mostly larger than haploid tetraspores (Ramus, 1968; Ngan and Price, 1979) so that they might have high nutritional value as prey for *Ostreopsis* species on the red algae. Third, benthic dinoflagellates, including *Ostreopsis*, are known to be capable of producing a mucopolysaccharide matrix to attach to substrates (Honsell et al., 2013; Escalera et al., 2014). In addition to the role for attachment, the mucopolysaccharide matrix might also act as a mucus trap for *Ostreopsis* to attach to and feed on red algal spores, which are released into the marine environment. If this is true, this mechanism would be effective when the red algae do not dominate the macroalgal community or rarely occur even if *Ostreopsis* is epiphytic on green or brown algae. These possibilities need to be addressed in the future to better understand the mixotrophic behavior and nutritional ecology of harmful benthic dinoflagellate *Ostreopsis* species.

AUTHOR CONTRIBUTIONS

All authors listed have made a substantial, direct and intellectual contribution to the work, and approved it for publication.

FUNDING

This work was supported by a research grant funded by the National Research Foundation of Korea (NRF-2016R1A6A1A03012647) and a program entitled Management of marine organisms causing ecological disturbance and harmful effects funded by KIMST/MOF.

ACKNOWLEDGMENTS

We gratefully acknowledge BS Jeon, A Kim, and JH Park for their assistance during sampling.

SUPPLEMENTARY MATERIAL

The Supplementary Material for this article can be found online at: https://www.frontiersin.org/articles/10.3389/fmars.2018.00217/full#supplementary-material

Figure S1 | Phylogenetic tree based on *rbc*L amino acid sequences from Rhodophyta, Haptophyta, Stramenopiles, and Cryptophyta. Sequences from the ingested food particles of *Ostreopsis* cells isolated from this study are indicated in bold face. Bootstrap values (>70%) from maximum likelihood are indicated at nodes. Double slash marks indicate shrink nodes length (70%).

Table S1 | Details of dominant macroalgal species collected at each sampling time and site in this study. R, red algae; B, brown algae; G, green algae.

REFERENCES

Accoroni, S., Romagnoli, T., Penna, A., Capellacci, S., Ciminiello, P., Dell'aversano, C., et al. (2016). *Ostreopsis fattorussoi* sp. nov.(Dinophyceae), a new benthic toxic *Ostreopsis* species from the eastern Mediterranean Sea. *J. Phycol.* 52, 1064–1084. doi: 10.1111/jpy.12464

Accoroni, S., Romagnoli, T., Pichierri, S., and Totti, C. (2014). New insights on the life cycle stages of the toxic benthic dinoflagellate *Ostreopsis* cf. ovata. *Harmful Algae* 34, 7–16. doi: 10.1016/j.hal.2014.02.003

Accoroni, S., and Totti, C. (2016). The toxic benthic dinoflagellates of the genus *Ostreopsis* in temperate areas: a review. *Adv. Oceanogr. Limnol.* 7, 1–15. doi: 10.4081/aiol.2016.5591

Aligizaki, K., and Nikolaidis, G. (2006). The presence of the potentially toxic genera *Ostreopsis* and *Coolia* (Dinophyceae) in the North Aegean Sea, Greece. *Harmful Algae* 5, 717–730. doi: 10.1016/j.hal.2006.02.005

Almada, E. V. C., Carvalho, W. F. D., and Nascimento, S. M. (2017). Investigation of phagotrophy in natural assemblages of the benthic dinoflagellates *Ostreopsis*, *Prorocentrum* and *Coolia*. *Braz. J. Oceanogr.* 65, 392–399. doi: 10.1590/s1679-87592017140706503

Baek, S. H. (2012). First report for appearance and distribution patterns of the epiphytic dinoflagellates in the korean peninsula. *Korean J. Environ. Biol.* 30, 355–361. doi: 10.11626/KJEB.2012.30.4.355

Carnicer, O., Guallar, C., Andree, K. B., Diogène, J., and Fernández-Tejedor, M. (2015). *Ostreopsis cf.* ovata dynamics in the NW Mediterranean Sea in relation to biotic and abiotic factors. *Environ. Res.* 143, 89–99. doi: 10.1016/j.envres.2015.08.023

Craigie, J. (1990). "Cell walls," in *Biology of the Red Algae*, eds K. M Cole and R. G. Sheath (Cambridge: Cambridge University Press), 221–257.

Delattre, C., Fenoradosoa, T. A., and Michaud, P. (2011). Galactans: an overview of their most important sourcing and applications as natural polysaccharides. *Braz. Arch. Biol. Technol.* 54, 1075–1092. doi: 10.1590/S1516-89132011000600002

Domozych, D. S. (2011). "Algal cell walls," in *eLS* (Chichester: John Wiley & Sons, Ltd). doi: 10.1002/9780470015902.a0000315.pub3

Escalera, L., Benvenuto, G., Scalco, E., Zingone, A., and Montresor, M. (2014). Ultrastructural features of the benthic dinoflagellate *Ostreopsis* cf. ovata (Dinophyceae). *Protist* 165, 260–274. doi: 10.1016/j.protis.2014.03.001

Faust, M. A. (1998). "Mixotrophy in tropical benthic dinoflagellates," in *VIII International Conference on Harmful Algae*, eds B. Reguera, J. Blanco, M. L. Fernández, and T. Wyatt (Vigo: International Oceanographic Comission of UNESCO), 390–393.

Faust, M. A., and Morton, S. L. (1995). Morphology and ecology of the marine dinoflagellate *Ostreopsis labens* sp. nov.(Dinophyceae). *J. phycol.* 31, 456–463. doi: 10.1111/j.0022-3646.1995.00456.x

Faust, M. A., Morton, S. L., and Quod, J. P. (1996). Further SEM study of marine dinoflagellates: the genus *Ostreopsis* (Dinophyceae). *J. Phycol.* 32, 1053–1065. doi: 10.1111/j.0022-3646.1996.01053.x

Fawcett, R. C., and Parrow, M. W. (2014). Mixotrophy and loss of phototrophy among geographic isolates of freshwater *Esoptrodinium*/*Bernardinium* sp.(*Dinophyceae*). *J. Phycol.* 50, 55–70. doi: 10.1111/jpy.12144

Fraga, S., Rodríguez, F., Bravo, I., Zapata, M., and Marañón, E. (2012). Review of the main ecological features affecting benthic dinoflagellate blooms. *Cryptogam. Algol.* 33, 171–179. doi: 10.7872/crya.v33.iss2.2011.171

Freshwater, D. W., and Rueness, J. (1994). Phylogenetic relationships of some European *Gelidium* (Gelidiales, Rhodophyta) species, based on rbcL nucleotide sequence analysis. *Phycologia* 33, 187–194. doi: 10.2216/i0031-8884-33-3-187.1

Hackett, J. D., Maranda, L., Yoon, H. S., and Bhattacharya, D. (2003). Phylogenetic evidence for the cryptophyte origin of the plastid of *Dinophysis* (*Dinophysiales, Dinophyceae*). *J. Phycol.* 39, 440–448. doi: 10.1046/j.1529-8817.2003.02100.x

Honsell, G., Bonifacio, A., De Bortoli, M., Penna, A., Battocchi, C., Ciminiello, P., et al. (2013). New insights on cytological and metabolic features of *Ostreopsis* cf. *ovata* fukuyo (*Dinophyceae*): a multidisciplinary approach. *PLoS ONE* 8:e57291. doi: 10.1371/journal.pone.0057291

Kim, M., Kim, S., Yih, W., and Park, M. G. (2012). The marine dinoflagellate genus *Dinophysis* can retain plastids of multiple algal origins at the same time. *Harmful Algae* 13, 105–111. doi: 10.1016/j.hal.2011.10.010

Laza-Martinez, A., Orive, E., and Miguel, I. (2011). Morphological and genetic characterization of benthic dinoflagellates of the genera *Coolia*, *Ostreopsis* and *Prorocentrum* from the south-eastern Bay of Biscay. *Eur. J. Phycol.* 46, 45–65. doi: 10.1080/09670262.2010.550387

Linton, E. (2005). *MacGDE: Genetic Data Environment for MacOS X*.

McManus, G. B., Zhang, H., and Lin, S. (2004). Marine planktonic ciliates that prey on macroalgae and enslave their chloroplasts. *Limnol. Oceanogr.* 49, 308–313. doi: 10.4319/lo.2004.49.1.0308

Mitra, A., Flynn, K. J., Tillmann, U., Raven, J. A., Caron, D., Stoecker, D. K., et al. (2016). Defining planktonic protist functional groups on mechanisms for energy and nutrient acquisition: incorporation of diverse mixotrophic strategies. *Protist* 167, 106–120. doi: 10.1016/j.protis.2016.01.003

Ngan, Y., and Price, I. R. (1979). Systematic significance of spore size in the *Florideophyceae* (Rhodophyta). *Br. phycol. J.* 14, 285–303. doi: 10.1080/00071617900650311

Nishitani, G., Nagai, S., Baba, K., Kiyokawa, S., Kosaka, Y., Miyamura, K., et al. (2010). High-level congruence of *Myrionecta rubra* prey and *Dinophysis* species plastid identities as revealed by genetic analyses of isolates from Japanese coastal waters. *Appl. Environ. Microbiol.* 76, 2791–2798. doi: 10.1128/AEM.02566-09

Park, K. A., Park, J. E., Choi, B. J., Byun, D. S., and Lee, E. I. (2013). An oceanic current map of the east sea for science textbooks based on scientific knowledge acquired from oceanic measurements. *Sea* 18, 234–265. doi: 10.7850/jkso.2013.18.4.234

Parsons, M. L., Aligizaki, K., Bottein, M.-Y. D., Fraga, S., Morton, S. L., Penna, A., et al. (2012). *Gambierdiscus* and *Ostreopsis*: reassessment of the state of knowledge of their taxonomy, geography, ecophysiology, and toxicology. *Harmful Algae* 14, 107–129. doi: 10.1016/j.hal.2011.10.017

Penna, A., Vila, M., Fraga, S., Giacobbe, M. G., Andreoni, F., Riob,ó, P., et al. (2005). Characterization of *Ostreopsis* and *Coolia* (Dinophyceae) isolates in the Western Mediterranean Sea based on morphology, toxicity and internal transcribed spacer 5.8 S rDNA sequences. *J. Phycol.* 41, 212–225. doi: 10.1111/j.1529-8817.2005.04011.x

Posada, D., and Crandall, K. A. (1998). Modeltest: testing the model of DNA substitution. *Bioinformatics* 14, 817–818. doi: 10.1093/bioinformatics/14.9.817

Ramus, J. S. (1968). *The Developmental Sequence of the Marine Red Alga Pseudogloiphloea Confusa in Culture*. Berkeley, CA: University of California.

Rhodes, L. (2011). World-wide occurrence of the toxic dinoflagellate genus *Ostreopsis* Schmidt. *Toxicon* 57, 400–407. doi: 10.1016/j.toxicon.2010.05.010

Ronquist, F., Teslenko, M., Van Der Mark, P., Ayres, D. L., Darling, A., Höhna, S., et al. (2012). MrBayes 3.2: efficient Bayesian phylogenetic inference and model choice across a large model space. *Syst. Biol.* 61, 539–542. doi: 10.1093/sysbio/sys029

Schmidt, J. (1901). Preliminary report of the biological result of the Danish Expedition to Siam (1899-1900). *Botanisk Tidsskrift*. 24, 212–221.

Selina, M. S., Morozova, T. V., Vyshkvartsev, D. I., and Orlova, T. Y. (2014). Seasonal dynamics and spatial distribution of epiphytic dinoflagellates in Peter the Great Bay (Sea of Japan) with special emphasis on *Ostreopsis* species. *Harmful Algae* 32, 1–10. doi: 10.1016/j.hal.2013.11.005

Selina, M. S., and Orlova, T. Y. (2010). First occurrence of the genus *Ostreopsis* (Dinophyceae) in the Sea of Japan. *Botanica Marina* 53, 243–249. doi: 10.1515/BOT.2010.033

Stamatakis, A. (2006). RAxML-VI-HPC: maximum likelihood-based phylogenetic analyses with thousands of taxa and mixed models. *Bioinformatics* 22, 2688–2690. doi: 10.1093/bioinformatics/btl446

Stoecker, D. K. (1998). Conceptual models of mixotrophy in planktonic protists and some ecological and evolutionary implications. *Eur. J. Protistol.* 34, 281–290. doi: 10.1016/S0932-4739(98)80055-2

Thompson, J. D., Higgins, D. G., and Gibson, T. J. (1994). CLUSTAL W: improving the sensitivity of progressive multiple sequence alignment through sequence weighting, position-specific gap penalties and weight matrix choice. *Nucleic Acids Res.* 22, 4673–4680. doi: 10.1093/nar/22.22.4673

Tichadou, L., Glaizal, M., Armengaud, A., Grossel, H., Lemée, R., Kantin, R., et al. (2010). Health impact of unicellular algae of the *Ostreopsis* genus blooms in the Mediterranean Sea: experience of the French Mediterranean coast surveillance network from 2006 to 2009. *Clin. Toxicol.* 48, 839–844. doi: 10.3109/15563650.2010.513687

Ukena, T., Satake, M., Usami, M., Oshima, Y., Naoki, H., Fujita, T., et al. (2001). Structure elucidation of ostreocin D, a palytoxin analog isolated from the dinoflagellate *Ostreopsis siamensis*. *Biosci. Biotechnol. Biochem.* 65, 2585–2588. doi: 10.1271/bbb.65.2585

Verma, A., Hoppenrath, M., Dorantes-Aranda, J. J., Harwood, D. T., and Murray, S. A. (2016). Molecular and phylogenetic characterization of *Ostreopsis* (Dinophyceae) and the description of a new species, *Ostreopsis rhodesae* sp. nov., from a subtropical Australian lagoon. *Harmful algae* 60, 116–130. doi: 10.1016/j.hal.2016.11.004

Vila, M., Garcés, E., and Mas,ó, M. (2001). Potentially toxic epiphytic dinoflagellate assemblages on macroalgae in the NW Mediterranean. *Aquat. Microb. Ecol.* 26, 51–60. doi: 10.3354/ame026051

West, J., and Mcbride, D. (1999). Long-term and diurnal carpospore discharge patterns in the *Ceramiaceae, Rhodomelaceae* and *Delesseriaceae (Rhodophyta*). *Hydrobiologia* 398, 101–114. doi: 10.1023/A:1017025815001

Yasumoto, T., Seino, N., Murakami, Y., and Murata, M. (1987). Toxins produced by benthic dinoflagellates. *Biol. Bull.* 172, 128–131. doi: 10.2307/1541612

Yoon, H. S., Hackett, J. D., and Bhattacharya, D. (2002). A single origin of the peridinin-and fucoxanthin-containing plastids in dinoflagellates through tertiary endosymbiosis. *Proc. Natl. Acad. Sci. U.S.A.* 99, 11724–11729. doi: 10.1073/pnas.172234799

Conflict of Interest Statement: The authors declare that the research was conducted in the absence of any commercial or financial relationships that could be construed as a potential conflict of interest.

frontiers in Marine Science

ORIGINAL RESEARCH
published: 02 February 2018
doi: 10.3389/fmars.2018.00013

Mixotrophic Activity and Diversity of Antarctic Marine Protists in Austral Summer

Rebecca J. Gast[1]*, *Scott A. Fay*[2,3] and *Robert W. Sanders*[2]

[1] Biology Department, Woods Hole Oceanographic Institution, Woods Hole, MA, United States, [2] Biology Department, Temple University, Philadelphia, PA, United States, [3] Invitae, San Francisco, CA, United States

Identifying putative mixotrophic protist species in the environment is important for understanding their behavior, with the recovery of these species in culture essential for determining the triggers of feeding, grazing rates, and overall impact on bacterial standing stocks. In this project, mixotroph abundances determined using tracer ingestion in water and sea ice samples collected in the Ross Sea, Antarctica during the summer of 2011 were compared with data from the spring (Ross Sea) and fall (Arctic) to examine the impacts of bacterivory/mixotrophy. Mixotrophic nanoplankton (MNAN) were usually less abundant than heterotrophs, but consumed more of the bacterial standing stock per day due to relatively higher ingestion rates (1–7 bacteria mixotroph^{-1} h^{-1} vs. 0.1–4 bacteria heterotroph^{-1} h^{-1}). Yet, even with these high rates observed in the Antarctic summer, mixotrophs appeared to have a smaller contribution to bacterivory than in the Antarctic spring. Additionally, putative mixotroph taxa were identified through incubation experiments accomplished with bromodeoxyuridine-labeled bacteria as food, immunoprecipitation (IP) of labeled DNA, and amplification and high throughput sequencing of the eukaryotic ribosomal V9 region. Putative mixotroph OTUs were identified in the IP samples by taxonomic similarity to known phototroph taxa. OTUs that had increased abundance in IP samples compared to the non-IP samples from both surface and chlorophyll maximum (CM) depths were considered to represent active mixotrophy and include ones taxonomically similar to *Dictyocha*, *Gymnodinium*, *Pentapharsodinium,* and *Symbiodinium*. These OTUs represent target taxa for isolation and laboratory experiments on triggers for mixotrophy, to be combined with qPCR to estimate their abundance, seasonal distribution and potential impact.

Keywords: protist, diversity, mixotrophy, Ross Sea, amplicon sequencing

OPEN ACCESS

Edited by:
Hongbin Liu,
Hong Kong University of Science and Technology, Hong Kong

Reviewed by:
Klaus Jürgens,
Leibniz Institute for Baltic Sea Research (LG), Germany
Bingzhang Chen,
Japan Agency for Marine-Earth Science and Technology, Japan

***Correspondence:**
Rebecca J. Gast
rgast @whoi.edu

Specialty section:
This article was submitted to Marine Ecosystem Ecology, a section of the journal Frontiers in Marine Science

Received: *25 July 2017*
Accepted: *16 January 2018*
Published: *02 February 2018*

Citation:
Gast RJ, Fay SA and Sanders RW (2018) Mixotrophic Activity and Diversity of Antarctic Marine Protists in Austral Summer. Front. Mar. Sci. 5:13. doi: 10.3389/fmars.2018.00013

INTRODUCTION

Phagotrophic protists are key constituents of aquatic food webs, transferring energy and organic matter to higher trophic levels (Caron et al., 2012). In the Southern Ocean, protists are reported to remove as much as 100% of the daily bacterial production (Becquevort et al., 2000; Anderson and Rivkin, 2001; Vaqué et al., 2004; Duarte et al., 2005), but compared to other oceanic areas, there are still relatively few data estimating bacterivory in Antarctic marine waters, and even less knowledge of the nature of the bacterivorous community. Information on bacterivorous protist abundance and activity can be realized via the use of fluorescent tracer particles of an appropriate

size since this approach allows visual confirmation of phagotrophy. For example, Becquevort (1997) used fluorescently labeled bacteria (FLB) to identify small (<5 μm) heterotrophic nanoflagellates (HNAN), especially dinoflagellates, as important bacterivores during early spring in the Atlantic sector of the Southern Ocean, while small choanoflagellates were the major bacterivores in the Indian Ocean sector (Becquevort et al., 2000). Over the past two decades, Antarctic marine bacterivory studies have used ingestion methods to examine the bacterial grazing rates and impacts of protists, with highly variable results reported (Putt et al., 1991; James et al., 1995; Leakey et al., 1996; Pedrós-Alió et al., 1996; Vaqué et al., 2002; Pearce et al., 2010, 2011). In most of these reports, HNAN had ingestion rates of <10 bacterial cells $HNAN^{-1}$ per day, although some were as high as 67 bacterial cells $HNAN^{-1}$ per day (Vaqué et al., 2002). The impact on daily bacterial production ranged from not detectable to greater than 120%. This variability is not unique to the Antarctic, or polar regions, (Sherr et al., 1989; Sanders et al., 2000; Vaqué et al., 2014) and is likely due to a combination of factors including HNAN species composition (Boenigk and Arndt, 2002), the patchy nature of aquatic environmental samples and the presence, abundance and activity of mixotrophic nanoplankton (MNAN).

Fluorescent tracers have also been important in identifying the widespread impact of phagotrophic phytoflagellates (mixotrophs) as bacterivores. Anecdotal accounts of mixotrophs have long existed, but in the last 30 years there has been a growing recognition of the wide geographic and taxonomic distributions of species that combine photosynthesis with consumption of particulate food (Sanders and Porter, 1988; Havskum and Hansen, 1997; Stoecker et al., 2017). Furthermore, the ecological impact of mixotrophs has the potential to be substantial. Mixotrophic phytoflagellates have been identified as important bacterivores in both coastal oceans and oligotrophic gyres, accounting for up to 70% of bacterivory (Hartmann et al., 2012; Unrein et al., 2014). In Antarctica, Moorthi et al. (2009) used the FLB method in the Ross Sea and found that mixotrophs potentially consumed 11–100% of the bacterial standing stock daily during spring, while Laybourn-Parry and colleagues found large impacts by mixotrophs in some Antarctic lakes (Roberts and Laybourn-Parry, 1999; Bell and Laybourn-Parry, 2003; Laybourn-Parry et al., 2005).

While bacterivory and mixotrophic activity in natural systems can be assessed and some taxonomic groups can be identified using tracer ingestion experiments, determining the identity of most bacterivorous taxa is difficult. This is particularly evident when studying nano- and picophytoplankton that often lack useful morphological features for discriminating between species with epifluorescence/light microscopy. Yet the ability to identify which species are mixotrophic is important in understanding their behavior and ecological roles. Phagotrophic phytoplankton species from culture collections have been valuable for determining the variable triggers of feeding, as well as grazing rates and overall impact on bacterial standing stocks (Rothhaupt, 1996; Gast et al., 2014; Johnson, 2015). However, we still miss much of the mixotroph species diversity in field surveys, which is important because feeding by different species may be stimulated by different mechanisms or resource limitations (Maranger et al., 1998; Wilken et al., 2014; Princiotta et al., 2016). Using molecular methods, we recently showed that three known Antarctic mixotroph species usually comprised only a small portion of the total mixotrophic nanoflagellate assemblage identified by tracer methods (Gast et al., 2014), indicating that there are likely a large number of unidentified species present or that the cultured species are not generally abundant in the environment.

In this project, two goals were addressed. First, to assess polar seasonal and regional differences in mixotroph abundance and activity we compared previously reported ingestion results on the impacts of bacterivory, including mixotrophy, during the austral summer in the Ross Sea (Gast et al., 2014) with data from the Ross Sea in austral spring (Moorthi et al., 2009) and from the Arctic in the fall (Sanders and Gast, 2012). Second, we used incubation experiments with bromodeoxyuridine (BrdU) labeled bacteria as food and the subsequent immunoprecipitation of BrdU-labeled DNA followed by amplification of the eukaryotic portion of the labeled DNA and high throughput sequencing. The incorporation of BrdU into protist DNA allows the identification of bacterivorous organisms, with putative mixotrophs identified by their taxonomic affiliation with phototrophic lineages (Fay et al., 2013). The results expand our understanding of the roles of bacterivorous mixotrophic and heterotrophic protists in the Antarctic marine environment and identify taxa for further study of trophic ecology.

METHODS

Sample Collection

Samples for shipboard experiments were collected in the Ross Sea during research cruise NBP-1101 aboard the R/V Nathaniel B. Palmer in the austral summer (20 January through 13 February 2011). Seawater was collected from two depths (surface and deep chlorophyll maximum) at 10 open water stations using 30 liter Niskin bottles on a CTD rosette. Two of those sites were sampled a second time on different dates (**Figure 1**, **Table 1**). The deep chlorophyll maximum (CM) was determined by fluorescence (WetLabs FLRTD fluorometer) during the downcast of the CTD and ranged from 30 to 90 m in depth depending on station. For chlorophyll *a* determination, 100 mL of whole water was filtered onto a 47 mm GF/F filter (Whatman) and frozen at −20°C until analyzed. Filters were later extracted in 90% acetone overnight at −20°C and fluorescence was determined with a Model TD-700 fluorometer (Turner Designs, Sunnyvale, CA, USA). Nutrient data (soluble reactive phosphate, nitrate, nitrate + nitrite, ammonia, silicate) from these stations is available in the Supplementary Material of Gast et al. (2014). In addition to water samples, we collected ice cores from land-fast ice (77° 43.70 S, 166° 08.50 E) with a motorized Sipre corer. Three replicate cores were taken within 15 cm of each other at each of three sites 10–12 m apart along an east-west transect. Core lengths ranged from 105 to 175 cm. For each core, the bottom 10 cm and a 10 cm section from mid-core (ranged from 20 to 80 cm from the top/surface of the core depending on the presence of brine channels or cracks) were removed and stored in separate 3.8 L

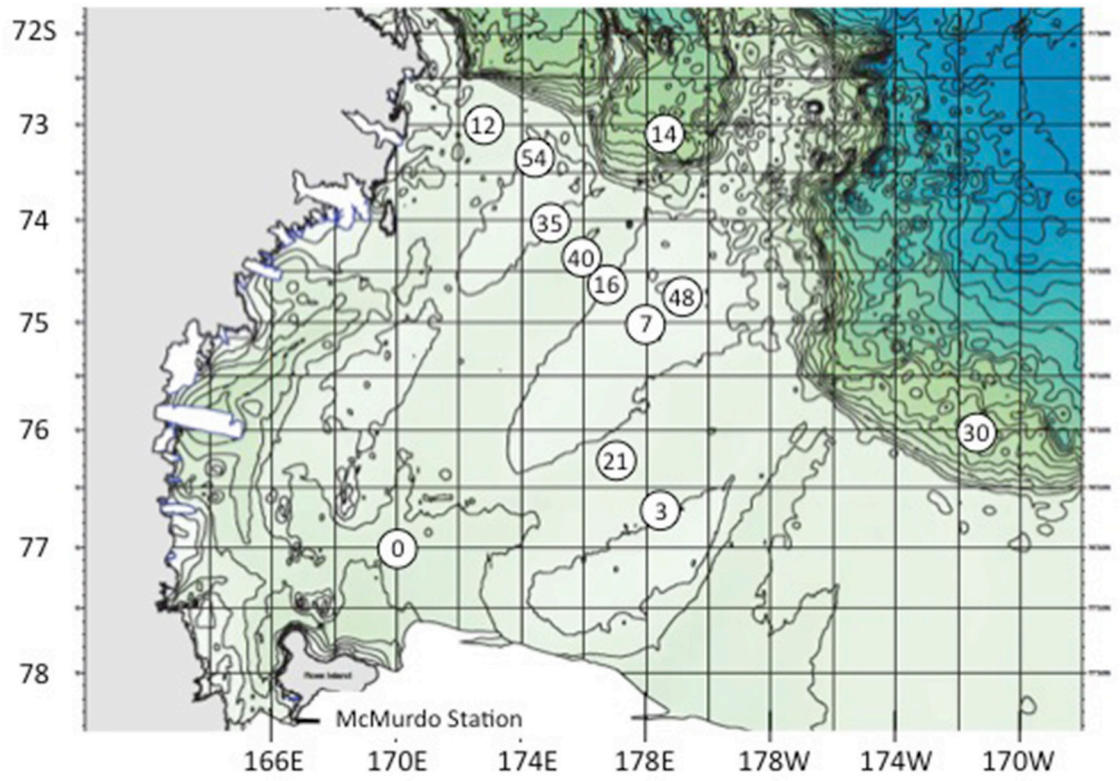

FIGURE 1 | Stations sampled in the Ross Sea, Antarctica, Jan/Feb 2011. BrdU experiments were accomplished at stations 14, 21, 30, and 54. Station 7 is also 61, and 16 is also 24.

freezer bags in a cooler until transfer to the ship for processing (see below).

Ingestion Experiments

Seawater samples were gently pre-filtered through acid-washed 200 μm nylon mesh followed by 35 μm Nitex mesh (Wildlife Supply, Yulee, FL, USA) to remove larger zooplankton. Since these experiments require a liquid phase, ice core replicates were pretreated by crushing the sea ice inside zip-lock bags and mixing with 0.2 micron filtered ice-cold seawater (Moorthi et al., 2009).

To determine the appropriate concentration of tracer particles to add, bacterial abundance was assessed by epifluorescence microscopy from samples filtered onto 25 mm black Poretics polycarbonate filters (0.2 μm pore size), stained and mounted with cover slips onto glass slides using VectaShield® mounting medium containing DAPI (Vector Laboratories, Inc., Burlingame, CA, USA). Ingestion experiments were run in triplicate (300 mL prescreened water in 500 mL Whirlpak bags) with 0.6 μm polycarbonate microspheres (Polysciences, Inc., Warrington, PA, USA) added at ∼25% of natural bacterial abundance. Fluorescent tracer stock solution was sonicated immediately prior to addition to disperse particles evenly. Replicate bags were incubated at −0.5°C under fluorescent lamps at irradiance levels of 1.5×10^{15} quanta s^{-1} cm^{-2} (for surface samples) and 2.9×10^{14} quanta s^{-1} cm^{-2} (for CM samples). Light level was measured with a QSL-100 Quantum-Scalar Irradiance meter (Biospherical Instruments, Inc., San Diego, CA, USA). To determine bacterivory, replicate bags were sacrificed immediately after particle addition (T_0) and at 60 min after particle addition (T_{final}), and fixed using the Lugol's/formaldehyde/$Na_2S_2O_3$ method to prevent egestion (Sherr et al., 1993). Additional subsamples were taken at T_0, fixed in 1% glutaraldehyde and filtered onto 0.2 μm polycarbonate filters with VectaShield® with DAPI as described above to determine bacterial and exact microsphere abundances. Hourly bacterial ingestion rates for both heterotrophic and mixotrophic nanoflagellates were calculated by multiplying the rates of microsphere uptake and the ratio of natural bacteria to microspheres in the sample after subtraction of background (T_0), which was always negligible. Grazing impact (bacteria d^{-1} ml^{-1}) of each nanoflagellate group was estimated by multiplying ingestion rate by abundance. This value was then used to determine the percentage of the bacterial assemblage removed daily as a result of grazing by HNAN or MNAN for comparison to literature values.

Abundances of phototrophic (PNAN), mixotrophic (MNAN), and heterotrophic (HNAN) nanoplankton were determined using 30 mL of sample collected from the WhirlPacs filtered onto 25 mm Poretics polycarbonate membranes (3 μm pore size, GE Osmonics, Minnetonka MN, USA). Filters were stained and mounted on glass slides using VectaShield® with DAPI

TABLE 1 | Station location, bacterial, and nanoplankton abundances, photosynthetically active radiation (PAR) and chlorophyll *a* concentrations for NBP-1101 austral summer cruise.

Station and depth (m)	Latitude/ Longitude	Abundances (no. mL^{-1})				PAR (photons m^{-2} d^{-1})	Chl *a* (μg L^{-1})
		Bacteria (× 10^5)	PNAN	MNAN*	HNAN		
STA 0 5	76° 29.98 S/	11.7	2,049	169	55	223	4.03
50	170° 0.05 E	12.1	2,170	99	165	0.1	n.d.
STA 3 5	76° 09.34 S/	5.75	1,311	75	165	136	0.74
45	178° 31.06 E	9.63	1,609	287	253	3.5	1.49
STA 7 5	74° 30.12 S/	6.02	1,289	157	231	164	4.62
40	178° 0.03 E	5.59	1,917	413	826	0.18	4.24
STA 12 5	72° 29.98 S/	3.16	1,686	301	925	181	1.58
45	172° 36.18 E	2.42	1,454	267	286	1.8	1.60
STA 14 5	72° 35.01 S/	3.41	1,256	338	529	n.d.	0.49
50	178° 30.05 E	2.14	1,355	252	705	n.d.	0.53
STA 16 5	74° 08.01 S/	3.22	1,840	630	264	87.25	0.42
70	176° 39.98 E	4.40	1,190	149	286	3.13	0.66
STA 21 5	75° 44.99 S/	8.62	1,377	133	925	59.22	3.72
35	177° 00.14 E	8.71	1,146	186	738	0.29	2.53
STA 24 5	74° 08.24 S/	2.29	463	198	848	84.45	0.55
60	176° 39.35 E	6.30	650	315	331	0.23	1.16
STA 30 5	75° 30.02 S/	2.54	3,261	123	1,289	170	6.03
30	171° 29.76 W	3.14	2,843	267	474	1.2	4.22
STA 35 5	73° 35.00 S/	3.14	2,071	192	430	95	1.40
45	174° 50.01 E	3.76	1,289	82	33	0.19	1.90
STA 40 5	73° 53.02 S/	2.33	948	183	1,168	173	n.d.
35	175° 50.00 E	3.49	1,245	208	253	8.2	n.d.
STA 48 5	74° 12.06 S/	2.38	793	55	132	35	0.63
40	178° 45.18 E	4.32	452	30	88	2.7	0.98
STA 54 10	72° 45.07 S/	2.61	793	55	132	13	0.47
90	174° 00.01 E	2.98	452	30	88	0.12	0.32
STA 61 20	74° 30.07 S/	2.47	1,179	44	99	5.29	n.d.
100	178° 0.18 E	3.92	165	11	88	0.00	n.d.

Stations 7 and 61 were in close proximity but were sampled on different dates, as were and stations 16 and 24. Italicized stations were sites of sampling for BrdU experiments.
**Previously reported in Gast et al. (2014).*

and frozen at −20°C to reduce loss of chlorophyll fluorescence until enumeration by epifluorescence microscopy at 1,000X magnification onboard the ship. Nanoplankton (3–20 μm) were counted in 20–40 fields per filter, or a minimum of 100 cells. PNAN were distinguished by the presence of a chloroplast and a DAPI stained nucleus, while HNAN were identified by presence of a nucleus and absence of a chloroplast. Mixotrophic cells were defined as those with chlorophyll and at least one ingested fluorescent tracer (microsphere) after background correction based upon the T_0 sample. All abundances of protists were calculated per milliliter seawater or milliliter brine. For the latter, the original brine volume was calculated by subtracting the amount of added filtered seawater (FSW, used to wash organisms out of sea ice) from the total amount volume of the experimental FSW/brine mixture drained from ice, assuming the remainder to be pure brine (Moorthi et al., 2009). For the brine experiments, differences in abundance between sites of collection and depth in the ice cores were tested with a two-way analysis of variance, ANOVA; data were (square root + 1)-transformed prior to statistical analysis.

The role of environmental variables in explaining variation in mixotroph abundances in the water samples was assessed using distance-based linear modeling (DistLM) in PERMANOVA+ (McArdle and Anderson, 2001). Mixotroph counts for each sample were square root transformed and a Bray Curtis resemblance matrix was built. Environmental data included temperature, salinity, oxygen, beam attenuation fluorescence, PAR, Julian day, latitude, longitude, total bacteria, soluble reactive phosphate (SRP), nitrate, nitrate + nitrite, ammonium, and silicate. The nutrient analyses of water were accomplished by a contractor technician following standard procedures for SRP (Bernhardt and Wilhelms, 1967), nitrate + nitrite (Armstrong et al., 1967), ammonium (indophenol blue method from ALPKEM), and silicate (Atlas et al., 1971) using a 5-channel Lachat Instruments QuikChem FIA+ 8000s series autoanalyzer in conjunction with a Lachat Instruments XYZ

AutoSampler (ASX-500 Series), two Lachat Instruments RP-100 Series peristaltic reagent pumps and OMNION Software, version 3.0.220.02. Depth and fluorescence were square root transformed, and PAR was transformed by log(1+PAR). The DistLM model building run utilized the Stepwise selection procedure and BIC as the selection criteria, with 9999 permutations.

Bacterivore Diversity Experiments (BrdU Incorporation)

A strain of bacteria, *Planococcus* sp., with a diameter <1 μm was labeled with BrdU (5′-bromo-2′-deoxyuridine, Sigma B5002) by inoculating into 50 mL of fresh media (1% yeast extract, 0.22 μm filtered seawater) with 20 μM BrdU (Fay et al., 2013). *Planococcus* for control incubations was treated identically except that BrdU was excluded from the media. The bacterial cells were harvested by centrifugation (3,000 × g, 10 min), washed 3 times, and dispersed and resuspended by pipetting with cold phosphate-buffered saline.

At a subset of stations (14, 21, 30, 54, **Table 1**), seawater was collected from the surface and the deep chlorophyll maximum, prefiltered through 200 μm nylon mesh screen and distributed into 20 L cubitainers. There were two treatments per experiment; the addition of BrdU-labeled *Planococcus* and the addition of unlabeled *Planococcus*. *Planococcus* was added at 10% of the natural abundance of bacteria for the first experiment and at 20% for the remaining three BrdU incubation experiments.

All cubitainers were incubated at −0.5°C in continuous fluorescent light at ∼7×10^{15} quanta s^{-1} cm^{-2} (surface samples) and ∼7×10^{14} quanta s^{-1} cm^{-2} (CM samples). Samples (1–2 L) were taken after 72 h of incubation for each depth/replicate, collected on 0.2 μm Durapore filters and frozen at −80°C for later extraction. DNA was extracted following the protocol in Gast et al. (2004), resuspended in 100 μL 1× Tris/EDTA and stored frozen at −80°C for transport. Immunoprecipitation of BrdU-labeled DNA was performed following the protocol modified and published by Fay et al. (2013). Samples of DNA from incubations that were fed unlabeled bacteria are identified as "Whole," whereas the samples fed BrdU-labeled bacteria are identified as "IP" (immunoprecipitated).

Primers to amplify the V9 region of the 18S ribosomal RNA gene (Amaral-Zettler et al., 2009; Stoeck et al., 2010) were used to generate products for amplicon high throughput sequencing. For each sample, 3 PCR reactions were performed at a volume of 50 μl each that contained 0.2 μM of each primer (Fay et al., 2013), 1× reaction buffer, 200 μM each dNTP, and 0.5U Phusion DNA Polymerase (New England Biolabs F-553). Cycling conditions were: 98°C for 120 s; 10 cycles of 98°C for 15 s, 67°C decreased by 1°C $cycle^{-1}$ for 20 s, and 72°C for 15 s; 25 cycles of 98°C for 15 s, 57°C for 20 s, and 72°C for 15 s; and a final extension step of 72°C for 120 s. Each sample was purified with AMPure XP beads (Beckman Coulter A63880) following the manufacturer's protocol. Sequencing was accomplished on pooled triplicate samples at the University of Pennsylvania DNA Sequencing Facility using a "1-way read" approach for amplicon pyrosequencing with the GS Junior emPCR Lib-L kit (454 Life Sciences Corp., 2010) on a Roche/454 GS-FLX. The resulting read data were deposited in the National Center for Biotechnology Information (NCBI) Sequence Read Archive (SRA) under accession number SRP076481.

High Throughput Sequence Analysis

The barcodes, primers and sequences with a quality score below 25 were removed from the 454 data files, and the data de-multiplexed using the split_libraries command in QIIME version 1.9.1 (Caporaso et al., 2010). Operational taxonomic units (OTUs) were clustered at 95% identity, and chimeras were checked for using blast_fragments in QIIME. Taxonomy was assigned to OTUs in QIIME using Blast and the Silva 119 database (all taxa). Singleton, bacterial, archaeal, fungal, higher plant and metazoan OTUs were removed from the final dataset. OTU tables were exported to PRIMER v. 6 (Clarke and Warwick, 2001) for analysis of community similarity. Experiments were also analyzed individually in Excel for the identification of putatively mixotrophic OTUs. The data was normalized by conversion of each OTU to a percentage of the total tag counts from each sample. QIIME analysis pipeline commands are documented in Supplemental Material.

RESULTS AND DISCUSSION

Phototrophic, Mixotrophic and Heterotrophic Nanoplankton Abundances and Bacterivory

Phototrophic nanoplankton (PNAN) typically were more abundant than the mixotrophic (MNAN), and heterotrophic (HNAN) nanoplankton combined, with the PNAN abundance usually an order of magnitude greater than either the MNAN or HNAN (**Table 1**, **Figure 2**). However, estimates of MNAN are based on presence of an ingested particle and not all MNAN necessarily ingested a particle during the incubations. Thus, the reported abundances of MNAN are considered a minimum estimate. Also, there have been previous studies indicating that some heterotrophic protists discriminate against microspheres based on size, phenotypic traits, motility, or taste (Sherr and Sherr, 1993), although we found that Arctic nanoplankton had higher grazing rates on microspheres than FLB as found in some other environments (Sanders et al., 1989; Sanders and Gast, 2012; Princiotta et al., 2016). In our summer Ross Sea samples, flagellates identified as MNAN were usually less abundant than HNAN (**Table 1**, **Figure 2**), but MNAN usually consumed more of the bacterial standing stock per day than the HNAN at both the surface and deep chlorophyll maximum (**Figures 2C,D**), a phenomena also observed in the Beaufort Sea and Canadian Basin when mixotrophic picoeukayotes (phytoplankton 0.2–2 μm in size) were included (Sanders and Gast, 2012). Comparison of our shipboard experiments in polar regions indicated that mixotrophs comprised 4–34% of the phototrophic and 3–75% of the bacterivorous flagellates (**Table 2**). However, mixotrophic flagellates are reported to account for 37–95%, 12–72%, and 9–42% of the total protistan bacterivory in the Southern and Northern Atlantic Ocean,

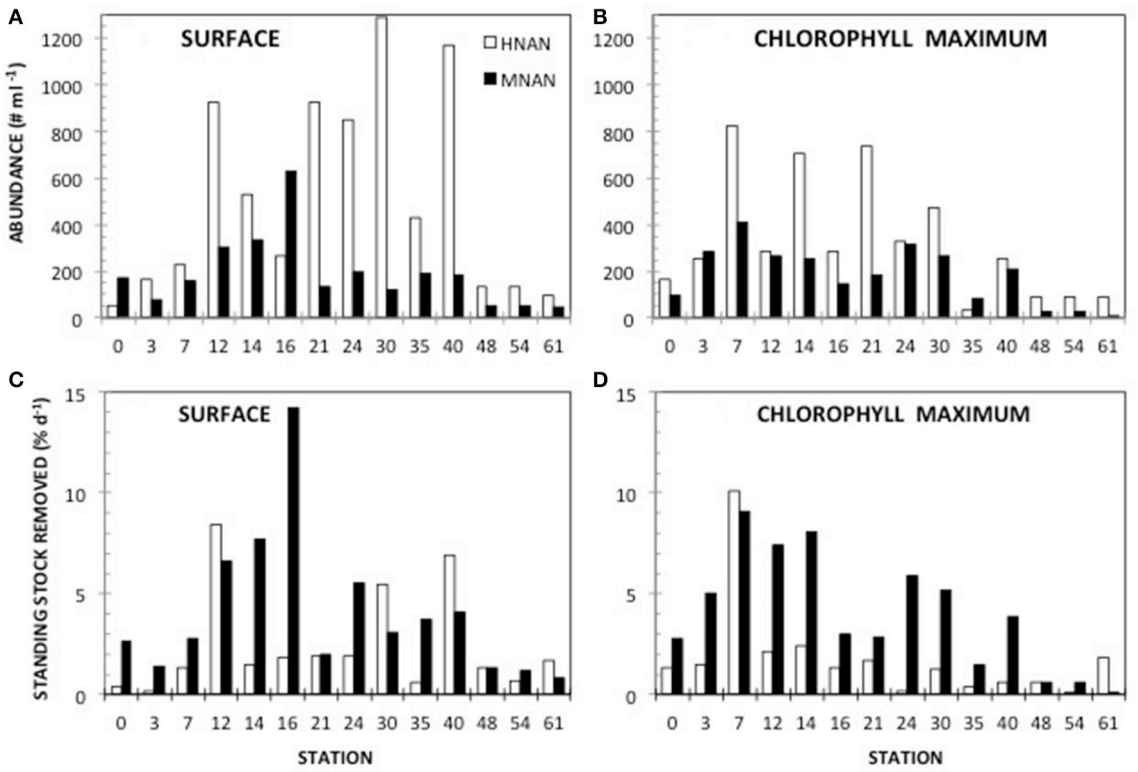

FIGURE 2 | Mixotroph abunance and grazing impact. Abundance of mixotrophic nanoflagellates (MNAN) and heterotrophic nanoflagellates (HNAN) determined by microscopy at **(A)** the surface and **(B)** the deep chlorophyll maximum. Amount of bacteria removed by MNAN or HNAN grazing at **(C)** the surface and **(D)** the deep chlorophyll maximum.

TABLE 2 | Mixotrophs as a percentage of phototrophic and bacterivorous flagellates in different seasons in Polar Oceans.

		Antarctic Spring 2005*		Antarctic Summer 2011		Arctic Autumn 2008‡	
		Surface	DCM	Surface	DCM	Surface	DCM
% Phototrophs	Mean	11	14	12	12	16	14
	Range	4–24	6–22	4–30	9–33	5–28	5–34
% Bacterivores	Mean	19	10	33	37	9	10
	Range	8–42	9–14	9–75	11–71	3–23	5–25

*The Arctic calculations include mixotrophic picoeukaryotes that were not observed in the Antarctic experiments. *Moorthi et al. (2009); ‡Sanders and Gast (2012).*

Western Pacific Ocean and Northwestern Mediterranean Sea, respectively, suggesting a ubiquitous and major role as bacterivores in the world's oceans (Zubkov and Tarran, 2008; Tsai et al., 2011; Hartmann et al., 2012; Unrein et al., 2014). Three environmental variables explained most of the variation in mixotroph abundance over our samples. The most influential was date of sample collection (Julian day; 76.09% total variation), followed by nitrate + nitrite (1.86% total variation) and depth of sample collection (0.11% total variation).

Comparing our mixotrophy studies in the Antarctic summer, Antarctic spring (Moorthi et al., 2009) and the Arctic autumn (Sanders and Gast, 2012), MNAN in the water column comprised the same percentage of phototrophs on average in all three sample sets, with similar overall abundance in the Antarctic studies, but much lower absolute abundances in the Arctic autumn (**Table 2**). This similar percentage of MNANs is despite the fact that FLB were used in the Antarctic spring study rather than beads, which could result in different ingestion rates and behavior. Also, the relatively low grazing impact of nanoflagellates in the Arctic was sometimes as high as 25% of bacterioplankton standing stock when mixotrophic picoeukaryotes were considered (Sanders and Gast, 2012). Mixotrophic picoeukaryotes were not observed in our Antarctic fluorescent tracer additions in either spring 2005 or summer 2011.

In the Antarctic summer, mixotrophs tended to have relatively high ingestion rates (1–7 bacteria $MNAN^{-1}$ h^{-1}, mean 3.4 bacteria $HNAN^{-1}$ h^{-1}) compared to heterotrophs (0.1–4 bacteria $HNAN^{-1}$ h^{-1}, mean 2.2 bacteria $HNAN^{-1}$ h^{-1}) and also made up a greater percentage of the total bacterivores compared to our other polar studies (**Table 2**). Despite this, the maximum impact on bacterioplankton was only 14 and 9% of the standing stock per day in the surface and chlorophyll maximum layer, respectively. This indicates that the effect of mixotroph bacterivory may be much higher in the Antarctic

spring, where we estimated an impact of up to 100% of standing stock calculated from our abundances and a conservative grazing rate of 1 bacterium $MNAN^{-1}$ h^{-1} (Moorthi et al., 2009). In the Arctic, MNAN may play a smaller role with respect to bacterivory due to the prevalence of picoeukaryotic phytoplankton that are also mixotrophic, though further study in different seasons is clearly needed. While we noted higher ingestion rates by MNAN than HNAN (mean 5.1 bacteria $MNAN^{-1}$ h^{-1} vs. 1.3 bacteria $HNAN^{-1}$ h^{-1}), this is not always the case. Ingestion rates for HNAN that are higher or equivalent to MNAN have been reported in several environments (Sanders et al., 1989; Unrein et al., 2007; Zubkov and Tarran, 2008). These differences are likely due to varying community composition and to environmental factors, such as light and nutrient concentration, which may be more likely to affect ingestion by MNAN than HNAN. Additionally, MNAN that have not ingested microspheres typically cannot be distinguished from PNAN in field-collected samples and this can lead to an overestimate of MNAN ingestion rates per cell, but not relative grazing impact, compared to HNAN (Sanders and Gast, 2012).

Calculated abundances of nanoflagellates in the brine channels at the fast ice station were generally greater than those observed in open water (**Tables 1**, **3**). Although the ice core samples generally had no visible color, with the exception of a very slight brownish coloration in the bottom 10 cm of the three replicates at site 2, PNAN, MNAN, and HNAN were found in all of the brine channel samples (**Table 3**). All three protistan groups had significantly greater abundance in the bottom part of the cores relative to mid-core and there also were significant differences in abundance between the three coring sites despite their proximity to each other (ANOVA, $p < 0.001$). The differences in abundance between depths in the core were consistent in all samples, but the differences between sites were driven by higher overall abundances at site 2, which had the slightly colored cores (**Table 3**). Across sites, HNAN had the highest abundances, followed by PNAN and mixotrophs (**Table 3**). A higher abundance of nanoflagellates, especially HNAN, in brine relative to open water was previously observed in the Antarctic spring (Moorthi et al., 2009). Mixotrophic nanoflagellates in the brine comprised 13–26% of all phototrophs (PNAN + MNAN) and 9–19% of all bacterivorous flagellates (**Table 3**). Similar proportions of mixotrophs were noted by Moorthi et al. (2009) for sea ice brine in widely separated stations in the Ross Sea during the austral spring (5–10% and 3–15% of phototrophs and bacterivorous flagellates, respectively).

Bacterivory by nanoflagellates from the brine channels was variable. HNAN had low ingestion rates and almost zero impact on bacterial populations at site 1 and 3, despite abundances ranging from 3,000 to 10,000 ml^{-1}. However, at site 2, HNAN could have ingested 4–8% of the bacterial standing stock daily. Conversely, MNAN were at much lower abundances than HNAN (**Table 3**), but with ingestion rates of 2–6 bacteria $MNAN^{-1}$ h^{-1}, could potentially have removed 12–18% of the brine standing stock daily, and up to 32% at the bottom of the cores at site 2 where both abundances and ingestion rates were highest. To our knowledge, this is the first report of experimentally-determined bacterivory for protists from brine channels.

Bromodeoxyuridine (BrdU) Experiments—Biodiversity of Protistan Bacterivores

The incubation experiments using BrdU-labeled bacteria as food and subsequent immunoprecipitation and amplification of the eukaryotic portion of the BrdU-labeled DNA allow identification of some of the major bacterivorous taxa. Putative mixotrophic taxa are identified by BrdU-labeling, indicating bacterivory, coupled with their taxonomic relationship to phototrophic organisms. The number of sequence tags and OTUs recovered in the surface and chlorophyll maximum for the total community (whole) and those that were bacterivorous (immunoprecipitated, IP) are given in Table S1. The data are reported both before and after removal of OTUs corresponding to singletons, bacteria, fungi, metazoa and higher plants. No chimeric OTUs were

TABLE 3 | Abundances of phototrophic (PNAN), mixotrophic (MNAN) and heterotrophic (HNAN) nanoflagellates in sea ice brine channels (station means of three replicate cores) from the middle and bottom of cores (see Methods) and the relative percentage of mixotrophs as total phototrophs and total bacterivores based on all replicates.

		Abundances (cells ml^{-1} brine)			Trophic mode (%)	
		PNAN	MNAN	HNAN	Phototrophs	Bacterivores
Mid-core	Site 1	2,664	839	4,760	20 (18–26)	12 (9–15)
	Site 2	4,102	790	8,065		
	Site 3	3,085	551	3,768		
	Mean	2,909	727	5,531		
	(S.E.)	(318)	(89)	(1,299)		
Bottom	Site 1	4,627	793	7,933	15 (13–17)	14 (9–19)
	Site 2	9,896	1,607	10,511		
	Site 3	5,604	742	3,173		
	Mean	6,060	1,048	7,206		
	(S.E.)	(1,594)	(280)	(2,145)		

Numbers in parentheses are S.E. of the mean for abundances and the range from all the cores taken at three nearby sites for percent of trophic mode.

detected. A similar number of total sequences were recovered for each sample, except for Experiment 1 surface Whole and Experiment 2 surface IP, which had about half the number of tags. After removal of non-protistan OTUs, the number of sequences per sample became more variable. This was due to the recovery of a relatively high number of Metazoan sequences in several samples (e.g., Experiment 2 surface whole and Experiment 3 CM whole; Table S1). The number of OTUs identified at 95% similarity varied for each experiment and sample, but in general the Whole samples had more OTUs than the IP samples. The notable exception to this was the CM IP sample from Experiment 3, which had a much greater number of OTUs, before and after removal of non-protistan OTUs (Table S1).

The OTUs with prevalence at >0.5% of the total tags at the Class level for each experiment are given in Supplemental Material (Figure S1), but can be briefly summarized. In experiment 1 (Station 14), diatoms comprise about half of all the sequences in all of the samples, although less in the IP fraction (surface Whole 64%, CM Whole 55%, surface IP 53%, CM IP 46%). Syndiniales (parasitic dinoflagellates) is the second most abundant OTU in all four samples (surface Whole 12%, CM Whole 20%, surface IP 23%, CM IP 36%) followed by the Prymnesiophyte, *Phaeocystis antarctica,* in the Whole samples (surface 10%, CM 11%). Experiment 2 (Station 21) also shows an abundance of diatom sequences in the Whole samples (surface 75%, CM 68%), but much fewer in the IP samples (surface 20%, CM 25%). Syndiniales sequences are the next most abundant OTUs (surface Whole 14%, CM Whole 16%, surface IP 30%, CM IP 42%), and both they and the dinoflagellates (surface 6%, CM 6%) show an increase in the IP samples (surface 23%, CM 12%). Interestingly, *P. antarctica* sequences increase in abundance in the IP samples compared to the Whole samples for this experiment (surface Whole 2%, CM Whole 1%, surface IP 10%, CM IP 7%). Diatoms were much less abundant in all samples for Experiment 3 at Station 30 (surface Whole 16%, CM Whole 12%, surface IP 14%, CM IP 14%). The OTUs corresponding to Syndiniales (surface Whole 34%, CM Whole 21%, surface IP 29%, CM IP 31%), free-living dinoflagellates (surface Whole 19%, CM Whole 25%, surface IP 14%, CM IP 34%) and cercozoa (surface Whole 6%, CM Whole 29%, surface IP 23%, CM IP 10%) were the most abundant representatives for Experiment 3. *Phaeocystis* OTU was only abundant in the surface Whole samples (11%), but did show a slight increase in the CM IP sample (2.8%) for this experiment. In Experiment 4 (Station 54), the diatom OTUs were once again abundant, with a decrease in the IP samples (surface Whole 48%, CM Whole 36%, surface IP 41%, CM IP 9%), followed by the Syndiniales OTUs (surface Whole 19%, CM Whole 13%, surface IP 27%, CM IP 10%). *Phaeocystis* was only detected in the Whole samples in Experiment 4 (surface Whole 9.6%, CM Whole 4.5%) and the Polycystinea were abundant in the CM whole and IP samples (CM Whole 35%, CM IP 69%).

Identification of Putative Mixotrophs

When comparing the Whole and IP results to examine site similarity and to identify putative mixotrophs, the data were not restricted to the >0.5% fraction, and the taxonomic classification was taken to the lowest available level. In Primer v. 6 the abundance data was normalized to the total for each sample, log(x+1) transformed and then a Bray-Curtis resemblance matrix was created. Cluster analysis with SIMPROF indicated that whole and IP samples from an individual experiment were usually more similar to each other than they were to the same treatment from a different experiment. This was not unexpected considering that the water samples were collected at very different sites (**Figure 1**), and that the IP samples are expected to represent the bacterivorous subset of the original whole water sample. This was confirmed by the comparison of abundance of individual OTUs (Table S2).

OTUs with a taxonomic similarity to known phototrophs that were present in the IP samples were considered putatively mixotrophic. There were a small number of these OTUs that showed increased abundance in both the surface and CM IP samples compared to the Whole sample (**Table 4**). In most cases, the OTU abundance in the IP sample was lower than in the Whole sample, or an OTU was present in only one of the IP samples. While the strongest support for putative mixotrophic OTU identification could be argued for ones that showed an increase in abundance in the IP samples from both depths at a station, the fact that the OTU was present in an IP sample suggests that there was mixotrophic activity (Table S2) because it might be differentially stimulated in different parts of the water column. Light and nutrient concentrations can affect ingestion by mixotrophs (e.g., Nygaard and Tobiesen, 1993; McKie-Krisberg et al., 2015) and consequently affect BrdU-labeling of the mixotroph DNA. Since light and nutrients typically vary with depth, differences in the mixotrophs identified from the surface and chlorophyll maximum layer could be a factor of environment as much as of species composition.

The presence of dinoflagellate OTUs in the IP samples was not unexpected, as many of these taxa are now considered to be able to consume particles (Jeong et al., 2010). Many of these dinoflagellates were less likely to have been observed in our microsphere ingestion experiments because they may be removed by the 35 μm prescreening or because their abundance was low and not observed on the filters for microscopy. In contrast, the presence of diatom OTUs in the IP samples was surprising as they have never been reported to ingest particles. Diatoms are often very abundant in Antarctic water samples and their DNA may persist through the selection process, although it would be expected to be much less in the IP samples. Another possible reason for the presence of diatom OTUs in the IP samples is that they may take up nucleotides released into the media by bacterivore grazing. The 72 h incubation period that was utilized to enhance incorporation into predator DNA may have increased the potential for breakdown of bacterial DNA and release of dissolved BrdU into the media for uptake by phytoplankton. Again, abundance in the IP sample should be less, and in most cases the number of diatom OTU tags observed in the IP portion was less than in the Whole portion.

The presence of *Phaeocystis* was noted by microscopy throughout the cruise. This Prymnesiophyte alga exists as

TABLE 4 | Operational taxonomic units (OTUs) that had increased abundance in IP relative to whole samples at both surface and deep chlorophyll maximum depths in at least one of the BrdU experiments (B1–B4).

OTU	Number of sequences recovered																Consensus lineage (≥90% Silva 119)
	B1 (Station 14)				B2 (Station 21)				B3 (Station 30)				B4 (Station 54)				
	Whole		IP		Whole		IP		Whole		IP		Whole		IP		
	Surface	CM	Surface	CM	Surface	CM	Surface	CM	Surface	CM	Surface	CM	Surface	CM	Surface	CM	
denovo297	44	75	193	93	0	0	0	0	2	0	0	0	65	10	0	2	Eukaryota; SAR; Stramenopiles; Ochrophyta; Dictyochophyceae; Dictyochales; *Dictyocha*; **uncultured marine eukaryote**
denovo341	3	15	1	11	0	0	76	0	1	0	3	2	20	10	0	7	Eukaryota; SAR; Alveolata; Dinoflagellata; Dinophyceae; Gymnodiniphycidae; Gymnodinium clade; *Gymnodinium*; **Gymnodinium aureolum**
denovo376	1	1	3	7	0	0	0	0	1	0	0	0	4	1	0	0	Eukaryota; SAR; Alveolata; Dinoflagellata; Dinophyceae; Gymnodiniphycidae; Gymnodinium clade; *Gymnodinium*; **uncultured marine eukaryote**
denovo384	16	25	97	171	3	14	0	23	79	21	145	8	55	1	75	0	Eukaryota; SAR; Alveolata; Dinoflagellata; Dinophyceae; Gymnodiniphycidae; Gymnodinium clade; *Gymnodinium*; **uncultured marine eukaryote**
denovo271	0	0	0	0	0	0	0	0	0	107	65	0	0	0	66	70	Eukaryota; SAR; Alveolata; Dinoflagellata; Dinophyceae; Gymnodiniphycidae; Suessiaceae; *Symbiodinium*; ***Symbiodinium* sp. CS-156**
denovo320	2	3	0	0	0	4	13	15	10	0	9	3	5	0	0	0	Eukaryota; SAR; Alveolata; Dinoflagellata; Dinophyceae; Peridiniphycidae; Thoracosphaeraceae; *Pentapharsodinium*; **Pentapharsodinium dalei**

Whole: whole DNA sample. IP: bromodeoxyuridine immunoprecipitated sample. Bold text in Consensus Lineage indicates lowest taxonomic affiliation.

both single cells and multicellular colonies, and forms dense blooms. The increase in *Phaeocystis* OTUs in the IP sample for Experiment 2 was unexpected. Although mixotrophy has never been reported for this particular alga, the presence of the sticky, mucilaginous material in the colonial form makes ingestion experiments difficult to interpret. There is the potential that BrdU nucleotides released by grazing could have been taken up, as is suggested for the diatoms, but why it only occurred in Experiment 2 is not apparent. The difference in experimental results might have reflected the presence of an appropriate (but unknown) trigger for stimulating grazing by the alga. In either case, the result is something to consider in future experiments with laboratory isolates of *Phaeocystis*.

The potentially parasitic Syndiniales OTUs also appear in IP samples. This leads to questions of whether they are acquiring label from an infected host, whether they consume bacteria when not infecting a host, or whether this OTU is not a parasite at all, but actually a heterotroph. Marine Stramenophile (MAST) OTUs also tend to be enriched in IP samples, as do some ciliates, although not as much as anticipated considering the potential capacity of many ciliates to consume large numbers of bacteria.

The OTUs listed in **Table 4** represent a very conservative assessment of mixotrophy and are taxonomically similar to *Dictyocha*, *Gymnodinium*, *Pentapharsodinium,* and *Symbiodinium*. The silicoflagellates (e.g., *Dictyocha*) are considered mixotrophic (Quéguiner, 2016) and there is growing experimental support for mixotrophy in many photosynthetic dinoflagellates, including a *Symbiodinum* strain (Jeong et al., 2010, 2012). We have not observed mixotrophic activity in these groups in our Antarctic ingestion experiments, which may be due to our focus on the more abundant nanoplankton, or that the conditions of our fluorescent-tracer experiments do not favor/induce the behavior in these groups. While it is unlikely that the OTUs with consensus lineages of $\geq$90% represent the exact taxa that have been assigned to them, they do suggest new target taxa for isolation and laboratory experiments on triggers for mixotrophic activity. The sequence data can also be used to develop qPCR assays to estimate their abundance in archived environmental samples to determine if, and under what conditions, they make up a significant portion of the mixotrophic community. Our previous work showed that three known Antarctic mixotroph species generally were only a small portion of the total mixotroph population identified by ingestion methods (Gast et al., 2014). However, the qPCR data also indicated that a single species, *Pyramimonas trychotreta*, was responsible for most of the mixotrophic feeding during at least one of the summer experiments (Gast et al., 2014). This indicated that while the overall mixotroph community is diverse, individual taxa have the capacity to dominate when appropriate conditions are met.

In the Antarctic marine environment, photosynthetic microbial eukaryotes sustain the food web. Although mixotrophy has been demonstrated in effectively every freshwater and marine environment for which the nutritional strategy has been studied, only recently has it been proposed as essential to the functioning of marine food webs (Unrein et al., 2007, 2014; Hartmann et al., 2012). When abundant, mixotrophs likely are an important food source for higher trophic levels. Mixotrophs generally have lower carbon to nutrient ratios (C:N, C:P) than strict phototrophs (Katechakis and Stibor, 2006), and protists with low ratios are considered to be better quality food for higher trophic levels (Sterner, 1990; Hessen et al., 2002; Bukovinszky et al., 2012). The quality of phytoplankton food could impact zooplankton growth and reproduction, which in turn would affect fish and other marine vertebrates.

To our knowledge, the only experimental field data on mixotrophy in the Southern Ocean comes from our work using microscopic and molecular approaches (Moorthi et al., 2009; Gast et al., 2014), with this study being the first to taxonomically identify putative mixotrophic species based upon ribosomal sequence data. Microscopy-based methods allow us to detect and enumerate mixotrophic nanoflagellates as a group, as well as determine their grazing rates and the amount of bacteria that they consume, but tell us little about the actual species present. In Antarctic marine systems, the extreme environmental circumstances of seasonal light deprivation (polar night) and depletion of nutrients including iron (after large seasonal blooms of diatoms and *Phaeocystis)* are conditions that are known to stimulate/enhance mixotrophic activity in cultured nanophytoplankton species (Nygaard and Tobiesen, 1993; Maranger et al., 1998; McKie-Krisberg et al., 2015). The combination of these conditions in the Antarctic may result in a diverse collection of mixotrophic taxa. Consequently, the species present and their relative abundance will alter the impact on the environment. Identifying mixotrophic taxa genetically allows us to target those organisms for recovery in culture and testing of stimulatory conditions that can be used to predict how species may respond to environmental conditions. In conjunction with measurements of bacterial ingestion rates and photosynthetic production, it is also possible to estimate the impact that those particular species may have on the cycling of nutrients. Understanding diversity of mixotrophic species, the amount of their photosynthetic and bacterivorous contributions, and the conditions under which they occur will greatly improve our interpretation of the function of the Antarctic food web.

AUTHOR CONTRIBUTIONS

All three authors contributed to the conception, design and execution of the work, as well as to the writing of the manuscript.

FUNDING

This work was supported by National Science Foundation Grants OPP-0838955 (RG) and OPP-0838847 (RS). Any opinions, findings, and conclusions or recommendations expressed in this material are those of the authors and do not necessarily reflect the views of the National Science Foundation.

ACKNOWLEDGMENTS

We gratefully acknowledge the captain and crew of Nathanial B. Palmer for logistical support and Elizabeth Halliday for assistance during the cruise.

SUPPLEMENTARY MATERIAL

The Supplementary Material for this article can be found online at: https://www.frontiersin.org/articles/10.3389/fmars.2018.00013/full#supplementary-material

REFERENCES

454 Life Sciences Corp. (2010). *GS Junior System Guidelines for Amplicon Experimental Design*. Branford, CT: 454 Life Sciences.

Amaral-Zettler, L. A., McCliment, E. A., Ducklow, H. W., and Huse, S. M. (2009). A method for studying protistan diversity using massively parallel sequencing of V9 hypervariable regions of small-subunit ribosomal RNA genes. *PLoS ONE* 4:e6372. doi: 10.1371/journal.pone.0006372

Anderson, M. R., and Rivkin, R. B. (2001). Seasonal patterns in grazing mortality of bacterioplankton in polar oceans: a bipolar comparison. *Aquat. Microb. Ecol.* 25, 195–206. doi: 10.3354/ame025195

Armstrong, F. A. J., Stearns, C. R., and Strickland, J. D. H. (1967). The measurement of upwelling and subsequent biological processes by means of the Technicon AutoAnalyzer^{TM} and associated equipment. *Deep Sea Res.* 14, 381–389.

Atlas, E. L., Hager, S. W., Gordon, L. I., and Park, P. K. (1971). *A Practical Manual for the Use of the Technicon AutoAnalyzer^{TM} in Seawater Nutrient Analyses: Revised*. Corvallis, OR: Oregon State University, Dept of Oceanography.

Becquevort, S. (1997). Nanoprotozooplankton in the Atlantic sector of the Southern Ocean during early spring: biomass and feeding activities. *Deep-Sea Res. II* 44, 355–373. doi: 10.1016/S0967-0645(96)00076-8

Becquevort, S., Menon, P., and Lancelot, C. (2000). Differences in the protozoan biomass and grazing during spring and summer in the Indian sector of the Southern Ocean. *Polar Biol.* 23, 309–320. doi: 10.1007/s003000050450

Bell, E. M., and Laybourn-Parry, J. (2003). Mixotrophy in the Antarctic phytoflagellate, Pyramimonas gelidicola (Chlorophyta: Prasinophyceae). *J. Phycol.* 39, 644–649. doi: 10.1046/j.1529-8817.2003.02152.x

Bernhardt, H., and Wilhelms, A. (1967). The continuous determination of low level iron, soluble phosphate and total phosphate with the AutoAnalyzer. *Tech. Symp.* 1:386.

Boenigk, J., and Arndt, H. (2002). Bacterivory by heterotrophic flagellates: community structure and feeding strategies. *Antoine van Leeuwenhoek* 81, 465–480. doi: 10.1023/A:1020509305868

Bukovinszky, T., Verschoor, A. M., Helmsing, N. R., Bezemer, T. M., Bakker, E. S., Vos, M., et al. (2012). The good, the bad and the plenty: interactive effects of food quality and quantity on the growth of different Daphnia species. *PLoS ONE* 7:e42966. doi: 10.1371/journal.pone.0042966

Caporaso, J. G., Kuczynski, J., and Stombaugh, J. (2010). QIIME allows analysis of high-throughput community sequencing data. *Nat. Methods* 7, 335–336.doi: 10.1038/nmeth.f.303

Caron, D. A., Countway, P. D., Jones, A. C., Kim, D. Y., and Schnetzer, A. (2012). Marine protistan diversity. *Ann. Rev. Mar. Sci.* 4, 467–493.doi: 10.1146/annurev-marine-120709-142802

Clarke, K. R., and Warwick, R. M. (2001). *Change in Marine Communities: An Approach to Statistical Analysis and Interpretation*. Plymouth, UK: Primer-E Ltd.

Duarte, C. M., Agustí, S., Vaqué, D., Agawin, N. S. R., Felipe, J., Casamayor, E. O., et al. (2005). Experimental test of bacteria-phytoplankton coupling in the Southern Ocean. *Limnol. Oceanogr.* 50, 1844–1854. doi: 10.4319/lo.2005.50.6.1844

Fay, S. A., Gast, R. J., and Sanders, R. W. (2013). Linking bacterivory and phyletic diversity of protists with a marker gene survey and experimental feeding with BrdU-labeled bacteria. *Aquat. Microb. Ecol.* 71, 141–153. doi: 10.3354/ame01674

Gast, R. J., Dennett, M. R., and Caron, D. A. (2004). Characterization of protistan assemblages in the Ross Sea, Antarctica by denaturing gradient gel Electrophoresis. *Appl. Env. Microbiol.* 70, 2028–2037. doi: 10.1128/AEM.70.4.2028-2037.2004

Gast, R. J., McKie-Krisberg, Z. M., Fay, S. A., Rose, J. M., and Sanders, R. W. (2014). Antarctic mixotrophic protist abundances by microscopy and molecular methods. *FEMS Microb. Ecol.* 89, 388–401. doi: 10.1111/1574-6941.12334

Hartmann, M., Grob, C., Tarran, G. A., Martin, A. P., Burkill, P. H., Scanlan, D. J., et al. (2012). Mixotrophic basis of Atlantic oligotrophic ecosystems. *Proc. Natl. Acad. Sci.U.S.A.* 109, 5756–5760. doi: 10.1073/pnas.1118179109

Havskum, H., and Hansen, A. S. (1997). Importance of pigmented and colourless nano-sized protists as grazers on nanoplankton in a phosphate-depleted Norwegian fjord and in enclosures. *Aquat. Microb. Ecol.* 12, 139–151. doi: 10.3354/ame012139

Hessen, D. O., Færøvig, P. J., and Andersen, T. (2002). Light, nutrients, and P:C ratios in algae: grazer performance related to food quality and quantity. *Ecology* 83, 1886–1898. doi: 10.1890/0012-9658(2002)083[1886:LNAPCR]2.0.CO;2

James, M. R., Pridmore, R. D., and Cummings, V. J. (1995). Planktonic communities of melt ponds on the McMurdo Ice Shelf, Antarctica. *Polar Biol.* 15, 555–567. doi: 10.1007/BF00239647

Jeong, H. J., Yoo, Y. D., and Kang, N. S. (2012). Heterotrophic feeding as a newly identified survival strategy of the dinoflagellate *Symbiodinium*. *Proc. Natl. Acad. Sci.U.S.A.* 109, 12604–12609. doi: 10.1073/pnas.1204302109

Jeong, H. J., Yoo, Y. D., Kim, J. S., Seong, K. A., Kang, N. S., and Kim, T. H. (2010). Growth, feeding and ecological roles of the mixotrophic and heterotrophic dinoflagellates in marine planktonic food webs. *Ocean Sci. J.* 45, 65–91. doi: 10.1007/s12601-010-0007-2

Johnson, M. D. (2015). Inducible mixotrophy in the dinoflagellate Prorocentrum minimum. *J. Eukaryot. Microbiol.* 62, 431–443.doi: 10.1111/jeu.12198

Katechakis, A., and Stibor, H. (2006). The mixotroph Ochromonas tuberculata may invade and suppress specialist phago- and phototroph plankton communities depending on nutrient conditions. *Oecologia* 148, 692–701. doi: 10.1007/s00442-006-0413-4

Laybourn-Parry, J., Marshall, W. A., and Marchant, H. J. (2005). Flagellate nutritional versatility as a key to survival in two contrasting Antarctic saline lakes. *Freshw. Biol.* 50, 830–838. doi: 10.1111/j.1365-2427.2005.01369.x

Leakey, R. J. G., Archer, S. D., and Grey, J. (1996). Microbial dynamics in coastal waters of East Antarctica: bacterial production and nanoflagellate bacterivory. *Mar. Ecol. Prog. Ser.* 142, 3–17. doi: 10.3354/meps142003

Maranger, R., Bird, D. F., and Price, N. M. (1998). Iron acquisition by photosynthetic marine phytoplankton from ingested bacteria. *Nature* 396, 248–251. doi: 10.1038/24352

McArdle, B., and Anderson, M. (2001). Fitting multivariate models to community data: a comment on distance-based redundance analysis. *Ecol. Lett.* 82, 290–297. doi: 10.1890/0012-9658(2001)082[0290:FMMTCD]2.0.CO;2

McKie-Krisberg, Z. M., Gast, R. J., and Sanders, R. W. (2015). Physiological responses of three species of Antarctic mixotrophic phytoflagellates to changes in light and dissolved nutrients. *Microb. Ecol.* 70, 21–29. doi: 10.1007/s00248-014-0543-x

Moorthi, S., Caron, D. A., Gast, R. J., and Sanders, R. W. (2009). Mixotrophy: a widespread and important ecological strategy for planktonic and sea-ice nanoflagellates in the Ross Sea, Antarctica. *Aquat. Microb.Ecol.* 54, 269–277. doi: 10.3354/ame01276

Nygaard, K., and Tobiesen, A. (1993). Bacterivory in algae: a survival strategy during nutrient limitation. *Limnol. Oceanogr.* 38, 273–279. doi: 10.4319/lo.1993.38.2.0273

Pearce, I., Davidson, A. T., Thomson, P. G., Wright, S., and van den Enden, R. (2010). Maring microbial ecology of East Antarctica (30-80 E): rates of bacterial and phytoplankton growth and grazing by heterotrophic protists. *Deep Sea Res. II* 57, 849–862. doi: 10.1016/j.dsr2.2008.04.039

Pearce, I., Davidson, A. T., Thomson, P. G., Wright, S., and Van den Ende, P. (2011). Marine microbial ecology in the sub-Antarctic Zone: rates of bacterial and phytoplankton growth and grazing by heterotrohpic protists. *Deep Sea Res. II* 58, 2248–2259. doi: 10.1016/j.dsr2.2011.05.030

Pedrós-Alió, C., Calderón-Paz, J. I., Guixa-Boixereu, N., Estrada, M., and Gasol, J. M. (1996). Microbial plankton across teh Drake Passage. *Polar Biol.* 16, 613–622. doi: 10.1007/BF02329059

Princiotta, S. D., Smith, B., and Sanders, R. W. (2016). Temperature-dependent phagotrophy and phototrophy in a mixotrophic chrysophyte. *J. Phycol.* 52, 432–440. doi: 10.1111/jpy.12405

Putt, M., Stoecker, D. K., and Alstatt, J. (1991). Bacterivory in McMurdo Sound: 1. Grazing by heterotrophic nanoflagellates. *Antarct. J.* 26, 139–140.

Quéguiner, B. (2016). *The Biogeochemical Cycle of Silicon in the Ocean*. Hoboken, NJ: Wiley.

Roberts, E. C., and Laybourn-Parry, J. (1999). Mixotrophic cryptophytes and their predators in the Dry Valley lakes of Antarctica. *Freshw. Biol.* 41, 737–746. doi: 10.1046/j.1365-2427.1999.00401.x

Rothhaupt, K. O. (1996). Laboratory experiments with a mixotrophic chrysophyte and obligately phagotrophic and phototrophic competitors. *Ecology* 77, 716–724. doi: 10.2307/2265496

Sanders, R. W., Berninger, U.-G., Lim, E. L., Kemp, P. F., and Caron, D. A. (2000). Heterotrophic and mixotrophic nanoplankton predation on picoplankton in the Sargasso Sea and on Georges Bank. *Mar. Ecol. Prog. Ser.* 192, 103–118. doi: 10.3354/meps192103

Sanders, R. W., and Gast, R. J. (2012). Bacterivory by phototrophic picoplankton and nanoplankton in Arctic waters. *FEMS Microbiol. Ecol.* 80, 242–253. doi: 10.1111/j.1574-6941.2011.01253.x

Sanders, R. W., and Porter, K. G. (1988). Phagotrophic phytoflagellates. *Adv. Microb. Ecol.* 10, 167-192. doi: 10.1007/978-1-4684-5409-3_5

Sanders, R. W., Porter, K. G., Bennett, S. J., and DeBiase, A. E. (1989). Seasonal patterns of bacterivory by flagellates, ciliates, rotifers, and cladocerans in a freshwater planktonic community. *Limnol. Oceanogr.* 34, 673–687. doi: 10.4319/lo.1989.34.4.0673

Sherr, B. F., and Sherr, E. B. (1993). "Protistant grazing rates via uptake of fluorescently labeled prey," in *Handbook of Methods in Aquatic Microbial Ecology*, eds P. F Kemp, B. F. Sherr, E. B. Sherr, and J. J. Cole (Boca Raton, FL: CRC Press, LLC), 695-701.

Sherr, B. F., Sherr, E. B., and Pedrós-Alió, C. (1989). Simultaneous measurement of bacterioplankton production and protozoan bacterivory in estuarine water. *Mar. Ecol. Prog. Ser.* 54, 209–219. doi: 10.3354/meps054209

Sherr, E. B., Caron, D. A., and Sherr, B. F. (1993). "Staining of heterotrophic protists for visualization via epifluorescence microscopy," in *Handbook of Methods in Aquatic Microbial Ecology*, eds P. F. Kemp, B. F. Sherr, E. B. Sherr, and J. J. Cole (New York, NY: Lewis Publishers), 213-227.

Sterner, R. W. (1990). The ratio of nitrogen to phosphorus resupplied by herbivores: zooplankton and the algal competitive arena. *Am. Nat.* 136, 209–229. doi: 10.1086/285092

Stoeck, T., Bass, D., Nebel, M., Christen, R., Jones, M. D. M., Breiner, H.-W., et al. (2010). Multiple marker parallel tag environmental DNA sequencing reveals a highly complex eukaryotic community in marine anoxic water. *Mol. Ecol.* 19, 21–31. doi: 10.1111/j.1365-294X.2009.04480.x

Stoecker, D. K., Hansen, P. J., Caron, D. A., and Mitra, A. (2017). Mixotrophy in the Marine Plankton. *Ann. Rev. Mar. Sci.* 9, 315–335. doi: 10.1146/annurev-marine-010816-060617

Tsai, A. Y., Gong, G. C., Sanders, R. W., Chen, W. H., Chao, C. F., and Chiang, K. P. (2011). Relative importance of pigmented- and heterotrophic nanoflagellates grazing on bacteria during the warm season in a coastal subtropical ecosystem of the Western Pacific. *Aquat. Microb. Ecol.* 63, 9–18. doi: 10.3354/ame01470

Unrein, F., Gasol, J. M., Not, F., Forn, I., and Massana, R. (2014). Mixotrophic haptophytes are key bacterial grazers in oligotrophic coastal waters. *ISME J.* 8, 164–176. doi: 10.1038/ismej.2013.132

Unrein, F., Massana, R., Alonso-Saez, L., and Gasol, J. M. (2007). Significant year-round effect of small mixotrophic flagellates on bacterioplankton in an oligotrophic coastal system. *Limnol. Oceanogr.* 52, 456–469. doi: 10.4319/lo.2007.52.1.0456

Vaqué, D., Agustí, S., and Duarte, C. M. (2004). Response of bacterial grazing rates to experimental manipulation of an Antarctic coastal nanoflagellate community. *Aquat. Microb. Ecol.* 36, 41–52. doi: 10.3354/ame036041

Vaqué, D., Calderón-Paz, J. I., Guixa-Boixereu, N., and Pedrós-Alió, C. (2002). Spatial distribution of microbial biomass and activity (bacterivory and bacterial production) in the northern Weddell Sea during the austral summer (January 1994). *Aquat. Microb. Ecol.* 29, 107–121. doi: 10.3354/ame029107

Vaqué, D., Alonso-Sáez, L., Arístegui, J., Agustí, S., Duarte, C. M., Montserrate Sala, M., et al. (2014). Bacterial production and losses to predators along an open ocean trophic gradient in the subtropical north east atlantic ocean. *J. Plankton Res.* 36, 198–213. doi: 10.1093/plankt/fbt085

Wilken, S., Verspagen, J. M. H., Naus-Wiezer, S., Van Donk, E., and Huisman, J. (2014). Comparison of predator–prey interactions with and without intraguild predation by manipulation of the nitrogen source. *Oikos* 123, 423–432. doi: 10.1111/j.1600-0706.2013.00736.x

Zubkov, M. V., and Tarran, G. A. (2008). High bacterivory by the smallest phytoplankton in the North Atlantic Ocean. *Nature* 455, 224–226. doi: 10.1038/nature07236

Conflict of Interest Statement: SF was employed by Invitae at the time of manuscript submission, but was a postdoctoral investigator at Temple during the cruise and data collection portion of this work.

The other authors declare that the research was conducted in the absence of any commercial or financial relationships that could be construed as a potential conflict of interest.

Advantages of publishing in Frontiers

OPEN ACCESS
Articles are free to read for greatest visibility and readership

FAST PUBLICATION
Around 90 days from submission to decision

HIGH QUALITY PEER-REVIEW
Rigorous, collaborative, and constructive peer-review

TRANSPARENT PEER-REVIEW
Editors and reviewers acknowledged by name on published articles

Frontiers
Avenue du Tribunal-Fédéral 34
1005 Lausanne | Switzerland

Visit us: www.frontiersin.org
Contact us: info@frontiersin.org | +41 21 510 17 00

REPRODUCIBILITY OF RESEARCH
Support open data and methods to enhance research reproducibility

DIGITAL PUBLISHING
Articles designed for optimal readership across devices

FOLLOW US
@frontiersin

IMPACT METRICS
Advanced article metrics track visibility across digital media

EXTENSIVE PROMOTION
Marketing and promotion of impactful research

LOOP RESEARCH NETWORK
Our network increases your article's readership